

STUDIES OF PHASE INVERSION AND AMBIVALENCE
IN LIQUID-LIQUID SYSTEMS

by

MEHRDAD ARASHMID

A thesis submitted to the University of Aston in
Birmingham for the degree of Doctor of Philosophy

Department of Chemical Engineering
The University of Aston in Birmingham

July 1980

This thesis is dedicated to my father, whose financial and moral support enabled me to complete this work.

SUMMARYSTUDIES OF PHASE INVERSION AND AMBIVALENCE
IN LIQUID-LIQUID SYSTEMS

MEHRDAD ARASHMID

Ph.D.

1980

The literature relating to liquid-liquid mixing, and the factors determining which phase is dispersed in batch or continuous systems, and studies of phase inversion have been reviewed.

A mathematical model has been developed to predict the limits of phase inversion. The model is based on the collision frequency and coalescence frequency of agitated dispersions in conjunction with models relating drop sizes and hold-up to agitator speed.

Experimental investigations were made into ambivalent phase inversion in a batch and continuous mixer-settler unit. Drop sizes and limits of phase inversion were measured.

The model was tested with the experimental results obtained, as well as published results. The agreement between predicted and experimental results is excellent.

Key Words

Phase inversion

Drop collision/coalescence

ACKNOWLEDGEMENTS

The author wishes to thank the following:

Professor G.V. Jeffreys,

for his encouragement and supervision and for providing
the facilities for research

Dr. C.J. Mumford,

for his continual help and constructive criticism

The Technical Staff of the Department of Chemical Engineering

for their assistance in fabricating the equipment and
in the photographic work

Ms. P.J. O'Gorman

for her diligence in typing this thesis.

I N D E X

CHAPTER ONE		<u>Page</u>
1	<u>INTRODUCTION</u>	1
CHAPTER TWO		
2	<u>MIXING FUNDAMENTALS</u>	3
2.1	Fundamental Processes in the Flow of Two Immiscible Liquids	3
2.2	Agitated Vessels	4
2.2.1	Propellers	4
2.2.2	Turbines	4
2.2.3	Paddles	4
2.2.4	High Shear Impellers	6
2.2.5	Reciprocating Impellers	6
2.3	Power Requirement	6
2.3.1	Dimensional Analysis	6
2.3.2	Fluid Property Effects	8
2.3.2.1	Average Density	8
2.3.2.2	Effective Viscosity	8
2.4	Flow Pattern in Agitated Vessels	12
2.5	Mixing in Agitated Vessels	13
2.5.1	Batch Mixing	13

	<u>Page</u>
2.5.2 Continuous Mixing	17
 CHAPTER THREE	
3 <u>LIQUID HYDRODYNAMICS</u>	18
3.1 Drop Formation	19
3.2 Drop Breakage Process	26
3.3 Drop Size Distribution	33
3.4 Droplet Coalescence	36
3.4.1 Drop-Interface Coalescence	39
3.4.2 Drop-Drop Coalescence	40
 CHAPTER FOUR	
4 <u>PHASE INVERSION</u>	46
4.1 Ambivalent Range	46
4.2 Phase Inversion in Agitated Columns	48
4.2.1 Phase Inversion in R.D.C. Columns	48
4.2.2 Phase Inversion in Oldshue-Rushton Columns	49
4.3 Phase Inversion in Agitated Vessels	49
4.3.1 Phase Inversion in Batch Mixing Tanks	50
4.3.2 Phase Inversion in Mixer-Settlers	52
4.4 Effect of Mass Transfer on Phase Inversion	53
4.5 Further Observation on Phase Inversion in a Mixer-Settler Unit	54

CHAPTER FIVE

Page

5	<u>MATHEMATICAL MODELLING</u>	64
5.1	The Theory of Phase Inversion	64
5.1.1	Drop-Size Model	66
5.1.2	Collision Frequency Model	67
5.1.3	Coalescence Frequency Model	69
5.1.4	Phase Inversion Model	71
5.2	Computer Programme	71

CHAPTER SIX

6	<u>EXPERIMENTAL INVESTIGATION</u>	77
6.1	Design and Equipment Considerations	77
6.1.1	Batch Mixing Vessel	78
6.1.2	Continuous Mixer-Settler	80
6.1.2.1	Mixer Unit	80
6.1.2.2	Constant Head Device	89
6.1.2.3	Gravity Settler	89
6.1.3	Other Equipment Considerations	91
6.2	Ancillary Equipment	92
6.2.1	Continuous Phase Detector	92
6.2.2	Photographic Equipment	93
6.3	Liquid-Liquid Systems	94
6.3.1	Determination of Physical Properties	95
6.3.2	Liquid-Liquid Systems	95

6.3.3	Saturated-System Preparation	96
6.4	Experimental Procedures	96
6.4.1	Batch System	97
6.4.1.1	Cleaning	97
6.4.1.2	Purity Test	97
6.4.1.3	Start-up Procedure	97
6.4.1.4	Analysis of Data	98
6.4.2	Continuous Rig	99
6.4.2.1	Cleaning	103
6.4.2.2	Purity Test	103
6.4.2.3	Start-up Procedure	103
6.5	Experimental Programme	105
6.5.1	Velocity Gradient Near Impeller ..	106
6.5.2	Drop-Size	106
6.5.3	Drop-Size Growth at Phase Inversion	106
6.5.4	Limits of Phase Inversion	110
6.6	Matching Refractive Indexes	110

CHAPTER SEVEN

7	<u>EXPERIMENTAL PROCEDURE AND RESULTS</u>	113
7.1	Batch Mixing Vessel	113
7.1.1	Drop-Size Vs Rotor Speed and Hold-up	113
7.1.2	Drop-Size at High Hold-up	119
7.1.3	Drop-Size Growth at Point of Inversion	119

	<u>Page</u>
7.1.4 The Limits of Phase Inversion ..	119
7.1.5 Matching Refractive Indexes	124
7.1.6 Flow Pattern Studies	129
7.2 Continuous Mixer-Settler	129
7.2.1 Phase Inversion Under Batch Condition	129
7.2.2 Phase Inversion Under Continuous Operation	130
7.2.3 Phase Inversion Vs Input Rate ..	132

CHAPTER EIGHT

8 <u>DISCUSSION OF RESULTS</u>	139
8.1 Batch Mixing Vessel	139
8.1.1 Drop-Size Studies	139
8.1.1.1 Drop-Size Distribution ..	139
8.1.1.2 Drop-Size Vs Hold-up and Rotor Speed	140
8.1.2 Drop-Size Near Phase Inversion ..	140
8.1.3 Drop Growth at Phase Inversion ..	143
8.1.4 Limits of Phase Inversion	146
8.1.5 Matching Refractive Indexes	150
8.1.6 Flow Pattern Studies	151
8.2 Continuous Mixer-Settler	151
8.2.1 Phase Inversion Under Batch Condition	151
8.2.2 Phase Inversion Under Continuous Operation	152
8.2.3 Phase Inversion Vs Input Flow Rate	153

	<u>Page</u>
8.3 Comparison of Phase Inversion Results ..	154
8.3.1 Phase Inversion Vs Mode of Operation	154
8.3.2 Phase Inversion Vs Vessel Geometry ..	154

CHAPTER NINE

9 <u>CONCLUSION</u>	155
-----------------------------	-----

CHAPTER TEN

10 <u>SUGGESTIONS FOR FURTHER WORK</u>	157
--	-----

APPENDICES

1 Extrapolation of Miller's results	A1
2 Computer Programme of Phase Inversion Model ..	A2
3 Continuous Phase Detector Unit	A3
4 Physical Properties of Liquid-Liquid Systems ..	A4
5 Calibration of Rotameters	A5
6 Physical Properties of Glycerine-Water System ..	A6
7 Drop Size Analysis Programme	A7
8 Batch Equipment Results	A8
9 Continuous Flow Equipment Results	A9

LIST OF FIGURES

	<u>Page</u>
Figure 2.1 Characteristic Impeller Power Curve for Axial Flow Impeller	9
Figure 2.2 Impeller Characteristics and Power	10
Figure 2.3 Relationships Between Variables in Liquid Extraction	11
Figure 2.4 Flow Pattern for a Typical Axial Flow Turbine Impeller	15
Figure 2.5 Reference Points in a Baffled Vessel	16
Figure 3.1 Drop Formation at a Nozzle	20
Figure 3.2 Drop Formation in a Stirred Tank	20
Figure 3.3 Drop Volume Vs Time of Formation	21
Figure 3.4 Comparison Between Predicted and Actual Drop Volume	25
Figure 3.5 A Typical Drop Size Distribution	37
Figure 4.1 Ambivalent Phase Inversion Hysteresis Predicted Vs Actual (Toluene - Water) ..	55
Figure 4.2 Ambivalent Phase Inversion Hysteresis Predicted Vs Actual (Kerosene - Water) ..	56
Figure 4.3 Flow Pattern near a Turbine Impeller	58
Figure 4.4 Regions of Suction and Discharge Near an Impeller	59
Figure 4.5 Effect of Surfactants on a Dispersion ..	61
Figure 4.6 Effect of surfactants on a High Concentration Dispersion	62
Figure 5.1 A Typical Plot of T Vs Hold-up	72
Figure 5.2 Computer Flow Chart	73
Figure 6.1 Batch Mixing Vessel	79

	<u>Page</u>
Figure 6.2 Flow Diagram of Continuous Mixer-Settler Unit	81
Figure 6.3 General Layout of the Continuous Mixer - Settler Unit With Front Panels Removed ..	83
Figure 6.4 General Layout of the Control Panel ..	84
Figure 6.5 Diagram of Gravity-Settler	85
Figure 6.6 Diagram of Mixer Unit	87
Figure 6.7 Diagram of Constant Head Device	90
Figure 6.8 A Typical Phase Inversion Sequence	100
Figure 6.9 Predicted Drop-Size Vs Actual Drop Size (N = 350)	107
Figure 6.10 Rate of Drop Growth Near Phase Inversion	108
Figure 6.11 A Typical Unstable Dispersion Nearing Phase Inversion	109
Figure 6.12 Arrangement of Matching Refractive Index Apparatus	111
Figure 7.1 Variation of Drop-Size With Hold-up (N = 300)	114
Figure 7.2 Variation of Drop-Size With Hold-up (N = 350)	115
Figure 7.3 Variation of Drop-Size With Hold-up (N = 400)	116
Figure 7.4 Variation of Drop-Size With Hold-up (N = 450)	117
Figure 7.5 Variation of Drop-Size With Hold-up (N = 500)	118
Figure 7.6 Drop-Size vs Rotor Speed	120
Figure 7.7 Rate of Drop-Size Growth vs Time (N = 400)	121
Figure 7.8 Rate of Drop-Size Growth vs Time (N = 300)	122
Figure 7.9 Ambivalent Phase Inversion Limits (Toluene/Water)	123
Figure 7.10 Ambivalent Phase Inversion Limits (CCl ₄ /Water)	125

	<u>Page</u>
Figure 7.11 Ambivalent Phase Inversion Limits (70% Toluene + 30% CCl ₄ /Water)	126
Figure 7.12 Ambivalent Phase Inversion Limits (63% Toluene + 37% CCl ₄ /Water)	127
Figure 7.13 Ambivalent Phase Inversion Limits (30% Toluene + 70% CCl ₄ /Water)	128
Figure 7.14 Ambivalent Phase Inversion Limits (Continuous Rig Under Batch Conditions) ..	131
Figure 7.15 Ambivalent Phase Inversion Limits Under Flow Conditions ($V_T = 6 \times 10^{-5} \text{ m}^3/\text{s}$)	133
Figure 7.16 Ambivalent Phase Inversion Limits Under Flow Conditions ($V_T = 8 \times 10^{-5} \text{ m}^3/\text{s}$)	134
Figure 7.17 Ambivalent Phase Inversion Limits Under Flow Conditions ($V_T = 10 \times 10^{-5} \text{ m}^3/\text{s}$)	135
Figure 7.18 Ambivalent Phase Inversion Limits Under Flow Conditions ($V_T = 12 \times 10^{-5} \text{ m}^3/\text{s}$)	136
Figure 7.19 Effect of Flow Rate on Phase Inversion Hysteresis	137
Figure 7.20 Effect of Mode of Operation on Phase Inversion Hysteresis	138
Figure 8.1 Calculated Drop-Size vs Predicted Drop- Size (N = 300)	141
Figure 8.2 Calculated Drop-Size vs Predicted Drop- Size ($\phi = 40$)	142
Figure 8.3 A Typical Concentrated Dispersion	144
Figure 8.4 Ambivalent Phase Inversion Limits Predicted vs Actual (CCl ₄ /Water, Batch Data)	147
Figure 8.5 Ambivalent Phase Inversion Limits Predicted vs Actual (Toluene/Water, Continuous Flow Data)	148

LIST OF TABLES

	<u>Page</u>
Table 2.1 Advantages and Disadvantages of various Contacting Devices	5
Table 2.2 Comparison of Discharge rates of Impellers ..	14
Table 3.1 Exponents for Single Tanks	22
Table 3.2 Summary of Effects Predicted by Generalised Correlation for Drop Sizes	29
Table 3.3 Effect of Drop Size Distribution on Dispersion Property	38
Table 3.4 Effect of System Property on Coalescence Time	41

CHAPTER ONE

I N T R O D U C T I O N

1 INTRODUCTION

In area dependent processes (e.g. heat transfer, mass transfer) where two immiscible liquids are used, the dispersion is sustained by the use of a contacting device. Many different devices have been developed in the past for this purpose and many reviews on equipment selection have been published (1, 2, 3). Most of the literature available on the fundamental studies of these devices is limited to the Oldshue-Rushton and R.D.C. columns (4, 5, 6, 7, 8, 9, 10).

Studies dealing with the mixer-settler have been mainly concerned with qualitative studies of these devices (11, 12, 13, 14). Due to the wide application of contacting devices in the chemical and allied industries it was considered that a quantitative study of the hydrodynamic processes involved in the mixing of two immiscible liquids could lead to an improved performance. In these mixing vessels one phase is dispersed as droplets in a continuous phase of the other by means of a rotating or a pulsating agitator and the nature of dispersed phase is of considerable importance since, in the case of a liquid-liquid extractor the rate of transfer (heat or mass), or in a reactor, the rate of reaction depends upon it. The nature of dispersed phase further effects the rate of coalescence hence the separation characteristics of the dispersion in gravity-settlers.

Most mixing vessels and settlers in commercial use are usually sealed and made of steel or G.R.P. and this makes it virtually impossible to assess the type of dispersion visually. It will, therefore, be advantageous to be able to determine from the operating conditions which phase is dispersed. It is well known, for example, that in the ambivalent region the nature of dispersion will depend on the method of initiation of the dispersion.

In this work the processes involved in ambivalent phase inversion in a mixer-settler are considered. Phase inversion is defined as a hydrodynamic condition under which, due to a rapid increase in the coalescence rate, the dispersed phase becomes continuous and vice versa. In the ambivalent region either phase, depending on the manner of initiation of the dispersion, may be dispersed and the aim of this study is to quantify the processes involved in phase inversion.

The variables under investigation, besides the physical properties of liquid systems, were impeller speed and vessel geometry and a continuous and a batch mixing vessel were used to carry out these studies.

Theoretical studies of phase inversion lead to the development of a mathematical model taking into account the variables effecting phase inversion. The development of the mathematical model is discussed in Chapter 5.

A supporting paper, published in A.I.Ch.E. Jnl. (16) is appended at the end of this thesis.

CHAPTER TWO

MIXING FUNDAMENTALS

2 MIXING FUNDAMENTALS

In a mixer settler unit the energy introduced into the system by an impeller causes movement of the liquid phases and generates eddies that break the interface between the liquids to form a dispersion. The mechanism of turbulent motion is so complex that, at present, there has been no general physical model on which to base an analysis of drop size or size distribution. In order to simplify turbulent motion, it is usually assumed that the turbulence of the system is homogeneous. This implies that the average turbulence characteristics are independent of the position in the fluid i.e. invariant to the axis of translation. In this chapter the terms used to describe a dispersion and to consider the factors regulating the power requirements etc. for choosing the most suitable contacting device will be reviewed.

2.1 FUNDAMENTAL PROCESSES IN THE FLOW OF TWO IMMISCIBLE LIQUIDS

The object of this section is to establish the basic hydrodynamics of fluid motion and their relevance to liquid-liquid contacting and the production of dispersions. Liquid-liquid mixing is frequently encountered in heat and mass transfer operations and always involves the dispersion

of one liquid into another by external mechanical energy. Mechanical devices are used to promote liquid motion and mixing and, therefore, it is necessary to review the design of the equipment and power input to promote the desired level of mixing by mechanical agitation.

A number of contacting devices have been developed for every kind of contacting application and the advantages and disadvantages of various liquid-liquid contacting devices are summarized in Table 2.1.

2.2 AGITATED VESSELS

The selection of impellers is usually dependent on the liquid systems employed. Impellers can be divided into five groups (17).

2.2.1 Propellers

Essentially high speed impellers of axial flow type, generally used in low viscosity liquids.

2.2.2 Turbines

The A.I.Ch.E "Standard Test Procedure for Impeller-Type Mixing Equipment" (16) defines a turbine as "an impeller with an essentially constant angle with respect to a vertical plane, over its entire length or over finite sections having blades either vertical or set at an angle less than 90° with the vertical". The blades may be curved or flat. The number of blades can be two or more.

2.2.3 Paddles

One of the oldest types of impeller and can

TABLE 2.1 ADVANTAGES AND DISADVANTAGES OF VARIOUS CONTACTORS (12)

	Capital Cost	Operating Cost	Efficiency	Total Capacity	Flexibility	Volumetric Efficiency	Space	
							Vertical	Floor
1 Spray Tower	5	5	1	2	2	1	1	5
2 Baffle Plate Tower	4	5	2	4	2	3	1	5
3 Packed Tower	4	5	2	2	2	2	1	5
4 R.D.C.	3	4	4	3	5	4	3	5
5 Pulsed Plate Column	3	3	4	3	4	4	3	5
6 Mixer-Settler	2	2	3	4	3	3	5	1
7 Centrifugal	1	2	5	3	5	5	5	5

be described as having two blades, horizontal or vertical, with a high D/T ratio.

2.2.4 High Shear Impellers

They operate in the higher Reynolds number range, the D/T is low, the speed is high and the blade area is small.

2.2.5 Reciprocating Impellers

These are very rarely used, they feature a perforated plate on a reciprocating shaft.

2.3 POWER REQUIREMENT

The estimation of power requirement in a mixing process is essential for economic operation. Thomson (18) was the first to study the friction of rotating discs. Unwin (19) furthered the work on discs and summarised the effect on frictional resistance of changes in speed, diameter, surface roughness, fluid viscosity and the ratio of the disc diameter to the tank. White et al (20, 21, 22) were the first to point out the possibility of correlating impeller power by dimensional analysis. Hixson et al (23, 24, 25, 26) substantiated and elaborated on the theory.

2.3.1 Dimensional Analysis

The general dimensionless equation for agitator power has been derived using dimensional analysis. Thus the pertinent dimensionless groups are:

$$f\left(\frac{D^2 N \rho}{\mu}, \frac{D N^2}{g}, \frac{P}{\rho N^3 D^5}, \frac{D}{T}, \frac{D}{Z}, \frac{D}{c}, \frac{D}{P}, \frac{D}{W}, \frac{D}{1}, \frac{n_2}{n_1}\right) = 0 \quad 2.1$$

Geometric, kinematic and dynamic dimensionless groups are the most relevant and, therefore, confining the general equation to this area of interest reduces the correlation to:

$$f\left(\frac{D^2 N \rho}{\mu}, \frac{D N^2}{g}, \frac{P}{D^5 N^3 \rho}\right) = 0 \quad 2.2$$

Equation 2.2 can be rewritten as

$$N_p = K (Re)^a (Fr)^b = 0 \quad 2.3$$

For a fully baffled tank $b = 0$

$$N_p = K (Re)^a \quad 2.4$$

At high Reynolds numbers the power can be obtained from

$$P = K N^3 D^5 \rho \quad 2.5$$

where K is a constant depending on the type of impeller.

Many workers have collected data on all types of impeller of a standard design, Martin (27), Brown et al (28) and Hooker have plotted the data of many investigators' various impellers (29).

Fortunately, the data collected for turbine impellers in recent years has been extensive and the results of these

workers are summarised in Figures 2.1 and 2.2.

2.3.2 Fluid Property Effects

Power data for two phase mixtures is very scarce. However, data for the effects of viscosity and density for Newtonian liquids has been published using average properties. The results are in good agreement with single phase data on Np vs Re plots. Figure 2.3 shows the relationships between variables in liquid extraction.

2.3.2.1 Average Density

The average density of a mixture is given by the correlation

$$\rho_{av} = \phi \rho_d + (1 - \phi) \rho_c \quad 2.6$$

2.3.2.2 Effective Viscosity

The effective viscosity of a mixture as a geometric mean is given by

$$\mu_m = (\mu_d)^\phi (\mu_c)^{1 - \phi} \quad 2.7$$

worked reasonably well for Miller and Mann (35) but it has been found by many other workers to be valid only for miscible low viscosity fluids.

Vermeulen et al (31) recommended for emulsions the use of

$$\mu_m = \frac{\mu_c}{(1 - \phi)} \left(1 + \frac{(1.5) (\phi) (\mu_d)}{\mu_c + \mu_d} \right) \quad 2.8$$

Vanderveen (32) in an extension of the work of

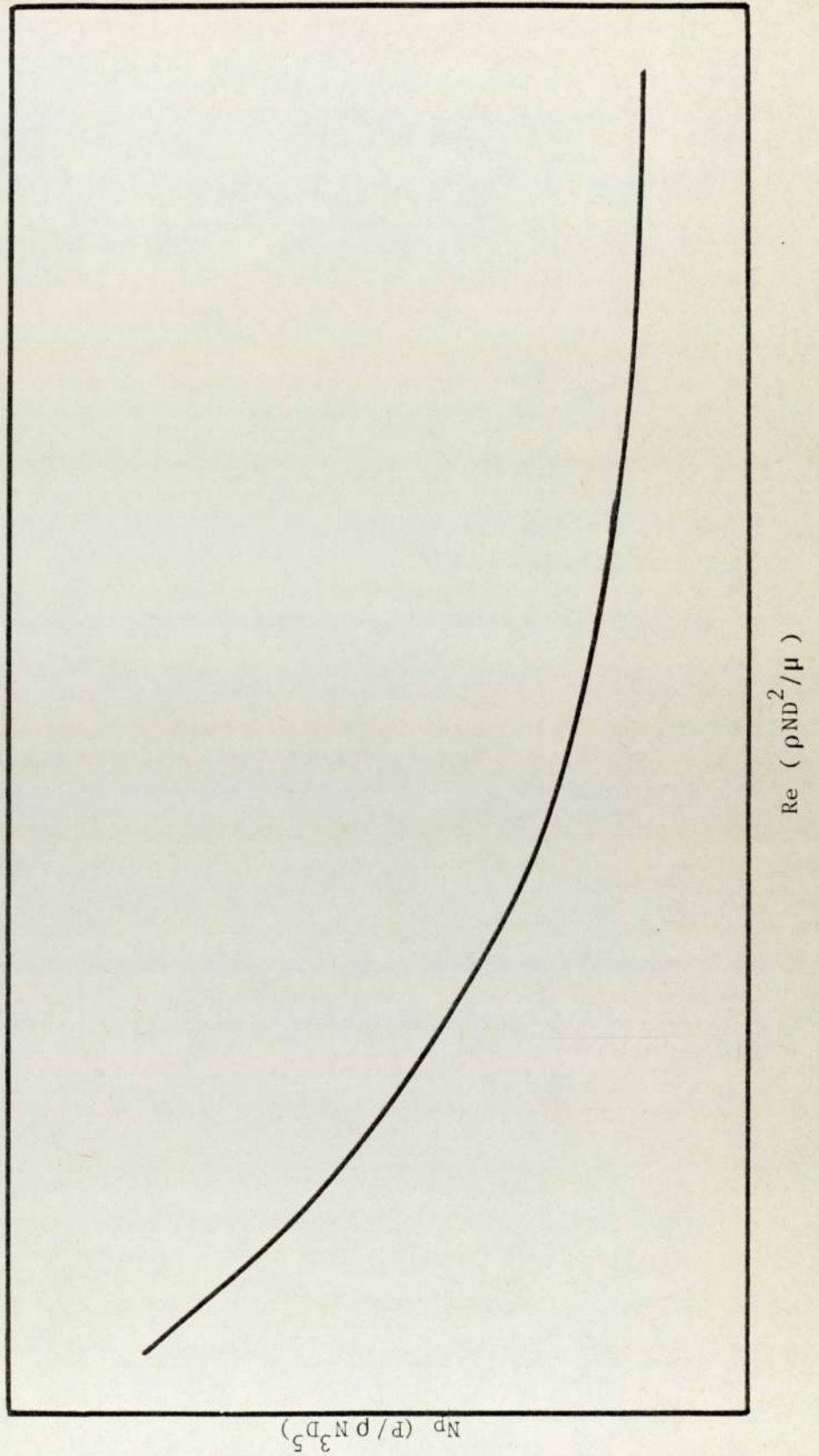


Figure 2.1 CHARACTERISTIC IMPELLER POWER CURVE FOR
AXIAL FLOW IMPELLER (17)

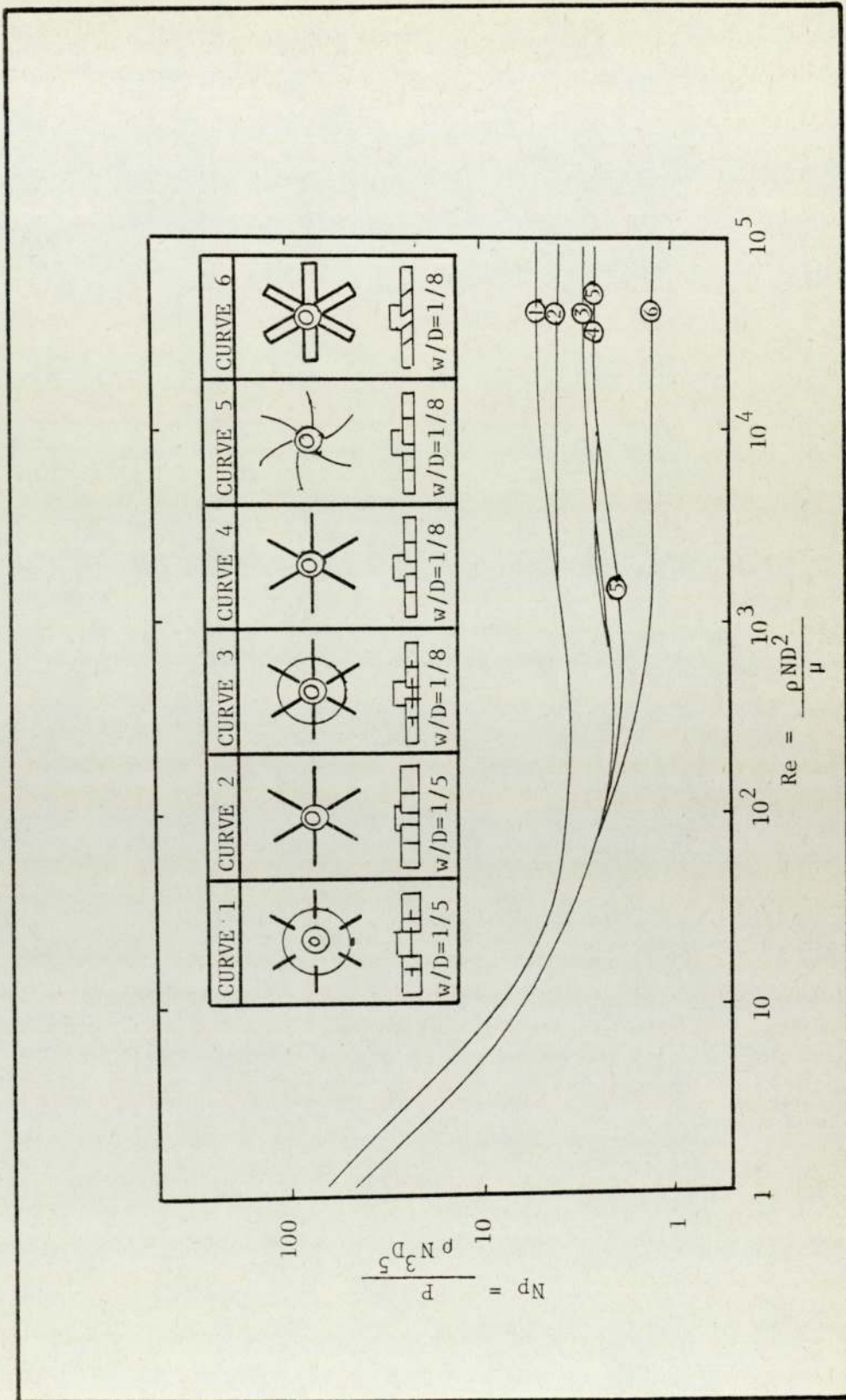
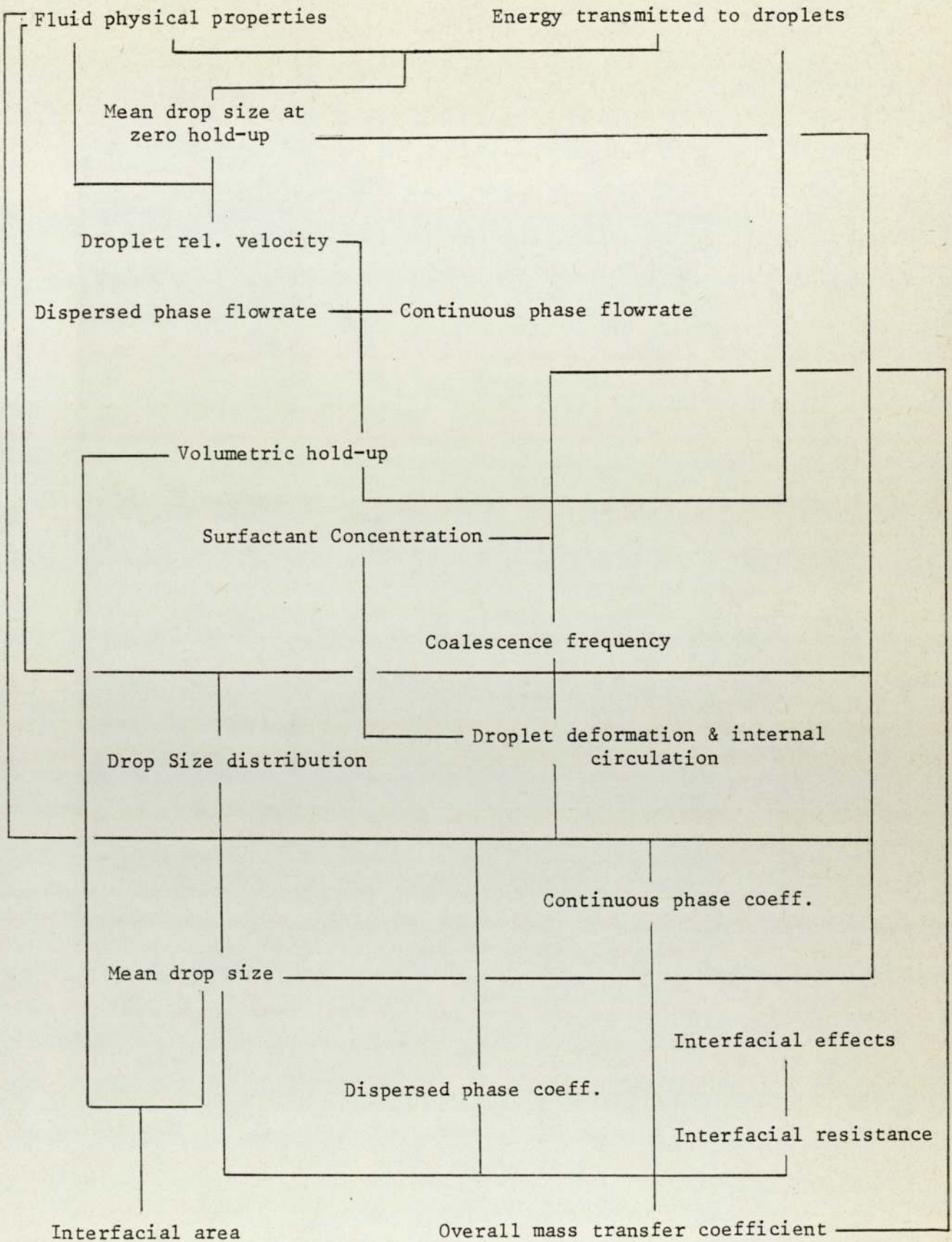


Figure 2.2 IMPELLER CHARACTERISTICS AND POWER (17)



RELATIONSHIPS BETWEEN VARIABLES IN LIQUID EXTRACTION (7)

Figure 2.3

Vermeulen et al, suggests an equation of the form

$$\mu_m = \frac{\mu_c}{(1 - \phi)^{1.5}} \left(1 + \frac{\phi \cdot \mu_d}{\mu_c + \mu_d} \right)^{1.5} \quad 2.9$$

2.4 FLOW PATTERN IN AGITATED VESSELS

Mixing is considered to be a process in which progressively greater uniformity is obtained as a result of various types of fluid motion. Here the fluid mechanics of the processes involved in a vessel, in which fluid motion is induced by impellers to promote mixing, is reviewed.

In turbulent flow there is a resultant direction and magnitude of velocity at each point and a random variation in these values, with time, these movements interchange fluid between different parts of the vessel. This interchange of fluid reduces the difference in properties and leads to uniformity of mixture or emulsion. The relationships between impeller geometry, rotational speed and other variables have been studied in detail for centrifugal pumps (33, 34). These basic principles which relate the head developed, fluid velocities, flow rates, power consumption and equipment geometry are also applicable to rotating impellers in agitated vessels. Figure 2.5 shows the reference point for calculating impeller discharge rates in baffled vessels (35). Table 2.2 provides a comparison of various impellers. In order to estimate the mixing time a knowledge of impeller discharge is of vital importance.

In brief:

- i In addition to rotational speed and impeller diameter, discharge rates of fluids from rotating impellers in vessels are affected by the axial blade width, the number of blades, the curvature or pitch of the blades and the ratio of the impeller to the fluid rotational velocity.

- ii Fluid discharge rates have not been calculated from theoretical relationships, but have been obtained from experimental measurements.

- iii The discharge coefficient $N_Q = Q/ND^3$ is a useful dimensionless group for correlating impeller discharge data.

2.5 MIXING IN AGITATED VESSELS

When two immiscible liquids are agitated in a vessel, the time required to obtain a homogeneous emulsion in the vessel depends on the flow pattern and velocities, which, in turn, depend on the vessel and agitator configuration, the velocity of moving parts, and upon fluid properties. The flow pattern for turbine impellers is shown in Figures 2.4, 2.5.

2.5.1 Batch Mixing

A brief summary of the batch mixing time studies is presented below:

- i. Methods of correlating mixing times have been

TABLE 2.2

Comparison of Discharge Rates of Impellers (17)

Impeller type	No. of blades	D/T	w/D	Z_i/T	Z/T	No. of baffles	D(in.)	Speed r.p.s.	$N_{Re} \times 10^{-5}$	N_Q
Propeller (p ^e)	3						6		1.6	0.40
Propeller (p = 1)	3	0.2-0.6		0.4-0.8	0.7-1.1	3	2-5	5-15	0.4-2	0.61
Propeller	3	0.17-0.6				4	3.6-12.3	2-15		0.42
Propeller (p = 1)	3									0.47
Propeller (p = 1)	3									0.60
Turbine	4	1/6	1/5	0.45	1.33	4	6	5-7	1-1.7	0.59
Turbine	3	1/6	1/5	0.45	1.33	4	6	6-10	1.5-2	0.50
Turbine	4	0.35	1/5	0.35	1.04	4	4	1.7-3.3	0.17-0.34	0.47
Turbine	6	0.53	1/5	0.35	2.8		6			2.9
Turbine	6	0.50	1/5	0.50	1	4			10	1.9
Turbine	8	0.51	1/5	0.50	1	8	11.8	1.45	1.3	1.34
Turbine			1/5							1.25
Turbine	8	0.31	1/3	0.50	1	8	7.1	2.3	0.76	2.9
Turbine			1/5			e				2.3
Pitched blade	8	0.51	0.14	0.50	1	8	11.8		1.3	0.87
Pitched blade			0.14							1
Turbine	8	0.51	1/5	0.50	1	8	11.8		1.3	1.2
Turbine			1/5							1.26

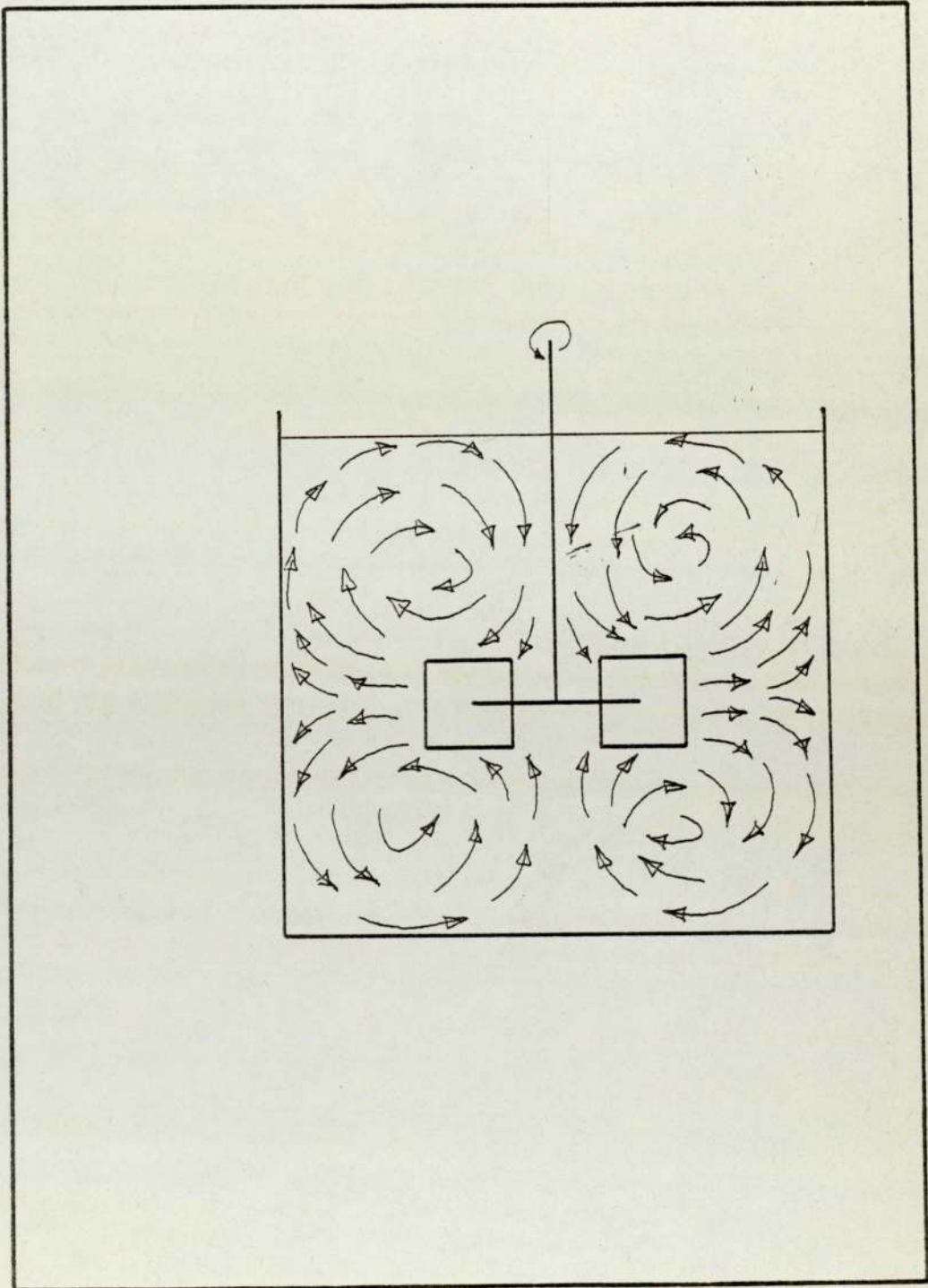


Figure 2.4 FLOW PATTERN FOR A TYPICAL AXIAL FLOW TURBINE
IMPELLER

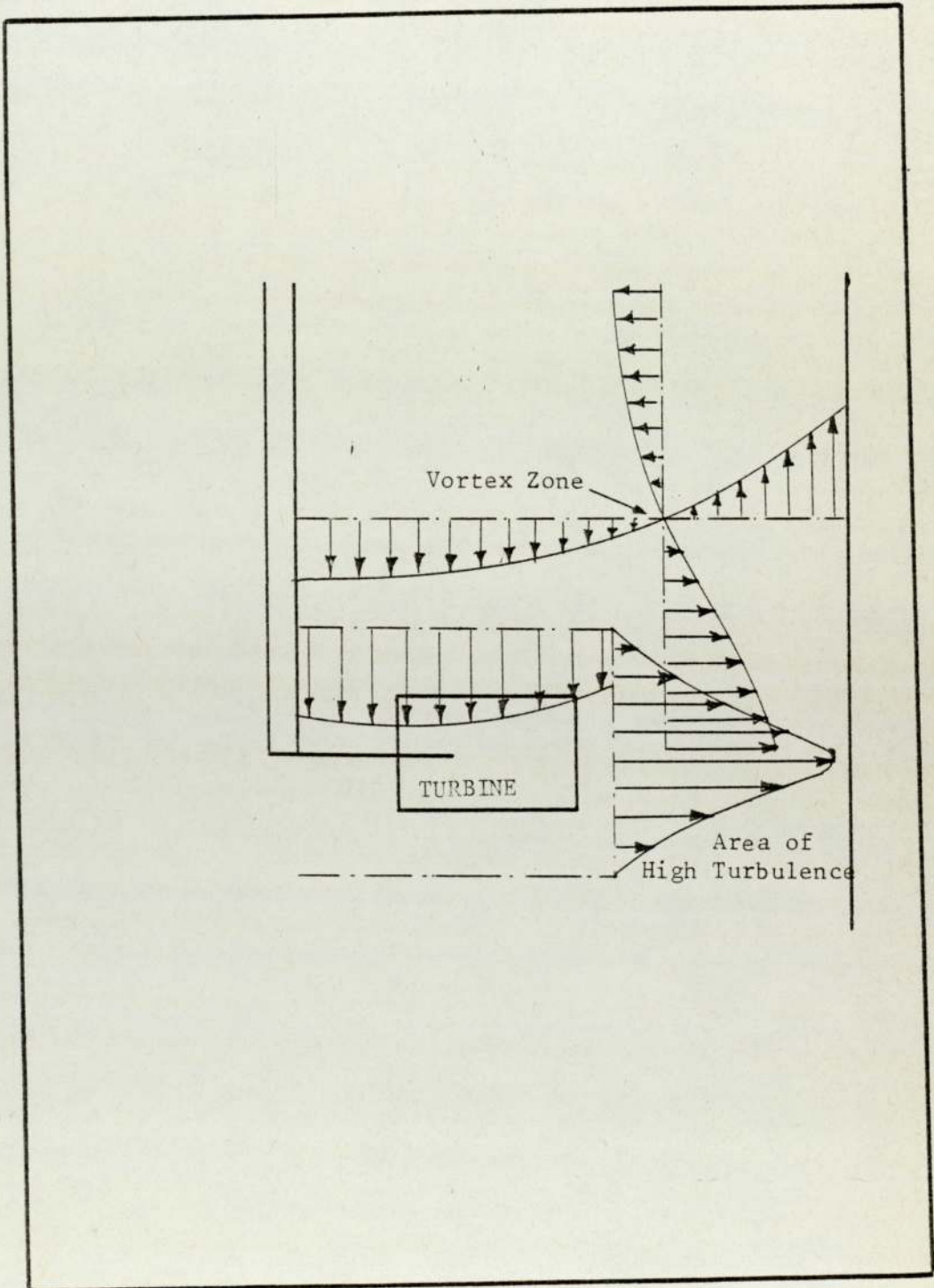


Figure 2.5 REFERENCE POINTS IN BAFFLED VESSEL (17)

developed for Newtonian fluids and the important variables which affect mixing time are:

- a) Equipment configuration, type and proportions.
- b) Equipment size.
- c) Velocity or rotational speed.
- d) Fluid properties.

ii. Significant dimensionless groups used for correlation mixing times are (ΘN) , $(D^2 N \rho / \mu)$, $(\Delta \rho / \rho)$ and $(N^2 D/g)$.

iii. Fluid circulation rate induced by impeller.

2.5.2 Continuous Mixing

Most modern processes tend to favour continuous operations, therefore a logical extension from the knowledge of the batch mixer will be the continuously operated mixer. The basic principles involved are the same as in batch mixing, however, certain considerations must be taken into account with regard to inlet and outlet positions to minimise short circuiting. The other consideration will be the residence time and that depends on a number of factors, the most notable of which will be the fluid properties and the type of process which it is hoped to achieve, as well as the rate of process, flow patterns, type of impeller, etc.

CHAPTER THREE

LIQUID HYDRODYNAMICS

3 LIQUID HYDRODYNAMICS

3 Introduction

When a pair of immiscible liquids is placed in a contactor, one of the two liquids is dispersed in the form of drops in the second phase and mechanical agitation keeps the dispersed phase in suspension. The dispersed phase simultaneously undergoes competing processes, 'breakage and coalescence' whose rates in equilibrium conditions will be both equal and opposite and will depend on the energy transmitted to the dispersed phase, the physical properties of the system and geometrical parameters of the contacting device. The distribution of drop sizes produced in an agitated system represents an equilibrium between competing effects of break-up and coalescence. Coalescence rates are related to inter-droplet distance, i.e. hold-up, but vary with position. However, at the high Reynolds numbers in the case of agitated tanks it has proved to be a satisfactory means of minimising the concentration gradient of the hold-up.

Many models have been developed by different research workers (95,31) to describe drop behaviour. However, it was decided that the model developed by Thornton and Bouyatiotis (47) was the most suitable for agitated vessels and was found to behave satisfactorily for concentrated dispersions. Although of course direct measurement of drop size (47) is the most reliable technique, because of the complexity of the behaviour of the drop against variable factors (e.g. rotor speed, high hold-up,

impurities, etc.).

Study of phase inversion is concerned with the conditions under which a change in rotor speed or hold-up will cause the rate of coalescence to exceed the rate of drop breakage by such a large amount that the dispersed phase will become continuous and vice versa. Therefore, it was decided that an insight into drop size distribution mechanism would be of benefit to this study.

3.1 Drop Formation

The most common use of liquid-liquid contacting devices is to promote large contacting areas for the purpose of heat or mass transfer operations. The area of contact depends largely on the rate of formation of the droplets.

Drop formation occurs when one phase is suddenly exposed to the hydrodynamic pressures of the continuous phase and this is most easily illustrated by drop formation at the nozzles. The stages involved in the production of a drop at a nozzle can be illustrated by figure 3.1. The dispersed phase entering a dispersion in the agitated vessel showed a similar behaviour to that of a drop formed at a nozzle, as shown in figure 3.2.

The recognised stages in drop formation are:

- 1 The volume of the drop as a function of the time of formation.
- 2 The surface area of the drop as a function of the said volume.

Figure 3.3 shows the volume of the drop as a function of the time of formation, it shows that four regions exist. Hayworth and Treyball (51) measured the drop volume produced from a nozzle.

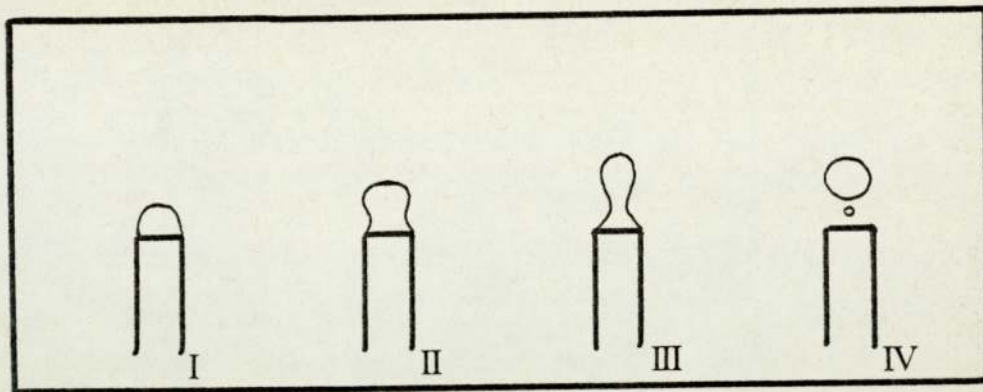


Figure 3.1 DROP FORMATION AT A NOZZLE (IN 4 STAGES)

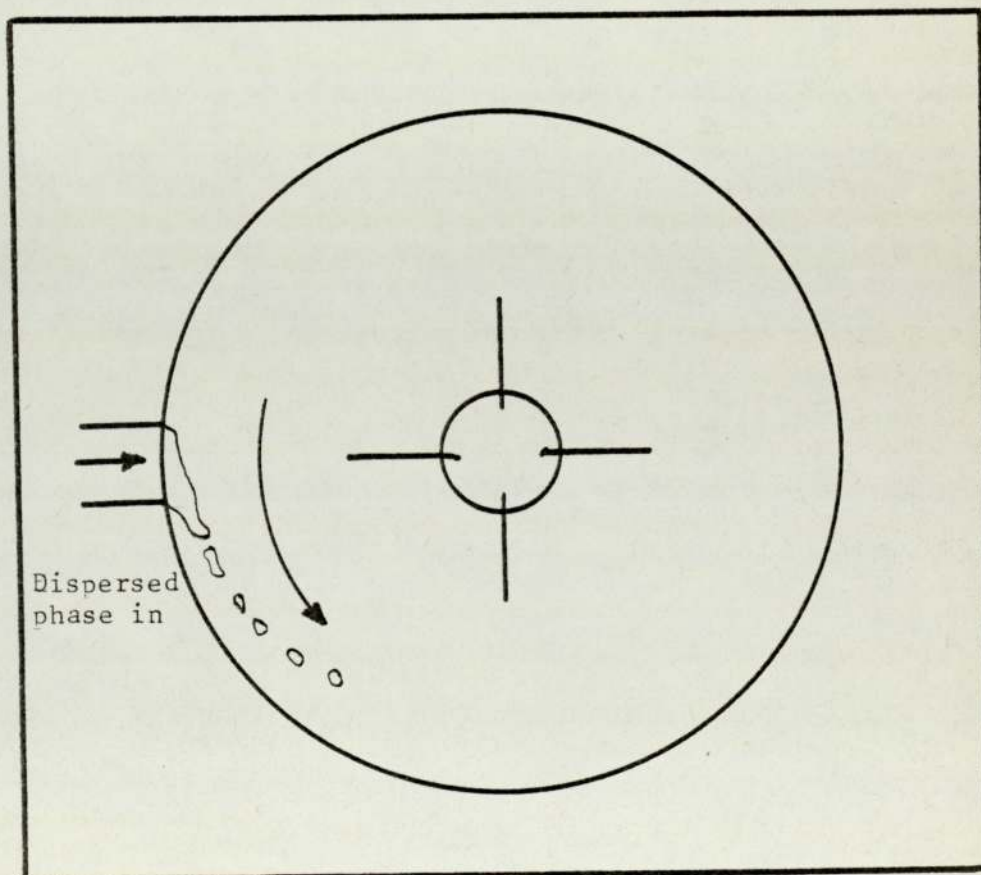


Figure 3.2 DROP FORMATION IN A STIRRED TANK

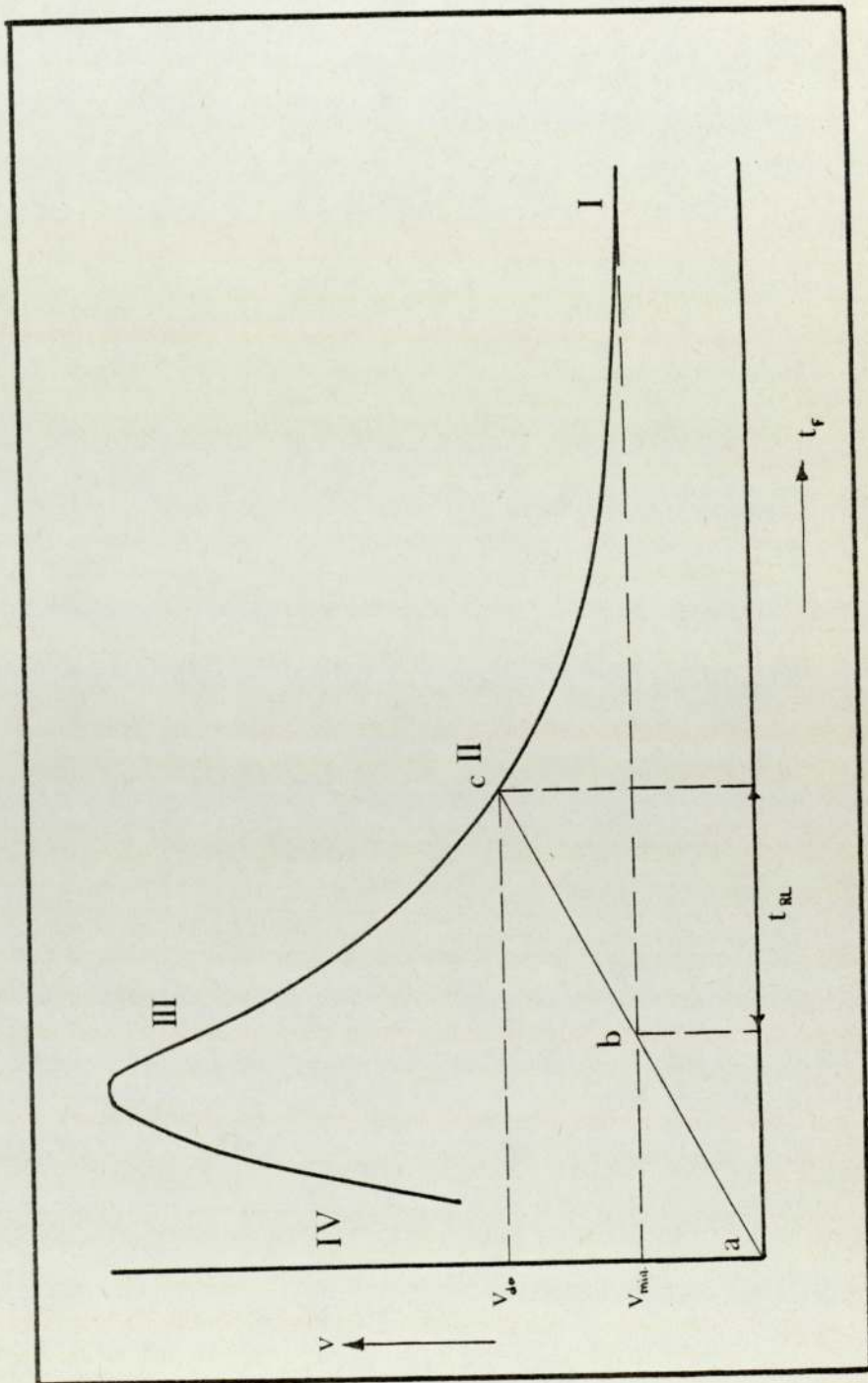


Figure 3.3 DROP VOLUME VS TIME OF FORMATION

TABLE 3.1 Exponents for Single Tanks, $d_{32} \sim N^a D^b$ (7)

<u>Author</u>	<u>a</u>	<u>b</u>
Kolmogorov	-1.2	-2.0
Vermeulen et al	-1.2	-0.8
Rodger et al	-0.7	-0.75
Shinnar	-1.2	-0.8
Shinnar and Church	-1.2	-0.8
Hinze	-1.2	-2.0
Luhning and Sawistowski	-1.2	
Giles et al	-1.2	
Giles et al	-1.0	
Myleck and Resnick	-1.2	-0.8
Taylor	-1.5	-1.0
Brown and Pitt	-1.2	-0.8
Calderbank	-1.1	-0.7
Pebalk and Mishev	-0.912	-1.624
Obukhov	-1.2	-2.0
Rea et al	-1.0	-1.5
Kafarov and Babanov	-1.1	-0.7
Pavlushenke et al	-1.0	-1.65
Yamoguchi et al	-1.5	-2.45

However, an important limitation of their studies was the use of surfactive materials to study the effect of interfacial tension on the drop diameter, since the effect of surfactants cannot be characterised solely by the resultant equilibrium lowering of interfacial tension. Scheele and Meister (50) first pointed out the drawbacks of using such methods for the lowering of interfacial tension. They concluded that the effect cannot be characterised simply by the resultant equilibrium, because for a given surfactant concentration the interfacial tension increases with increasing velocity through the nozzle as a result of the slow diffusion of the surfactant to the interface. This causes a much greater increase in the drop volume with increasing nozzle velocity than is observed for pure liquids.

Null and Johnson (48) presented an empirical correlation based on experimental observation of the drop geometry. Hartius and Brown (49) derived a correlation for the drop volume by equating buoyancy forces acting to detach the drop from the nozzle. Ryan (52) presented a semi-empirical correlation based on a wide range of experiments. Working with unsaturated systems Rao et al (53) and Heertzes and de Nie (54) have proposed a two stage model. Both used a similar approach; if a drop is formed at a constant rate, the drop volume will increase linearly with time from zero volume. The two stages refer to high and low viscosity liquids.

In all recent publications on drop formation, theoretical considerations have been given to the correlations predicting drop volumes, with all the studies distinguishing between the two periods during drop formation. The correlation given by

Null and Johnson (43) was based on experiments with a large number of systems and with the advantage that no surface active agents were used. The work of Rao et al (53) has some limitations since the volume is certainly influenced by the speed of formation. Scheele and Meister (50) used an elaborate application of force balances to predict the drop volume at the nozzle. Like others, they presented an expression fitting their own observations.

The accuracies of the prediction by the various correlations are uncertain. A comparison of the results obtained by Scheele and Meister (50) and Ryan (52) is shown in figure 3.4. The conclusion from the comparison can be that the differences are due to inaccuracies in experimentation or in the physical constants used in the correlation. Scheele and Meister's method of predicting drop volume has certain advantages over the other methods since

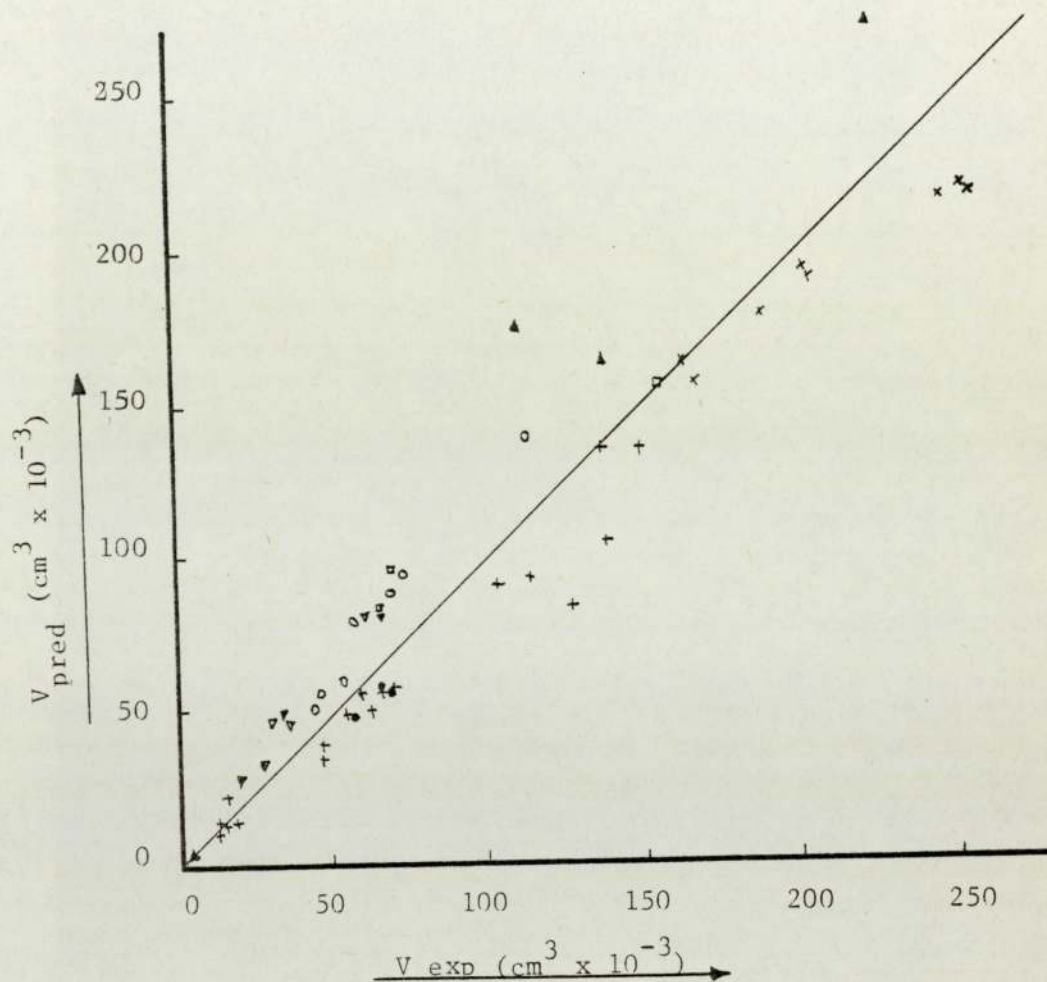
- (i) It is based on a sound momentum balance
- (ii) It covers a wide range of conditions of drop formation
- (iii) Predicted values agree with those determined

experimentally within the accuracy limits shown in figure 3.4.

Table 3.1 summarises the correlations proposed by various workers.

Until recently the drop surface was commonly determined by considering the drop as a perfect sphere. However, many workers have reported this is not the case (58,99), Dixon and Russell (56) proposed a linear relationship between the mean surface area and mean volume during drop formation, Nodberg (55) determined a relationship between the two independent of time. Angels, Lightfoot and Howard (57) measured the change of

Figure 3.4 COMPARISON BETWEEN PREDICTED DROP VOLUME (V_{pred}) AND EXPERIMENTS (V_{exp}) FROM DIFFERENT AUTHORS.



Symbol Used	Author	System No.	Dispersed phase	Reference
X	Meister	10 - 12	Paraffine oil-heptane Different ratios	56 "
●	id	13	Benzene	"
▲	id	7	Butanol	"
+	id	1, 3 - 6	Heptane	"
○	Ryan	-	Cyclohexanol	52 "
△	id	-	Benzene	"
▽	id	-	MIK	"
□	id	-	Hexane	"
▽	id	-	Phenetol	"

Continuous phase is water except for the systems 3 - 6 where a glycerol-water mixture has been used in different ratios.

surface area with time and the change of volume with time for the system isopar-Hx-water. The results point to a linear relationship between surface area and volume.

3.2 Drop Breakage Process

Drop breakage mechanisms have been considered by many investigators in turbulent conditions. Droplet deformation may be caused by a number of interdependent forces. Thus it may be caused by energy transmitted by the impeller, or viscous drag by the continuous phase and interfacial tension of the dispersed phase as well as impact against walls or baffles. Although the effect due to the latter is small when the surface area of the walls and baffles are small in comparison with the dispersion volume, e.g. agitated tanks.

When the extent of deformation exceeds a critical limit owing to the hydrodynamic forces (dependent on the system properties) droplet break-up occurs. Energy transmitted by the impeller causes the agitation of the dispersion and creation of turbulent streams, the drop sufficiently exposed to turbulent eddies will break up under the influence of these eddies.

This phenomenon was first studied experimentally and theoretically by Baranayeu et al (65). The theory of this phenomenon is based on the theory of homogeneous, isotropic turbulence developed by A. N. Kolmogoroff (59). He proposed that the fragmentation phenomenon is related to the fact that the velocity in a turbulent liquid stream varies from one point to another. The velocity of the liquid at the surface of the drop also varies from point to point. Therefore, different dynamic pressures will be exerted at different points on the surface of

the drop. Under certain conditions this will inevitably lead to deformation and break-up of the drop.

Many authors have used the theory of local isotropy to derive expressions for the stable drop size in a turbulent field and supported it with experimental results. Hinze (60) considered the fundamentals of the break-up process and characterised them by two dimensionless groups. A Weber group We and a viscosity group N_{vi} . The analysis covered the mechanism of disintegration and all the constituent stages, from a bulk liquid into globules of fluid and finally the break-up into small size droplets. The forces postulated as a deformation force τ , a surface (σ/d) and a viscous stress $\frac{\mu_d}{d} \left(\frac{\tau}{\rho_d} \right)^{\frac{1}{2}}$. These three forces per unit area control the deformation and break-up of a globule. For one of the dimensionless groups the combination $We = \tau d / \sigma$ is a generalised Weber group. The other dimensionless group selected was $N_{vi} = \frac{\mu_d}{\sqrt{\rho_d \sigma d}}$. The greater the value of We the greater the external force τ compared with the counteracting interfacial tension force σ / d , the greater the deformation. At a critical value $(We)_{crit.}$, break-up occurs.

Hinze extended Kolmogoroff's (59) energy distribution law to predict the size of the maximum stable drop in a turbulent field as:

$$d_{\max} \left(\frac{\rho_c}{\sigma} \right)^{3/5} E^{2/5} = c \quad 3.1$$

where c is a constant. The value of c was calculated as 0.725 from the experimental data of Clay (94). The difference in density between the dispersed and continuous phase was concluded to have an important effect on the way in which the break-up

occurs. Rushton et. al (61) derived the following correlation for a fully baffled vessel.

$$d = \frac{k}{D} \left(\frac{D^3 N^2 \rho_c}{\sigma_i} \right)^{0.36} \left(\frac{D}{T} \right)^k \left(\frac{v_d}{v_c} \right)^{1/5} \left(\frac{t}{t_0} \right)^{1/6} \left(\exp 3.6 \frac{\Delta \rho}{\rho_c} \right) F(s) \quad 3.2$$

Table 3.2 shows the summary of effects predicted by generalised correlation.

Shinnar and Church (62) proposed a similar expression relating the drop size to energy input in a batch system:

$$\frac{E}{\sigma d^2} = 0.26 \quad 3.3$$

where E is the kinetic energy, equal to the difference between the total energy of the parent drop and the energy associated with the two daughter droplets produced by break-up.

The assumption made for the development of their correlation was that a drop with the same viscosity and density as the continuous phase will oscillate with it, and, as such, is only applicable to liquid systems with similar viscosity and density. Levich (63) considered the case of drop fragmentation in a field of homogeneous, isotropic turbulence. The assumption made was that the break-up of a drop is caused by eddies, the scale of which is large compared to the interior scale of turbulence λ_0 . A further assumption was made by considering the density of the continuous phase and dispersed phase to be close. The difference in dynamic pressures exerted on opposite sides of a drop with a diameter of d is

$$\Omega = k \frac{\rho (v_1^2 - v_2^2)}{2} \quad 3.4$$

where v_1 and v_2 are the velocities of the medium at points

TABLE 3.2

Summary of Effects Predicted by Generalised Correlation

$$\text{Relationship: } d = \left(\frac{K}{D}\right) \left(\frac{D^3 N^2 \rho_c}{\sigma_i}\right)^{0.36} \left(\frac{D}{T}\right)^k \left(\frac{v_d}{v_c}\right)^{1/5} \left(\frac{t}{t_0}\right)^{1/6} \exp 3.6 \left(\frac{\Delta \rho}{\rho_c}\right) F(s)$$

INCREASE	RELATIONSHIP	EFFECT ON d
Weber No. a) by increasing N b) by decreasing σ_i c) by increasing D	$d \sim We^{0.36}$	Increases Increases with $N^{0.72}$ Increases with $\sigma_i^{-0.36}$
Kinematic Viscosity Ratio	$d \sim D^k + 0.08$	Increases nearly directly with D and effect is larger with increasing Weber No.
$\Delta \rho / \rho_c$	$d \sim \left(\frac{v_d}{v_c}\right)^{1/5}$ $d \sim \exp \left(3.6 \frac{\Delta \rho}{\rho_c}\right)$	Increases slowly Increases exponentially

...

TABLE 3.2 (Continued)

INCREASE	RELATIONSHIP	EFFECT ON d
Settling Time	$d \sim \left(\frac{t}{t_0}\right)^{1/6}$	Increases slowly
D/T (at constant We)	$d \sim D^k - 1$	Decreases below We = 500
a) by increasing D		Increases above We = 500
b) by decreasing T	$d \sim \frac{\phi}{T^k}$	Effect is small
		Increases

separated from each other by a distance d . From the above correlation it is clear that large-scale eddies compared with the drop diameter do not effect the drop and that deformation and fragmentation are caused by relatively small eddies. The change of eddy velocity over a region of length d can be expressed as

$$v_\lambda = (\varepsilon_0 \lambda)^{1/3} \quad 3.5$$

where $\varepsilon_0 = \frac{\varepsilon}{\rho}$ is the energy dissipation per unit mass and λ is the eddy length, Ω can be expressed as

$$\Omega = \frac{k \rho}{2} \varepsilon_0^{2/3} (d)^{2/3} \quad 3.6$$

Substitution of the value of Ω gives:

$$\frac{k \rho v^2}{\lambda^{8/3}} (d_{cr})^{2/3} \sim \frac{\sigma}{d_{cr}}$$

whence the radius of the formed drop

$$d_{cr} = \left(\frac{\sigma}{k \rho v^2} \right)^{3/5} \lambda^{8/3} \quad 3.7$$

The latter formula was developed by Kolmogoroff (59). This concludes that the radius of drops being formed decreases with an increase in velocity, almost inversely with the velocity, and is also a function of the scale of turbulence.

On examination of the studies of previous workers Levich (63) noted that for a given velocity of the homogenous, isotropic flow, drops formed in it must be of a single size. He concluded that if drops are not in the flow for a sufficiently long period of time an equilibrium with respect to drop size may not have time to be established. In addition, the law of $v \lambda^{1/3}$ gives only an average value for the difference in velocities over a

distance .

Levich suggested that in order for a difference in dynamic pressure exerted on a drop to cause its deformation and fragmentation, the dynamic thrust acting on the drop must be expressed by the quadratic law i.e. the Reynolds number of the liquid flow past the drop must satisfy the condition

$$Re = \frac{v d_{\min}}{\nu} \sim 2a \sim 10$$

Therefore d_{\min} satisfies the condition

$$\frac{a^2 v^2}{d_{\min}^2} \sim \frac{\sigma}{d_{\min}}$$

or

$$d_{\min} \sim \frac{\rho a^2 v^2}{\sigma} \quad 3.8$$

Substituting equation 3.8 into 3.7 and rearranging gives:

$$\lambda_0 > \left(\frac{\rho v^2}{\sigma} \right) a^{5/4} \quad 3.9$$

which limits the value of the inner turbulence scale for which condition $\frac{d}{2} > \lambda_0$ is satisfied.

Misek (102) considered droplet break-up in an R.D.C. and postulated that, as the rate of flow of both liquid phases is negligible compared with the peripheral velocity of agitation, the break-up of drops in an agitated contactor can be considered as identical to the break-up of drops in an agitated tank. It was further argued that there was a similarity between the mixing and break-up processes associated with a turbine mixer and the rotating disc. It was emphasised that theoretical derivations basically deal only with the break-up of a single drop and no attention is given to the correct choice of the mean drop size

for the practical solution involving a large number of drops.

The final correlation presented for the turbulent region, i.e. $Re_{cr} = 5.74 \times 10^4$, with the exponents evaluated experimentally, was:

$$d_{vs} \frac{N^2 D^2 \rho_c}{\exp(0.0887 \Delta D)} = 16.3 \left(\frac{H}{D}\right)^{0.46} \quad 3.10$$

On diminishing the mixing intensity below a critical value of Reynolds number $(Re)_{crit} = 5.74 \times 10^4$ the splitting of drops occurs in a transitive region in which viscous shear forces have some effect. The expression then valid is

$$d_{vs} = \frac{N^2 D^2 \rho_c}{\exp(0.0887 \Delta \rho)} = 1.345 \times 10^{-6} \times \left(\frac{D^2 N^2 \rho_c}{\mu_c}\right)^{1.42} \quad 3.11$$

A further decrease in the mixing intensity into the laminar region results in other forces becoming significant.

Endoh and Oyama (64) elaborated the theory of the break-up of a drop entrained in a turbulent stream and verified it experimentally. The resultant relation depends on the energy dissipated by the agitator and according to their work, drop sizes can be estimated from the following relations:

$$\frac{d_{10}}{D} \sim We^{1/3} Re^{-1/3} \gg d \quad 3.12$$

$$\frac{d_{10}}{D} \sim We^{-3/5} \gg d \quad 3.13$$

where $We = D^3 N^2 \rho_c / \sigma$; $Re = \frac{D^2 N}{V_c}$. Transition between the

regimes is gradual. Vermeulen et al (31) arrived at similar results from their experimental work. This can be taken as confirmation of the correlations obtained by Endoh and Oyama.

In their investigations the sizes of the drops were measured in a system agitated by a six-bladed turbine. By means of light diffraction the Sauter mean diameter was correlated by the relation,

$$\frac{d_{vs}}{D} \sim F_1(x) We^{-0.6} \quad 3.14$$

$F_1(x)$ denotes the empirically determined function of the hold-up of the dispersed phase, which corrects the results for the effect of the coalescence of the drops. Similar results were reported by Kafanov and Babanov (73), who determined the mean diameter of drops by means of sedimentation analysis. They assumed that the drop size is related to the physical state of the system and correlated their results on the basis of dimensional analysis by the relation,

$$\frac{d_{vs}}{D} \sim F_2(x) We^{-0.5} Re^{-0.1} \quad 3.15$$

where $F_2(x)$ is a system constant.

Stephenson (97) studied the effect of agitation on drop-size. Using high-speed cine film photographs he concluded that the drop break-up mechanism is a random process and is confined to the high shear region of the stirrer. The body forces that act on a dispersed phase in the vortices influence the mechanism of break-up.

In matching refractive studies carried out in this work it was observed that drop elongation occurred in vortices and depending on the hydrodynamic conditions resulted in coalescence or breakage. It was further noticed that as the concentration of the dispersed phase changed the flow pattern also changed.

3.3 Drop Size Distribution

A drop size distribution is created in any mechanically agitated liquid-liquid mixing device as a result of competing drop breakage and coalescence processes. For the purpose of the calculation of the transfer area in such a medium it is necessary to compute an average drop size.

Olney (75) studied the variation of drop size distribution with rotor speed, dispersed phase hold-up and system properties. It was found that rotor speed had a marked effect on the average drop size but very little effect on the size distribution. Vermeulen (31) studied the effect of volume fraction on the mean diameter in a stirred tank.

$$\frac{d}{D\phi} = G We^{-0.6} \quad 3.16$$

Calderbank (74) proposed a similar correlation:

$$\frac{d}{D} = (1 + \phi) We^{-0.6} \quad 3.17$$

Shinnar and Church (62) confirmed the above findings and proposed the following correlation for acollusive conditions:

$$\frac{d}{D} = C_3 We^{-0.6} \quad 3.18$$

They further added an extra term, the energy of adhesion between two drops, for high hold-ups and gave the following expression,

$$\frac{d}{D} = C_4 We^{0.375} \left(\frac{A(h)}{YL} \right)^{0.375} \quad 3.19$$

They also showed that for very small drops, where the drop diameter was small compared with the Kolmogoroff length ψ which is given by

$$\psi = \left(\frac{v_c^3}{\epsilon} \right)^{1/3} \quad 3.20$$

The drop break-up will be a function of kinematic viscosity and the energy dissipated per unit mass.

Sprow (76) developed a correlation for the maximum drop size existing in an emulsion. Bouyatiotis and Thornton (47) found that for batch and continuous operations in an agitated tank the measured distribution approximates a normal one, which was also confirmed in this work, figure 3.5. Similar results for different systems have been reported by various workers (66,67). However, Pebalk and Misher (68) and Giles et al (69) reported a log-normal distribution, in the case of the former the same systems as (47,66,67) were used, this suggests that the equipment type can influence the drop size distribution. Whether the drop size distribution is normal or log-normal is of significant importance in estimating the average drop size and transfer area in the design of a liquid contactor. For a mixed volumetric throughput, a comparison of the two types of dispersion is given in table 3.3. For the prediction of hydrodynamic and mass transfer performance the ideal distribution would be a mono dispersion with a consequent standard deviation of zero. This is impracticable but a distribution where the mode is equal to the mean results in more drops being nearer the mean size than with a log-normal distribution.

3.4 Drop - Drop Coalescence

Coalescence processes are of importance in agitated contacting devices, since interdroplet coalescence, or coagulation, is an important factor determining the equilibrium drop size generated.

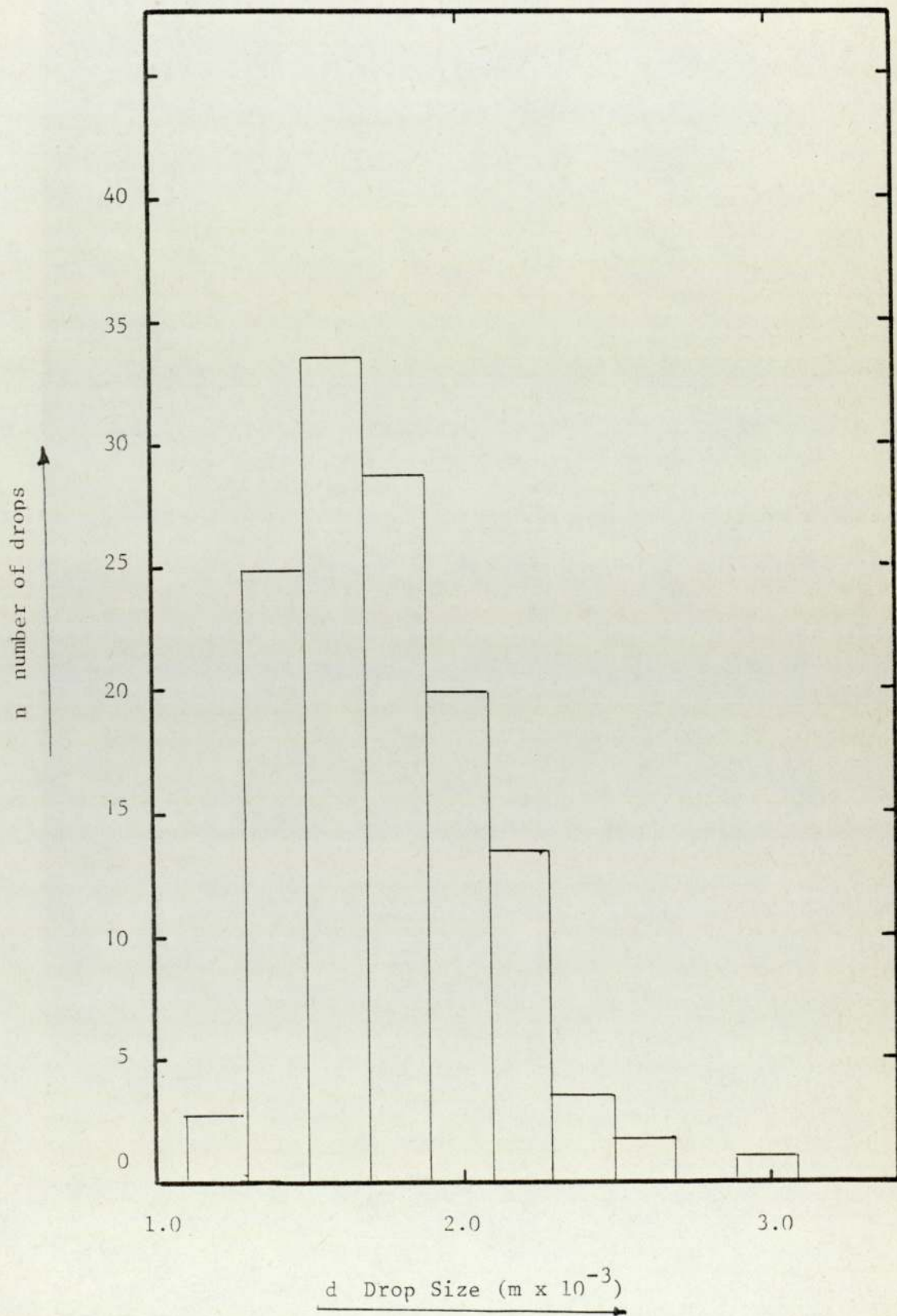
Figure 3.5 A TYPICAL DROP SIZE DISTRIBUTION

TABLE 3.3

PROPORTION OF DISPERSION	NORMAL	LOG-NORMAL
Proportion of smaller droplets	Lower	Higher
Mean mass transfer coefficients	Higher because more drops are circulating	Lower - more stagnant drops
Interfacial area	Lower	Higher
Settling rate	Higher	Lower

Effect of Drop Size Distribution on Dispersion Property

In the agitated zone the drop size is determined by the balance between the break-up and coalescence. This size determines the interfacial area and hence the rate of the transfer operation promoted by the transfer area. Furthermore, study of phase inversion necessitates the understanding of the factors involved in coalescence. There are two types of coalescence:

- 1 Drop - Interface Coalescence
- 2 Drop - Drop Coalescence

Both types will be reviewed here although drop-interface will be very briefly covered, it is considered here that the drop-globule coalescence is similar in behaviour to drop-interface. Drop-drop coalescence will be more thoroughly investigated as this type of coalescence usually occurs in flow conditions in a dispersion. In order to complete this subject the effect of mass transfer will also be reviewed.

3.4.1 Drop - Interface Coalescence

It is generally agreed that the coalescence processes take place in five consecutive stages, as follows:

- (i) The approach of the drop to the interface resulting in deformation of both the drop and the interface.
- (ii) The damped oscillation of the drop at the interface.
- (iii) The formation of a film of the continuous phase between the drop and its bulk phase.
- (iv) The drainage of the film, its rupture and removal with the initiation of the coalescence process proper.
- (v) The transference of the contents of the drop (partially or wholly) into its bulk phase.

Most research workers have come to the conclusion that stages (i) and (ii) occur immeasurably fast, and that the time taken for stages (iii), (iv) and (v) is about 0.06 to 0.08 of a second, with most of the time taken up by drainage. A survey of the work in this field is beyond the scope of this work, a summary of the findings in this type of coalescence is shown in table 3.4.

3.4.2 Drop - Drop Coalescence

Drop-drop coalescence has not been extensively studied in agitated liquid-liquid contacting systems. The study of drop-drop coalescence is the study of a dynamic situation, liquid-liquid dispersions are usually thermodynamically unstable systems. Since the free energy associated with the large interfacial area between the phases can decrease by aggregation or coalescence of the dispersed phase, from energy balance considerations coalescence of a liquid dispersion would be expected, until ultimately two liquid layers are formed.

Drop-drop coalescence occurs in two stages.

- (a) The drainage of the continuous phase from between drops until a critical film thickness is achieved.
- (b) The rupture of the critical film.

Therefore, the rate of coalescence is dependent on the forces impelling the droplets towards each other, the resistance to liquid film drainage and the thickness and ultimate strength of the critical film. This is dependent on the physical properties of both phases, however the presence of a third component can drastically change the expected behaviour of an interdroplet coalescence. These effects are similar to those

Effect of System Property on Coalescence Time

TABLE 3.4

VARIABLE (INCREASE)	EFFECT ON COALESCENCE TIME	EXPLANATION IN TERMS OF EFFECT ON PHASE 2 FILM DRAINAGE RATE
Drop size	Longer	More phase 2 in film
Length of fall	Longer	Drop 'bounces' and film is replaced
Curvature of interface towards drop (a) concave	Longer	More phase 2 in film
(b) convex	Shorter	Less phase 2 in film
Interfacial tension	Shorter	Less phase 2 in film (more rigid drop)
Phase ratio $\frac{\mu_d}{\mu_c}$	Shorter	Either less phase 2 film or increase in drainage rate
Phase $\Delta \rho$	Longer	More deformation of drop more phase 2 film
Temperature	Shorter	Increases phase ratio

.../

TABLE 3.4 (continued)

VARIABLE (INCREASE)	EFFECT ON COALESCENCE TIME	EXPLANATION IN TERMS OF EFFECT ON PHASE 2 FILM DRAINAGE RATE
Temperature gradients	Shorter	Thermal gradients 'weaken' film
Vibrational effects	Shorter	Assist drainage rupture
Electrostatic effects	Shorter	Increase effective gravitational force
Applied electric field	Shorter	Increase effective gravitational force
Presence of a third component (a) stabiliser	Longer	(a) form 'skin' around drop
(b) mass transfer into drop	Longer	(b) sets up interfacial tension gradients which oppose flow of film
(c) mass transfer out of drop	Shorter	(c) sets up interfacial tension gradients which assist flow of film

of drop-interface coalescence. In systems in which mass transfer is taking place, coalescence is favoured when the direction of the transfer is from the dispersed to continuous phase and hindered when it is in the opposite direction (10, 100, 101).

Work in this area has been relatively little, this is because the analysis of drop-drop coalescence, which represents a dynamic situation in agitated systems is rather difficult as,

- (a) It is difficult to reproduce a controlled collision between two drops which have not been restrained in some way.
- (b) There is an inherent randomness in the manner in which the drops rebond or coalesce.
- (c) In this work it was noticed (by means of matching refractive indexes) that, due to bulk flow the average properties of the system vary, this is most noticeable in low agitation intensity.

From the first two considerations and using a purely theoretical approach, Howarth (70) developed an equation to relate the frequency of coalescence with hold-up in a homogeneous isotropic turbulent flow,

$$N_c = k_z \frac{\phi \left(\frac{d \cdot d}{d \cdot t} \right)}{d^4} \quad 3.21$$

This is based on a simplified model of coalescence in a mono dispersion of drops smaller than the characteristic length of the turbulent field and in which most of the collisions result in cohesion or immediate coalescence. Madden and Damerell (71) studied water drops in toluene using a

tracer and reported the rate of coalescence frequency to be increasing as $N^{2.4}$, and increasing as $\phi^{0.5}$.

Davies (96) reported the coalescence frequency to be dependent on the tracer impurity, the coalescence rate of commercial toluene was only 65% of that of refined toluene. In another work Miller (90) studied the effect of third phase concentration and concentrated dispersed solution, table 3.4 shows the variation of power of N with increasing ϕ . Misek (72) characterised the dispersion by a hydraulic mean drop diameter and assumed that these drops exactly followed the turbulent fluctuations in the continuous phase. He developed the collision theory by Levich (63) suggesting that coalescence will result from each collision. Misek proposed two correlations one for the bulk of the liquid and one at the wall,

$$W_t = z_1 n^3 d^3 \psi^{\frac{1}{2}} \sqrt{vD_k} \quad 3.22$$

For drop coalescence at the wall:

$$W_t = z_2 n^2 d^3 \psi / v \quad 3.23$$

Coefficients z_1 and z_2 were determined indirectly based on phase flowrate measurement using equation

$$\psi = k_4 \sqrt{\sigma/d\rho} \quad 3.24$$

Drop size d was calculated from the terminal falling velocities of solid spheres, k_4 is a universal constant.

Nakada and Tanaka (98) evaluated coalescence frequency rates and their findings imply that coalescence frequency between smaller drops is greater than that between larger drops. The results obtained by them compared well with the results of Howarth. They confirmed the dependence of coalescence

frequency on the power of the impeller. For their dispersion they found it to be proportional to the 2.5 power of the impeller and 0.8 power of the hold-up.

CHAPTER FOUR

PHASE INVERSION

4 PHASE INVERSION

When two immiscible or partially miscible liquids are agitated together a dispersion is formed in which one of the liquids is distributed in the form of droplets in the other liquid. The liquid distributed is called the dispersed phase and the other the continuous phase. In batch systems it has been observed that the addition of the dispersed phase will lead to certain hydrodynamic conditions under which the dispersed phase becomes continuous and vice versa, this phenomena is called phase inversion.

Phase inversion was first reported by Oswaldt (79), he reported that dispersions containing more than 75% of the dispersed phase will undergo phase inversion, this value is generally termed as "Oswaldt ratio" and is based on the assumptions that drops are spherical and therefore this will be the maximum packing value. This, however, has been proved to be not the case, many workers have reported higher values of inversion hold-ups, Al-Hemiri (8) reported inversion hold-ups up to 94%.

4.1 Ambivalent Range

When agitation initiates in a liquid-liquid system, the factors effecting which phase will be dispersed in an agitated tank are phase ratio and impeller location. At certain phase ratios depending on the start-up either phase can become dispersed. The said phase ratio is in the ambivalent region, in other words ambivalent range is an area in which either phase can be dispersed, phase inversion occurs when the limits of ambivalence are reached.

by the following correlation:

$$\frac{V_c}{V_d} = 1 - 3/2 \left(\frac{1}{X} \right) + \frac{1}{2} \left(\frac{1}{X^2} \right) \quad 4.1$$

by rearranging the above correlation he found that where X is the inversion concentration and V_c is the characteristic continuous phase velocity and V_d is the characteristic dispersed phase velocity.

Recently Sarkar (10) using the system butyl acetate-water and toluene-water found, contrary to Al-Hemiri's (8) findings, the phase inversion to be cyclical in RDC. Reinversion occurred in each compartment after a finite time, the whole process being repeated indefinitely. A model for predicting hold-up was proposed:

$$\frac{V_c}{V_d} = 1 - \frac{a}{X_i} + \sum_{k=2}^{k=s} b^k / X_i \quad 4.2$$

where X_i = hold-up at inversion, $a = 1.5$, $b = 0.5$. The model was tested for $\frac{V_c}{V_d} = 1.0$ and was found to be in good agreement with

the experimental results. The time for re-appearance of the inversion slug in a compartment was correlated by:

$$t = 0.048 (Z)^{0.66} (X)^{0.33} (D)^{-1.0} \quad 4.3$$

where Z is the volume of the compartment, X is the dispersed phase hold-up and D is the drop diffusion coefficient. Khandelwel (9) reported, phase inversion is assisted using dispersed phase wetted rotors, the studies were carried out in a 30.48×10^{-2} m diameter RDC column. The wall effects due to the large diameter were minimal.

The latitude of this region depends on the physical properties of the liquid-liquid system and in particular the viscosity and interfacial tension of the system. Ambivalent phase inversion was first reported by Selker and Sleicher (83).

4.2 Phase Inversion in Agitated Columns

Phase inversion studies in agitated columns can be divided into two groups:

- 1 RDC columns
- 2 Oldshue-Rushton columns

Phase inversion studies have been very limited and most of the studies have only been a secondary study in this field, to date no quantitative study has been carried out to quantify the factors leading to phase inversion. In this section a summary of works done on phase inversion in agitated columns will be reported.

4.2.1 Phase Inversion in RDC Columns

The data reported on phase inversion in a RDC column is very limited. Al-Hemiri (8) reported phase inversion in a RDC column, he stated that the onset of phase inversion occurred in the bottom compartment giving rise to a very large 'slug', possessing a high terminal velocity, which travelled up the column and eventually dispersed in higher compartments. With further increase in dispersed phase flow the same effect was repeated at an increased frequency until other compartments reached their phase inversion hold-ups. At this stage the column still operated countercurrently. A further increase in the flow rate of either phase, or the agitator speed, caused a proportion of the phase to flow in the reverse direction, i.e. "flooding proper". Al-Hemiri attempted to characterise phase inversion phenomena

Studies carried out by these workers in phase inversion have been of a secondary nature. Both models proposed rely only on the geometrical considerations and can only be applied to a particular column design and very narrow range of chemical systems.

4.2.2 Phase Inversion in Oldshue-Rushton Column

Arnold (7) was the first to report the phenomena of cyclic phase inversion in an Oldshue-Rushton Column, one particular compartment became inverted, the inversion passed to the next compartment after a certain time and proceeded up the column, ultimately coalescing with the bulk interface. After the 'slug' of inverted phases had left that compartment, normal operating conditions continued. Subsequently the hold-up built up to a value sufficient to give inversion, and the process was repeated. The rate of advance of the cyclic inversion was found to be inversely proportional to the rotor speed. It was found that the phase inversion always occurred in one particular compartment or group of compartments for any specific set of operating conditions. Arnold (7) found that the volumetric hold-up of the dispersed phase reached a steady state value in each compartment for certain operating conditions, hence the start of inversion in a particular compartment can be explained in these terms. Sarkar (10) using a 10.16×10^{-2} m diameter Oldshue-Rushton column used the same correlation developed for the RDC column, suggesting the same processes exist in the columns.

4.3 Phase Inversion in Agitated Vessels

Phase inversion studies in agitated tanks can be divided into two parts:

1 Batch Mixing Tank

2 Continuous Mixer-Settler

Published data in this field is very limited, to date no attempt has been made to characterise phase inversion in Agitated Vessels.

4.3.1 Phase Inversion in Batch Mixing Tanks

Oswaltdt (79) was the first to report phase inversion in an agitated tank, he observed that it is difficult to produce a dispersion containing more than 75% by volume of the dispersed phase, this ratio is generally known as 'Oswaltdt ratio'. Quinn and Sigloh (84) found that for a fixed impeller speed the inversion concentration ϕ_i expressed as a volume fraction in the organic phase was given by:

$$\phi_i = \phi_o + a/P \quad 4.4$$

where ϕ_o is the constant asymptotic inversion concentration a is a system constant and, P the power input given by:

$$P = k \rho N^3 \quad 4.5$$

where k is a constant, they concluded that a large number of variables affect the phase continuity in concentrated dispersion. Moreover, for some dispersions both phases are subdivided throughout the tank and there is no continuous phase. Ahmad (66) studied phase inversion at high rotor speeds and found, after phase inversion, secondary droplets of the continuous phase in the primary drops. Selker and Sleicher (83) were first to report the existance of the ambivalence range. They found that within this range the phase that becomes continuous is prescribed by the manner of initiating the dispersion. The ambivalence range was reported to be principally of the viscosity ratio.

Selker and Sleicher found that vessel geometry does not have a primary effect on the width of the ambivalence range. Ali (87) confirmed the position of the impeller as the determinant of the nature of the dispersed phase, if the impeller is placed in the organic phase, the aqueous phase will become dispersed and vice versa, if the impeller is placed at the interface, either phase can be dispersed. Rodger et al (103) reported that one phase is dispersed at low impeller speeds and the other at high impeller speeds when the impeller is positioned at interface. This phenomena was observed in this work too, but with the difference that high rotor speeds did not yield the same dispersion, although statistically one phase was becoming dispersed for a particular speed. It was further observed that water was more difficult to disperse than the organic solvent. Yeh et al (85) studied the effects of temperature, interfacial tension and density and concluded that there was no general correlation applicable to the systems studied. They further proposed a correlation based on statistical forces, namely surface tension, density, geometry, etc., and dynamic forces, namely flow pattern and velocity distribution, the following correlation was proposed:

$$\frac{a}{b} = \sqrt{\frac{\mu_1}{\mu_2}} \quad 4.6$$

where a is the thickness of phase 1 and b is the thickness of phase 2 and μ_1 is the interfacial viscosity of phase 1 and μ_2 is the interfacial viscosity at the interface.

The above correlation is very difficult to evaluate since it is essential to calculate the interfacial viscosities

of both phases. Further, the experimental and calculated values show that other factors must be included in the above correlation. Its application is further complicated when a large density difference exists and interfacial forces rather than viscous forces are dominant. Another limitation of this correlation is that it does not take into account the effects of varying energy input.

Luhning and Sawistowski (81) studied phase inversion in stirred tanks and showed graphically that phase inversion was characterised by a metastable or ambivalence region, it was found to be strongly dependent upon the viscosity ratio of the phases and the interfacial tension and to a lesser extent on the stirrer speed. The presence of a solute under conditions of phase equilibrium increased the range of ambivalence, while mass transfer (dispersed \rightarrow continuous) considerably narrowed it. The propionic acid was the solute used in the above investigation and the binary systems studied were benzene-water and p-xylene-water.

4.3.2 Phase Inversion in Mixer-Settlers

Published reports are very limited in this area. McClarey and Mansoori confirmed the factors effecting phase inversion in their studies. However, no attempt was made to quantify their findings. Hussein (/12) was the first to report this phenomena in the cascade of mixer-settler units. The following correlation was proposed:

$$\frac{V_c}{V_d} = 1 - \left(\frac{4}{3X} \right) + \left(\frac{1}{9X^2} \right) + \left(\frac{2}{27X^3} \right) + \left(\frac{4}{81X^4} \right) \quad 4.7$$

where V_c is the characteristic velocity of the continuous phase, V_d is the characteristic velocity of the dispersed phase, X is

the inversion hold-up. The above model is restricted to a very limited range of physical properties and a particular mixer-settler unit.

4.4 The Effect of Mass Transfer on Phase Inversion

Clarke and Sawistowski (86) investigated the behaviour of phase inversion under mass transfer conditions in a stirred tank. They found that sudden injection of the solute into the dispersion had primarily two effects. Firstly, it lowers the interfacial tension and thereby shifts the position of dynamic equilibrium between the drop break-up and coalescence towards smaller drop sizes and, secondly, the mass transfer results in the appearance of the Marangoni effect. It was further reported that there is a time lag between the attainment of a new value of interfacial tension and the corresponding drop size distribution, this is to be expected as is the case when rotor speed change requires a time lag to establish new equilibrium levels. This disturbance in energy distribution under certain conditions may lead to permanent inversion. Clarke and Sawistowski showed that the combination of lowering interfacial tension and the appearance of the Marangoni effect resulted in a narrowing of the hysteresis gap. Study of coalescence of two drops shows that for mass transfer out of the drop, coalescence is practically instantaneous. Hence, once the system inverts, the Marangoni effect results in a rapid decrease in the interfacial area. Subsequently, the Marangoni effect decays with time as the system approaches equilibrium and a new equilibrium drop size distribution is attained (86). The Marangoni effect is therefore only present when there is mass transfer. This effect necessitates the use of

mutually saturated phases for reproducible results.

Sarkar (10) found that mass transfer hinders or promotes inversion depending on its direction. When the direction of transfer is from continuous to dispersed phase the resistance of the dispersed phase to inversion is increased and when the situation is reversed the resistance is lowered. This, however, is a simple view of the problem, other aspects such as the lowering of interfacial tension and viscosity in particular can change the direction and shift the phase inversion boundary. Other factors such as chemical reaction and order of reaction can also be influential.

4.5 Further Observation on Phase Inversion in a Mixer-Settler Unit

The survey shows that knowledge in the area of phase inversion is very limited, in both columns and stirred tanks. This work has attempted to characterise phase inversion in stirred tanks. A number of systems were studied to examine the model proposed in Chapter 5. The agreement was excellent and furthermore it confirmed results of other workers. Figures 4.1 and 4.2 show some of the results (16).

Within the range of flowrates studied i.e. $6 \times 10^{-5} \text{ m}^3/\text{s}$ to $12 \times 10^{-5} \text{ m}^3/\text{s}$ there was no noticeable difference in phase inversion values obtained from similar rotor speeds and temperature in continuous and batch modes of operation. This was thought to be due to the low dynamic pressure of the flow systems relative to that of the dynamic pressure of the agitation flow in the vessel, although it can be expected that high input flowrates can cause shortcircuiting and, hence, effect the inversion phenomena.

It was noticed that as the concentration of the dispersed

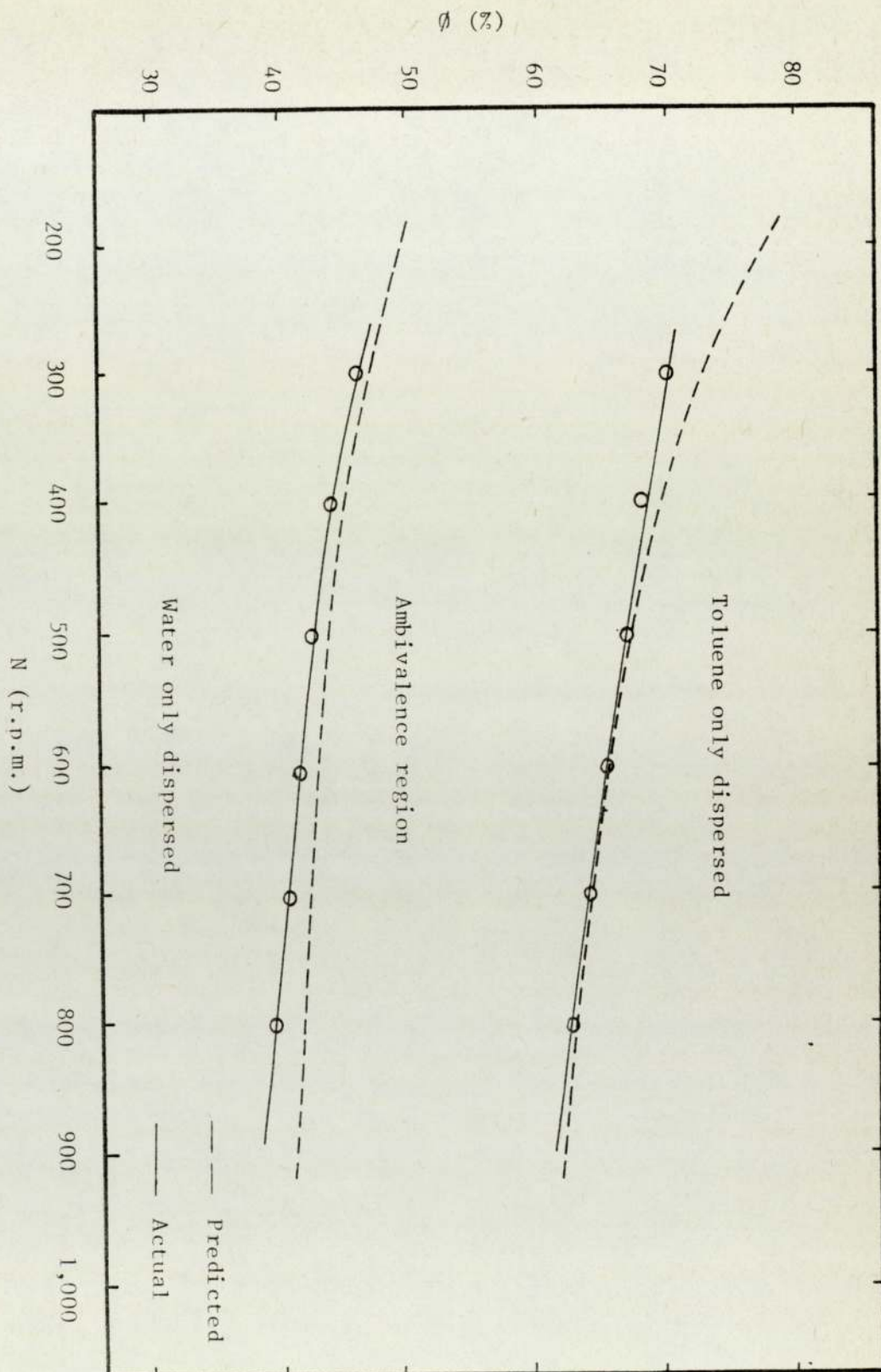


Figure 4.1 AMBIVALENT PHASE INVERSION HYSTERESIS
PREDICTED VS ACTUAL (TOLUENE-WATER)

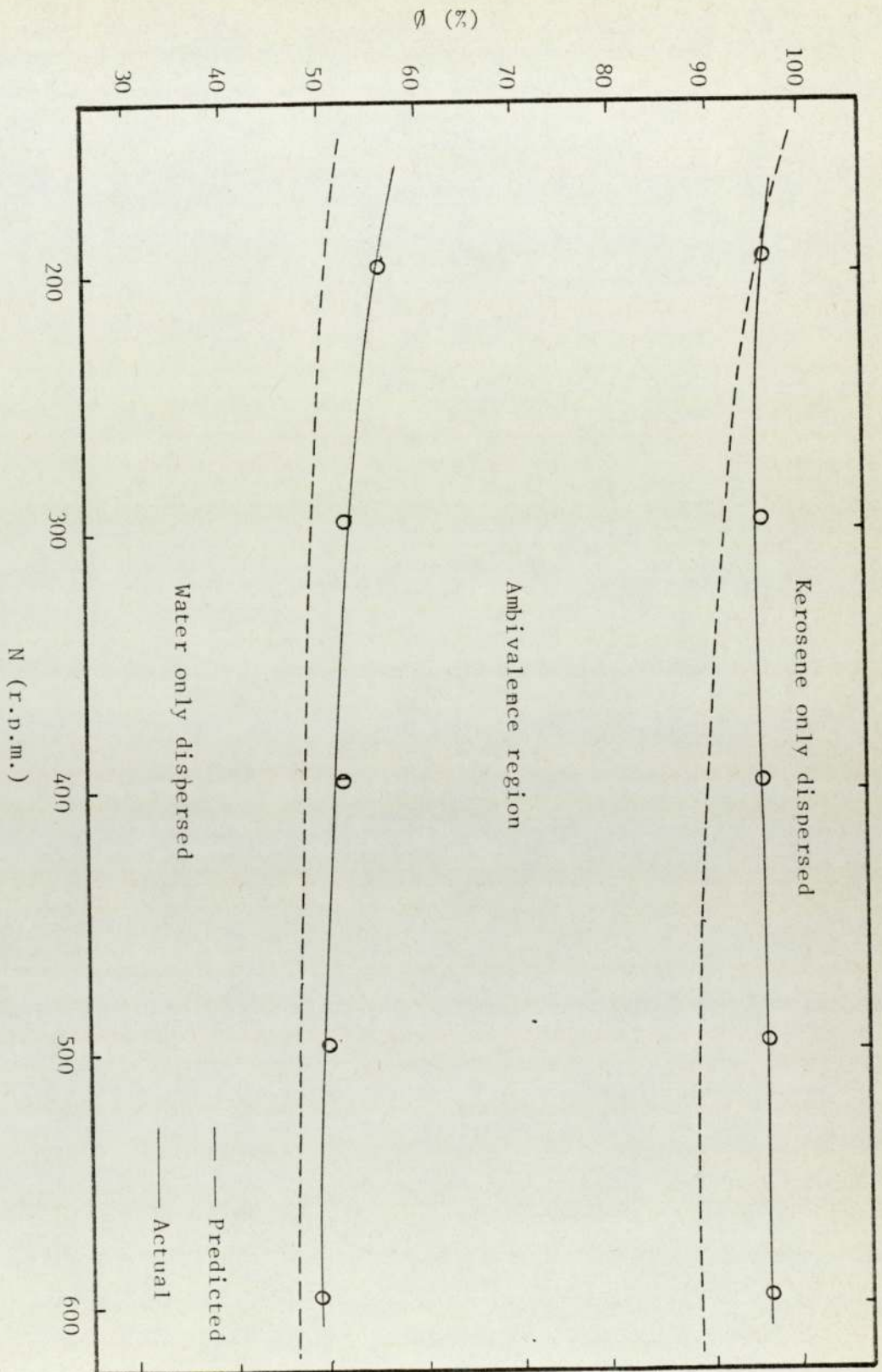


Figure 4.2 AMBIVALENT PHASE INVERSION HYSTERESIS
PREDICTED VS ACTUAL (KEROSENE/WATER)

phase increased the flow pattern changed and the system tended to become less isotropic. Matching refractive index studies proved this and showed that the largest drops were not formed away from the impeller but in the regions close to discharge, where the dispersion leaves the vortexes formed by the impeller, as shown in figure 4.3. This phenomenon only occurs when the dispersed phase concentration passes a critical value where the resistance to isotropic condition prevails, this hold-up is directly proportional to the rotor speed. The best indication of this phenomena is the appearance of the globules of the dispersed phase from the impeller region. Phase inversion follows as the frequency of the appearance of these globules increases. A video and a cine film of this phenomenon is recorded in the departmental film library, which clearly shows the source of the appearance of these globules. It was observed that phase inversion is initiated from the discharge regions of the impeller, figure 4.4 shows the phase inversion region. Phase inversion characteristics appear to be dependent on the physical properties of the dispersed phase. The globules of the organic phase were bigger for the same rotor speed than those of the aqueous phase. The latter's resistance to dispersion was greater than that of the organic phase, the inversion time also seemed to be much shorter than that of the organic phase. These could be explained in terms of the viscosity and surface tension and of the angle of contact of the phases. The film of the organic phase has a much lower critical thickness than that of the aqueous phase, which explains the smaller globules, as well as the fact that organic drops are also larger. The higher surface



Figure 4.3 FLOW PATTERN NEAR A TURBINE IMPELLER

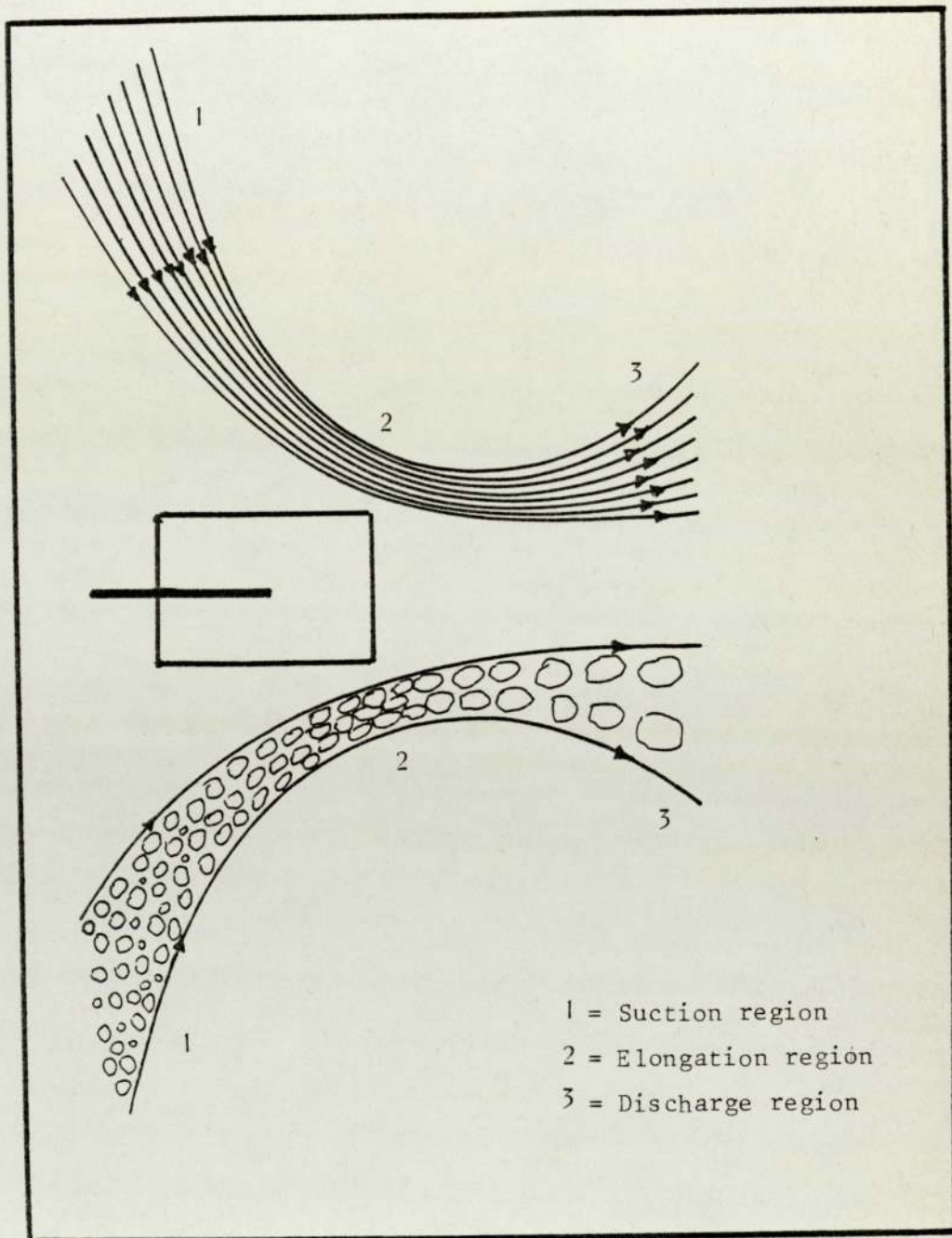


Figure 4.4 REGIONS OF SUCTION AND DISCHARGE NEAR AN
IMPELLER

tension of the aqueous phase facilitates its coalescence in the lower turbulence regions, therefore explaining the very fast and seemingly instantaneous occurrence of the phase inversion. This theory can be further supported by the observations below:

- 1 The time for inversion increases with an increase in rotor speed.
- 2 The dispersed phase hold-up increases with an increase in rotor speed.

Increase in the time for inversion can be due to the fact that the higher agitation intensity reduces the areas of low turbulence and the coalescence of these areas is lower, so that a bigger portion of the coalescence happens in the vortex areas. The increase in dispersed aqueous phase hold-up can be explained in terms of the resistance of the organic film to rupture and the presence of high intensity turbulence areas reducing the amount of coalescence leading to an increase in the hold-up.

Surfactants can effect the phase inversion to an unpredictable amount; in extreme cases the phase inversion can be completely resisted and some of the dispersed phase may be rejected completely from the main dispersion. Figures 4.5 and 4.6 show such a case which was studied under batch conditions. In appearance it looks like flooding, but flooding is only encountered in continuous operations. One of the characteristics of this was its stability, even the addition of large amounts of the dispersed phase did not cause inversion. Relatively large amounts of discharge which can resemble continuous flow operations (discharge of 25% of the total content) did not cause any change in the nature of the dispersion. The only way to achieve


A black and white micrograph showing a cross-section of a material with a textured, porous appearance. A ruler is visible at the bottom of the image for scale. The text "Figure 4.5 EFFECT OF SURFACTANTS ON A DISPERSION" is printed in the center of the image.

Figure 4.5 EFFECT OF SURFACTANTS ON A DISPERSION



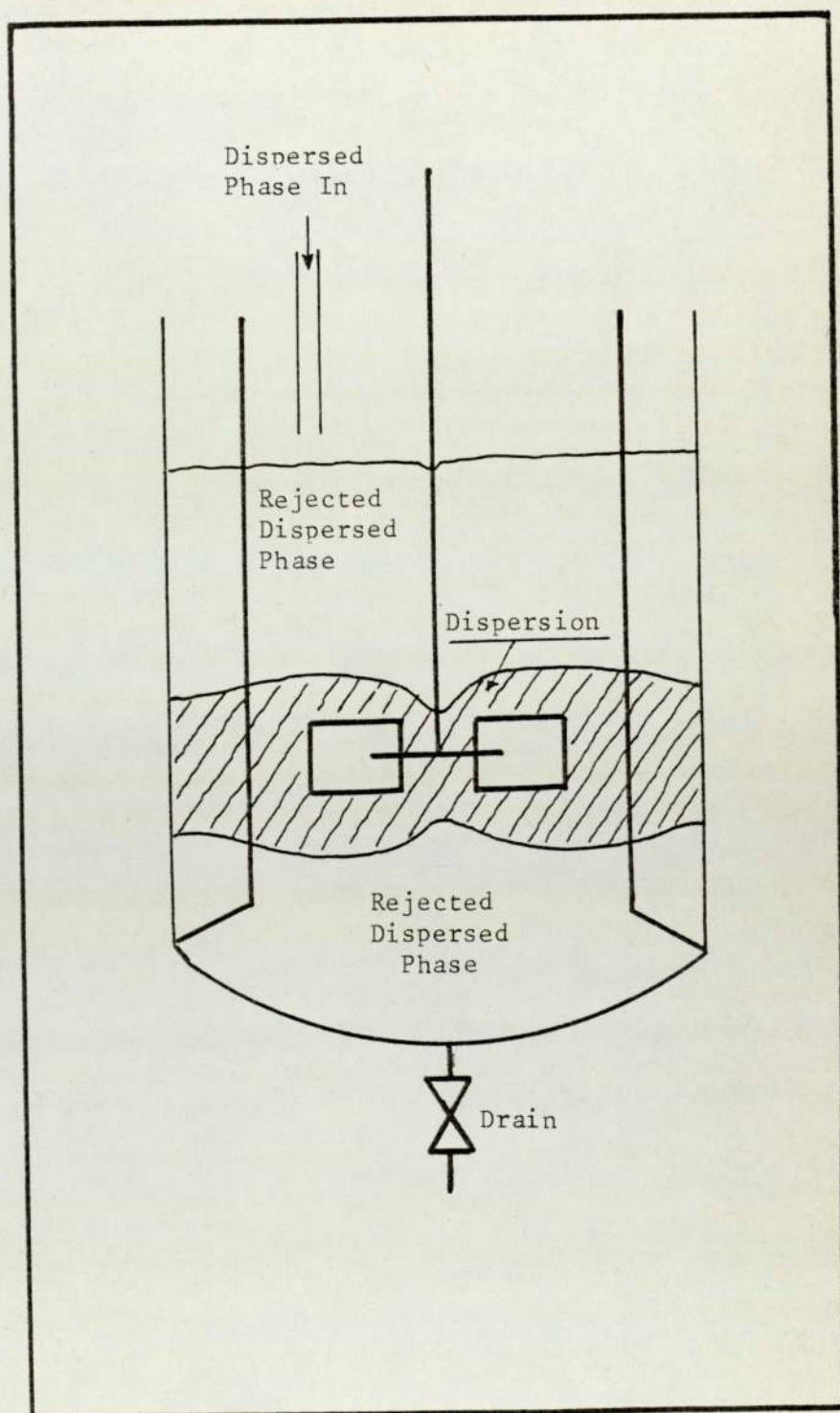


Figure 4.6 EFFECT OF SURFACTANTS ON A HIGH CONCENTRATION DISPERSION

phase inversion was through a sudden change in rotor speed. This condition, however, only exists above a certain agitation intensity. Any factor which can enhance coalescence frequency can effect the limits of phase inversion. Sawistowski (104) found that using a mixing vessel which was soaked in the dispersed phase overnight narrowed the ambivalence region. However, there is no correlation describing their dependance.

CHAPTER FIVE

MATHEMATICAL MODELLING

5 MATHEMATICAL MODELLING

Mathematical modelling of phase inversion phenomenon is of significant importance in the design of liquid-liquid contacting devices. To date no quantitative analysis has been made of this phenomenon. Phase inversion will lead to changes in the area of contact, hence affecting mass transfer or heat transfer rates, since liquid-liquid dispersions nearing phase inversion become unstable.

In this chapter the theoretical assumptions made to develop a mathematical model to describe phase inversion in an agitated tank are discussed.

5.1 The Theory of Phase Inversion

Phase inversion is described as a phenomenon in which the dispersed phase becomes continuous and vice versa. The hydrodynamic conditions leading to this phenomenon are discussed below.

In an agitated tank of suitable dimensions, by the introduction of sufficient kinetic energy isotropic condition can be assumed throughout its contents. Under steady-state conditions there will be equilibrium between the kinetic energy transmitted from the agitator, causing a drop break-up, and the energy of adhesion inducing the drops to coalesce, a mean drop size is then produced representing the equilibrium level present. Under steady-state conditions both the break-up and coalescence processes will proceed simultaneously and equally throughout the

contents of the tank.

A change in kinetic energy or dispersed phase hold-up will result in upsetting the equilibrium conditions and the rates of coalescence and breakage will be adjusted accordingly to establish a new equilibrium, a time lag is usually needed before a new steady-state condition is reached.

An increase in dispersed phase hold-up will then proceed with an increase in the rate of coalescence, phase inversion occurs when the coalescence frequency rate exceeds that of breakage.

Such an approach to the phase inversion problem therefore requires a thorough investigation into the coalescence phenomenon.

It is generally known that when two drops collide this does not always result in coalescence. Before two drops can coalesce they have to overcome a number of opposing forces. Shinnar and Church (62) discussed coalescence in concentrated dispersions, stating that coalescence seldom occurred when two droplets collide because the turbulent pressure fluctuations and kinetic energy of the oscillations induced in the coalescing droplet pair is larger than the energy between them, so that contact will be broken before coalescence can take place. Under steady state conditions:

$$E \supset A(h) \quad 5.1$$

where E is the kinetic energy imported to the dispersion by the impeller and $A(h)$ is the energy of adhesion between the drops.

At phase inversion

$$E \ll A(h) \quad 5.2$$

which indicates that every collision will result in coalescence.

The following phase inversion model is treated in four parts:

- 1 Drop size prediction model
- 2 Collision frequency model
- 3 Coalescence frequency model
- 4 Phase inversion model

Combination of the above models leads to the phase inversion model which includes physical properties of the dispersion systems.

5.1.1 Drop Size Model

The steady-state drop size is a function of both the agitator speed and the dispersed phase hold-up, and the effects of hold-up on the drop size have been the subject of a large number of research studies. These have been summarised by Tavalalarides and Coualaloglou (89) who stated that the different correlations proposed are equally valid within the limits of their derivation. Therefore, in this study the correlations of Thornton and Bouyotiotes (47) will be applied to estimate the mean drop size at different dispersed phase hold-ups. Thornton and Bouyotiotes showed that the drop size and hold-up were related by the following correlation:

$$d = d_0 + m\phi \quad 5.3$$

where d_0 is the drop size at zero hold-up, m is a constant depending on the physical properties of dispersion, ϕ is the dispersed phase hold-up. Drop size at zero hold-up could be correlated by the expression

$$\left(\frac{d_0 \rho_c^2 g}{\mu_c^3} \right) = 29.0 \left(\frac{P^3 g_c}{\rho_c^2 \mu_c g^4} \right)^{-0.32} \left(\frac{\rho_c \sigma^3}{\mu_c^4 g} \right)^{0.14} \quad 5.4$$

where P is the power induced by the impeller. Levich (63) showed that the power transmitted by the impeller can be

expressed as follows:

$$P = k \rho_c N^3 \quad 5.5$$

where k is the impeller geometrical constant.

Substituting 5.5 in 5.4 and converting to S.I units and then rearranging the equation 5.4 gives:

$$d_o = k_3 m_1 N^{-2.88} \quad 5.6$$

where k_3 is a geometrical constant and the parameter m_1 is correlated to be:

$$m_1 = \left(\frac{\mu_c^3}{\rho_c^2 g} \right) \left(\frac{\rho_c \sigma^3}{\mu_c^4 g} \right)^{0.14} \left(\frac{\rho_c}{\mu_c g^4} \right)^{-0.32} \quad 5.7$$

Combining equations 5.6 and 5.3 leads to:

$$d = k_3 m_1 N^{-2.88} + m \phi \quad 5.8$$

where m is correlated by the following expression:

$$m = k_4 \left(\frac{\mu_c^2}{\rho_c^2 g} \right) \left(\frac{\Delta \rho \sigma^3}{\mu_c^4 g} \right)^{-0.62} \left(\frac{\Delta \rho}{\rho_c} \right)^{0.05} \quad 5.9$$

where k_4 is a geometrical constant.

5.1.2 Collision Frequency Model

The study of the laws governing drop motion in a fluid medium has been the subject of many researches. The motion of liquid drops has shown to be closely tied to the size of the diffusional flux to the drop-solution interface. Smoluchowski (78) used the theory of convective diffusion to estimate the number of collisions encountered in dispersed systems for small particles.

$$\frac{\delta_n}{\delta_r} = D \frac{1}{r^2} \frac{\delta}{\delta_r} \left(r^2 \frac{\delta_n}{\delta_r} \right) \quad 5.10$$

where the term $\frac{\delta_n}{\delta_r}$ represents the number of collisions per

unit time, D is a kind of diffusivity constant of the droplets

and r is the radius.

Using the above correlation Levich (63) developed correlations for collision mechanisms of various dispersions of small size particles. Misesk (72) using the correlation developed by Levich (63) proposed the following:

$$N_t = k_2 n_o^2 d^3 v_o^{1/2} \sqrt{\xi_c D_t} \quad 5.11$$

where N_t is the number of collisions, k_2 is a geometrical constant and n_o is the number of drops, d is the drop diameter, v_o is the characteristic turbulence velocity, ξ is the kinematic viscosity and D_t is the turbulence diffusion constant. However, on examination of the assumptions made by Levich in developing the above correlation it was decided to develop a more suitable correlation.

A second mechanism for the coagulation of aerosol particles in turbulent flows was developed by Levich, since primary drops, as with aerosol particles, are not fully entrained by turbulent eddies. Different drops will have different velocities and encounters with each other will happen as a result. This will lead to substantially higher values than that produced from the diffusion mechanism model.

The number of encounters experienced by particles of size a with particles of size r per unit time is equal to

$$n \frac{(a+r)^2 (a^2 - r^2)}{1} \frac{\rho_d}{\rho_c} \frac{P^{3/4}}{\xi_c^{5/4}}$$

where $(a+r)^2$ in the area $(a^2 - r^2) \frac{\rho_d}{\rho_c} \frac{P^{3/4}}{\xi_c^{5/4}}$ is the

height of the cylinder swept out by a particle of radius a in its motion relative to a particle of radius r , and n is the average

number of particles per unit volume given by:

$$n = \frac{6 \phi}{\pi d^3}$$

The number of encounters experienced by particles of size a with all particles of size $r \leq a$ is equal to

$$\int_0^a \pi (a+r)^2 (a^2 - r^2) n f(r) \frac{\rho}{\rho_0} \frac{P^{3/4}}{\xi^{5/4}} dr$$

where $f(r)$ is a function of the size distribution of drops.

The total number of collisions per unit time and volume is equal to

$$N_t = \pi \frac{\rho_d}{\rho_c} n^2 \frac{P^{3/4}}{\xi_c^{5/4}} \overline{(a+r)^2 (a^2 - r^2)} \quad 5.12$$

where the overbar indicates the average over the entire drop size distribution.

The above mechanism only applies to polydispersed systems.

The actual value of

$$\overline{(a+r)^2 (a^2 - r^2)}$$

depends to a great degree on the form of the function of drop size distribution. Without formulating a specific form for this function it may be shown as:

$$\overline{(a^2 + r^2) (a^2 - r^2)} = \bar{a}^2 \quad 5.13$$

where \bar{a} is the average drop size.

Substituting 5.13 into 5.12 the collision rate can be obtained:

$$N_t \sim \pi \frac{\rho_d}{\rho_c} n^2 \frac{P^{3/4}}{\xi_c^{5/4}} \bar{a}^4 \quad 5.14$$

Expressing P in terms of N from equation 5.5, equation 5.14 can be expressed as:

$$N_t = k_4 \rho_d \rho_c \left(\frac{N^{9/4} \mu_d \phi^2}{\mu_c^{9/4} d^2} \right) \quad 5.15$$

where k_4 is a geometrical constant.

5.1.3 Coalescence Frequency Model

Coalescence frequency of drops in a dispersion in an agitated tank has also been studied by a number of workers, notably by Howarth (70) who stated that the coalescence frequency could be estimated by:

$$N_c = \frac{6.0 \phi (dd/dt)}{(2.0 - 2.0^{0.667}) d^4} \quad 5.16$$

Howarth found that the rate of change of drop size with time following a disturbance was proportional to $N^{1.9 - 2.25}$ for agitator speeds in the range 200 - 400 r.p.m.'s. Whereas Madden and Damerell (71) found that the coalescence frequency dependence on agitator speed was proportional to $N^{1.5 - 3.3}$. This range of the exponent of the agitator speed agrees with the tabulated results of Miller (90).

Extrapolation of Miller's results for a turbine agitator and dispersed phase hold-ups greater than 60% gives an exponent of 1.8 (see Appendix 1). That is

$$\frac{dd}{dt} \propto N^{1.8} \quad 5.17$$

is the most suitable relationship to substitute into equation 5.15 for the variation of drop size with time following a disturbance.

Rearranging equation 5.16 and substituting equation 5.17 gives the following relationship:

$$N_c = k_5 \frac{\phi N^{1.8}}{d^4} \quad 5.18$$

where k_5 is a constant depending on the agitator and mixing vessel.

5.1.4 Phase Inversion Model

As discussed earlier it is assumed that phase inversion phenomenon relates to certain hydrodynamic conditions where every collision between two drops results in coalescence. Therefore at phase inversion

$$N_c = N_t \quad 5.19$$

Substituting the values of N_c and N_t in equation 5.19 and rearranging it gives:

$$T = k \phi d^2 N^{0.46} \quad 5.20$$

where $T = \frac{N_c}{N_t}$ and its value will be equal to 1.0 at the point of inversion, k is a system constant.

The value of k depends on the liquid-liquid system, mixing vessel and agitator design, its dependence on physical properties of the liquid-liquid system is given by:

$$k_1 = \frac{\rho_d}{\rho_c \mu_c^{0.25} \mu_d} \quad 5.21$$

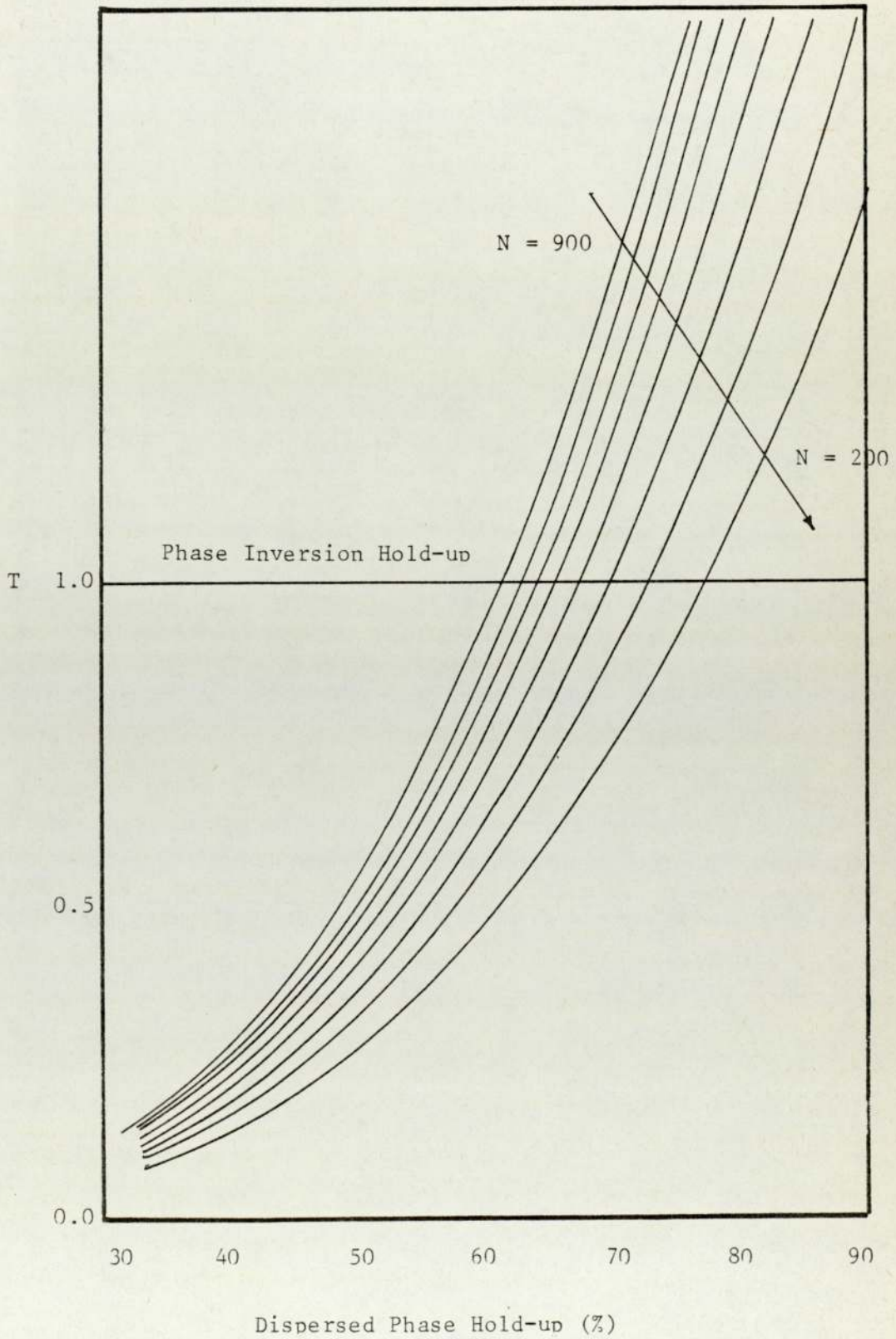
and the geometrical constant for the batch equipment was experimentally found to be 4.701×10^{-2} and for the mixer-settler unit it was found to be 5.102×10^{-2} .

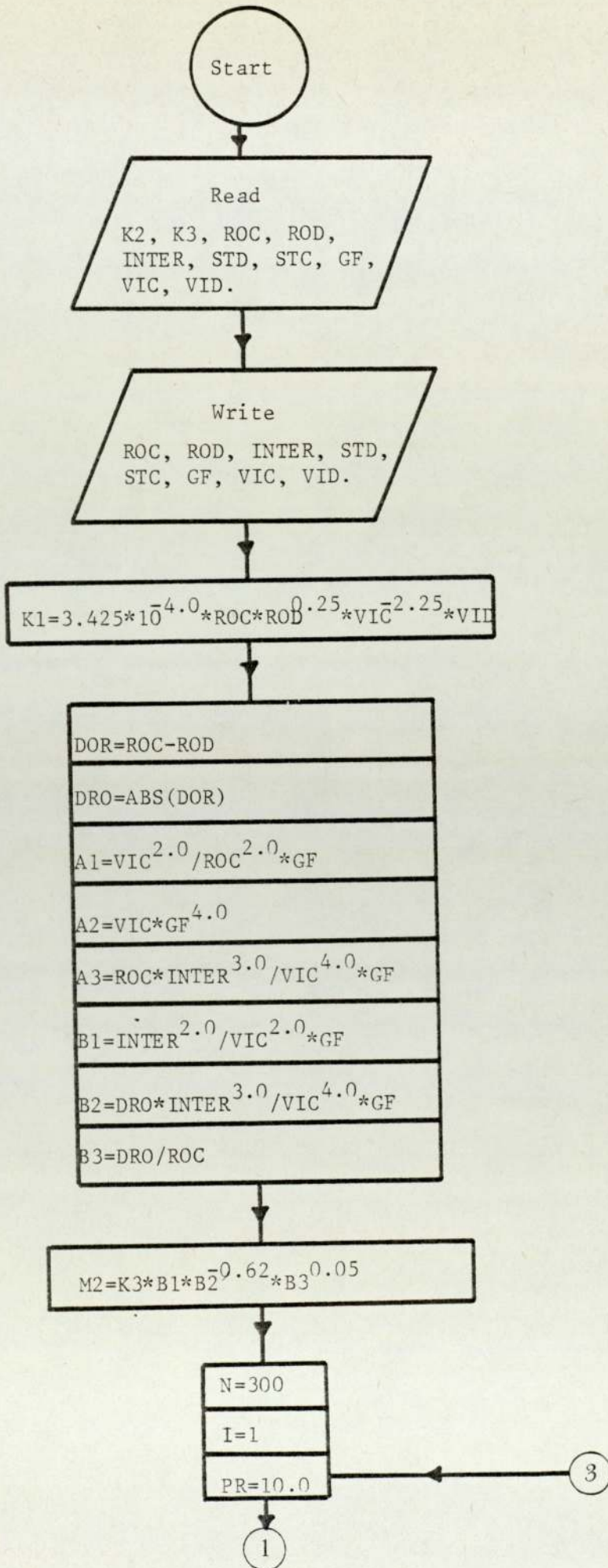
Figure 5.1 shows a typical plot of T vs hold-up.

5.2 Computer Programme

A computer programme was prepared for the prediction of phase inversion. The input data includes the physical properties and geometrical constant of the system.

Figure 5.2 shows the flowchart of the programme. The programme listing is shown in Appendix 2 together with some

Figure 5.1 A TYPICAL PLOT OF T VS HOLD-UP



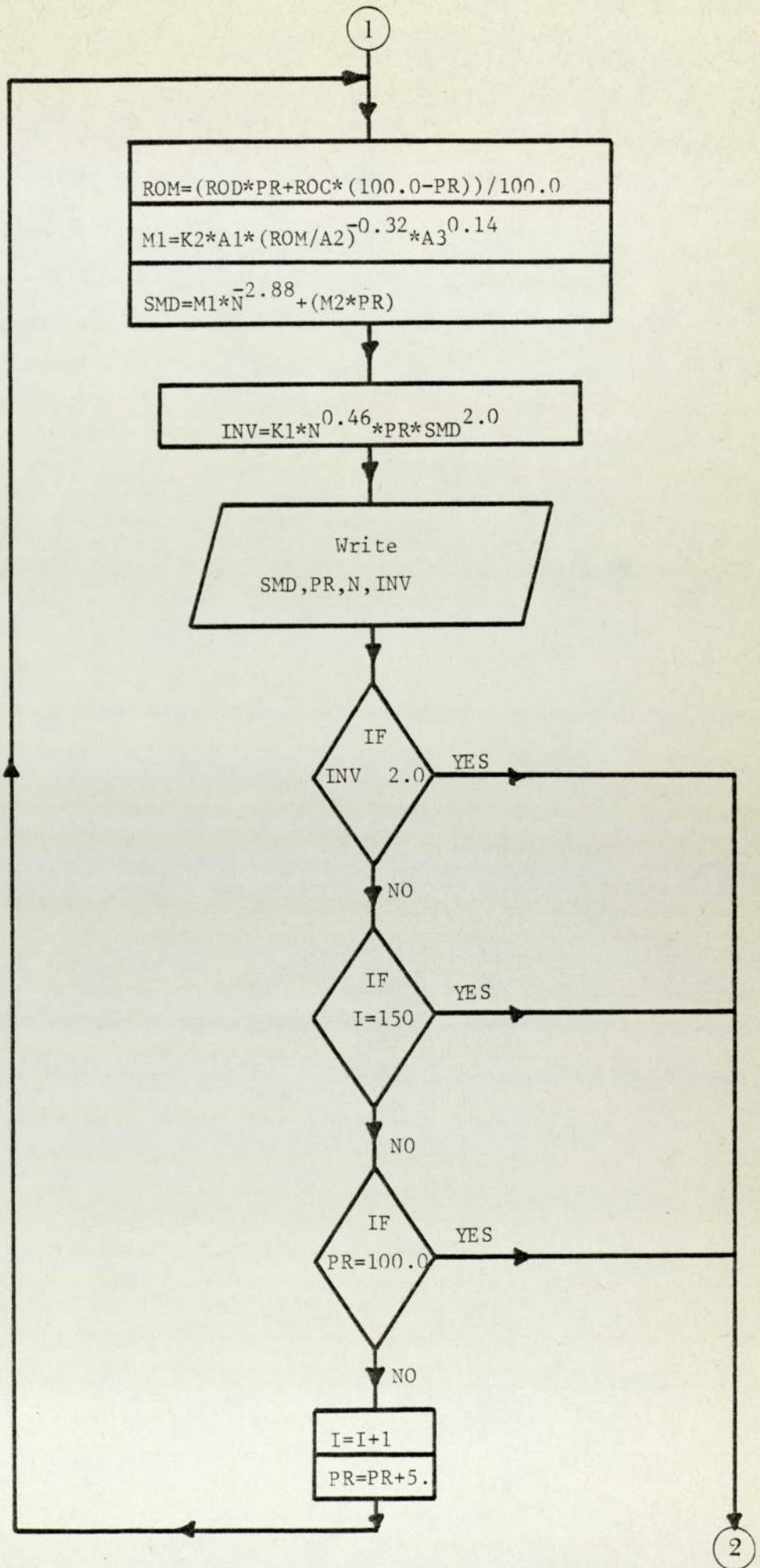
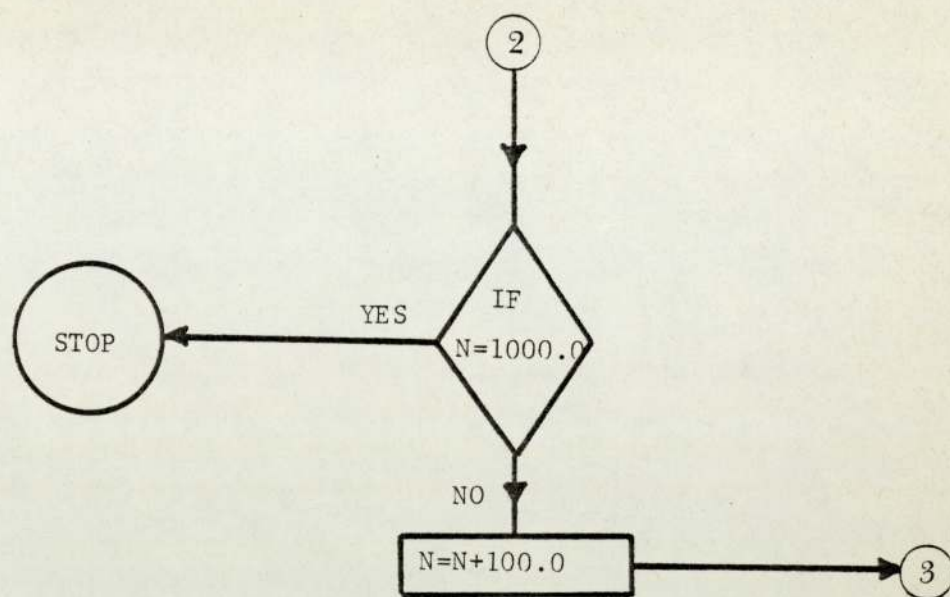


Figure 5.2 (continued)



typical results obtained.

CHAPTER SIX

EXPERIMENTAL INVESTIGATION

6 EXPERIMENTAL INVESTIGATION

The characterisation of liquid-liquid dispersions is an important requirement in many industrially important chemical engineering operations, such as solvent extraction, direct contact heat exchangers and batch and continuous heterogeneous reactors. This promotes the importance of establishing the processes and limitations encountered in such operations. Phase inversion is one of the most important limitations in many of these engineering operations and the study of this phenomenon requires very detailed attention to all the factors effecting it.

Two specific apparatus were constructed for the study of phase inversion; one for the batch experiments and the other for continuous operation experiments. Each was constructed of Q.V.F. glass and stainless steel with p.t.f.e. and Viton seals to eliminate contamination due to interaction with the equipment.

6.1 DESIGN AND EQUIPMENT CONSIDERATIONS

Experiments were carried out in two separate apparatus

- (i) A batch mixing vessel
- (ii) A continuous mixer-settler.

These will be separately discussed.

6.1.1 Batch Mixing Vessel

The batch apparatus consisted of a 10.16×10^{-2} m diameter mixing vessel with a four bladed turbine positioned centrally and of diameter 5.08×10^{-2} m. The agitator was located about 11.0×10^{-2} m (i.e. one tank diameter) from the bottom of the vessel and supported at the top for geometrical uniformity, Figure 6.1 shows the agitator and its dimensions.

The mixing vessel was a round bottom glass vessel with a glass valve located in its base for drainage. The tank was fully baffled, the four baffles were 1.02×10^{-2} m wide and 12.5×10^{-2} m long and made of stainless steel, arranged vertically at 90 degree intervals and supported at the top by a stainless steel plate forming the cover of the tank. The cover contained a port for the agitator shaft and, in addition, there were two other ports, one was connected to a glass funnel for the addition of the continuous phase or dispersed phase and the other was used for the addition of small quantities of the dispersed phase near the point of phase inversion, by means of an automatic burette.

Electrodes of the Continuous Phase Detector were supported on the baffles just below the impeller. The agitator was driven by a Citenco electric motor, type KQ 502, with a built-in variable speed control. The speed range was between 100 - 750 rpm. Figure 2.1 shows the power characteristics of a turbine agitator in the fully baffled mixing tank. The agitation rate was

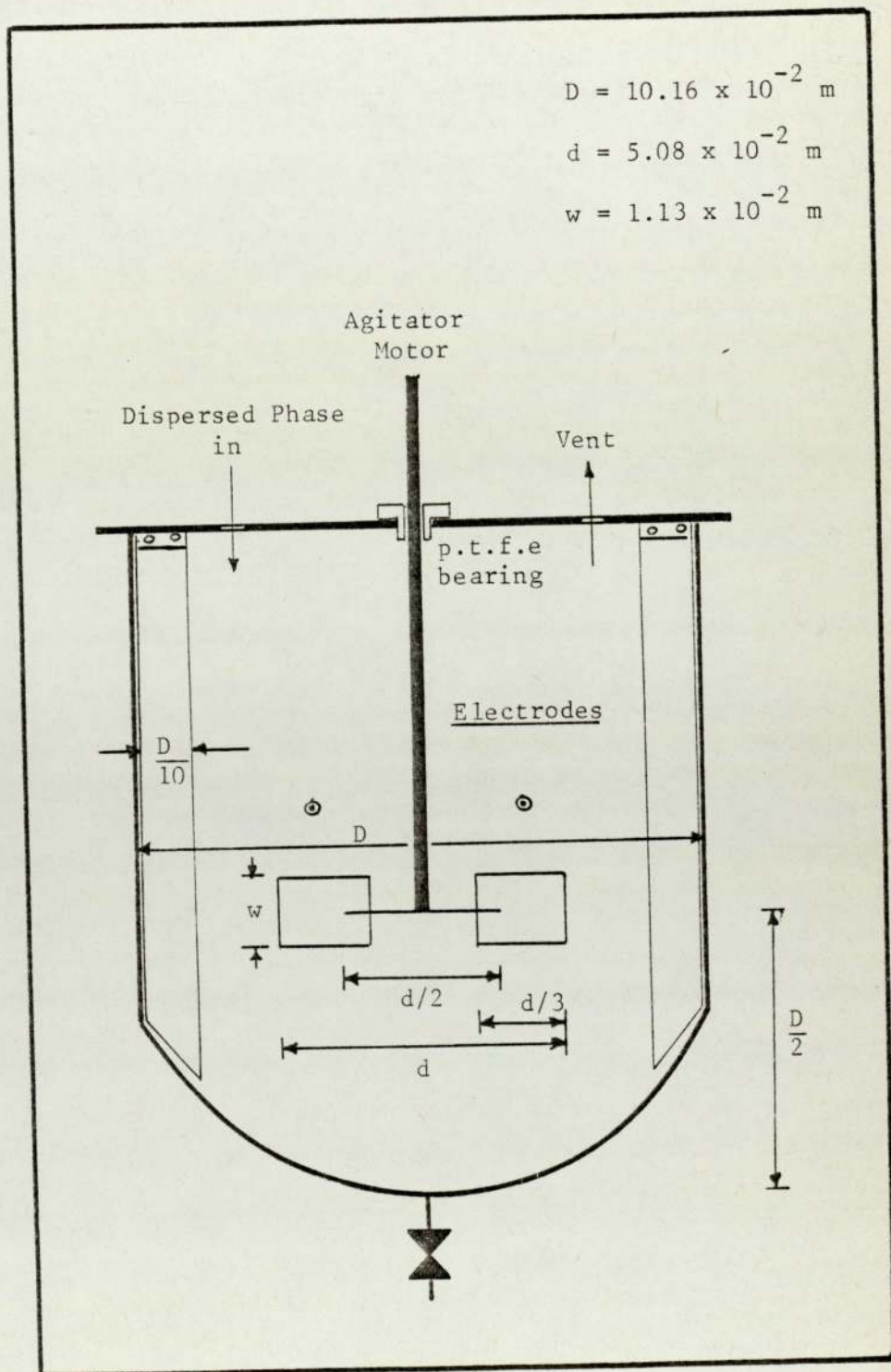


Figure 6.1 BATCH MIXING VESSEL

measured continuously by a Comark Electric Tachometer.

The dispersion was illuminated by a Kodak Carosol Projector which was found to be satisfactory for photographing the dispersion, the light source fitted with a Kodak Carosol Slide Projector Zoom Lens was particularly suitable for this type of work.

6.1.2 Continuous Mixer-Settler

A flow diagram of the equipment is shown in Figure 6.2 and details are presented in Figure 6.3-6.4. This was arranged so that the major components were easily accessible. The instrumentation and the flow control valves were located conveniently for easy reach.

All fluid reservoirs could be used as feed tanks or receivers. A recycle line was provided for each phase. Drain points were incorporated at the lowest points in the system.

The mixer-settler is illustrated in Figure 6.3 and consisted of a round bottom glass mixing tank of 15.24×10^{-2} m diameter and 33.0×10^{-2} m high, which was connected to the horizontal settler 31.0×10^{-2} m long, constructed from a Q.V.F. pipe section with stainless steel flanges, as shown in Figure 6.5

6.1.2.1 Mixer Unit

The phases were mixed in the mixer by a four bladed turbine agitator. A mixing vessel of 5.0 litre capacity was used and contained two inlets of 1.78×10^{-2} m diameter, positioned 15.0×10^{-2} m apart. The lower port was positioned just below the impeller. The two

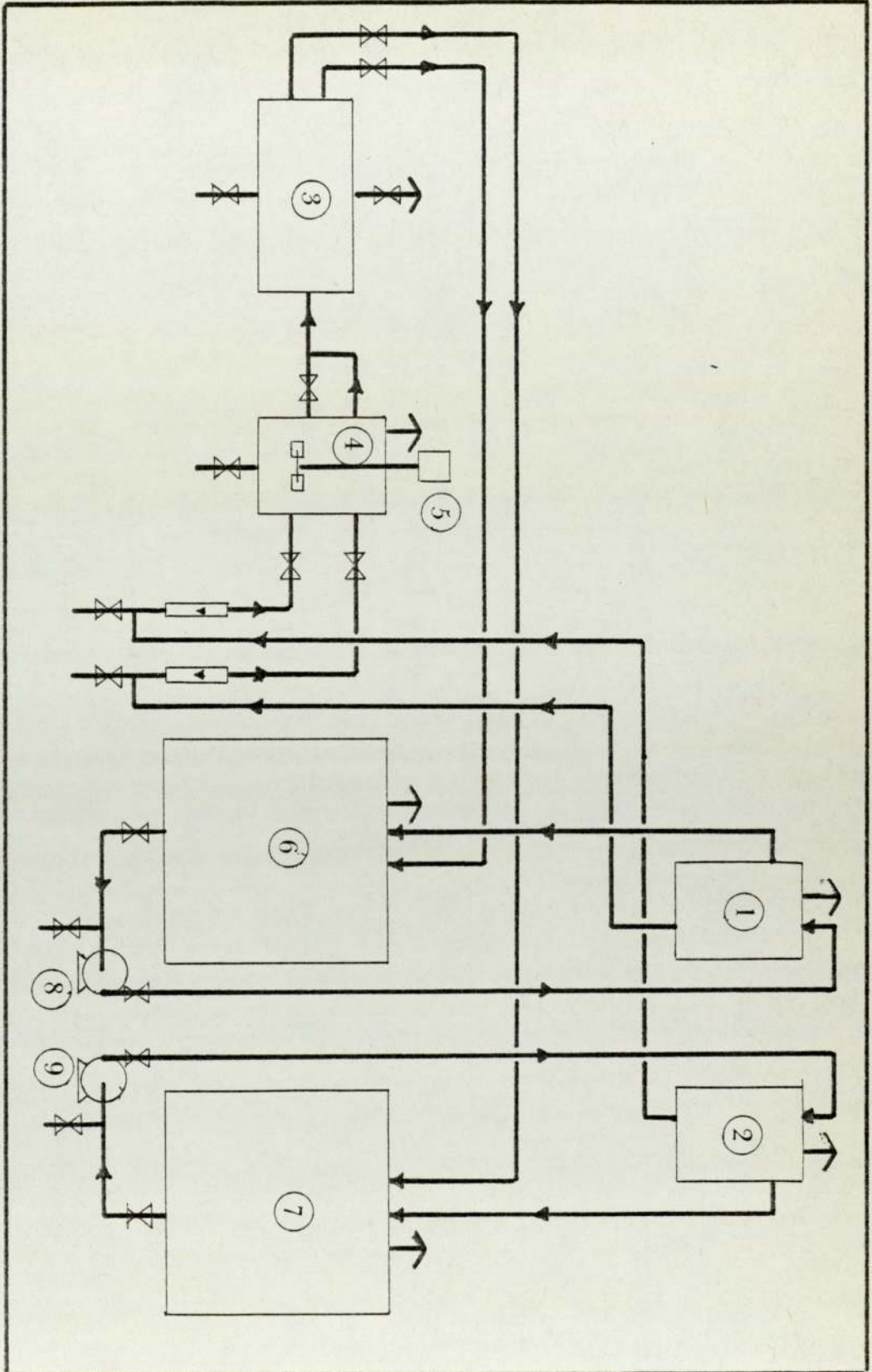


Figure 6.2 FLOW DIAGRAM OF CONTINUOUS MIXER-SETTLER UNIT

Figure 6.2 (continued)

- 1 & 2 Constant Head Devices
- 3 Gravity-Settler Unit
- 4 Mixing Vessel
- 5 Turbine Mixer Unit
- 6 & 7 Collecting Reservoir
- 8 & 9 Recirculating Pumps

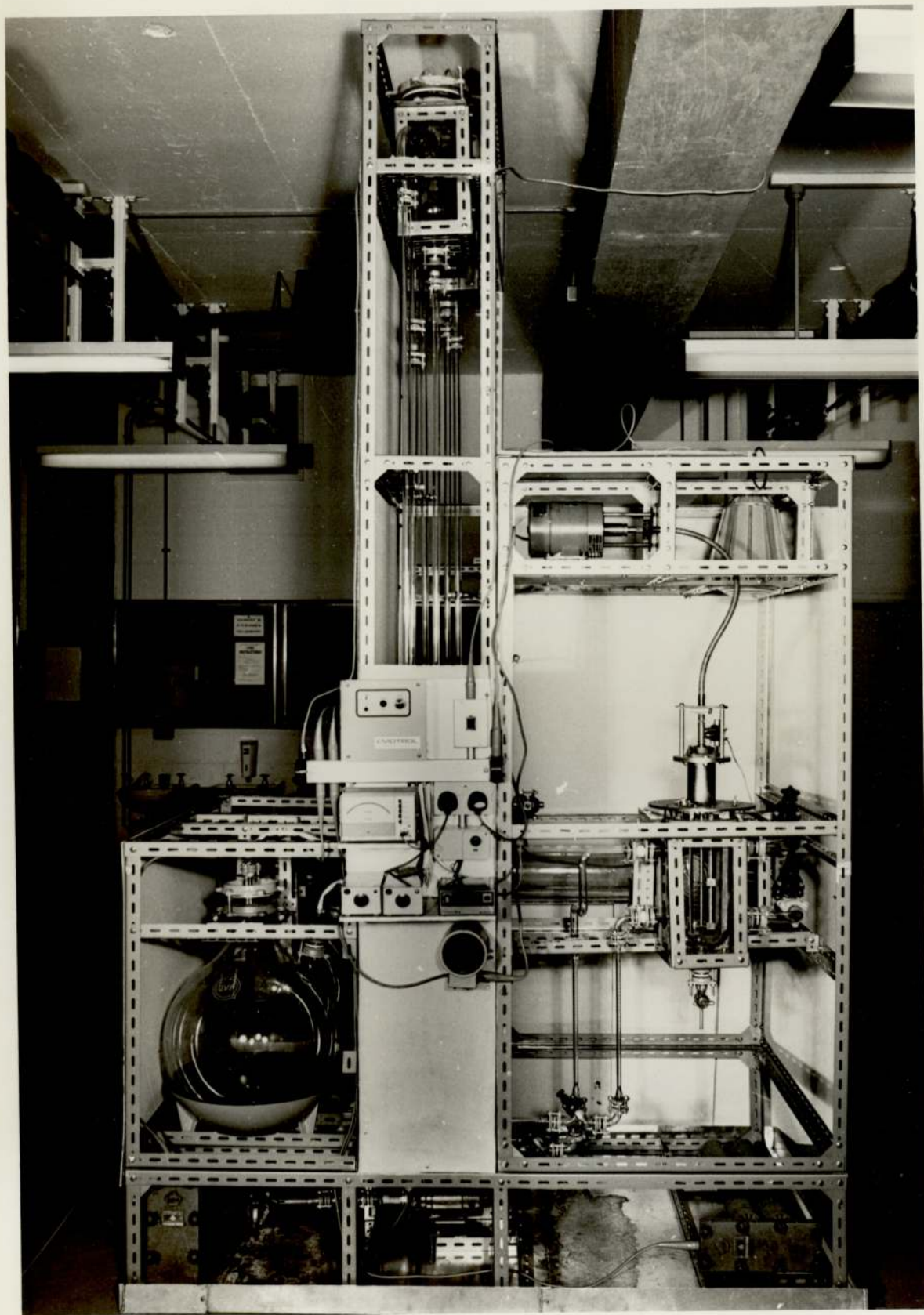


Figure 6.3 GENERAL LAYOUT OF THE CONTINUOUS MIXER-SETTLER UNIT
WITH FRONT PANELS REMOVED

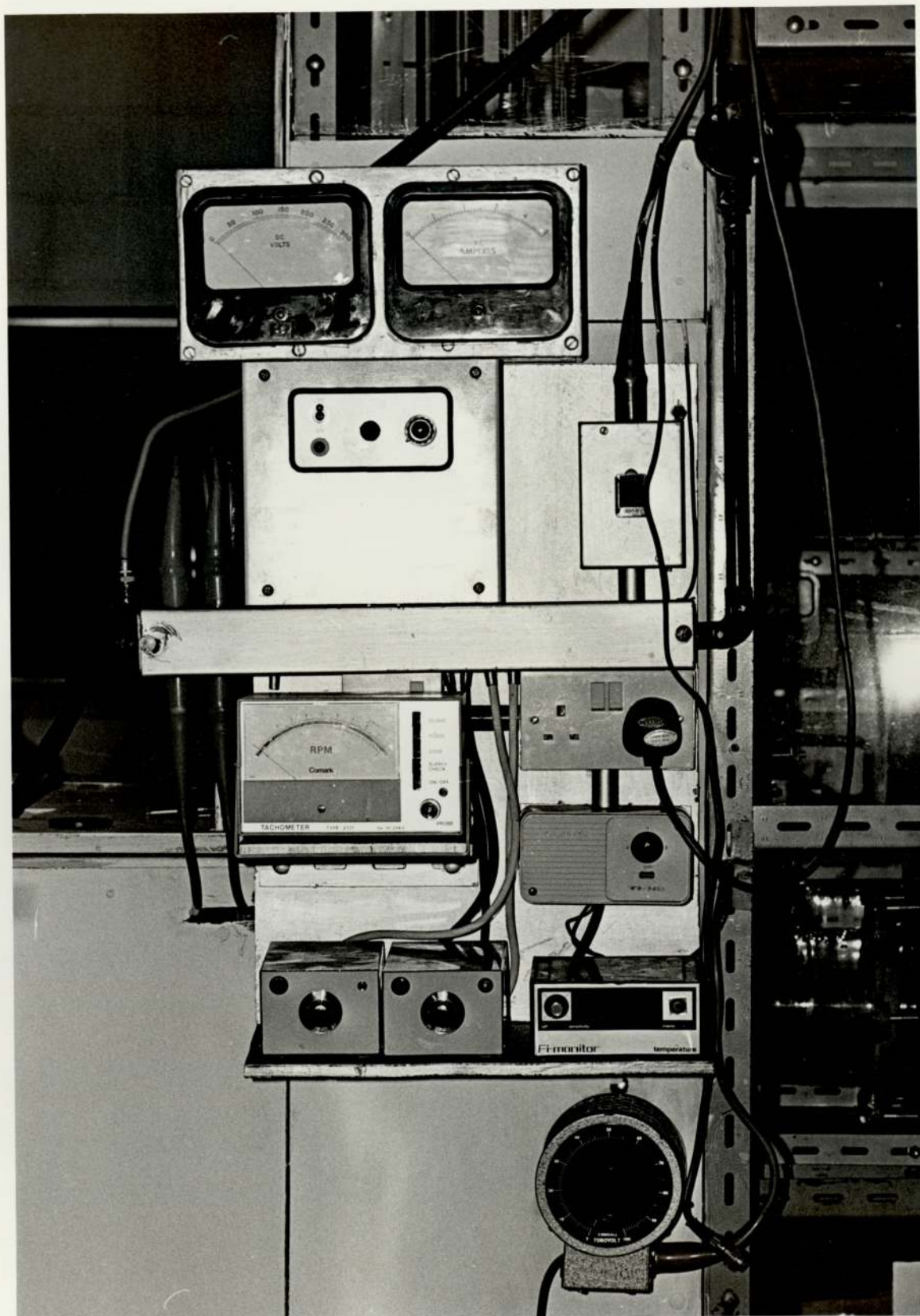
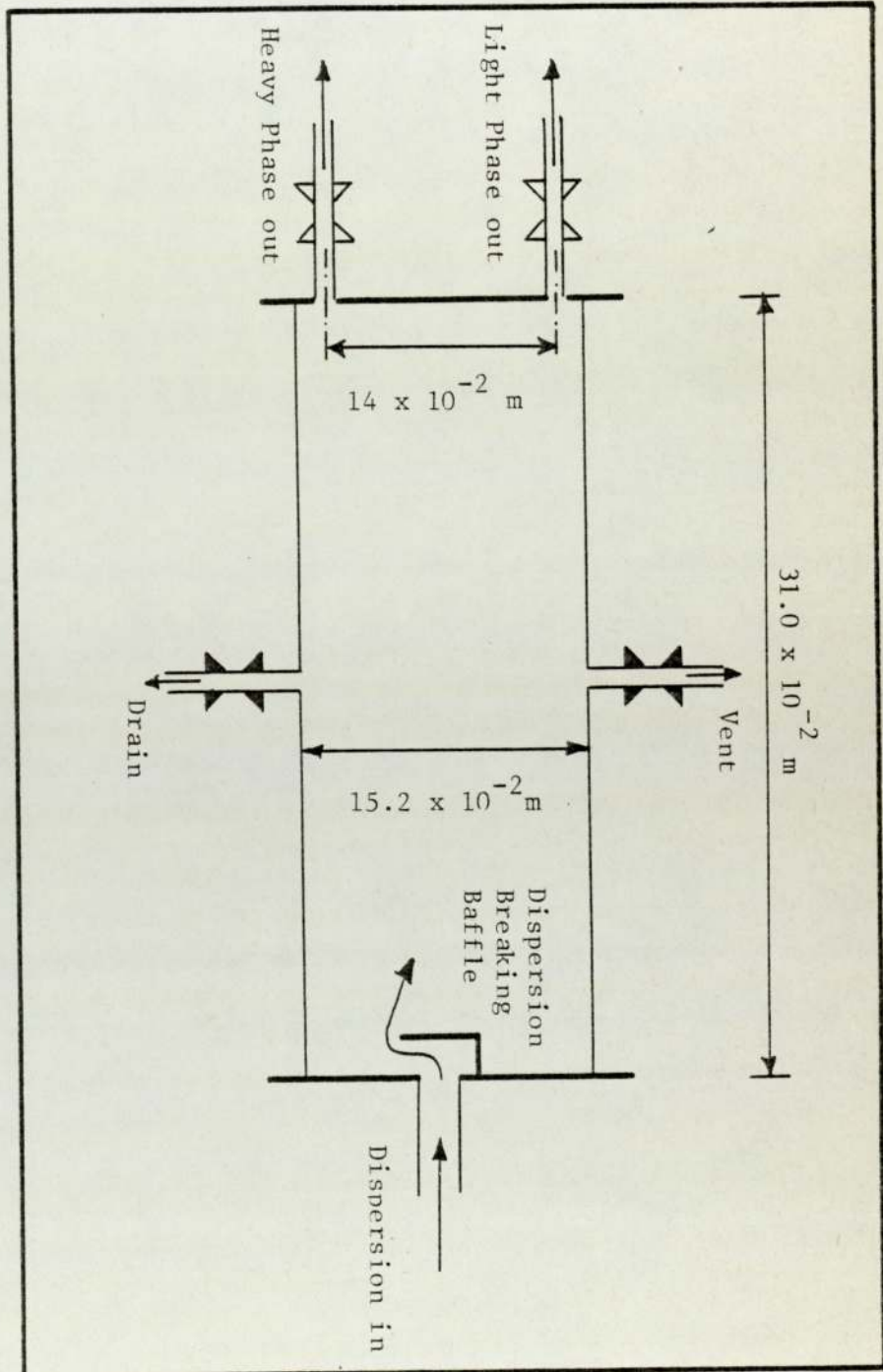


Figure 6.4 GENERAL LAYOUT OF THE CONTROL PANEL

Figure 6.5 DIAGRAM OF GRAVITY-SETTLER

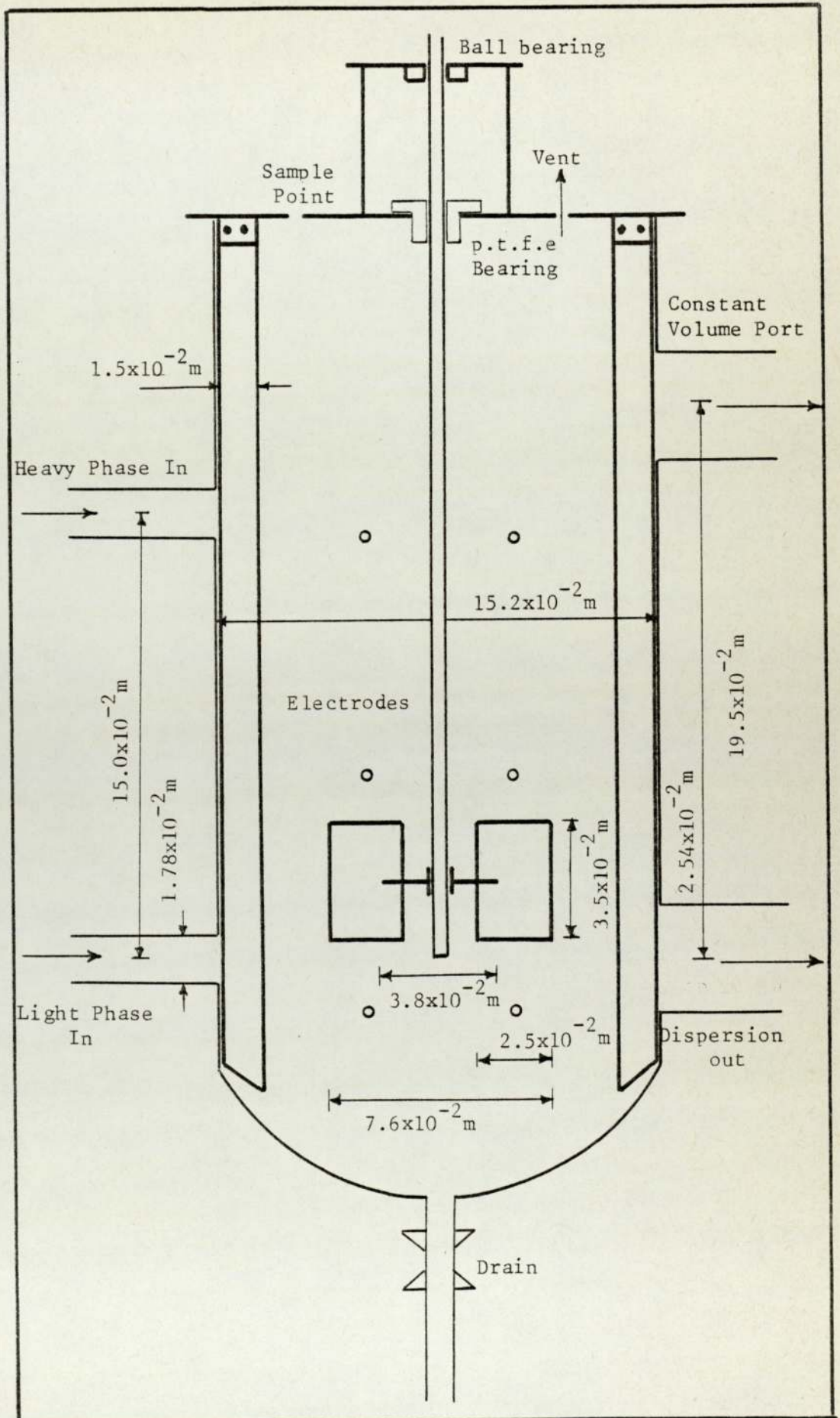
outlets were each of diameter 2.54×10^{-2} m and were positioned at a distance of 19.5×10^{-2} m apart. The lower outlet was used to study the effect of the outlet position on the phase inversion and a Q.V.F. glass control valve was inserted to regulate the outlet flow. The other outlet port was used for two purposes. One to study the effect of the outlet position, secondly to act as an overflow port, no valve was placed in this outlet line.

The inlet flow rates of each phase were regulated by a Q.V.F. glass valve and the flow rates of each stream were measured by a rotameter with a stainless steel float. The calibrations of these rotameters are presented in Appendix 4. The mixing vessel contained four stainless steel baffles 1.52×10^{-2} m wide and 28×10^{-2} m high, with stainless steel reinforcements as shown in Figure 6.6 the baffles were arranged vertically at 90 degrees intervals and supported at the top by a stainless steel plate covering the tank.

Three pairs of continuous phase detectors were inserted through the wall of the mixer, at equal distances of 7.0×10^{-2} m from each other and with each terminal being 4.0×10^{-2} m apart, so as to cover as much of the dispersion volume as possible.

A drain with an all glass on - off valve was located at the bottom of the vessel.

A 5 litre Q.V.F. vessel was used in order to minimise wall effects and possible fluctuations in the flowrates.

Figure 6.6 DIAGRAM OF MIXER-UNIT

Due to the height of the mixing vessel an adjustable double turbine impeller was used, but preliminary observations indicated that two agitation zones of different dispersion densities were produced. Therefore, a single four bladed turbine of 7.62×10^{-2} m diameter replaced the double agitator. Details of this unit are presented in Figure 6.6. The impeller height was adjustable by means of two screws shown in the Figure 6.6; the impeller height could, therefore, be easily adjusted and the required height for optimum performance was found to be 18.0×10^{-2} m from the base of the vessel. The single turbine impeller proved to be very efficient in promoting uniform flow throughout the vessel and hence eliminating any dead zones, even at relatively low rotor speeds (120 r.p.m.). The agitator shaft was supported by two bearings at the top, one p.t.f.e. and one ball bearing, the bearings were supported on the stainless steel cover.

The agitator was driven with a General Electric DC motor of 1/3 h.p. type and the speed was regulated with a General Electric type 502 DC speed regulator with an accuracy better than $\pm 2.5\%$. The electric motor was connected to the impeller shaft by a flexible shaft in order to reduce the amount of vibration transmitted by the motor. The motor itself was placed on four shock absorbers. A Colmark type 2101 **electronic** tachometer was used to read the impeller speed.

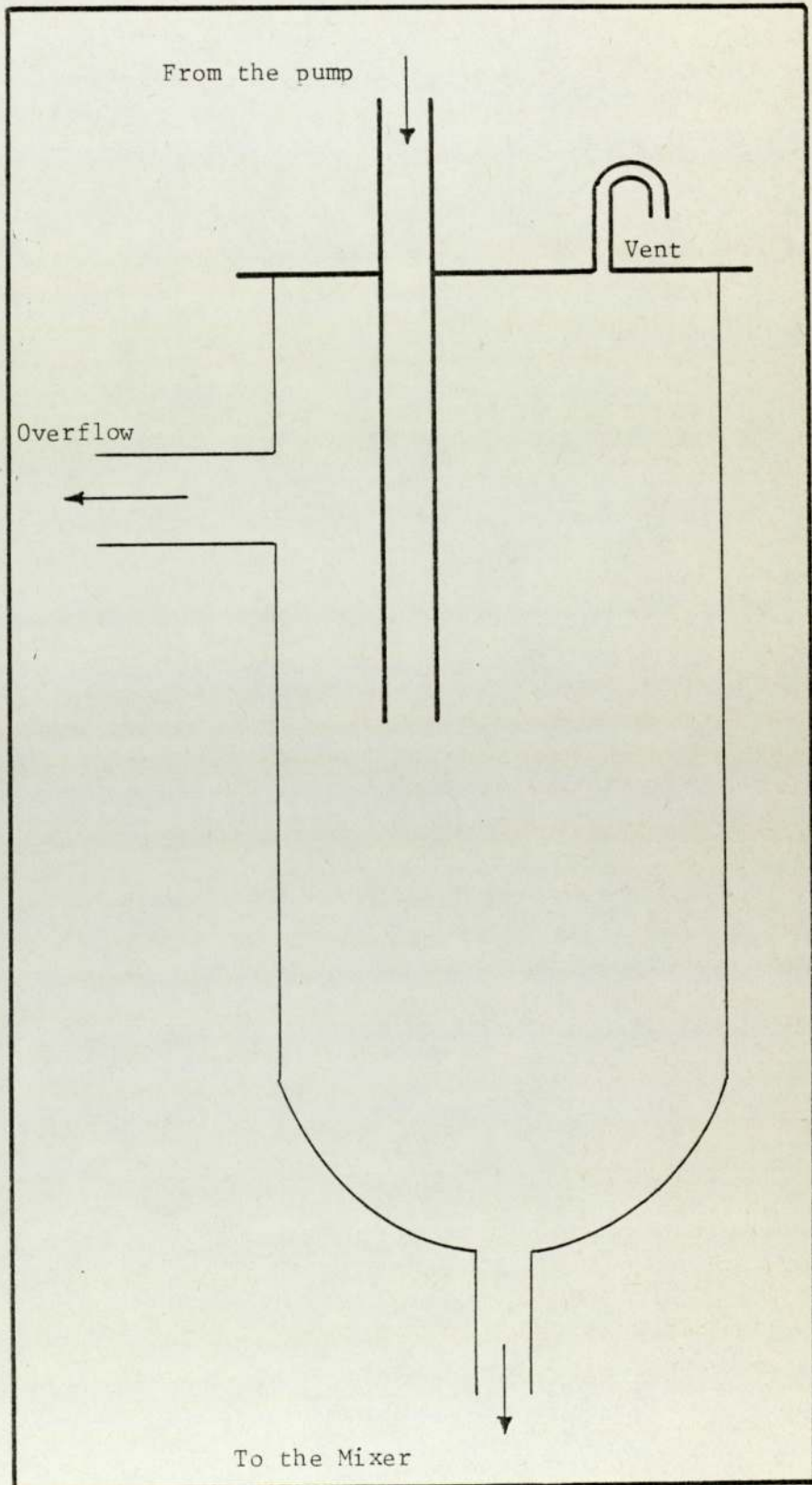
6.1.2.2 Constant Head Device

Most centrifugal pumps have an output which fluctuates around a mean value and, therefore, to overcome variations in flowrates a constant head device was installed. This device consisted of a 5 litre Q.V.F. glass vessel with a glass side port, the cover of the vessel was made of a stainless steel plate with an inlet port and a vent. Figure 6.7 gives details of this overhead device and it was found that this design ensured constant flow of liquid throughout an experiment. The constant head was fed by a Stuart No. 12 Centrifugal Pump, and the flowrate was controlled and was adjusted so that the liquid level in the constant head device was always at the same level as the side (overflow) port. The overflow was returned to the reservoir. The flowrate was adjusted by a type KV07 Q.V.F. glass control valve.

Two such devices were installed, one for each phase and each was separately controlled.

6.1.2.3 Gravity Settler

A gravity settler of 5 litre capacity, 31.0×10^{-2} m long and 15.2×10^{-2} m diameter was constructed from a Q.V.F. pipe section with two stainless steel end plates. One plate was connected to the mixer and had a single inlet of 2.54×10^{-2} m diameter. A stainless steel baffle was placed near the point of entry to ensure break-up of the dispersion. Such a baffle was recommended by Hussein (12) to reduce the length of the dispersion.

Figure 6.7 DIAGRAM OF CONSTANT HEAD DEVICE

band. The other end plates had two outlets, one for each phase. The flow of each phase was regulated by a Q.V.F. valve. Figure 6.5 illustrates the two end plates with their dimensions.

In practice it was observed that the settler was too large because of the two bends in the line connecting the mixing vessel and the gravity settler. In effect these two bends acted as baffles in coalescing the dispersed phase. This, however, enables low interfacial tension systems to be studied in future investigations.

6.1.3 Other Equipment and Considerations

Two storage vessels each of 5.0 litre capacity were included in the apparatus to receive and recirculate the phases. A stainless steel cover with three ports, one to receive the overhead flow from the constant head device, one connected to the outlet of the relevant phase from the settler and one acting as a vent was used. A two way valve was connected to the drain, one way for drainage and the other to the circulating pump.

All the connecting pipework was of standard Q.V.F pipe sections, the gaskets used were p.t.f.e. O ring type. Viton seal was also used where necessary. The infra-structure was made of ~~the~~ Andy Angle and the whole apparatus was enclosed in a cabinet. A mild steel drip tray with a drain was placed under the rig.

The temperature was controlled by two 1 kw flame proof radiation heaters and adjusted with Fisons Fi-monitor to an

accuracy of $\pm 1^{\circ}$ C.

Due to the fact that inflammable solvents were used all of the wiring was insulated to eliminate sparks and the whole frame was earthed to eliminate static charge. Steel covers were placed on all vessels to prevent contamination of the solvents and an extractor fan was installed to remove any vapour build-ups in the cabinet.

6.2 ANCILLARY EQUIPMENT

6.2.1 Continuous Phase Detector

An electric device based on completion of a circuit using electrical properties of water was developed to detect which phase was the continuous phase, the technique normally applied is a conductivity meter, which requires a certain amount of electrolyte. However, Lawson (106) as cited by Arnold (7) reported that even very small amounts of impurities can alter, to an unknown extent, the rate of coalescence and droplet break-up. For this reason it was decided to employ some other means and the Continuous Phase Detector was constructed. The unit is shown in Appendix 3. It was designed so that it required a very small current to complete the circuit. Therefore, the necessity of the addition of any electrolyte to the liquid phases was eliminated. The sensitivity of the detector could be adjusted by an external dial to function for very pure organic solvents, or even unsaturated deionised distilled water. When the continuous phase was aqueous, the circuit was complete and the signal was given in the form of a light. Disconnection of the circuit

occurs when organic phase exists between the two electrodes so that the light goes out, indicating that the continuous phase is organic. Near phase inversion, where the concentration of the dispersion is high, the close packing of drops causes the circuit to be completed or disconnected momentarily, resulting in flickering of the light, this indicated the approach of the limits of ambivalence, hence giving an advance warning of phase inversion.

Other advantages of the Continuous Phase Detector were its low cost and safety against fire, since it was powered by a 9 volts battery. It was compact and easy to operate and the signal of the continuous phase was very clear.

6.2.2 Photographic Equipment

Analysis of phase inversion mechanism in this study required the observation of the behaviour of drops under various conditions. This was most conveniently achieved by photography and a 35 mm Nikkormat camera with a 50 mm Nikon macro lens and a 35 mm Chinon ME with a power winder, with intravoltmeter facility to allow exposures to be produced at required intervals, was used. An Asahi Pentax Macro lens was used with the Chinon Camera Body. This combination allowed the best use of the film as it permitted a reasonable portion of the negative to be exposed by the required section of the dispersion. Photographing dispersions requires high speed films and a number of films, including the Kodak 2475 Recording Film, were used to find the most suitable combination. It was decided that Kodak Tri-X rated at 1200 A.S.A. and developed

in a full strength solution of D 76 Kodak Developer at 22° C for twenty minutes was the most suitable technique. The development time was adjusted to suit the new speed setting.

A Kodak Carosol Projector with a 150 mm Kodak lens was used as a light source with batch equipment. This enabled a shutter speed setting of 1/1000 second at f 5.6. In addition, a National P.E. 28 electronic flash gun with detachable sensor was used with the gun behind the vessel and the sensor placed in the top of the camera. This allowed the camera to be set at around f 11. Carosol was not used as the light source, as it was not sufficiently strong to penetrate the 0.152 m diameter vessel of the continuous equipment.

Photographs of dispersion in conjunction with a scale were made using the above technique. The photographs were printed on Grade 4 high contrast Kodak photographic paper. The counting of drops was performed using a Carl Zeiss TG 3 Particle Counter. A constant distance, established by trial and error, between the mixing vessel wall and the film was maintained using a simple spacing adaptor.

6.3 LIQUID-LIQUID SYSTEMS

A number of liquid-liquid systems were studied with a wide range of physical properties. These systems can be divided into two groups:

- a) systems studied in the Continuous Equipment
- b) systems studied in the Batch Equipment

This division was necessary for a number of reasons, thus:-

- 1 The economic considerations
- 2 Safety hazard due to large quantity of solvent involved.
- 3 Reasonable assumptions could be made to extend the batch results to the continuous.

6.3.1 DETERMINATION OF PHYSICAL PROPERTIES

Density

Density was estimated by the specific gravity bottle method. The density of mutually saturated liquid was determined to a fraction of 10^{-8} kg. All density estimations were made at a temperature of 20° C.

Viscosity

A Technico Cannon-Fenske type viscosity meter was used with a temperature controlled bath. The temperature was set up at 20° C and the samples were left for one hour before measurement. Depending on the consistency of the results the viscosity was checked between three to five times.

Surface Tension

A Torsion Balance with a ring, having a circumference of 0.04 m, was used to determine surface tension and interfacial tension.

6.3.2 LIQUID-LIQUID SYSTEMS

a) Batch Mixing Vessel

A number of solvents with various physical properties have

been used.

- 1 Toluene - Water
- 2 Carbon Tetrachloride - Water
- 3 Octanol - Water
- 4 Carbon Tetrachloride/Toluene - Water

A combination of mixtures of the Carbon Tetrachloride/Toluene was used to find the effects of low interfacial tension on phase inversion.

b) Continuous Mixer-Settler Unit

In order to compare the results obtained in the batch system with those of the continuous system similar operating conditions were chosen. This enabled study of the effect of mode of operation and system geometry, the results of which enlarge on the conclusions already drawn concerning the batch system.

A Toluene - Water system was chosen to compare the results in the two apparatus.

6.3.3 Saturated - System Preparation

G.P.R. grade of solvents were used throughout the experimental work and the aqueous phase was deionised distilled water. The two phases were poured into the same container and were mixed periodically by a slow moving paddle (100 r.p.m.) for about 48 hours to ensure that the phases were fully saturated before the start of any experiments.

6.4 EXPERIMENTAL PROCEDURES

The batch and continuous experimental procedures are

discussed separately below:

6.4.1 Batch System

6.4.1.1 Cleaning

Periodically the mixing vessel, the baffles and impeller were removed and washed in a 2% solution of 'Decon 90' detergent and were left to soak in the detergent solution over night. Following this they were washed under running tap water for an hour after which each item was rinsed three times with deionised distilled water.

6.4.1.2 Purity Test

Equal volumes of each phase were placed in the mixer and the agitator was switched on and set at a fixed rotor speed (400 r.p.m.), so that no secondary dispersion was produced. The agitation was continued for about ten minutes. Then the agitator was switched off and the time required for the phases to separate was measured. This was checked with the original data, a limit of $\pm 10\%$ of the original time was considered to represent a satisfactory level of the system purity.

6.4.1.3 Start-up Procedure

The phase to be continuous was introduced into the empty vessel so that the impeller was immersed. The impeller was switched on and set at the required speed of agitation. Dispersed phase was then added to the system until the mixture consisted of about 20% of the phase inversion composition. At this stage small quantities of the dispersed phase were added repeatedly

by means of an automatic burette, at a rate of approximately 50 cc per ten minutes. The volume of the solution was then kept constant by withdrawing 50 ml of solution very slowly to allow the steady-state condition to be reestablished. When the light signal of the Continuous Phase Detector started to flicker the rate of the addition was reduced to half. The total volume of dispersion was maintained $800 \text{ ml} \pm 50 \text{ ml}$. Addition of the dispersed phase was stopped when phase inversion started.

After phase inversion the stirrer was switched off, having noted its speed. After the phases were completely separated they were transferred and their volumes were recorded.

6.4.1.4 Analysis of Data

The construction of phase inversion diagram requires very little data other than accurate readings of the corresponding volumetric phase ratios and rotor speeds. However, the theoretical studies required a knowledge of the hydrodynamical behaviour of the system and a study of the latter was also carried out. The reasons behind the study of the hydrodynamical behaviour and also its findings will be discussed in Chapter 8.

Two studies were carried out as follows:

- 1 Drop-size vs Hold-up and Impeller speed.
- 2 Drop-size growth vs time at phase inversion.

Still photography was used to follow these studies.

1. Drop-size vs Hold-up and Rotor Speed

These studies were carried out to obtain the data in order to establish the most suitable correlation for phase inversion. As mentioned earlier, a modified version of the correlation 5.8 proposed by Thornton and Bouyatiotis was selected and, in order to be able to count a representative number of drops, three frames were taken, so that about two hundred drops could be counted for analysis.

2. Drop-size growth vs Time at Phase Inversion

These studies were carried out to confirm the theory of coalescence frequency. For this purpose a still frame was taken every 0.5 seconds prior to inversion and was continued until the start of the inversion. The series of photographs presented in Figure 6.8 shows a typical phase inversion.

3. Effect of Impurities

These experiments were carried out to assess the effect of impurities on the phase inversion hysteresis band for fully saturated liquid-liquid systems. The inversion vs rotor speed was determined as previously.

6.4.2 Continuous Rig

Due to the size, volume and complexity of the continuous rig the experimental procedures were modified where necessary from that of the batch apparatus.

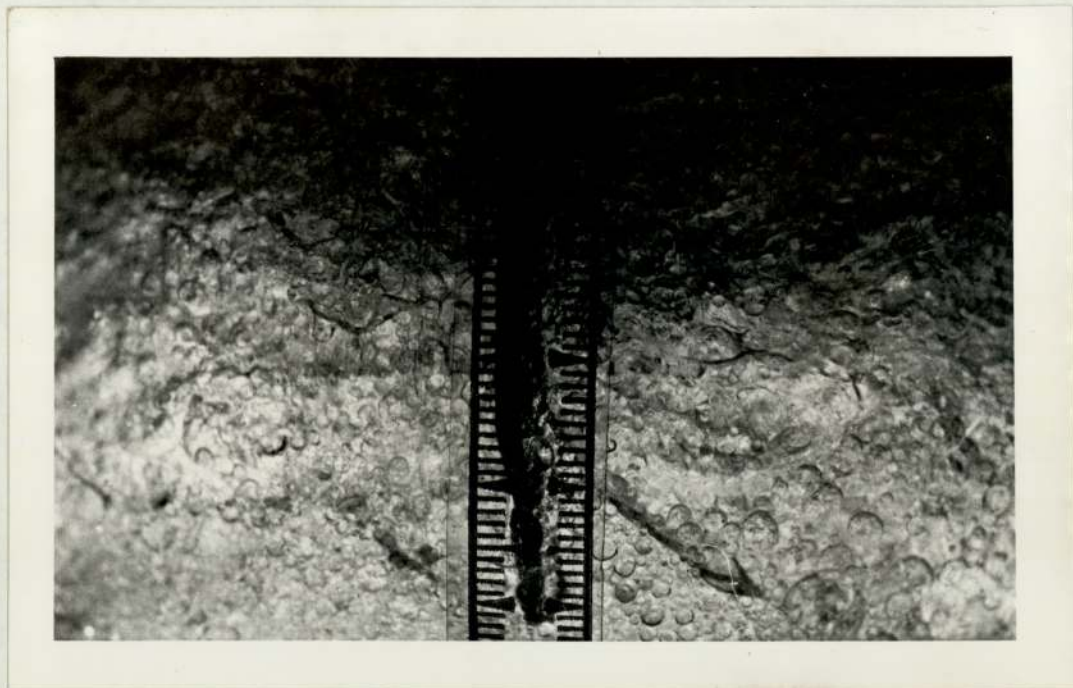
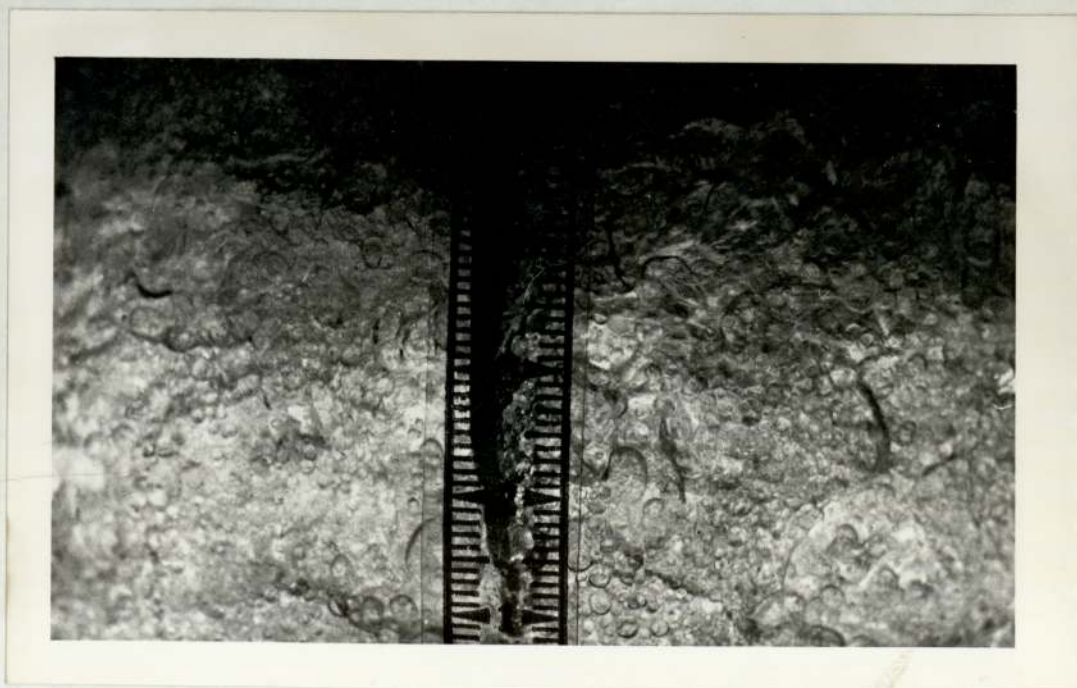
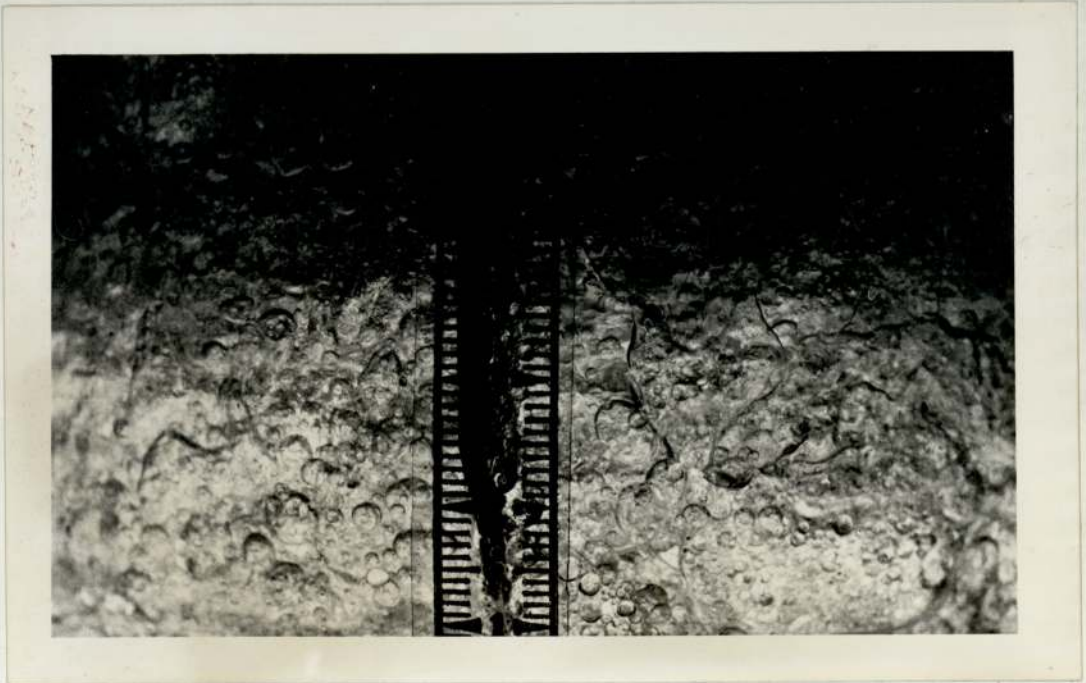
Figure 6.8 PHASE INVERSION SEQUENCE IN SIX STAGES(i) $t = 0.0$ seconds(ii) $t = 0.5$ seconds

Figure 6.8 (continued)

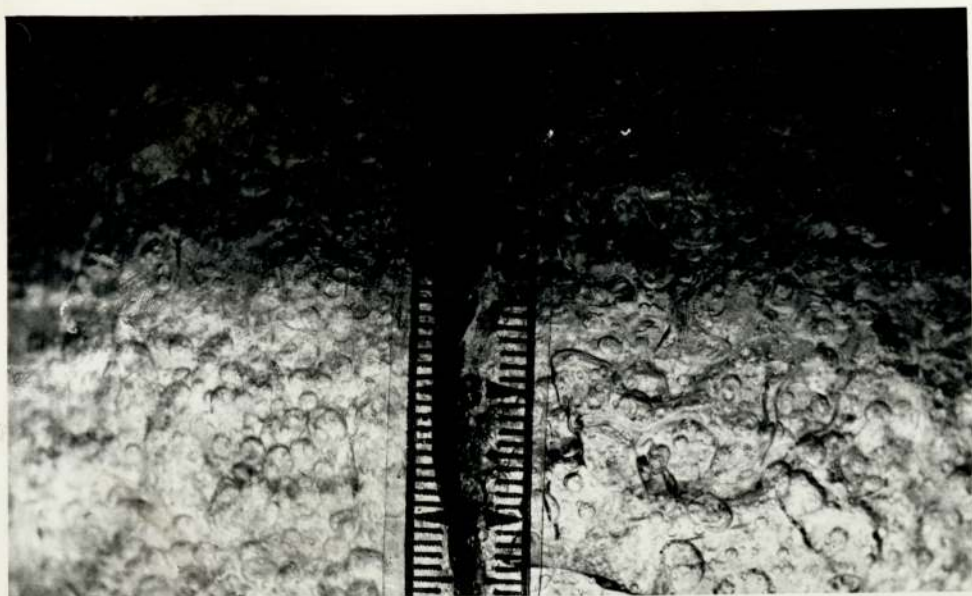


(iii) $t = 1.0$ seconds

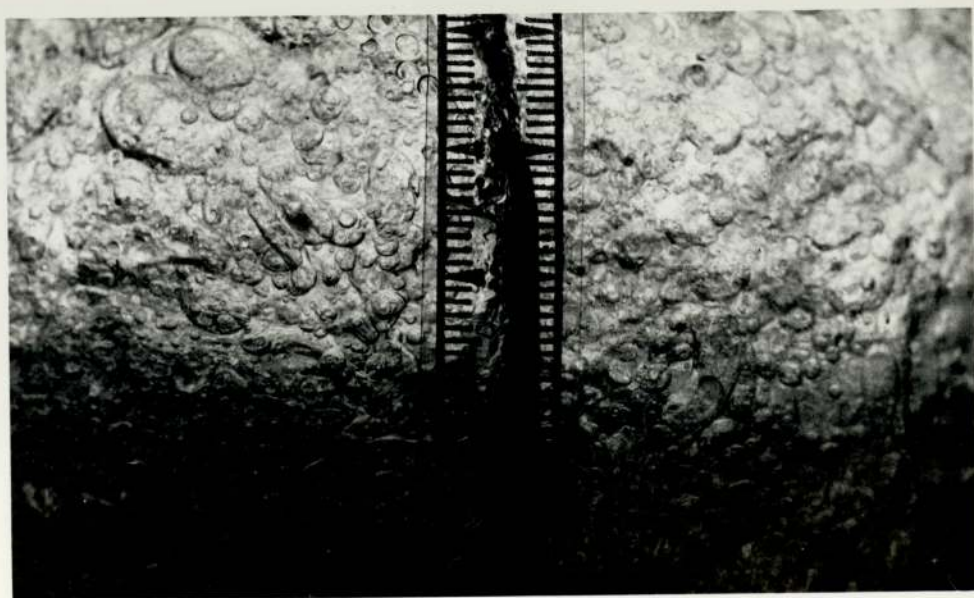


(iv) $t = 1.5$ seconds

Figure 6.8 (continued)



(v) $t = 2.0$ seconds



(vi) $t = 2.5$ seconds

6.4.2.1 Cleaning

An aqueous solution of Decon 90 of 1% concentration was used to clean the system, 25 litres of the solution were made. The solution was placed in each reservoir, the pumps were started and the flowrate was set at the maximum ($12 \times 10^{-5} \text{ m}^3/\text{s}$), the stirrer was switched on and set at maximum speed (750 r.p.m.) and the liquids were allowed to re-circulate for about 12 hours. The mixing vessel was then filled, together with as many connecting pipes as possible, and the settler was left to soak overnight. The system was completely drained, after which the apparatus was filled with tap water and all the pumps and the stirrer were switched on. The system was then drained. It was filled with tap water again and left to soak for ten hours. Finally, the system was drained and rinsed three times with deionized distilled water.

6.4.2.2 Liquid-Liquid Purity Test

This test was carried out in the same way as the batch experiments.

6.4.2.3 Start-up Procedure

The start-up procedure depends on the mode of operation, the continuous rig was operated in two modes:

- 1 Semi-batch
- 2 Continuous

This was done to enable the application of the results obtained from batch experiments to those of the continuous flow experiments.

6.4.2.3.1 Semi-batch Mode

As mentioned earlier these studies were performed by operating the continuous equipment under batch conditions, in order to compare the results obtained from batch experiments with those obtained by continuous operation.

The vessel was filled with the phase to be continuous. The inlet of this phase was then closed, the stirrer was switched on and set at the required level. The dispersed phase was then added through the respective inlet, and the flow rate was gradually reduced from approximately $1.5 \times 10^{-6} \text{ m}^3/\text{s}$ to $2 \times 10^{-7} \text{ m}^3/\text{s}$ as the phase inversion was approached. The inlet and outlet were closed immediately when the inversion commenced. The stirrer was then switched off and the phases left to settle. Respective volumes were then read from the calibration on the mixing vessel.

6.4.2.3.2 Continuous Mode

The pumps were switched on and the phases were introduced into the vessel, allowing the continuous phase to cover the impeller, the inlets were then closed. The impeller was then turned slowly and gradually brought to the required speed. The inlets were opened and the flowrates were adjusted to a ratio slightly lower than the expected phase inversion ratio (10%).

There were two positions for the outlet:

- 1 no flow from the top outlet
- 2 no flow from the bottom outlet

This was done in order to check the effect of the outlet position as regards phase escape.

In the event of condition 1 the bottom valve had to be adjusted so that the dispersion height remained constant.

The phase ratio was then altered by changing the dispersed phase flow rate by small amounts, allowing 30 minutes for steady-state conditions to be reached. This was then continued reducing the rate of increase of the flow rate of the dispersed phase as the limits of phase inversion were reached. Immediately after phase inversion the inlets and outlets were shut off and then the stirrer was switched off, the phases were allowed to settle and the volumes of the respective phases read as mentioned above.

This series of studies was carried out for varied total flow rates to study the effect of flow rate in short circuiting and escape frequency.

6.5 EXPERIMENTAL PROGRAMME

The experimental programme was designed to investigate different aspects on which the mathematical model was based.

6.5.1 Velocity Gradient Near Impeller

The collision frequency model is based on the fact that different drops move at different speeds, Figure 4.4 shows such a velocity gradient near the impeller region, which confirms the validity of assumptions made in the model.

These studies were carried out by using a shot of dye in an agitated tank having water as the solution.

The tank was placed in a photographic dark room and a strobe light source was used. The light frequency was adjusted so that the impeller appeared stationary. The shutter of the camera was then opened for one minute, during which time a shot of red dye was added. The dye used was Red Azo Dye.

6.5.2 Drop Size

These studies were set to find the most suitable drop size model. Figure 7.1 shows drop size variation with hold-up and Figure 7.6 shows drop size variation with rotor speed. The model selected was considered to be the best to describe the behaviour of drops under different conditions of hold-up and rotor speed. Figure 6.9 shows the predicted values with the actual values.

6.5.3 Drop Size Growth at Phase Inversion

These studies were carried out to confirm the main theory of the model which assumes that every collision causes coalescence, this was confirmed by study of the rate of growth of drops at phase inversion. Figure 6.10 shows the rate of drop growth at phase inversion and Figure 6.11 shows a typical dispersion undergoing phase

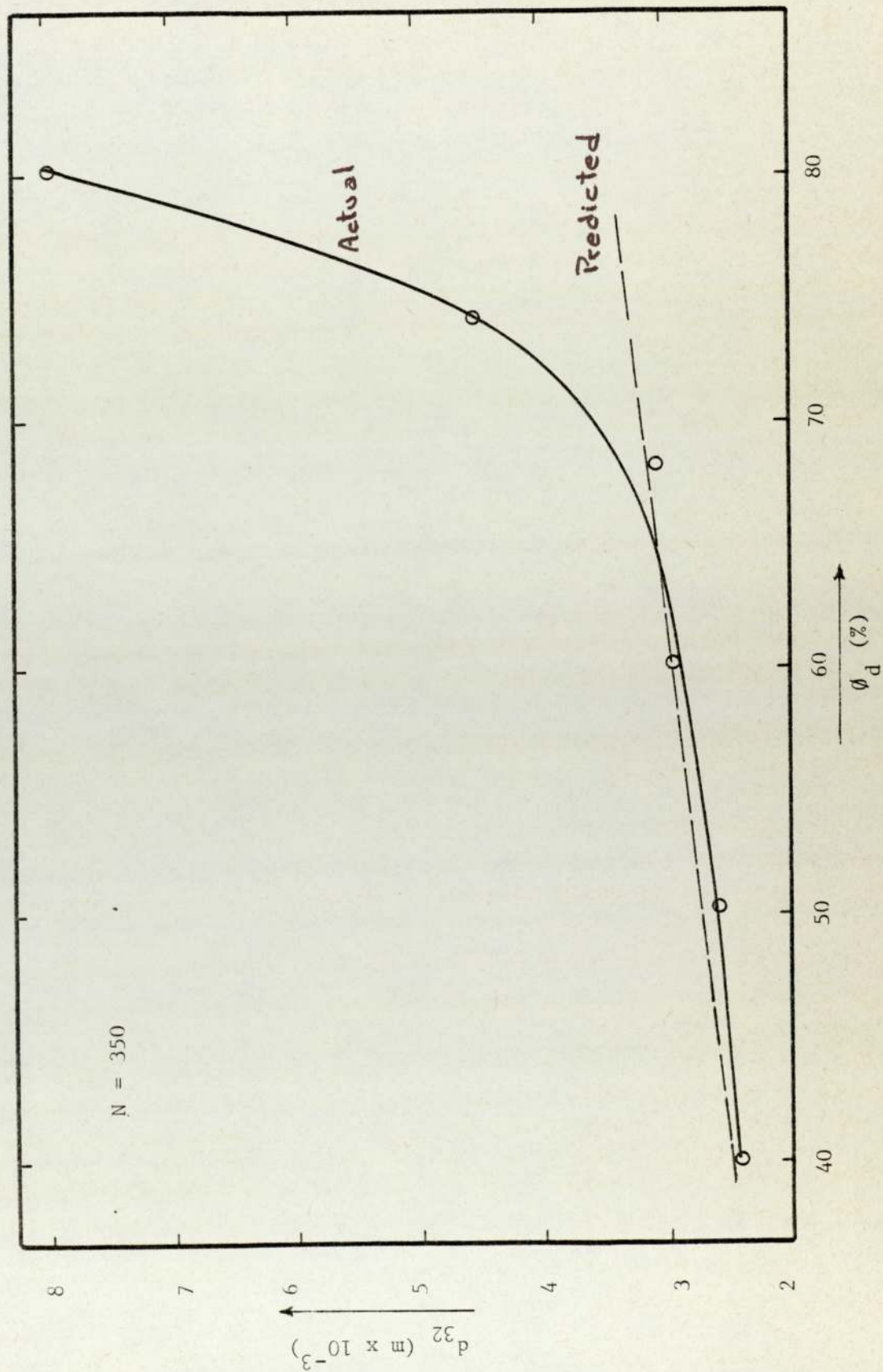
Figure 6.9 PREDICTED DROP SIZE VS ACTUAL DROP SIZE

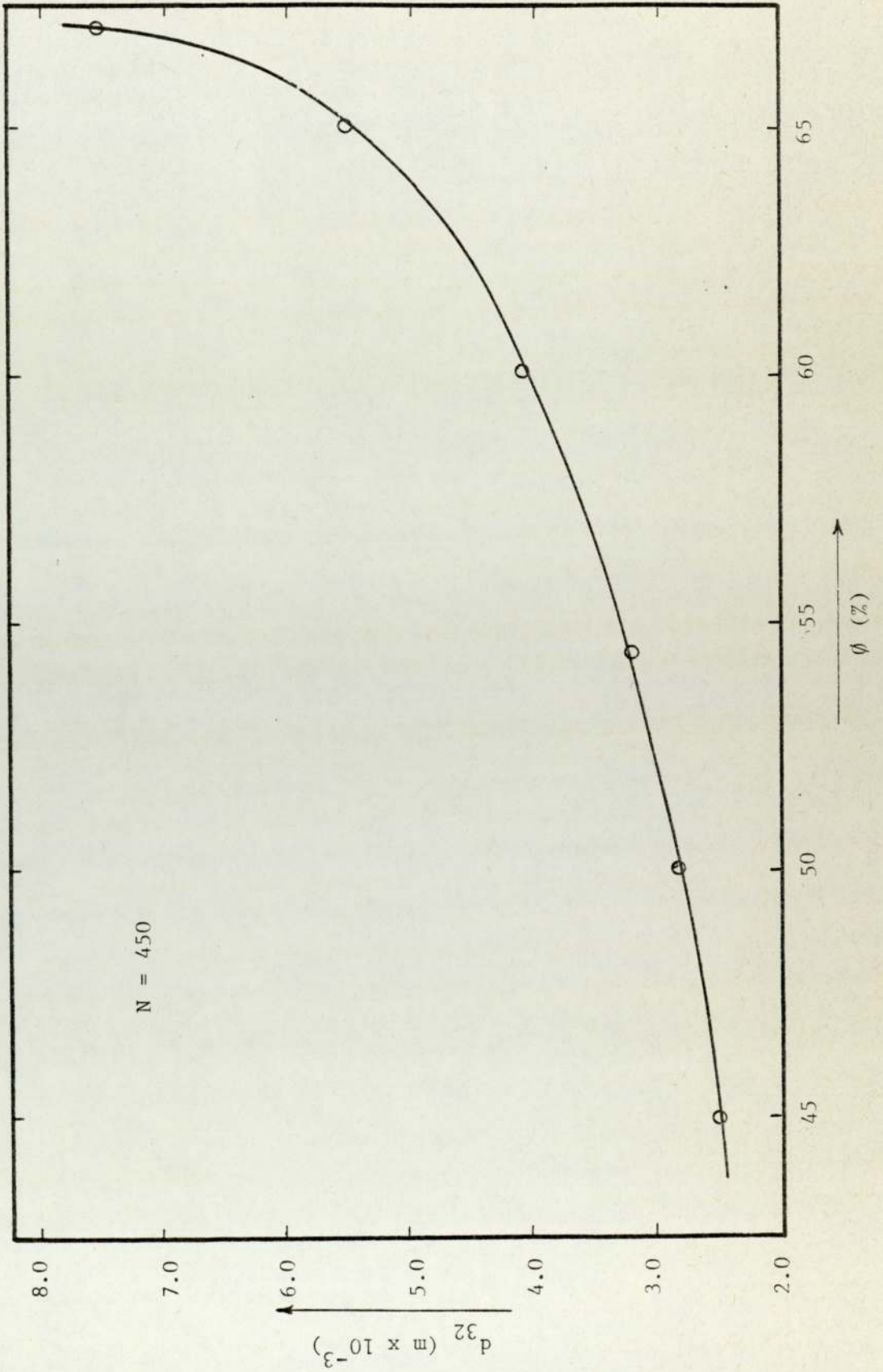
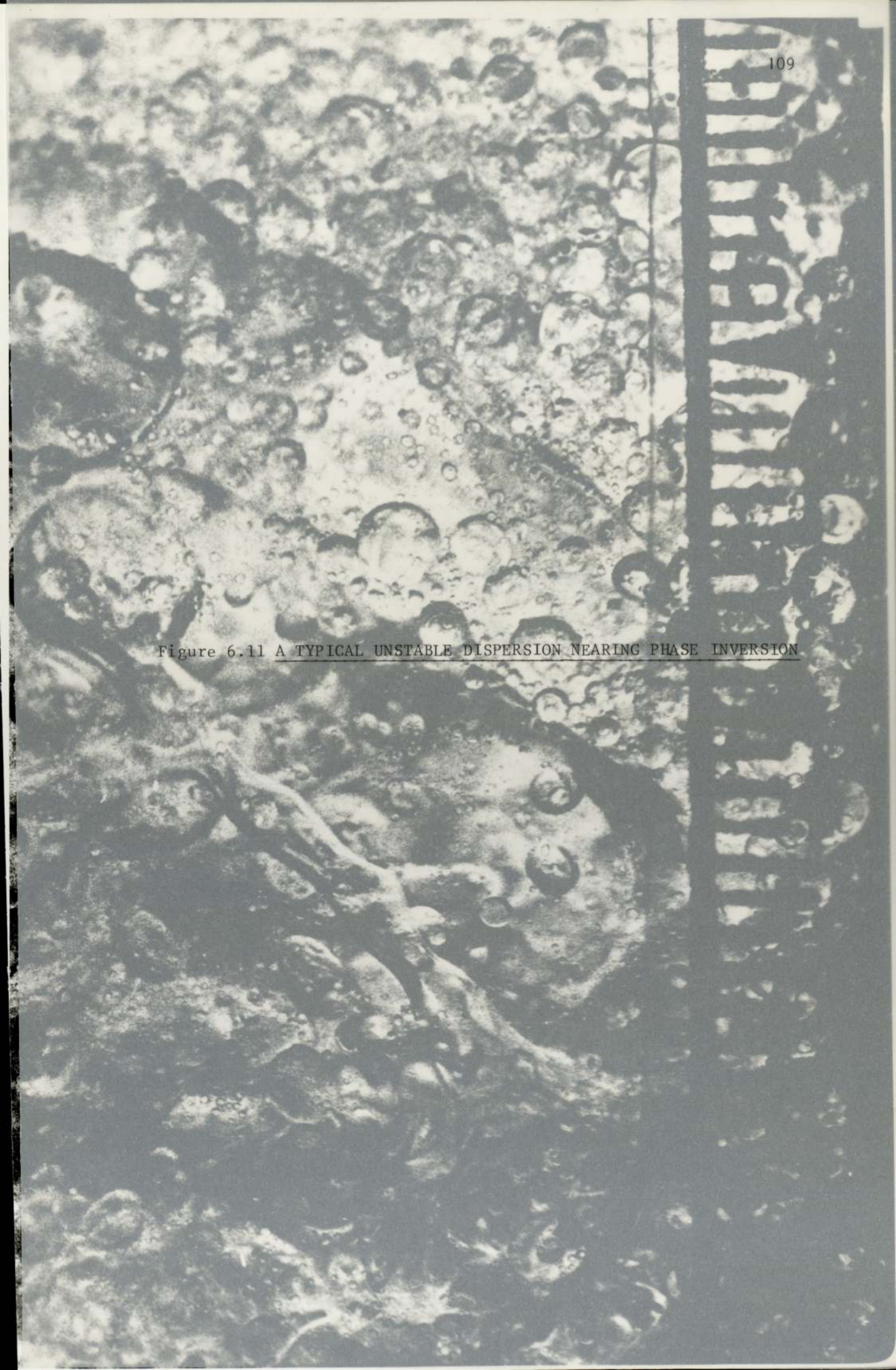
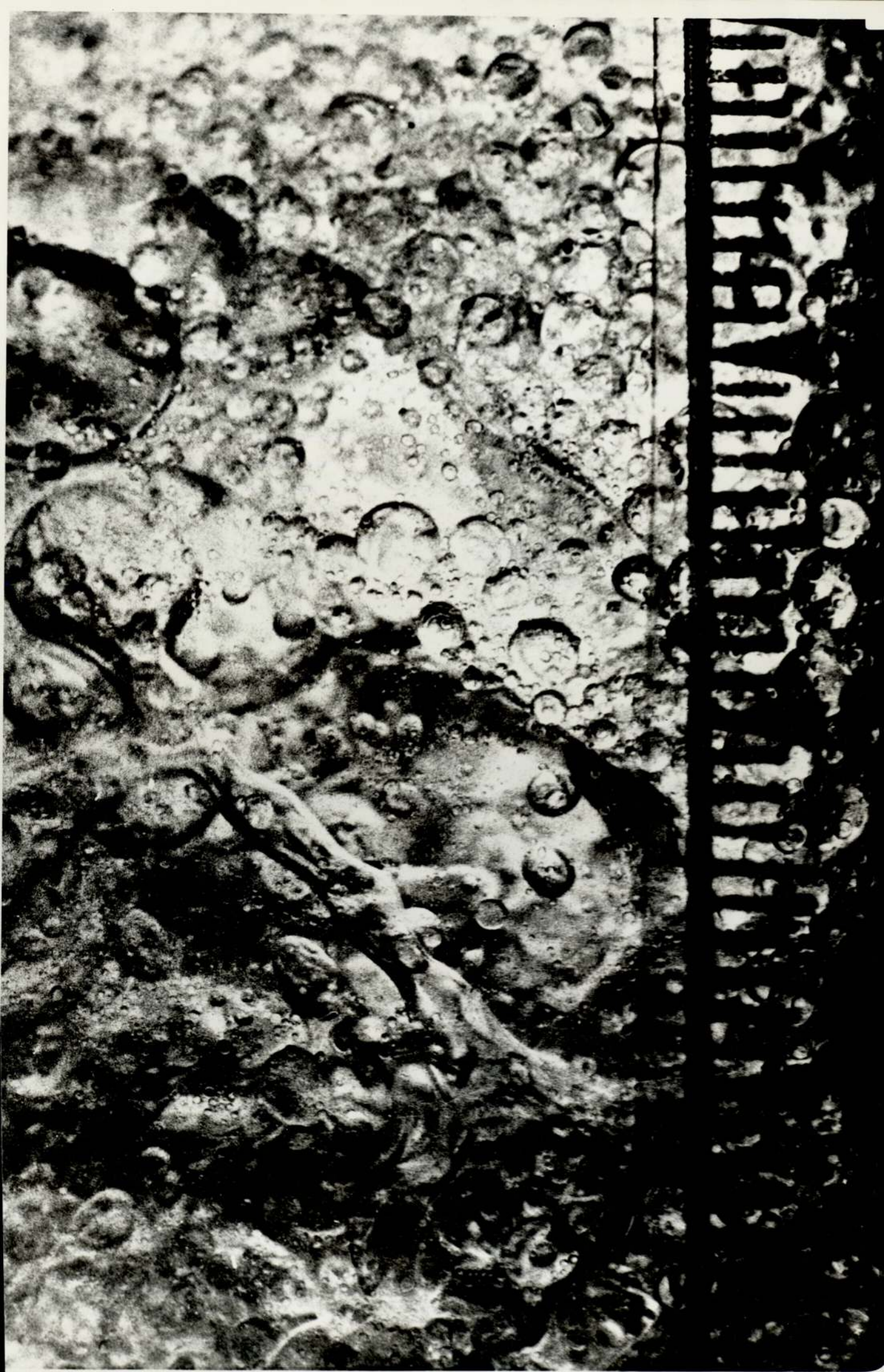
Figure 6.10 DROP GROWTH WITH HOLD-UP NEAR PHASE INVERSION

Figure 6.11 A TYPICAL UNSTABLE DISPERSION NEARING PHASE INVERSION





inversion.

6.5.4 Limits of Phase Inversion

Hold-ups at inversion were plotted for different systems to produce the limits of ambivalence. These results were then compared with the predicted results. Figure 4.1 shows a typical system with calculated values plotted to compare the mathematical model proposed with the actual experimental results.

6.6 MATCHING REFRACTIVE INDEXES

The most convenient method of formulating a model for phase inversion is to observe the processes involved in the phenomenon. Due to the lensing effect it is not possible to study zones of coalescence and breakage. However, this problem can be overcome by the matching of the refractive indexes, with the result that a clear solution is observed in which the drops will not be visible. It was found that the most suitable dye was a fluorescent dye which would become activated instantaneously by light, the most suitable light is ultraviolet light. The degree of activation depends on the intensity of the light which reaches the dye. Unfortunately, ordinary glass absorbs approximately 80% of the light, this made it impossible to collect photographic records of processes in the vessel, one was therefore limited to visual observation. It is however possible to make the vessel from special glass which would allow approximately 90% of the ultraviolet light to reach the vessel, Figure 6.12 shows the arrangement of apparatus.

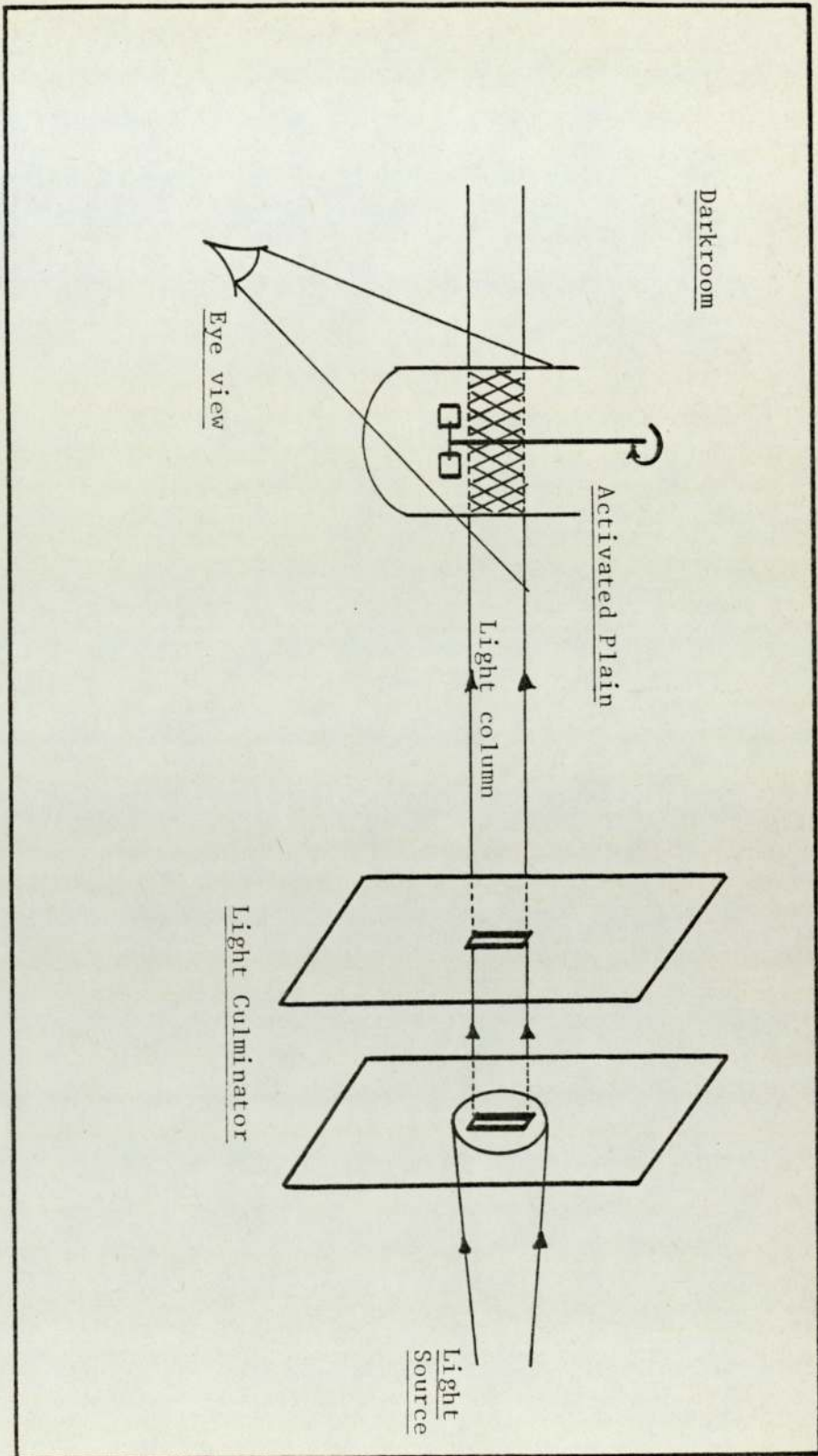


Figure 6.12 ARRANGEMENT OF MATCHING REFRACTIVE INDEX APPARATUS

Appendix (6) shows the variation of refractive indexes of water and glycerine and details of the dyes used.

CHAPTER SEVEN

EXPERIMENTAL PROCEDURE

AND RESULTS

7 EXPERIMENTAL PROCEDURE AND RESULTS

7.1 BATCH MIXING VESSEL

7.1.1 Drop Sizes vs Rotor Speed and Hold-up

The study was conducted to select a suitable correlation for the prediction of drop sizes. The study was carried out in two parts as follows:

- a) Drop Size vs Rotor Speed.
- b) Drop Size vs Hold-up.

The procedure and results obtained are discussed in the following sub-sections.

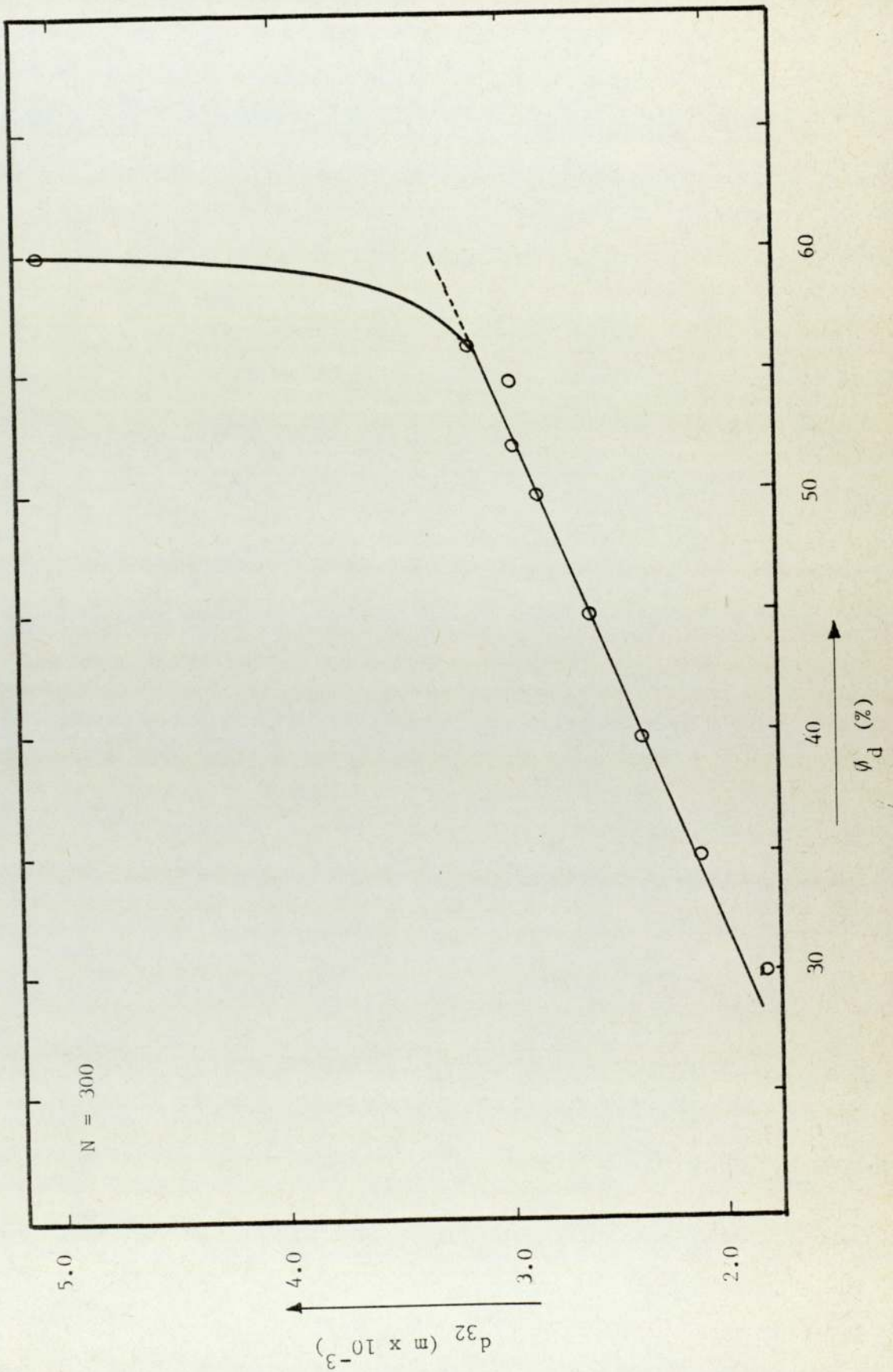
a) Drop Size vs Rotor Speed

These studies were conducted to assess the variation of drop size with rotor speed at different hold-ups in a range varying from 25% to 55% of the dispersed phase. The results obtained are presented in figures 7.1 to 7.5.

The speed of the impeller was adjusted to the desired value for a fixed hold-up. Ten minutes were allowed for the establishment of steady state conditions, and then three photographs were taken using a 35 mm camera with an uprated HP5 film to enable the counting of approximately 300 droplets. This was repeated for various rotor speeds.

b) Drop Size vs Hold-up

The procedure for these studies was similar to that

Figure 7.1 VARIATION OF DROP SIZE WITH HOLD-UP

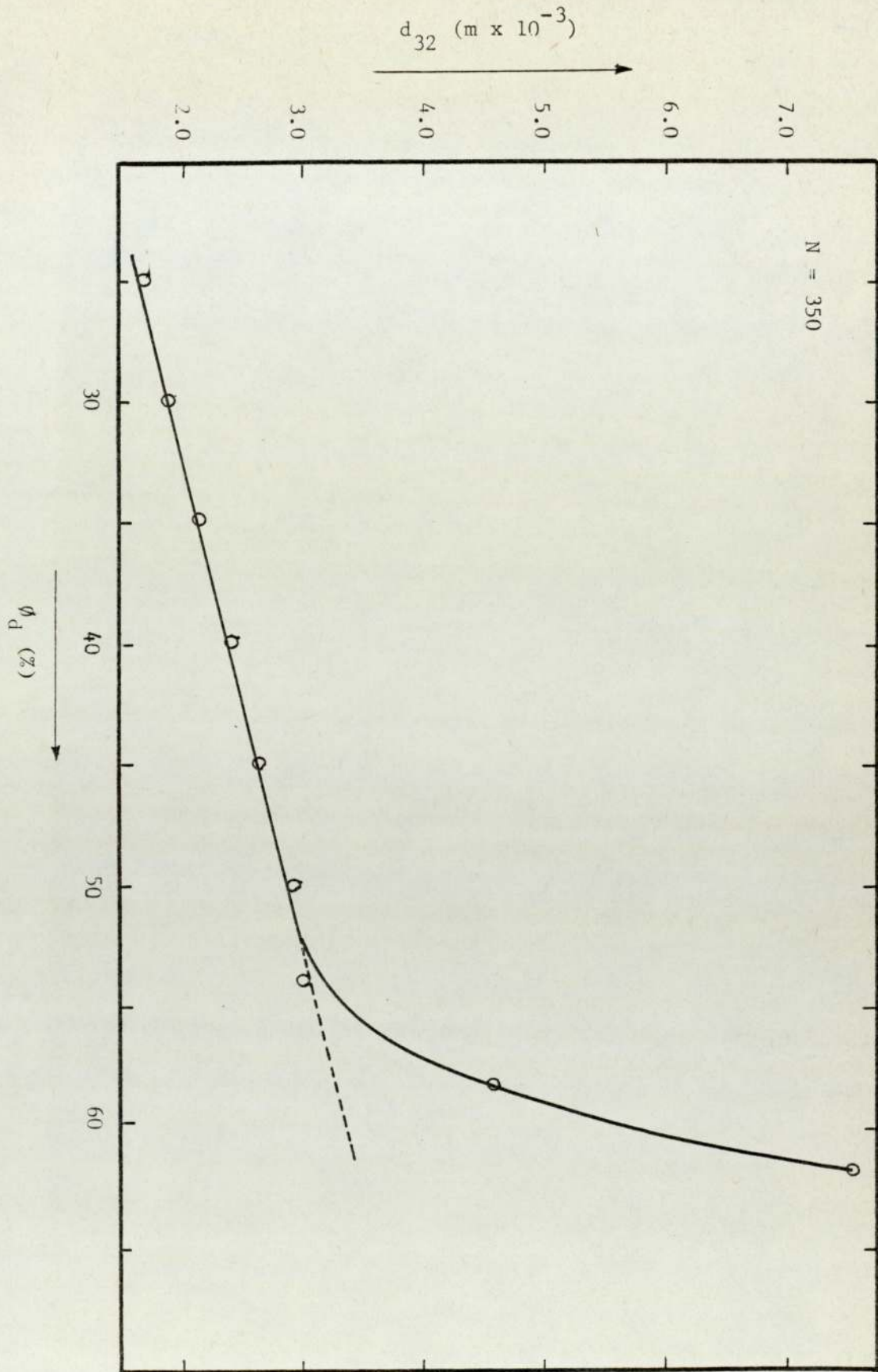


Figure 7.3 VARIATION OF DROP SIZE WITH HOLD-UP

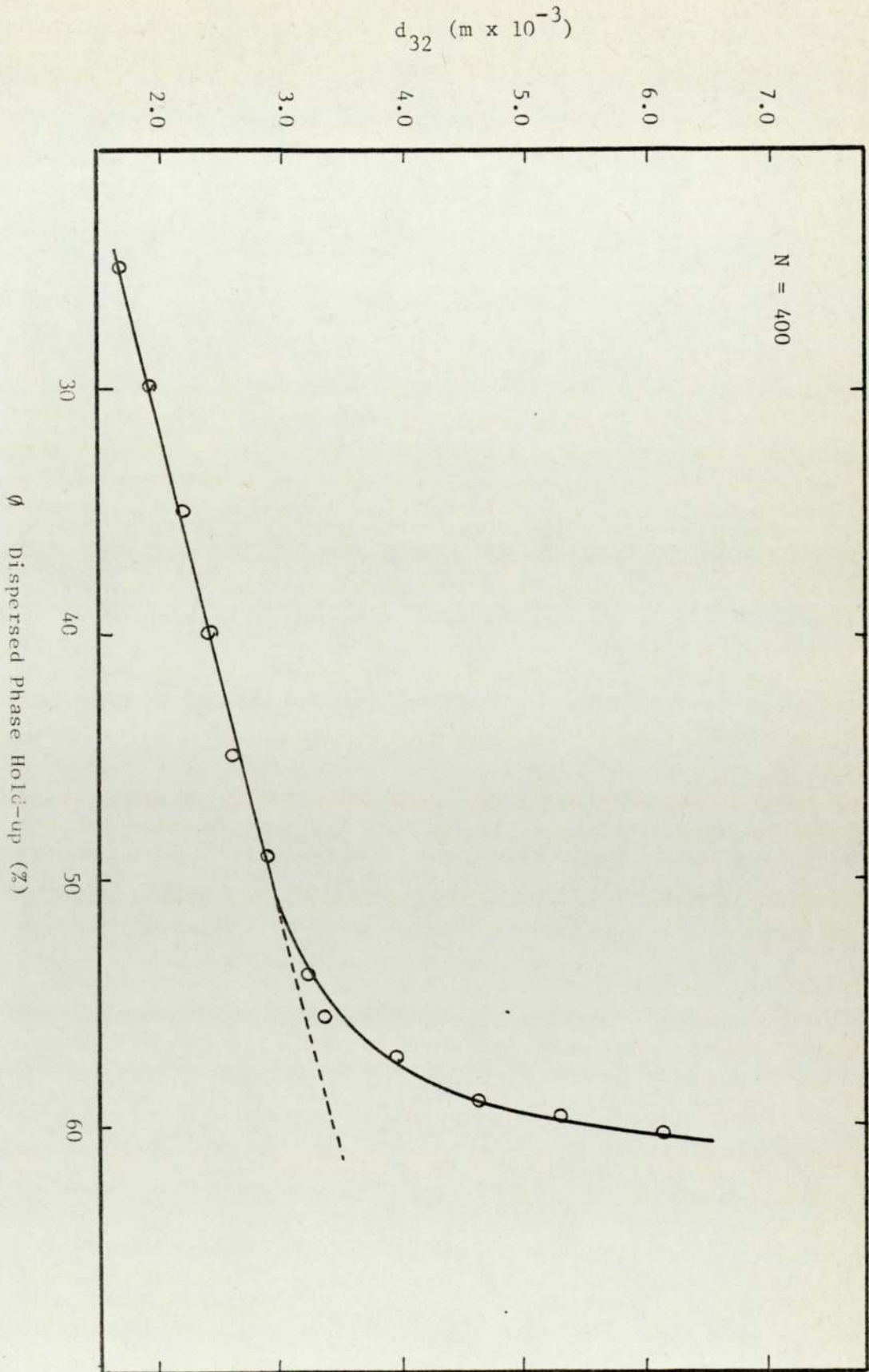


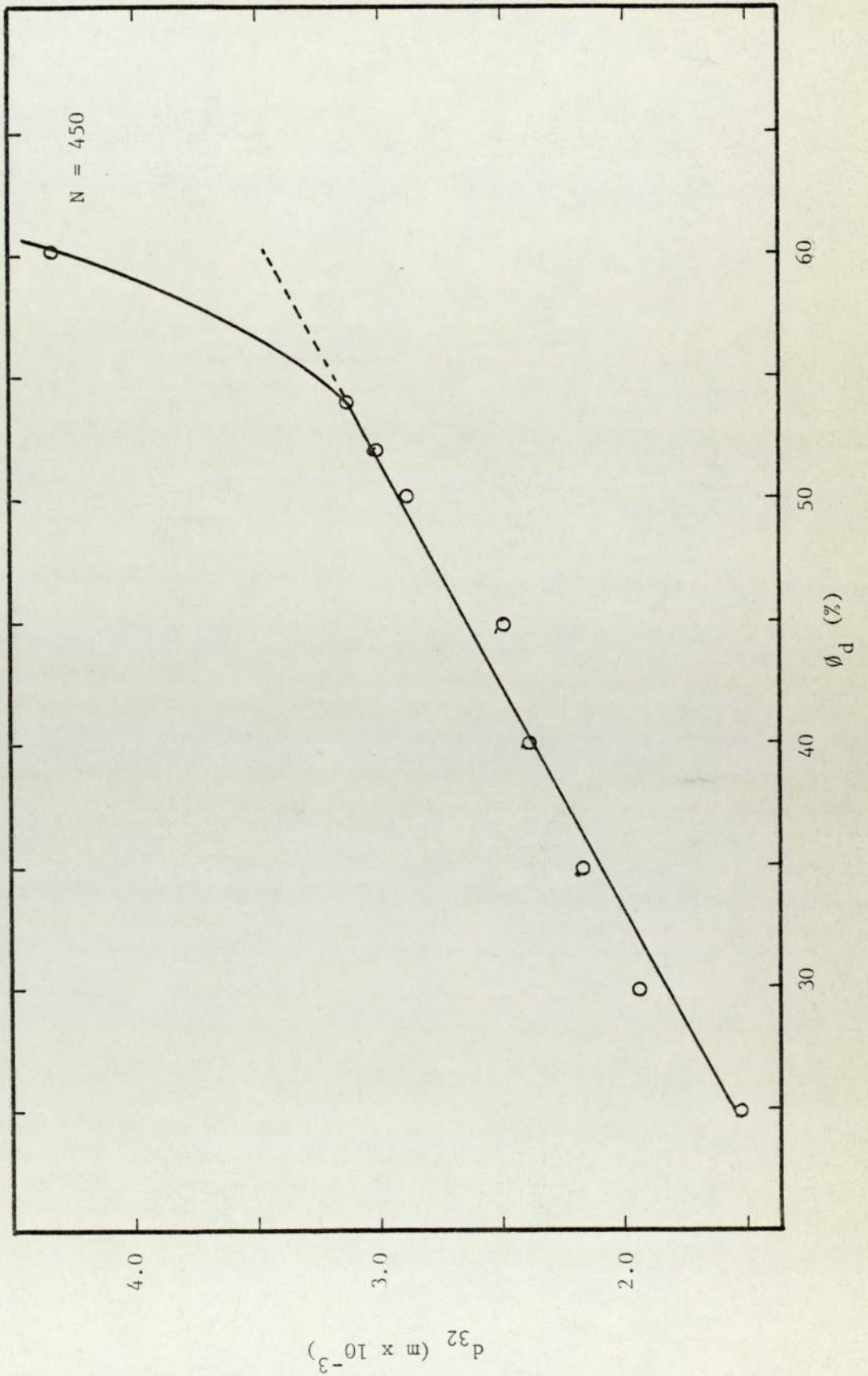
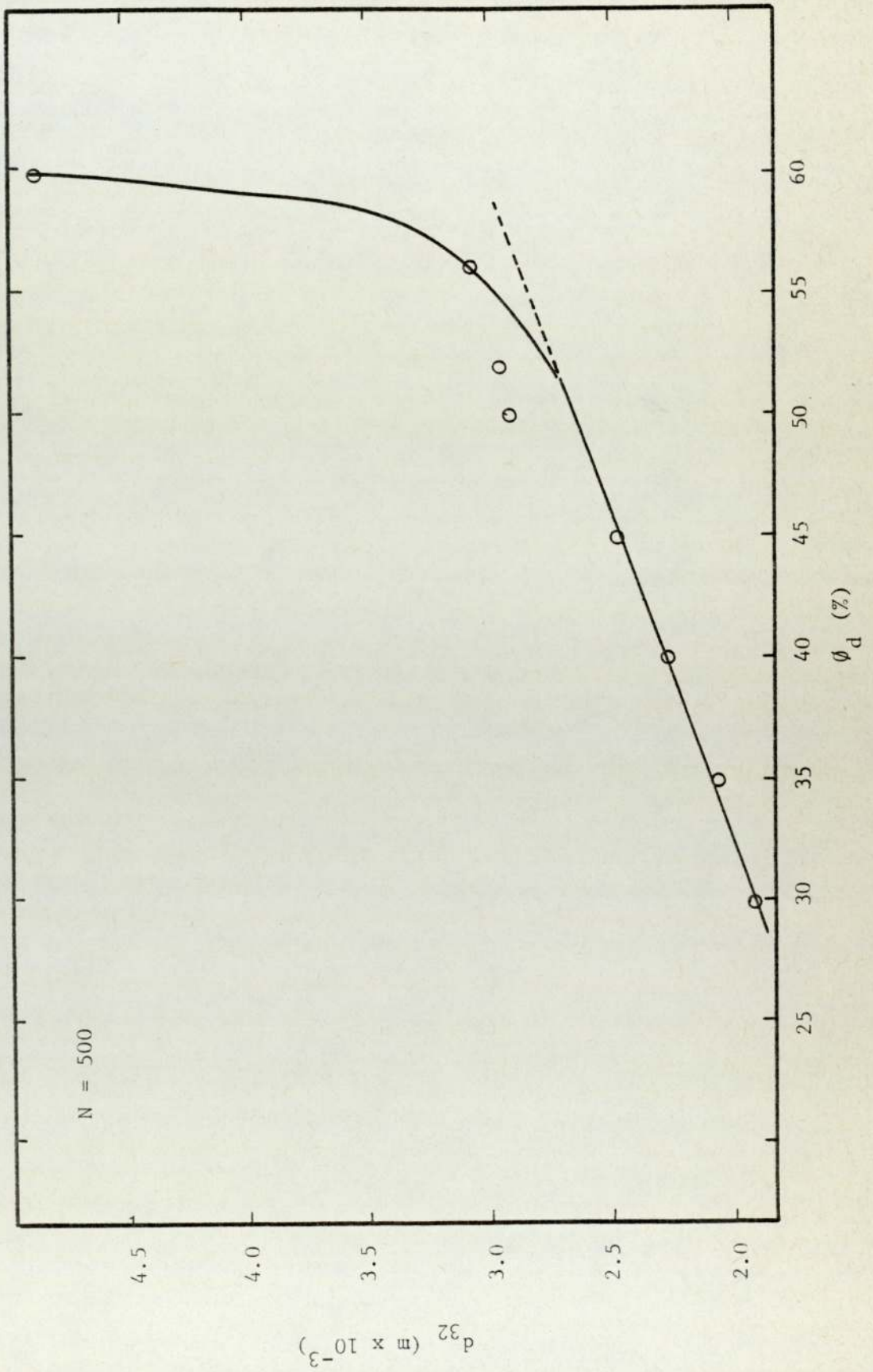
Figure 7.4 VARIATION OF DROP SIZE WITH HOLD-UP

Figure 7.5 VARIATION OF DROP SIZE WITH HOLD-UP

of the above experiments. In these studies the rotor speed was kept constant and drop sizes were measured for various hold-ups.

The results are presented in figure 7.6.

7.1.2 Drop Size at High Hold-up

These studies were in effect a continuation of the above studies at high hold-ups. They were carried out, as before, in two parts using the same techniques as discussed in previous sections.

The results of these studies are presented in figures 7.7 to 7.9.

7.1.3 Drop Size Growth at Point of Inversion

The study of the growth rate of drops at phase inversion involved setting the hydrodynamic conditions so that the limits of phase inversion were about to be achieved. A Chinon ME 35 mm camera with a motor drive set at 2 frames per second was prefocused and set to operate. Small amounts of dispersed phase were then added at minute intervals from an automatic burette. As the phase inversion was about to commence the camera was switched on and operated through the whole phase inversion. The photographs were then analysed as discussed previously in Chapter 6.

These studies were carried out for a number of phase inversion experiments and figures 7.7 - 7.8 show typical phase inversion sequences.

7.1.4 The Limits of Phase Inversion

The limit of phase inversion was determined for a number of systems and the results obtained are shown in

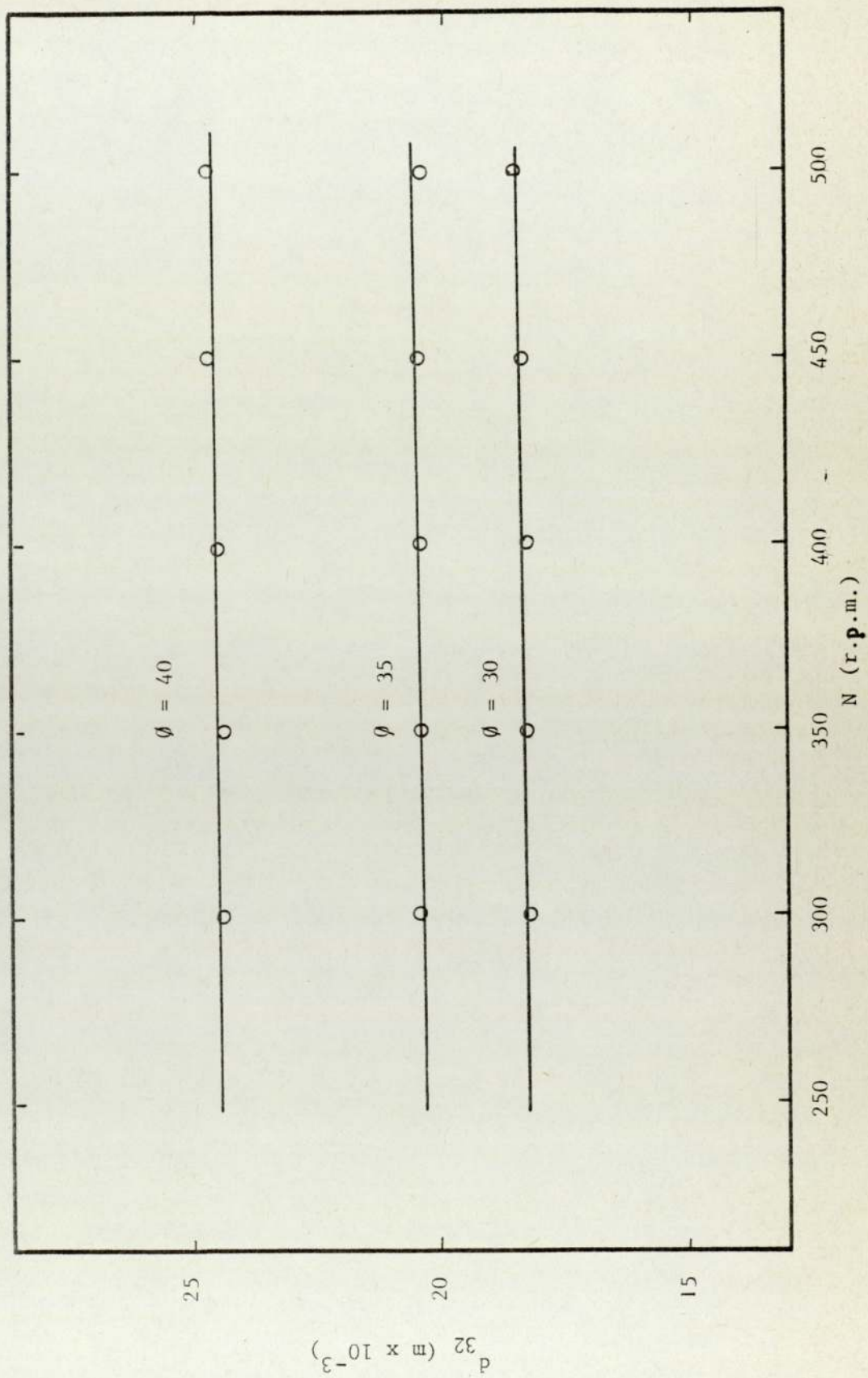
Figure 7.6 DROP SIZE VS ROTOR SPEED

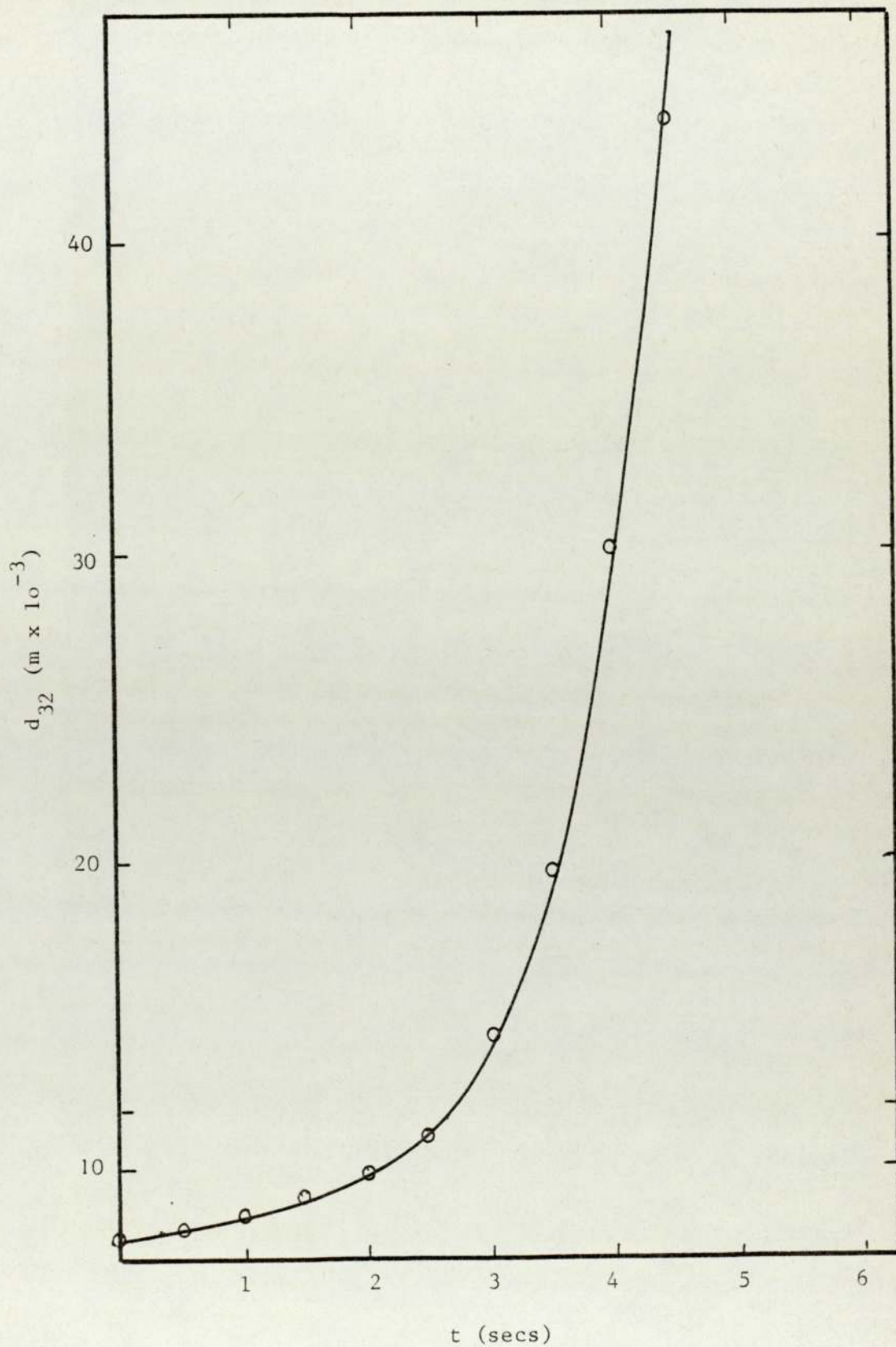
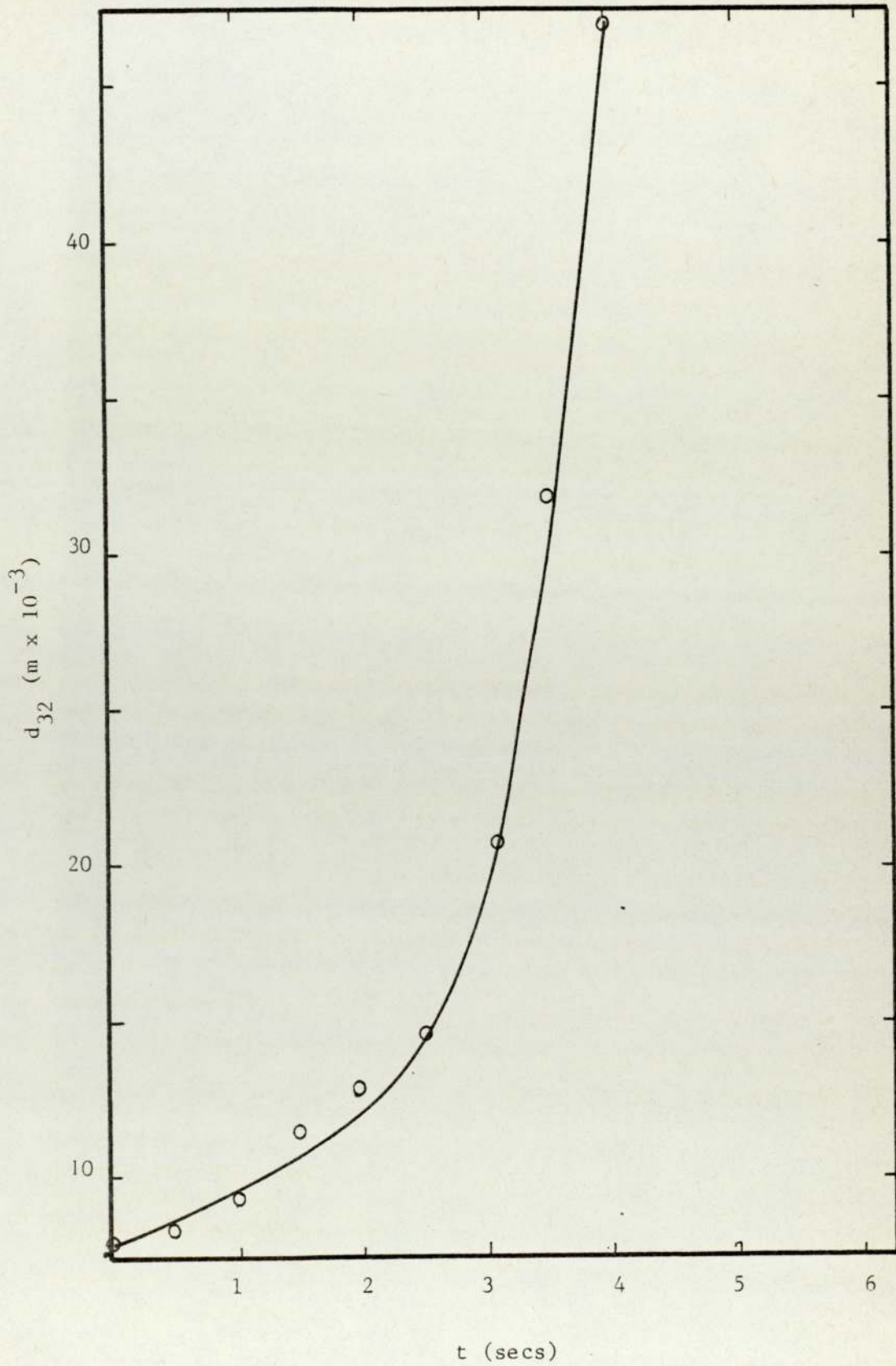
Figure 7.7 DROP SIZE GROWTH VS TIME AT PHASE INVERSION(N = 400)

Figure 7.8 DROP SIZE GROWTH VS TIME AT PHASE INVERSION

(N = 300)



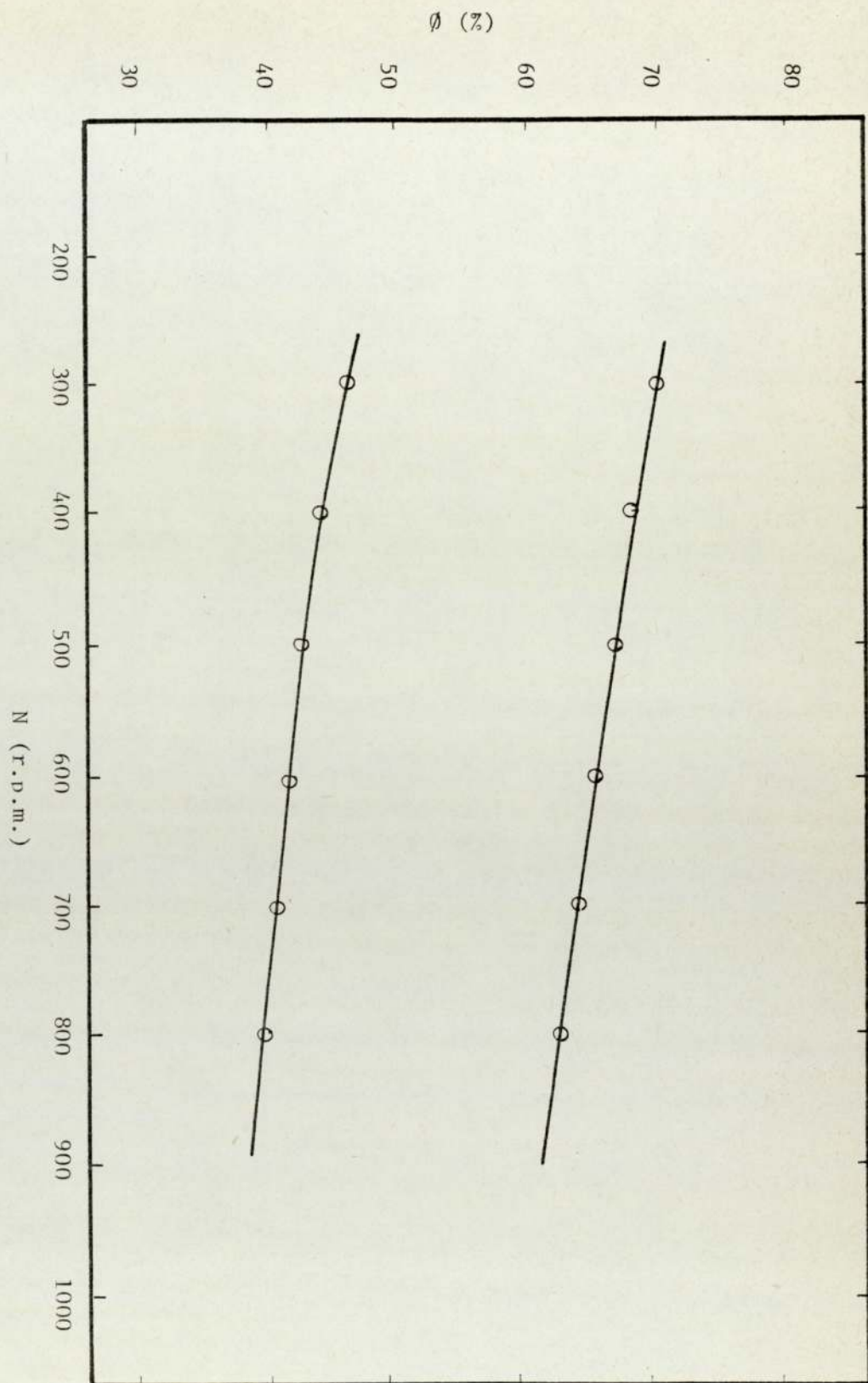


Figure 7.9 AMBIVALENT PHASE INVERSION LIMITS
(TOLUENE/WATER)

figures 7.9 - 7.13.

The tank was filled so that the impeller was immersed with the continuous phase; i.e. about 450 mls of the continuous phase. The impeller was switched on and the speed was set at the required rate. Dispersed phase was added until the total volume became 825 ml. Then 50 mls of the dispersion were slowly withdrawn. About 15 minutes were allowed so that steady state conditions were reached and then dispersed phase was added until the total volume again became 825 ml. The process was repeated until the frequency of the globules increased. Great care was taken in withdrawing the 50 mls portions. The process was repeated until the Continuous Phase Detector Signal became frequent. 5.0 mls. of dispersed phase were added at 5 minute intervals until phase inversion commenced. After inversion the dispersed phase hold-up was measured and plotted against the rotor speed. The experiments were repeated at least three times for each set of conditions and the results of phase inversion limits are shown in Appendix 8.

7.1.5 Matching Refractive Indexes

Matching of the refractive indexes was carried out to observe the processes involved in phase inversion and to ascertain the regions where initiation occurred. The addition of a second liquid changes the refractive index of a liquid mixture. Appendix 6 shows the change of refractive index of a mixture of water glycerol with varying concentrations of glycerol. When the refractive

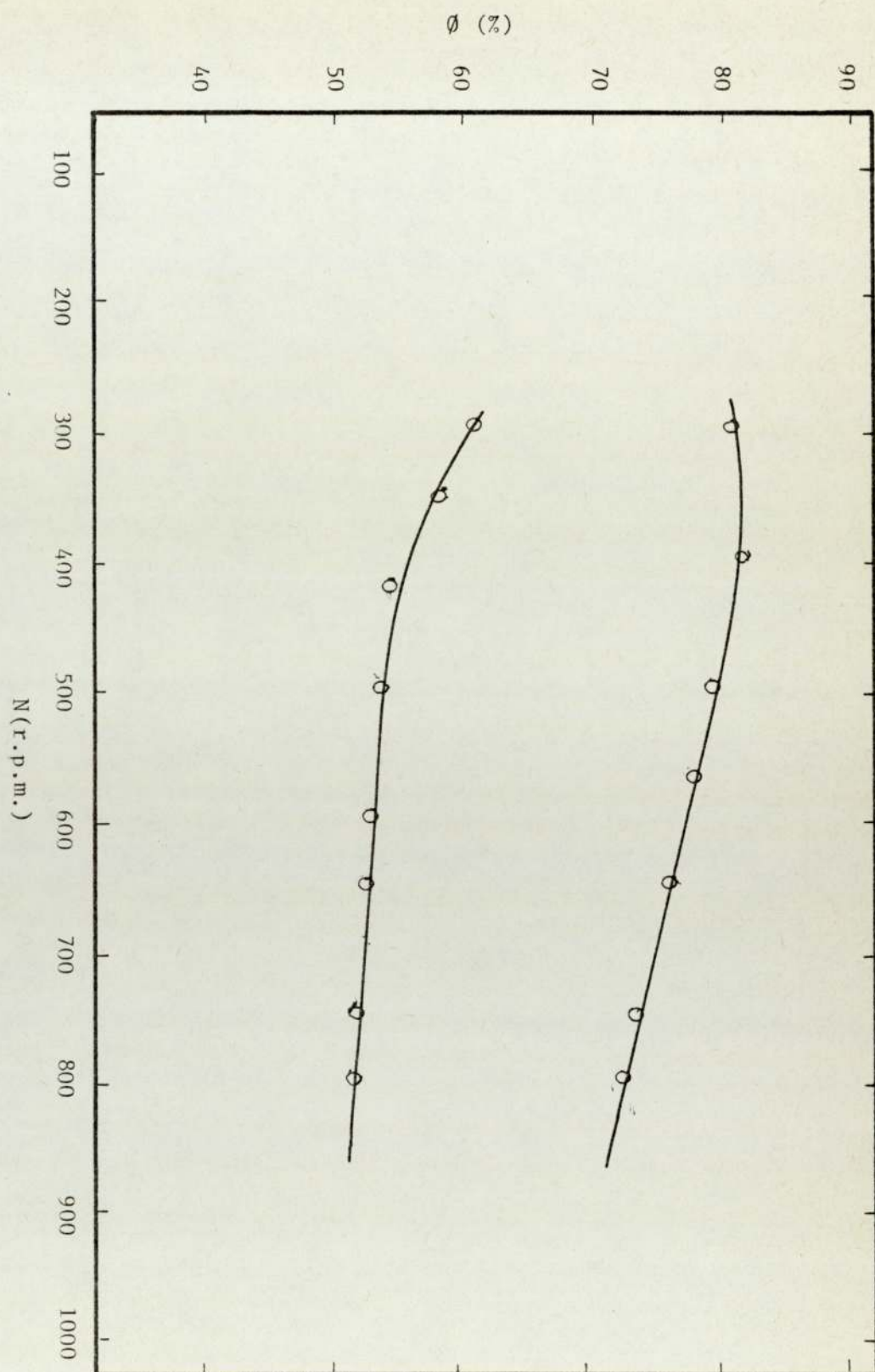


Figure 7.10 AMBIVALENT PHASE INVERSION LIMITS

(CC14/WATER)

Figure 7.11 AMBIVALENT PHASE INVERSION LIMITS (70% TOLUENE
+ 30% CCl₄/WATER)

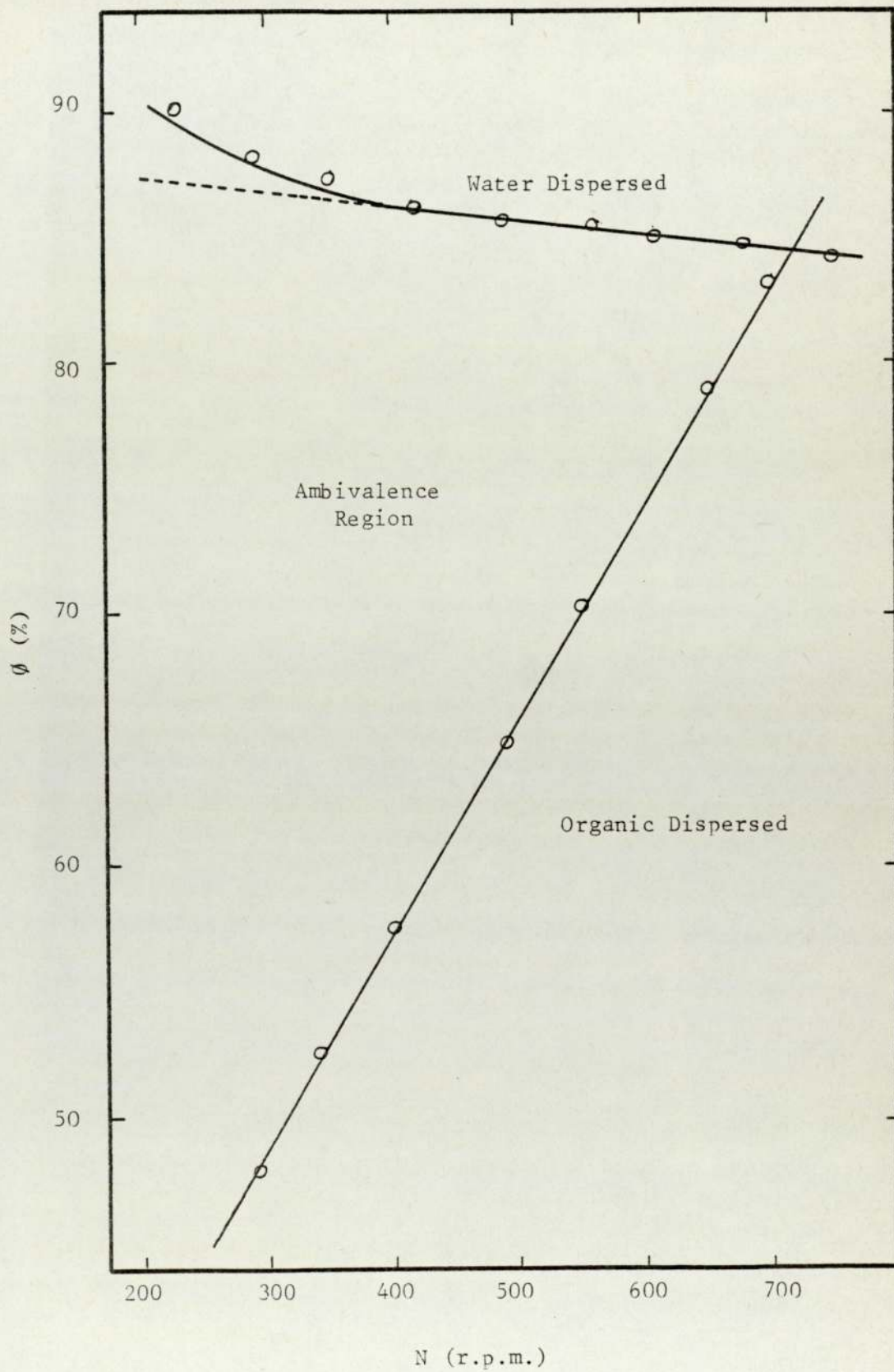


Figure 7.12 AMBIVALENT PHASE INVERSION LIMITS (63% TOLUENE
+ 37% CCl₄/WATER)

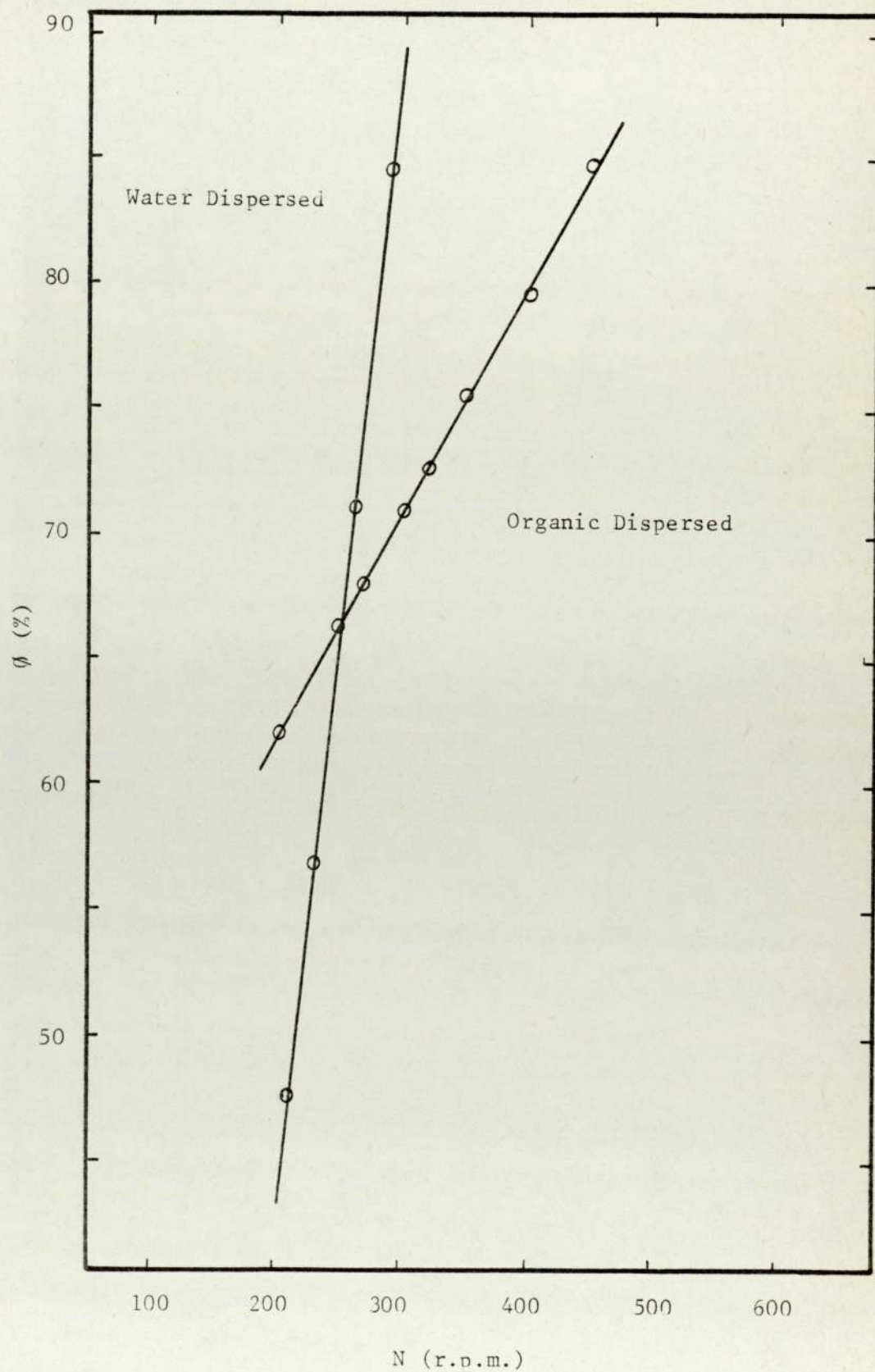
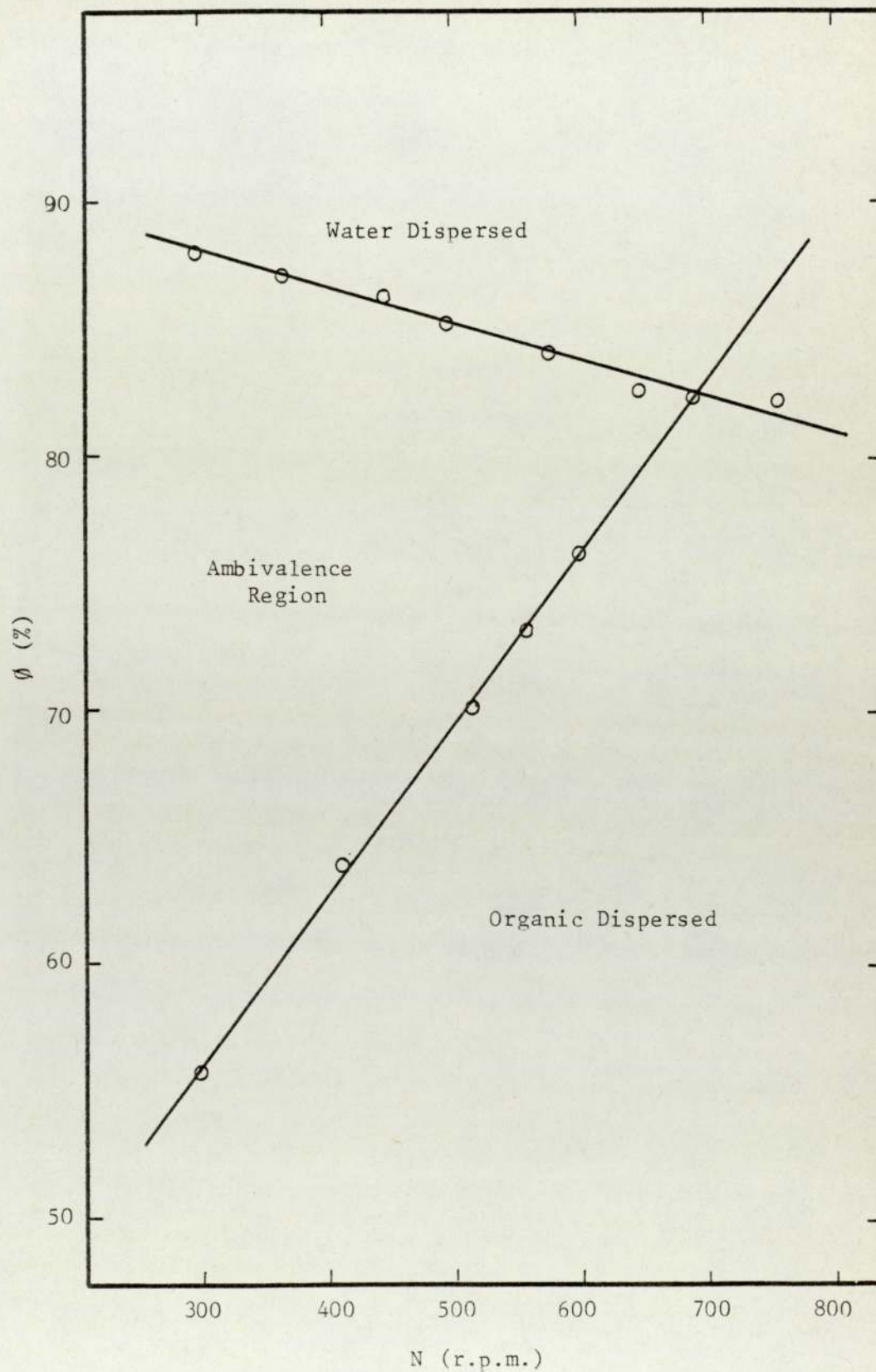


Figure 7.13 AMBIVALENT PHASE INVERSION LIMITS (30% TOLUENE
+ 70% CCl₄/WATER)



indexes of two immiscible liquids are matched the dispersion formed will be clear because the lensing effect is removed. The addition of a light sensitive dye, in this case a yellow fluorescent organic soluble and yellow fluorescent water soluble, enables selected areas of the dispersion to be viewed by using a powerful beam of light. The water soluble fluorescent dye was fluorescive and the oil soluble dye was Tratan Yellow.

Fluorescent dye was found to be most suitable as only small amounts need to be used, the only difficulty was the light source. The ideal light source would be an ultraviolet laser light in conjunction with a special glass vessel which will allow most of the ultraviolet light to pass, which would then enable a photographic survey of various parts of dispersion to be conducted. The present set up, however, only permitted a visual observation to be carried out. The results of these observations will be discussed in Chapter 8.

7.1.6 Flow Pattern Studies

These experiments were performed in a totally dark room. The lighting source used was a stroboscope giving 50 flashes per second. The agitator was set at a fixed speed and small quantities of dye were added. The flow pattern was then recorded using a 35 mm camera with a shutter speed setting of 1 second. A typical flow pattern study is shown in Figure 4.2.

7.2 CONTINUOUS MIXER-SETTLER

7.2.1 Phase Inversion Under Batch Condition

The vessel was filled with the phase to be continuous until the impeller was fully immersed. The other phase was then introduced and the agitator was turned slowly until the

interface was broken gradually, after which the speed was increased and set at a value desired for the experiment. The dispersed phase was added from the inlet port and the level was automatically adjusted by the upper outlet port. The dispersed phase was added until the liquid detector signal was consistent i.e. the light in the circuit flashed in and out uniformly, the inlet rate was then reduced to $2.0 \times 10^{-7} \text{ m}^3/\text{s}$. Immediately after the phase inversion commenced the inlet port was closed. After phase inversion the impeller was switched off and the hold-ups noted from the graduated vessel. This was done to reduce the possibilities of solvents becoming contaminated in handling. The experiment was repeated at least three times for each set of rotor speed and the results of these experiments are shown in Figure 7.14. The shape of phase inversion hysteresis shows a remarkable similarity to that obtained in the batch mixer unit shown in Figures 7.9 - 7.13.

7.2.2 Phase Inversion Under Continuous Operation

The start up procedure was similar to that discussed in the above section. After the initiation of dispersion the inlet flow rates were adjusted so that the phase ratio was about 10% below the limit of phase inversion. About half an hour was allowed so that the phase ratio inside the mixing vessel was the same as that of the flow. The flow rate was adjusted keeping the total flow rate constant so that over two hours the phase ratio was about 2% to 3% below the phase inversion limit. The

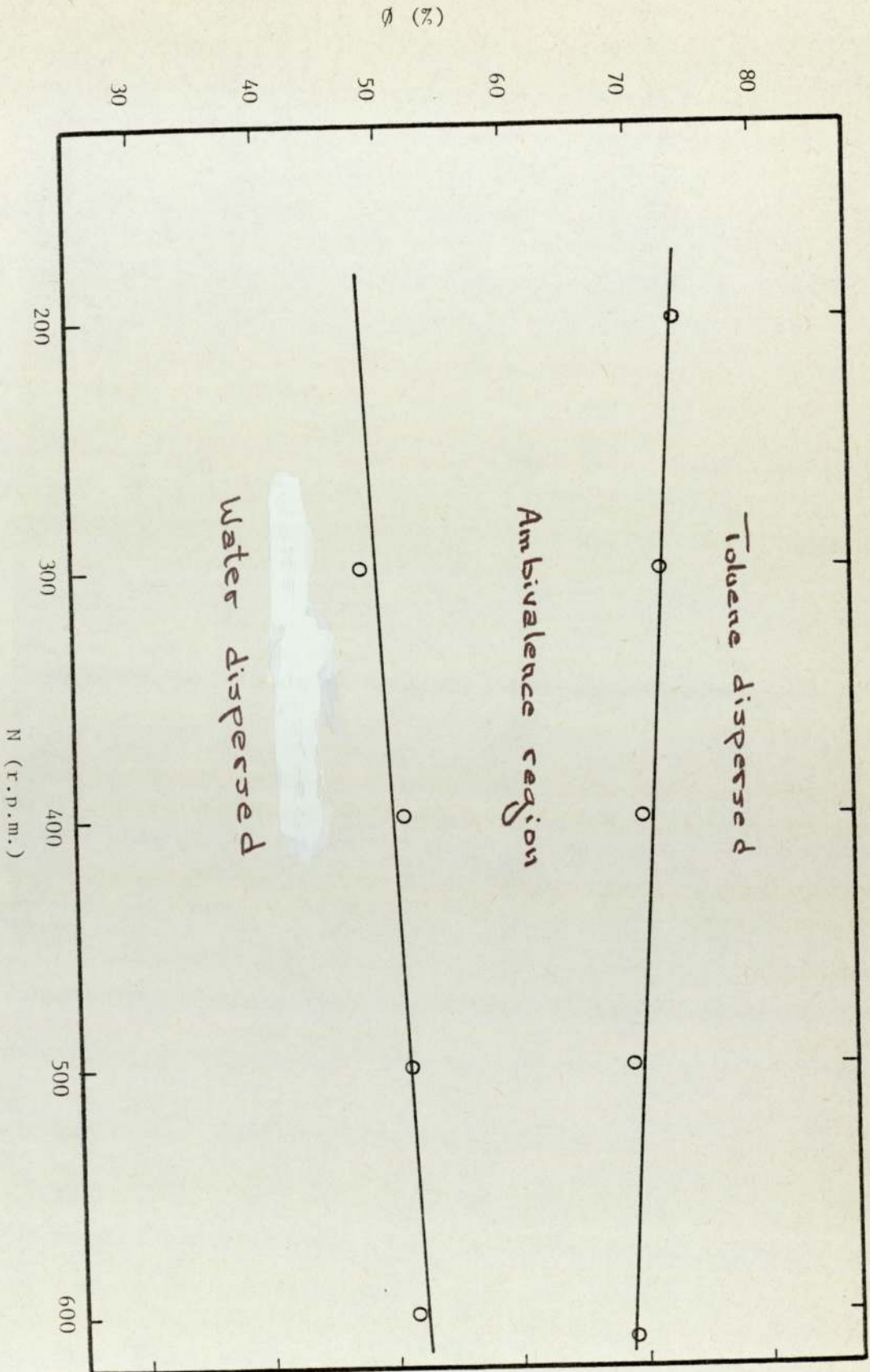


Figure 7.14 AMBIVALENT PHASE INVERSION LIMITS FOR THE CONTINUOUS RIG UNDER BATCH CONDITIONS

phase ratio was then changed by small increments at 15 minute intervals until phase inversion commenced. All the ports were immediately closed after phase inversion. The hold-up was measured as in the previous section. The experiments were repeated for the same conditions at least three times. Experiments were carried out to determine the limits of phase inversion versus various operating conditions, i.e. rotor speed, flow rate and the effect of the outlet port, Figures 7.15 - 7.18.

The results are presented in Appendix 9.

7.2.3 Phase Inversion Versus Input Rate

The operating procedure was similar to that discussed in section 7.2.2. The effect of flow rate was studied for three levels of agitation intensity. The results are shown in Figure 7.19. The effect of mode of operation is shown in Figure 7.20.

Figure 7.15 PHASE INVERSION IN THE CONTINUOUS

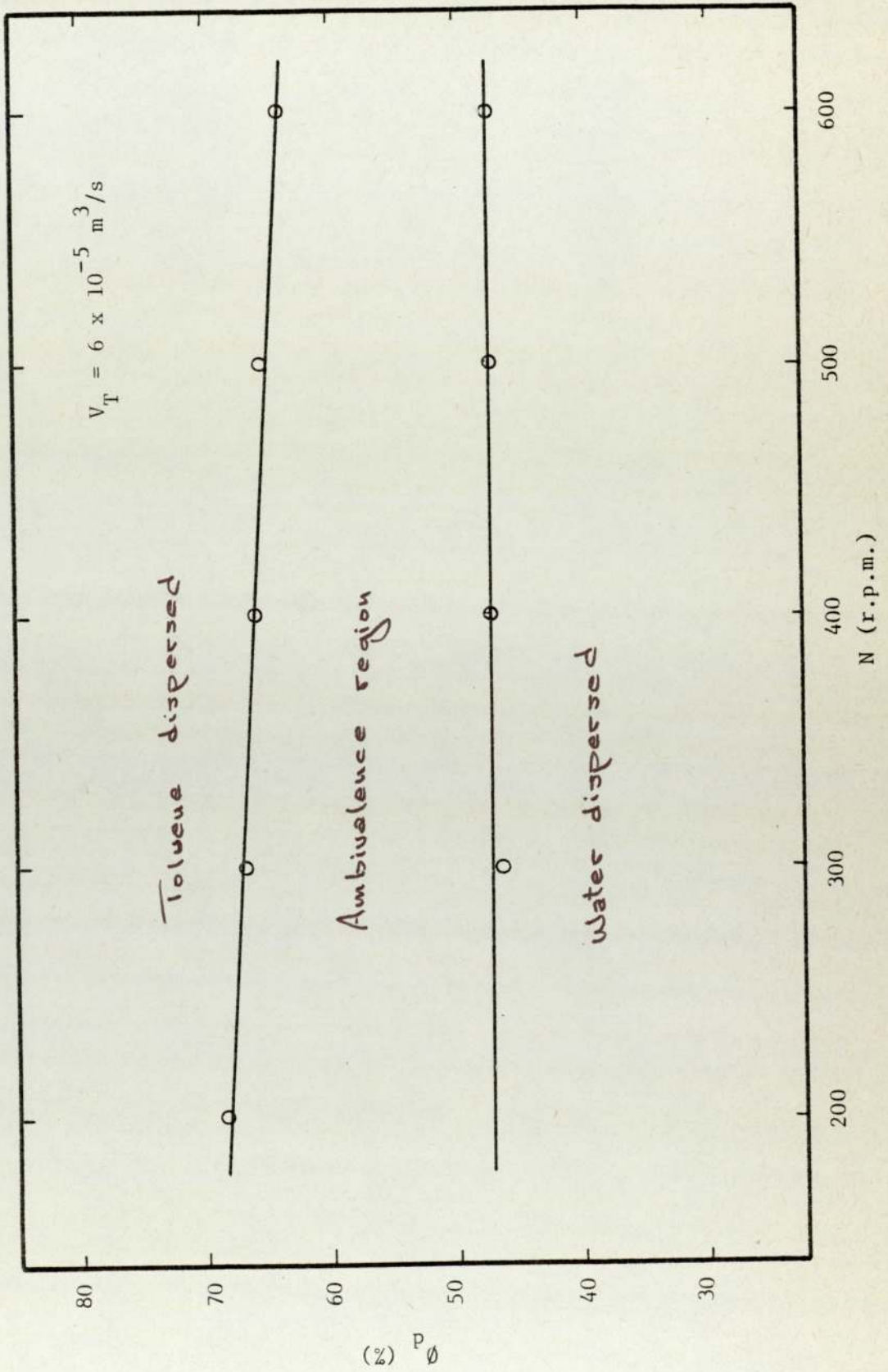
MIXER-SETTLER

Figure 7.16 PHASE INVERSION IN THE CONTINUOUS
MIXER-SETTLER

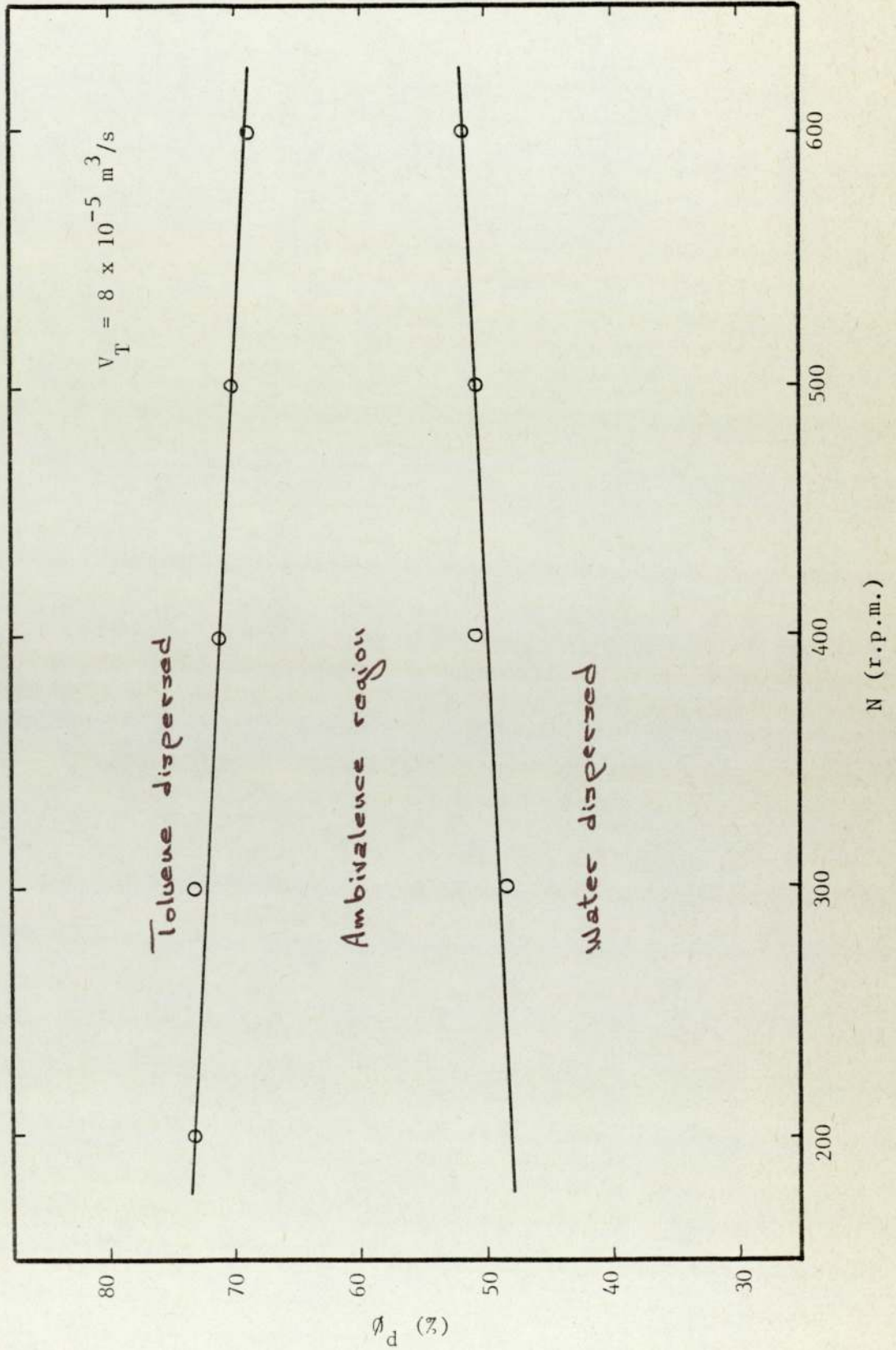


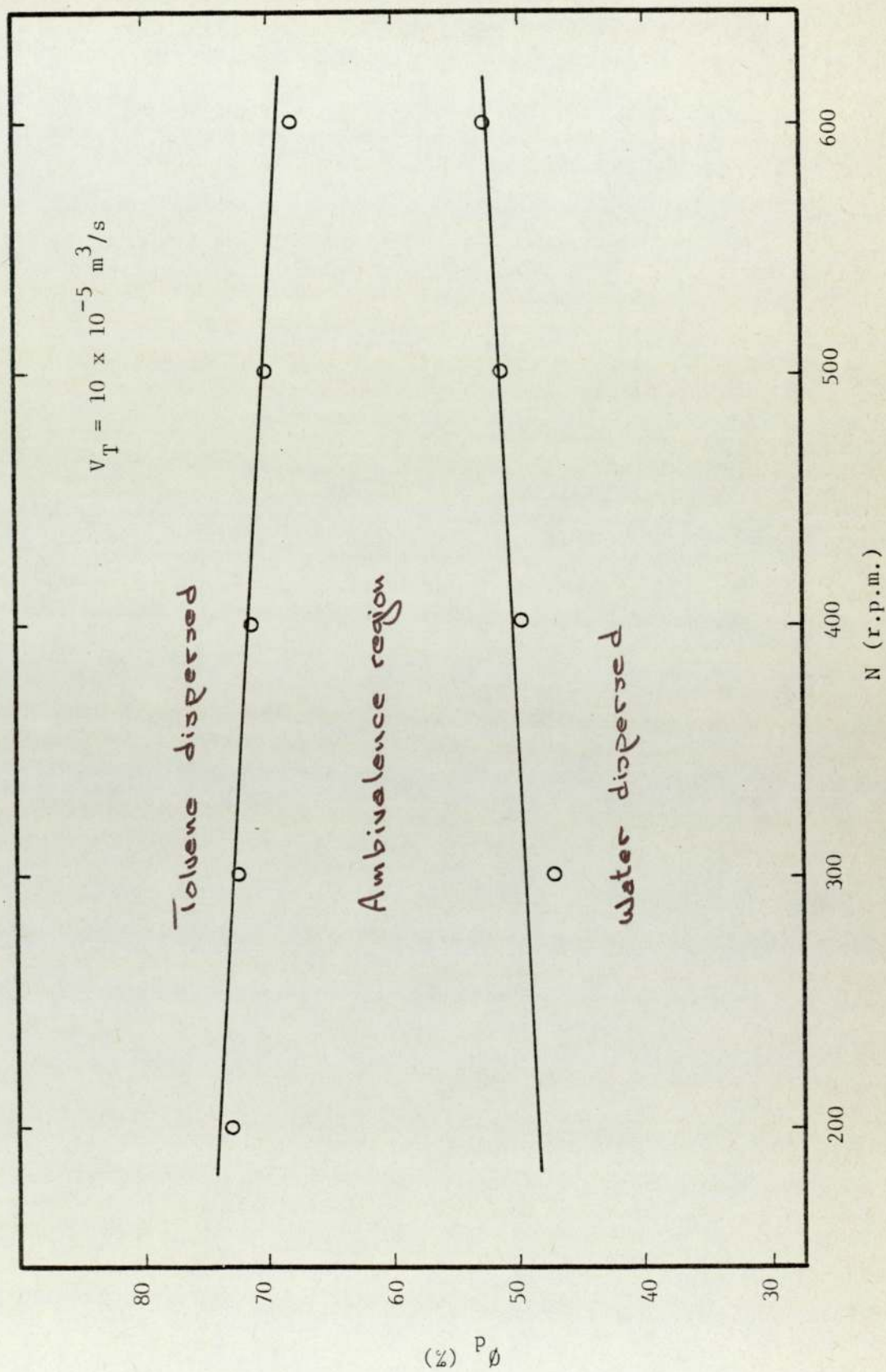
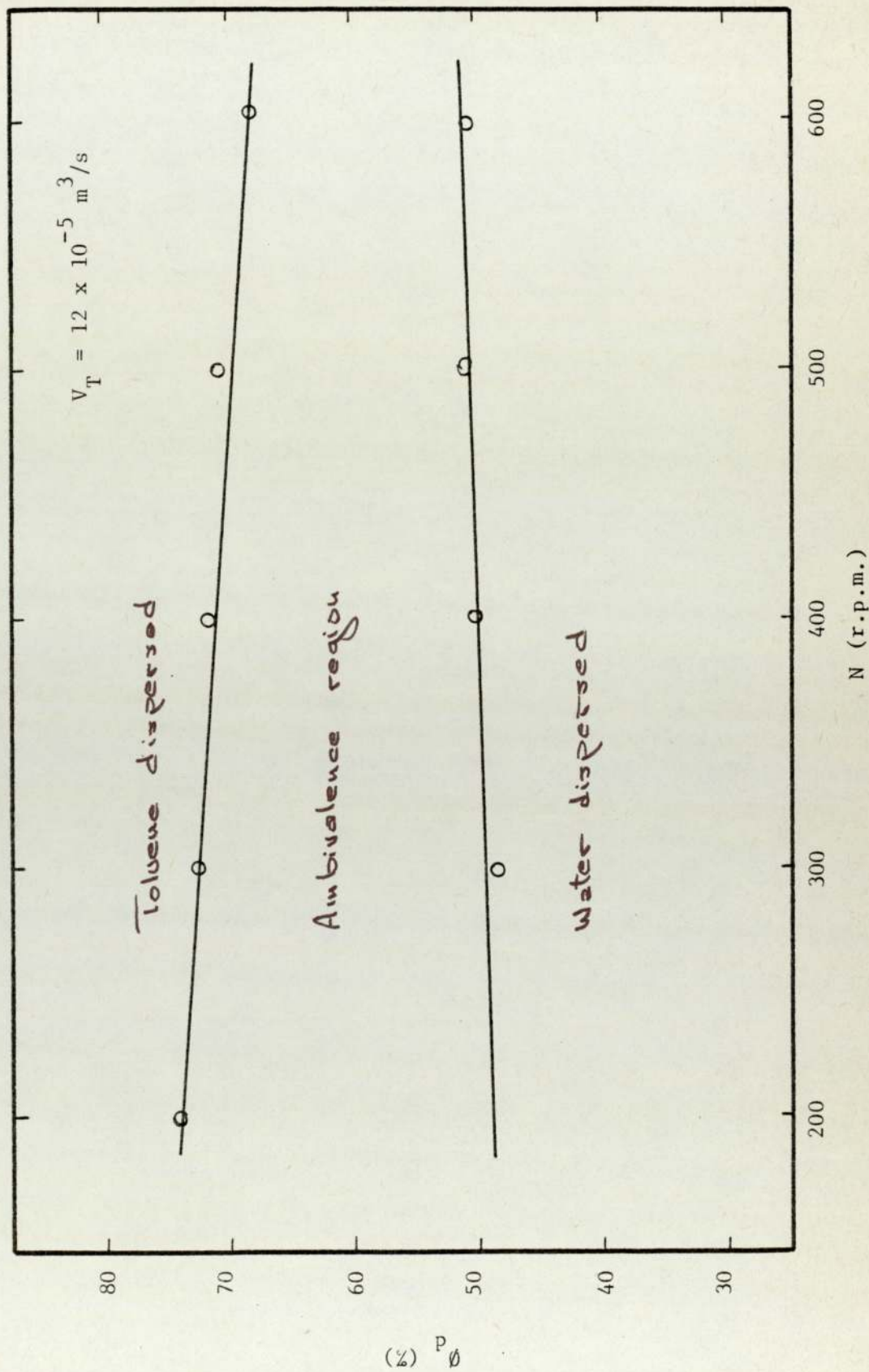
Figure 7.17 PHASE INVERSION IN THE CONTINUOUSMIXER-SETTLER

Figure 7.18 PHASE INVERSION IN THE CONTINUOUS

MIXER-SETTLER



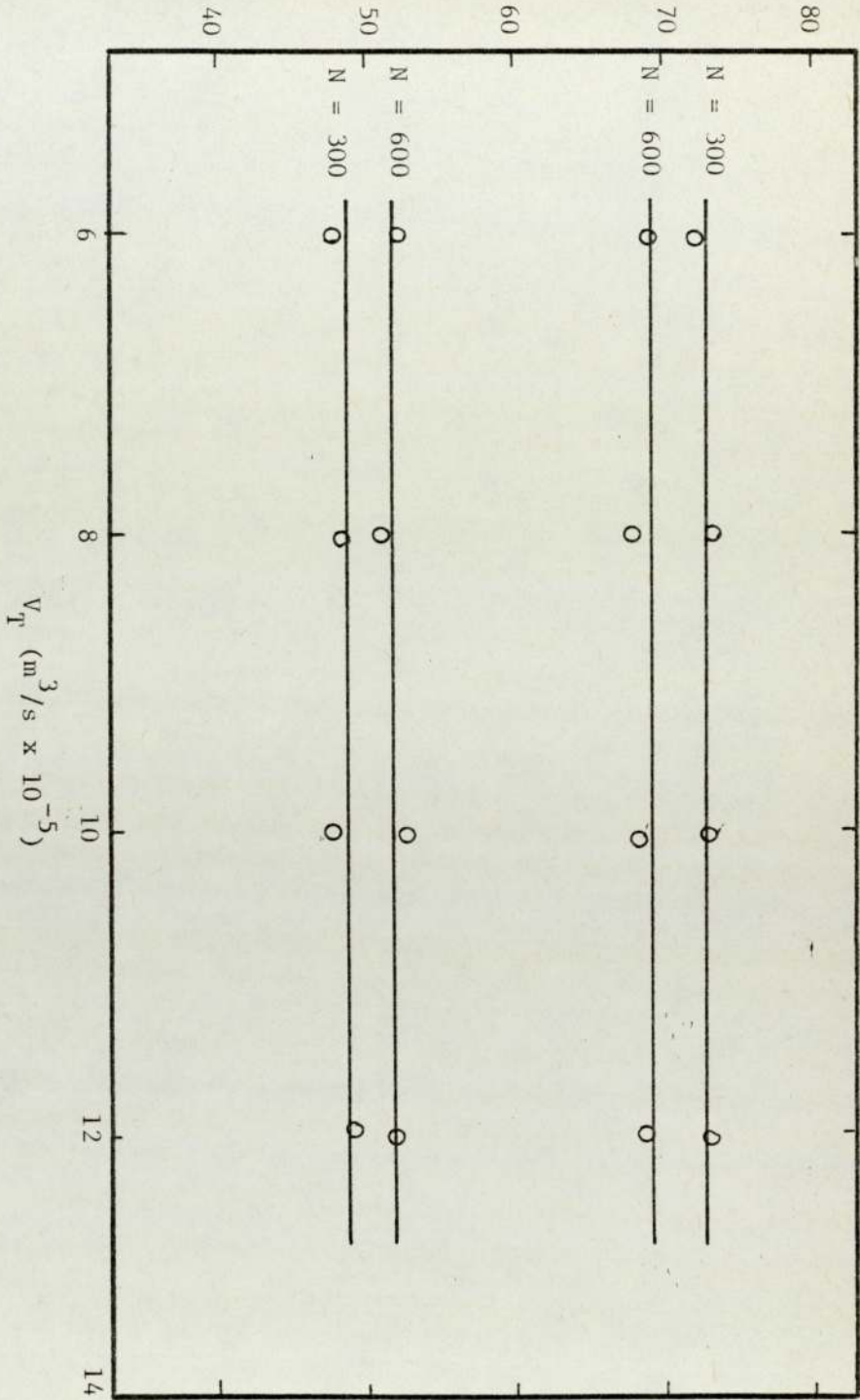


Figure 7.19 EFFECT OF FLOW RATE ON PHASE

INVERSION HYSTERESIS

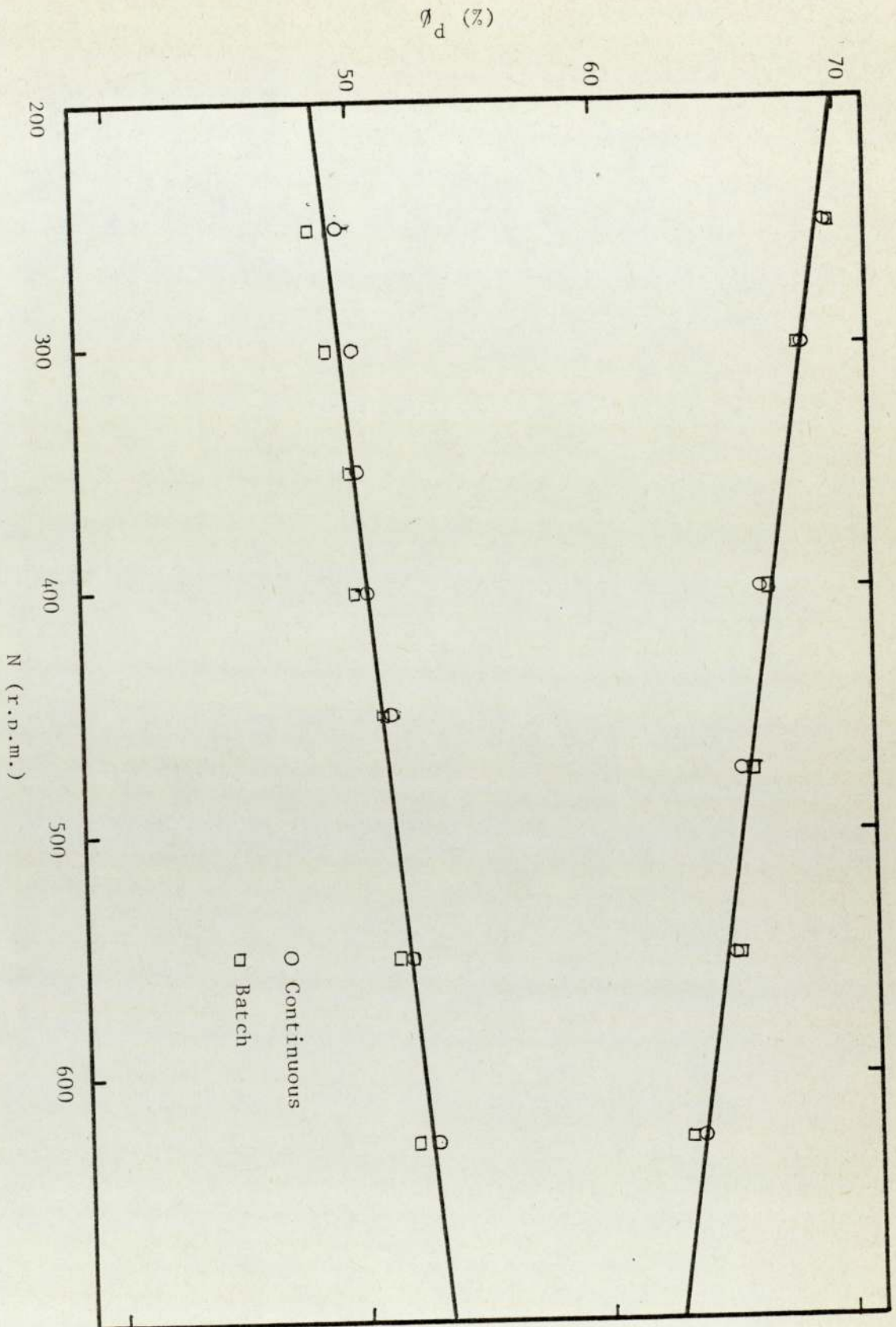


Figure 7.20 THE EFFECT OF MODE OF OPERATION
ON PHASE INVERSION HYSTeresis

CHAPTER EIGHT

D I S C U S S I O N O F R E S U L T S

8 DISCUSSION OF RESULTS

8.1 BATCH MIXING VESSEL

8.1.1 Drop Size Versus Rotor Speed and Hold-up

These studies were carried out to select a suitable correlation for the prediction of drop size. The results of these studies can be divided into two groups as follows:

8.1.1.1 Drop Size Distribution

Drop size distributions were measured for varying rotor speeds and phase ratios. Figure 3.4 is typical of the distributions obtained.

There has been considerable discussion over the shape of drop size distributions in agitated systems, as discussed in section 3.3. Some investigations reported normal and some log-normal distributions. For mass transfer studies the use of Sauter mean diameter is preferred, since the transfer across the interface is an area-dependent process. Conversely, for reaction studies, the volume mean is more applicable.

In this study Sauter mean diameters were found to be consistently log-normally distributed, and volume mean diameters of the same dispersions normally distributed. This is consistent with

previous studies.

8.1.1.2 Drop Size Versus Hold-up and Rotor Speed

Sauter mean drop size, subsequently termed 'drop size', was found to vary with hold-up and rotor speed. The equation 5.3 of Thornton and Bouyatiotis (47), described in section 5.1.1, with some modifications to the constants, was found to predict the drop sizes. In Figure 8.1 calculated and predicted drop sizes are plotted against hold-up at fixed rotor speed. Figure 8.2 presents the calculated and predicted drop size against rotor speed at fixed hold-ups. From these figures it can be seen that the correlation developed by Thornton and Bouyatiotis can be satisfactorily used to predict drop sizes in a stirred tank at high hold-ups. The agreement of results is particularly good from low hold-ups up to medium hold-ups (40%), at high hold-up values the agreement can be considered fairly satisfactory. The relative failure of the equation at high hold-ups may be due to the increased rate of coalescence, which leads to larger drops than predicted. This is because the equation depends on a linear relationship between hold-up and drop size at all concentrations. However, for most practical purposes this correlation is satisfactory.

8.1.2 Drop Size Near Phase Inversion

As discussed earlier, deviations in calculated drop

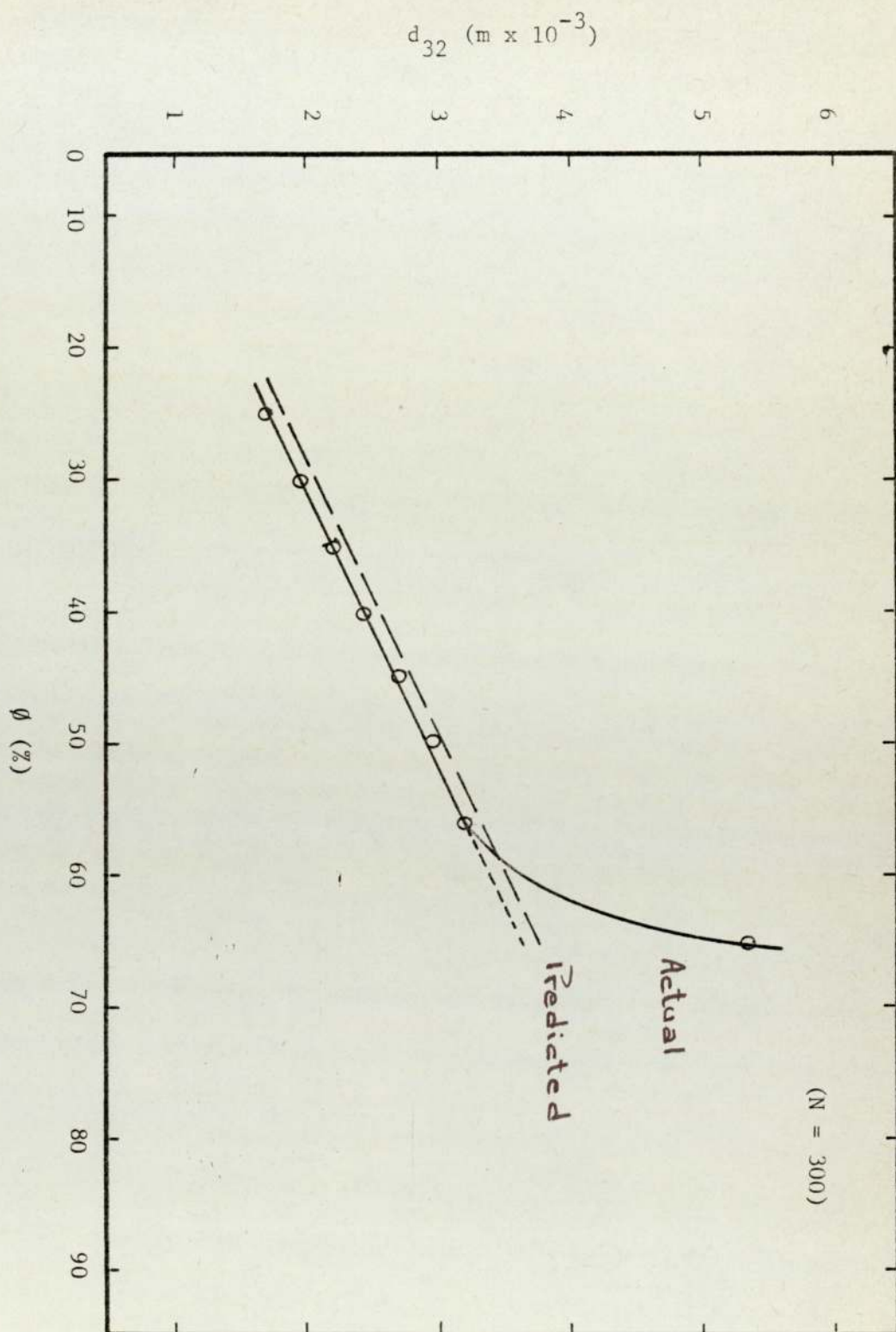


Figure 8.1 CALCULATED DROP SIZE VS PREDICTED

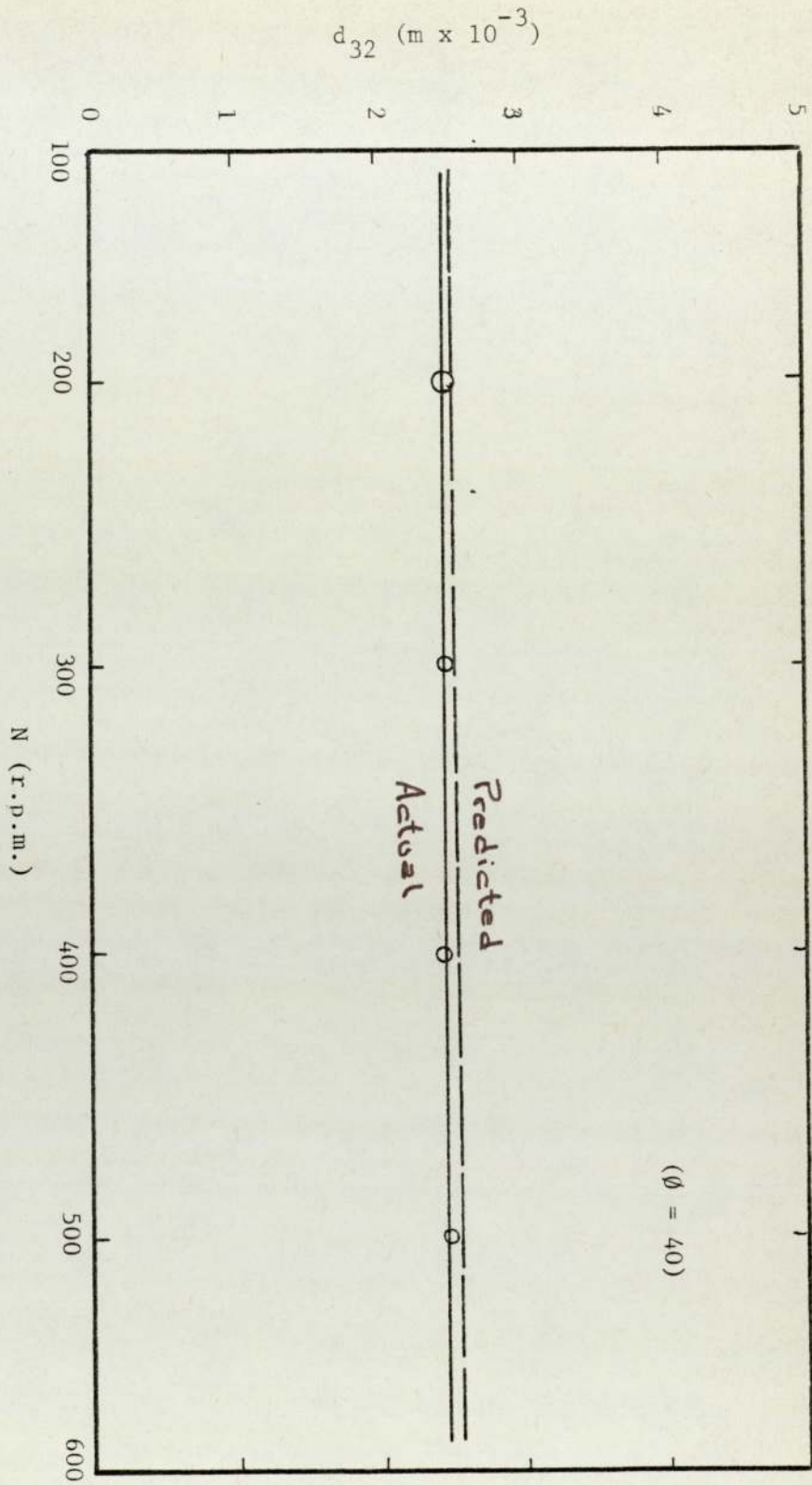


Figure 8.2 CALCULATED DROP SIZE VS PREDICTED

size compared with experimentally estimated drop sizes increased as the dispersed phase hold-up increased. Figures 7.7 to 7.9 show drop sizes near phase inversion. The shape of the slope suggests a curve. However, it was decided that, as the Thornton and Bouyatiotis model was satisfactory up to within 5% of the inversion hold-up, their correlation could be used for most practical purposes. The behaviour of drop size growth can be expected and can be used as an indication for the support of the phase inversion theory discussed in Chapter 5. Figure 8.3 shows a typical concentrated dispersion.

One of the characteristics of dispersions near phase inversion is the appearance of large slugs, this is discussed in more detail in the next section.

8.1.3 Drop Growth at Phase Inversion

Study of drop growth at phase inversion is in fact the observation of the sudden increase in the rate of the coalescence frequency. A very small addition of dispersed phase at the point of inversion leads to this sudden change in the drop size which has been plotted against time in Figures 7.7 and 7.8 to show drop size growth rate.

The results obtained from low agitator speeds ($N = 300$) suggest a divergence from isotropic conditions and the Reynolds number at this speed is 300. According to Kolmogoroff (59) a Reynolds number of the order of 10,000 is sufficient for isotropic turbulent conditions and higher rotor speeds showed a

Figure 8.3 A TYPICAL CONCENTRATED DISPERSION

reduced tendency for deviation. A close observation of phase inversion reveals a distinct change in flow pattern as the concentration of dispersed phase approaches that of phase inversion. A cine film and a video film of this process were made and have been deposited in the film library of this department. The approach of phase inversion is characterised by the formation of globules of dispersed phase, usually twenty times the average drop size. The globules usually appear from the discharge region of the impeller and the frequency of these globules increases as the point of inversion is approached. The measurement of drop sizes takes into account the effect of these globules which become a dominant feature at the point of phase inversion. At lower impeller speeds the rate of appearance of these globules fluctuates, hence leading to variation of drop sizes. At higher impeller speeds this becomes more regular, leading to a decrease in the fluctuation of drop size.

It can be concluded that, at phase inversion, a higher Reynolds number is necessary to ensure isotropic conditions. The time taken for the growth of the drops (hence the time taken for the completion of phase inversion) as shown in figures 7.7 - 7.8 shows that this phenomena depends to a large extent on the physical properties of dispersion and to a lesser extent it is inversely proportional to the rate of agitation. The latter observation at first may look unexpected. A closer examination reveals the contrary, at the lower impeller rates the isotropic

tendencies are lower, the concentration of dispersed phase is distributed unevenly, hence leading to areas which partially invert, which results in a very unstable dispersion. Phase inversion in these conditions is a matter of upsetting the balance in a very critical condition, this, therefore, results in a short time for inversion. At higher rotor speeds, the phase inversion process is due to increase in the rate of coalescence and hence the process is more orderly as the coalescence between two drops requires a finite time, the time for completion of this process will become longer. At intermediate speeds phase inversion can be due to both the processes discussed, as the rotor speed increases phase inversion becomes more dependant upon the second process, hence the time for phase inversion increases. Ponter (105) showed that the wettability of solids in contact with a dispersion played a key role in the drainage of drops, hence facilitating coalescence. Sawistowski (104) confirmed that materials of construction have an effect on phase inversion hysteresis. However, there are no correlations to relate the change in coalescence frequency with wettability and hence its effect on phase inversion. Further studies are needed to characterise the effect of wettability on an unstable dispersion under critical hydrodynamical conditions.

8.1.4 Limits of Phase Inversion

The limits of phase inversion were obtained for a number of organic - solvents and Figures 4.1-4.2 and Figures 8.4-8.5 present the results obtained vs results predicted from the phase inversion model discussed in Chapter 5. The

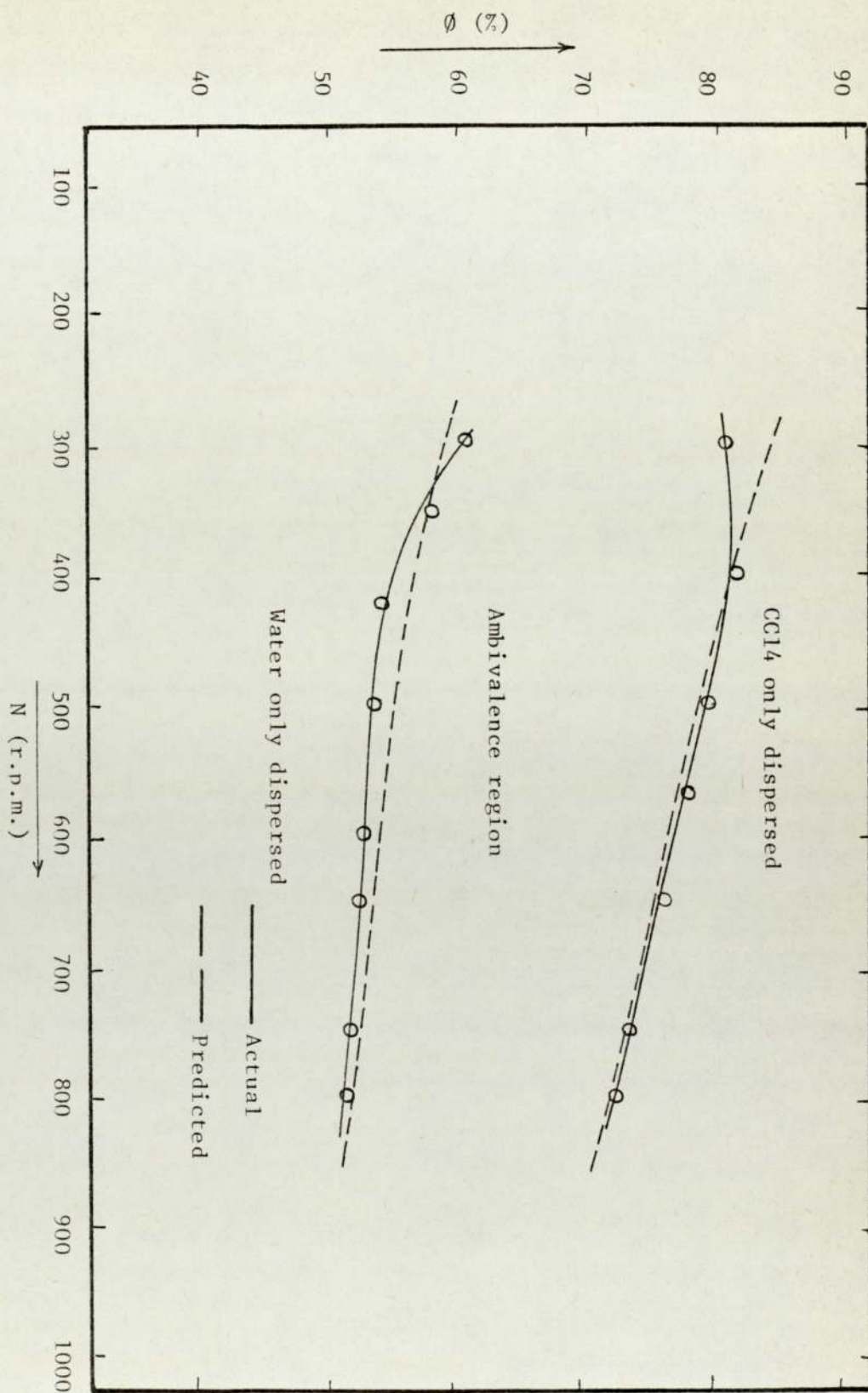
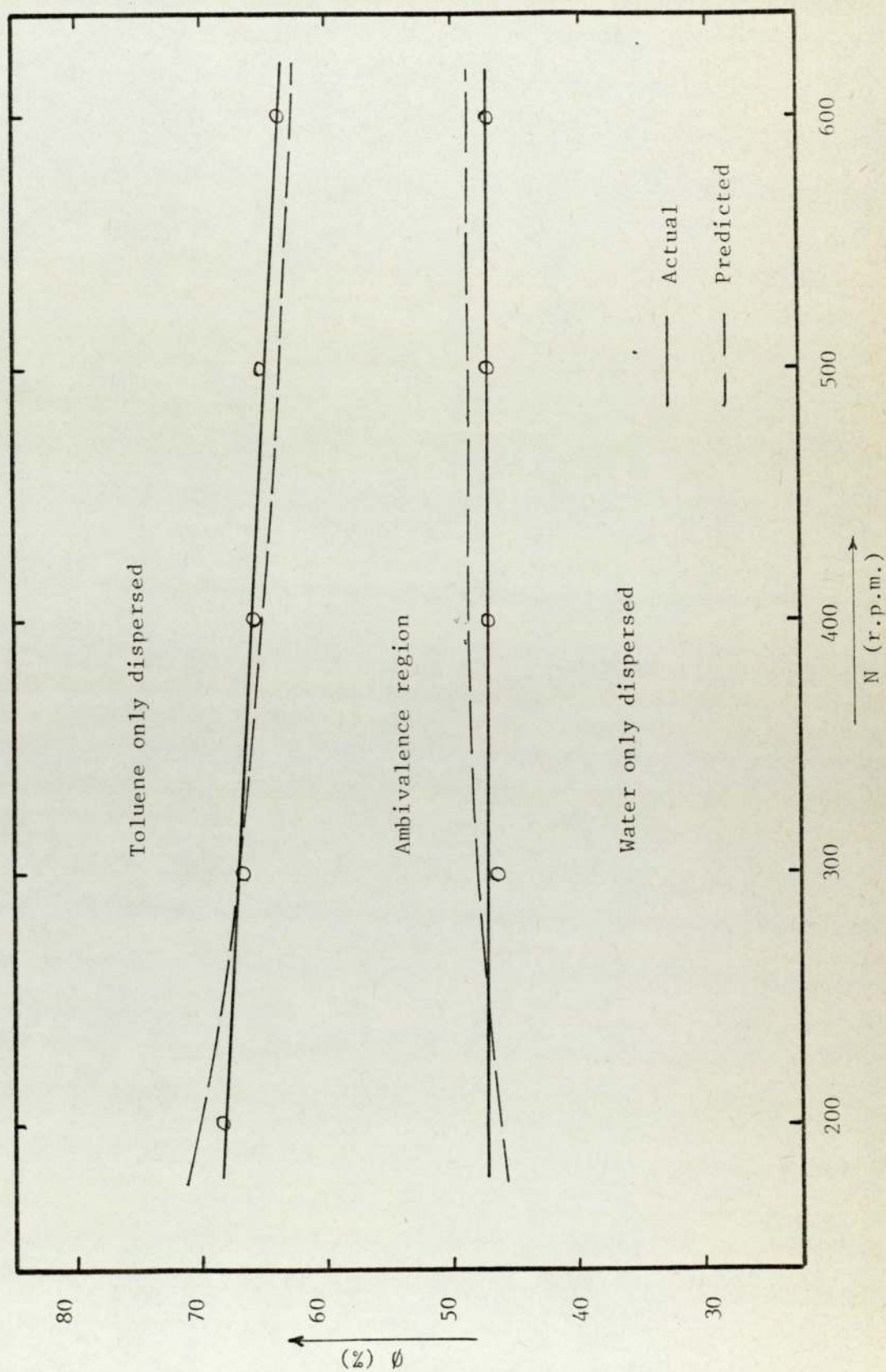


Figure 8.4 AMBIVALENT PHASE INVERSION LIMITS PREDICTED VS
ACTUAL (CCl₄/WATER, BATCH DATA)

Figure 8.5 AMBIVALENT PHASE INVERSION LIMITS PREDICTED VS
ACTUAL (TOLUENE/WATER, CONTINUOUS FLOW DATA)



general conclusion is that the model describes the processes involved very well indeed for the systems studied.

Considering the ambivalence boundary of phase inversion for systems with no surfactants as presented in Figures 7.9 to 7.14 it shows that an increase in rotor speed decreases phase inversion hold-up for the organic phase while it increases phase inversion hold-up for the aqueous phase. These different behaviours can be explained in the following way. The appearance of globules from the impeller region indicates that at phase inversion the bulk of coalescence occurs in the discharge region of the impeller, Flow pattern studies have shown that there is a vortex region in the discharge area, as illustrated in Figure 4.4 leading to an area of high impact as well as elongation. At phase inversion every impact will lead to coalescence. The ease of coalescence will be dependent on the stability and critical thickness of the film surrounding the drop Harkin (106) reported that the critical oil film thickness is $1.5 \times 10^{-6} \text{m}$ and that of water $8 \times 10^{-6} \text{m}$. The high resistance of a viscous oil film will resist the coalescence therefore, a higher value of the hold-up is achieved with an increase in rotor speed.

This case does not occur in the discharge region of the impeller, this also explains why the globules are smaller and do not appear frequently for water dispersions, even during phase inversion. The phase inversion time is very small compared with that of the organic phase dispersed, a typical time for phase inversion of aqueous phase was three seconds, compared with the 15 seconds it

took for organic phase.

An advance indication of phase inversion was obtained by the Continuous Phase Detector; this further suggested that the bulk of the coalescence of the water phase occurs in the area of low turbulence. However, the short time taken for inversion supports the theory presented in Chapter 5 suggesting that every impact at phase inversion leads to coalescence.

8.1.5 Matching Refractive Indexes

The results of these studies confirm the mechanisms considered above, although these studies cannot be quantitative as discussed in Chapter 7. They show visually that at phase inversion for the organic phase coalescence occurs in the high turbulence zones and zones where there is vortexing. The characteristics of the flow patterns change gradually as the dispersed phase concentration increases. At phase inversion the growth of drops was rapid and the large globules would not break up, despite Kolmogoroff's correlation for drop sizes, suggesting that locally the turbulent shear had been damaged. At the point of inversion the large globules contained drops of the continuous phase, such that the mass resembled a "grape". Phase inversion was different for the water dispersed phase, in that coalescence occurred in low turbulence zones and the size of globules was small. Although these studies cannot be representative, as the viscosity of the aqueous phase was high, they show the processes involved. This suggests that the potential of the

technique can be fully exploited for some quantitative assessment.

8.1.5 Flow Pattern Studies

This study was carried out to seek the reasons for the appearance of big globules in the discharge region since most workers suggested that breakage occurs in high turbulence zones. The flow pattern studies as shown in Figure 4.4 indicated vortex zones just outside the impeller discharge zones. At high hold-ups elongation of the drops coincided with the removal of continuous phase, hence the contact of drops over large regimes leads to rapid coalescence of large numbers of droplets before elongation could result in breakage. At phase inversion the frequency of these globules is so high that the globules coalesce, Figure 6.11 shows some of these globules at the point of inversion. The dispersed phase concentration changes, as well as the viscosity of the liquid-liquid dispersion, and study of the cine film of phase inversion indicates the presence of many vortex zones. Figure 6.8 shows a phase inversion sequence.

8.2 CONTINUOUS MIXER-SETTLER

8.2.1 Phase Inversion under Batch Condition

From the results shown in Figures 7.9 and 7.15 it can be concluded that phase inversion hysteresis is similar to that obtained from the batch mixing vessel. It also shows that the geometrical constants can change

the limits of the ambivalence range to a considerable extent. From the observations made in these studies it can be seen that the liquid detector indicates that the most unstable region at phase inversion is the impeller region when the dispersed phase is organic. Also the random signals obtained from the high and low electrodes shows that the density of the dispersed phase does not have any noticeable effect on the place of initiation of phase inversion. From observations made with the liquid detector it has been concluded that, in this case, the phase inversion is initiated in low turbulence areas, signals were most frequent from the high and low electrodes and the signals from the middle electrode (near the discharge of the impeller) were not frequent. This confirms the assumptions made in Chapter 5 to explain phase inversion behaviour.

8.2.2 Phase Inversion Under Continuous Operation

Phase inversion studies under continuous flow operation, shown in Figures 7.19-7.20 reveal that for a well mixed dispersion where both phases are fully dispersed the mode of operation has no significant effect on the position of the point of initiation of inversion. From these the following can be proposed:

- 1 The point of phase inversion for a particular hydrodynamic condition is unique.
- 2 The hydrodynamic condition prevailing at inversion are remarkably stable and external forces such as low level vibration etc., cannot

alter the position of the force balance significantly.

3. The time taken for the completion of phase inversion under batch and continuous operation is identical.

The above observations therefore, imply that it is possible to use the mathematical model for both cases. Figures 8.4 and 8.5 confirm that the mathematical model developed in Chapter 5 describes the phase inversion for both modes with the same constants. It can be argued that the bulk flow can affect the flow patterns, hence having a significant effect on the point of phase inversion. This is examined in the following section.

8.2.3 Phase Inversion Vs Input Flow Rate

The results of these studies are shown in the Figure 7.19. It can be seen that the effect of the flow rate on phase inversion for the range of flow rates studied is minimal. The effect of the flow rate appears to change slightly the position of the point of initiation of inversion at low impeller speeds. As mentioned in section 8.2.2 this could be due to interference in the flow pattern, as well as some short circuiting. The design of the agitator, however, prevented any major effect on the flow pattern or possibility of short circuiting. However, it can be intuitively argued that such factors can affect the hydrodynamical balances existing in the flow system and hence cause an alteration in the balance resulting in alteration of the position of the inversion point.

8.3 COMPARISON OF PHASE INVERSION RESULTS

8.3.1 Phase Inversion Vs Mode Of Operation

As discussed in the earlier section the mode of operation does not have any effect on the phase inversion under non-mass transfer conditions.

From this it can be concluded that the behaviour of the liquid-liquid systems studied in the batch mixing vessel is similar when operated in the continuous mixer-settler apparatus.

8.3.2 Phase Inversion Vs Vessel Geometry

From comparison of the results presented in Figures 7.9 - 7.14 it can be seen that the geometrical factors can have a very significant effect on the position of phase inversion. The characterisation of the geometrical factors was outside the scope of this work. The most important factor affecting the geometrical constants is the impeller design, materials of construction and dimensions. This has been reported by McClarey et al (82) in his studies of coalescence frequency.

CHAPTER NINE

CONCLUSION

9 CONCLUSION

This work is an attempt to characterise the parameters for the construction of a mathematical model to describe the phase inversion characteristics of liquid-liquid dispersions, using the physical properties of liquid-liquid systems and geometrical constants.

The main conclusions may be summarised as follows:

1. The phase inversion model based on the collision and coalescence frequencies of an agitated dispersion predicts the limits of phase inversion in good agreement with actual results.
2. The time taken for completion of phase inversion is inversely proportional to the agitation intensity and is finite.
3. The effect of flow on phase inversion limits is found to be negligible.
4. The vessel geometry has a significant effect on ambivalence hysteresis.
5. The phase inversion is initiated near the impeller region.

6. The surfactants effect dispersion behaviour in an unpredictable manner.
7. Interfacial tension has a significant effect on the characteristics of phase inversion.
8. Once phase inversion is commenced no reinversion occurs.

CHAPTER TEN

RECOMMENDATIONS FOR
FURTHER WORK

10 RECOMMENDATIONS FOR FURTHER WORK

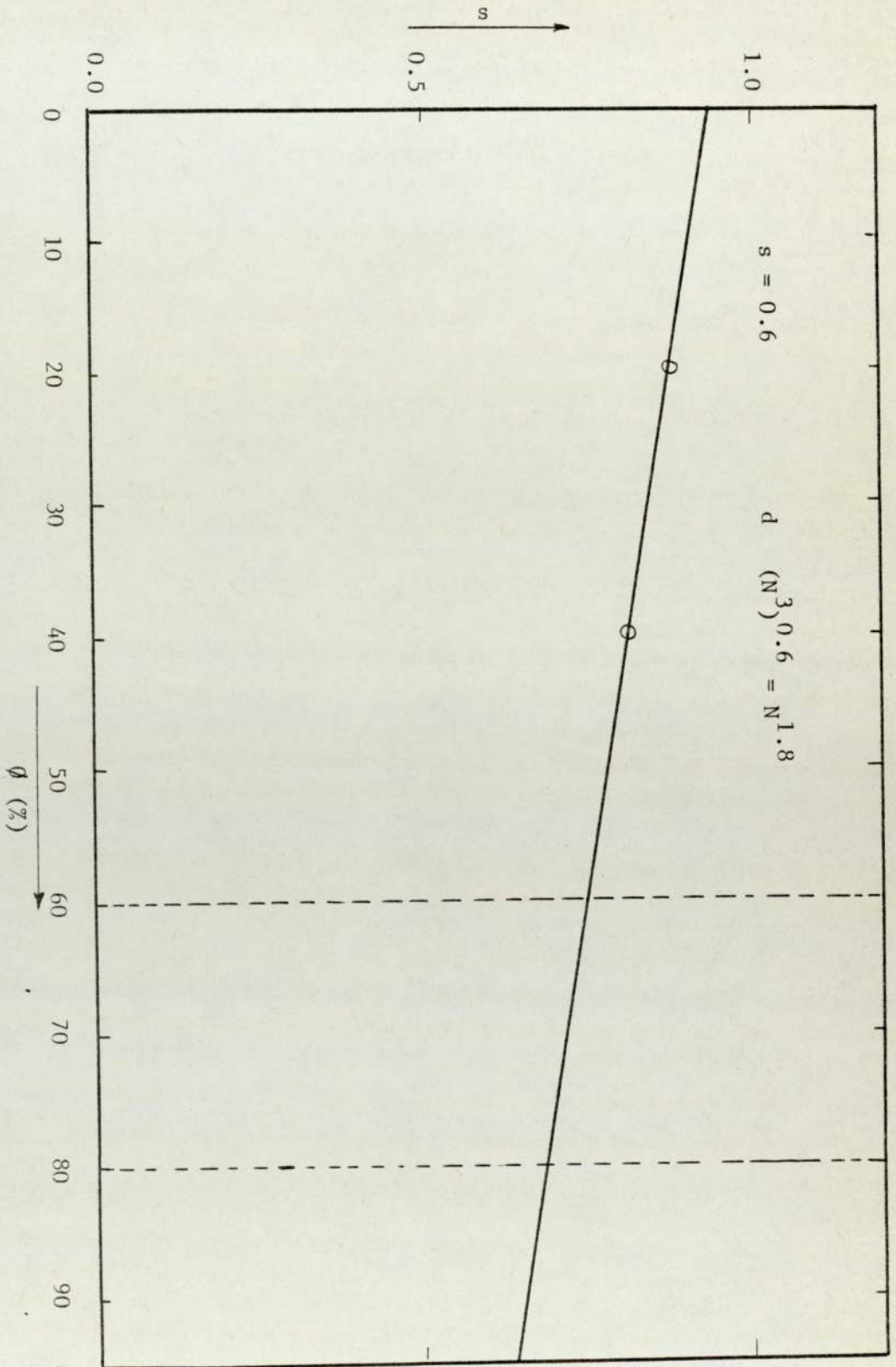
1. The phase inversion studies in this work relate to non-mass transfer conditions. However, an extension to this work should include the effects of mass and heat transfer and also chemical reaction. These factors need to be characterised. Extension of some of the techniques developed in this work may well prove useful (e.g. matching refractive indexes) in carrying out these studies. The above studies will be aimed to extend this work into industrial applications.
2. The low interfacial tension system displayed some interesting characteristics. This system needs to be investigated in a further work in order to complement the factors studied in this work.
3. Vessel geometry has a significant effect on the phase inversion characteristics of a liquid-liquid dispersion. Further work needs to be done to characterise the geometrical constants in the mathematical model developed here. It is of vital importance to carry out such studies as industrial scale-up is of considerable significance.
4. Phase inversion model needs to be applied to a variety of liquid-liquid systems, especially to viscous systems and any necessary adjustments made to various physical property effects.

5. There are no correlations to relate the effect of material of construction on phase inversion limits. Further work must be done in this area to characterise the effect of wettability on liquid systems, especially those with a strong tendency to wet the surface (i.e. low angle of contact).

APPENDIX ONE

EXTRAPOLATION OF MILLER'S RESULTS

Howarth (70) found that the rate of change of drop size with time following a disturbance was proportional to $N^{1.9-2.25}$ for agitator speeds in the range of 200 - 400 r.p.m. Whereas Madden and Damerell (71) found coalescence frequency dependence on agitator speed was proportional to $N^{1.5-3.3}$. This range of the exponent of the agitator speed agrees with the results of Miller (90). Extrapolating Miller's results for a turbine agitator and dispersed phase hold-up greater than 60% gives an exponent of 1.8.



APPENDIX TWO

COMPUTER PROGRAMME OF PHASE INVERSION MODEL


```

0020 WRITE(2,600)
2 0021 FORMAT(////)
2 0022
4 0023 WRITE(2,150)
4 0024 WRITE(2,601)
6 0025
6 0026 WRITE(2,700)(LINE(J),J=1,100)
8 0027
8 0028 WRITE(2,602)
10 0029
10 0030 WRITE(2,151)RHO,FOC
12 0031
12 0032 WRITE(2,603)
14 0033
14 0034 WRITE(2,603)
16 0035
16 0036 WRITE(2,152)GF
18 0037
18 0038 WRITE(2,604)
20 0039
20 0040 WRITE(2,153)STD,STC
22 0041
22 0042 WRITE(2,605)
24 0043
24 0044 WRITE(2,154)INTER
26 0045
26 0046 WRITE(2,606)
28 0047
28 0048 WRITE(2,155)VID,VIC
30 0049
30 0050 WRITE(2,156)DISPERSID,PHASE,VISCOSITY=,F8.3,2X,*,N/M*,3X,
32 0051 *CONTINUOUS,PHASE,VISCOSITY=,F8.3,2X,*,N/M*
34 0052
34 0053 WRITE(2,710)(LINE(J),J=1,100)
36 0054
36 0055 WRITE(2,607)
38 0056
38 0057
40 0058
40 0059
40 0060
42 0061
42 0062
44 0063
44 0064
46 0065
46 0066
48 0067
48 0068
50 0069
50 0070
52 0071
52 0072
54 0073
54 0074
56 0075
56 0076
58 0077
58 0078
60 0079
60 0080
62 0081
62 0082
64 0083
64 0084

```

PH=10.0
WRITE(2,200)
200 FORMAT(16X,*,DROG DIAMETER*,3X,*,PHASE RATIO*,4X,*,ROTAR SPEED*,
15X,*,RODEL ONE*,6X,*,RODEL TWO*,7X,*,ONE-TWO*)
609 FORMAT(//)
720 WRITE(2,720)(LINE(J),J=1,100)
720 FORMAT(10X,100A1)
WRITE(2,613)
WRITE(2,613)

```

0086 2 0087 0088 0089 0090 0091 0092 0093 0094 0095 0096 0097 0098 0099 0100 0101 0102 0103 0104 0105 0106 0107 0108 0109 0110 0111 0112 0113
END OF SEGMENT, LENGTH 541, WARE AWASH
END

```

```

30 END OF SEGMENT, LENGTH 541, WARE AWASH
32
34 0114 IRISH

```

```

36 END OF COMPILATION - NO ERRORS

```

```

38 S/C SUBFILE : 15 PUCKETS USED

```

```

40 CONSOLIDATED BY XPER 12H DATE 27/06/70 TIME 10/45/70

```

```

42 *SMGRLIST

```

```

44 *IN ED (FOOTSETECOMP)

```

```

46 *LIB ED (SUBGROUPS/F4,SUBROUTINES)

```

```

48 *WORK ED (CHECKWORKFILE)

```

```

50 *****

```

```

52 PROGRAM FXXX
54 EXTENDED DATA (Z2FN)
56 COMPACT PROGRAM (C0FF)
58 SCOME 5360

```

```

60 DISPLAY : TRICE 2 USED
62 ALLOT *CRU N
64 O.14: MONITOR
66 ALLOT ALPD N
68 O.15: MONITOR
70 ALLOT ALPD N
72 O.16:46.11 FREE *CRU 4 TRANSFERS
74 O.17:46.11 FREE *ALPD 501 TRANSFERS
76
78
80
82
84
86
88
90
92
94
96
98
100

```

10.46.14 JOBTIME USED 20 ; MAXIMUM CORE USED 52576
10.46.14 JOB UNITS 64

8*UUUUUUUU NUMBER OF PAGES 4

10*UUUUUUUU

12

14

16

18

20

22

24

26

28

30

32

34

36

38

40

42

44

46

48

50

52

54

56

58

60

62

64

2

4

6

8

10

12

14

16

18

20

22

24

26

28

30

32

34

36

38

40

42

44

46

48

50

52

54

56

58

60

62

64


```

2 *****
3 *****
4 *****
5 *****
6 *****
7 *****
8 *****
9 *****
10 *****
11 *****
12 *****
13 *****
14 *****
15 *****
16 *****
17 *****
18 *****
19 *****
20 *****
21 *****
22 *****
23 *****
24 *****
25 *****
26 *****
27 *****
28 *****
29 *****
30 *****
31 *****
32 *****
33 *****
34 *****
35 *****
36 *****
37 *****
38 *****
39 *****
40 *****
41 *****
42 *****
43 *****
44 *****
45 *****
46 *****
47 *****
48 *****
49 *****
50 *****
51 *****
52 *****
53 *****
54 *****
55 *****
56 *****
57 *****
58 *****
59 *****
60 *****
61 *****
62 *****
63 *****
64 *****

```

PHYSICAL PROPERTIES OF LIQUID-LIQUID SYSTEM

DISPERSED PHASE DENSITY=660.0 KG/M**3 CONTINUOUS PHASE DENSITY=999.0 KG/M**3

ACCELERATION DUE TO GRAVITY=+9.81 M/S**2

DISPERSED PHASE SURFACE TENSION=.0284 N/M CONTINUOUS PHASE SURFACE TENSION=.0565 N/M

INTERFACIAL TENSION=.0350 N/M

DISPERSED PHASE VISCOSITY=.126E-03 N/M CONTINUOUS PHASE VISCOSITY=.995E-03 N/M

DROP DIAMETER PHASE RATIO ROTAM SPEED MODEL ONE MODEL TWO ONE-TWO

0.0000549 10.00 300.00 0.000640 0.01166 -0.01127

0.0001521 15.00 500.00 0.00132 0.02614 -0.02481

0.0005073 20.00 300.00 0.00372 0.04637 -0.04525

10MLISTING OF :HOKKILE-7A800075164(1/) PRODUCED ON 27JUN80 AT 10.46.11

12#68-63EC AT ASTON IN :ECP7016-ARASH ON 27JUN80 AT 10.47.46 USING U15

1#DOCUMENT 1

	DEEP	DIAMETER	PHASE	RATIO	KOTAK	SPEED	MODEL	ONE	MODEL	TWO	ONE-TWO
2											
4		0.0001058		30.00		300.00		0.01050		0.10412	-0.09363
6		0.0001210		35.00		300.00		0.01665		0.14164	-0.12499
8		0.0001313		40.00		300.00		0.02244		0.18493	-0.16009
10		0.0001555		45.00		300.00		0.03534		0.23397	-0.19862
12		0.0001727		50.00		300.00		0.04846		0.28877	-0.24032
14		0.0001960		55.00		300.00		0.06447		0.34934	-0.28437
16		0.0002072		60.00		300.00		0.08366		0.41966	-0.33200
18		0.0002244		65.00		300.00		0.10634		0.48775	-0.38141
20		0.0002417		70.00		300.00		0.13278		0.56560	-0.44282
22		0.0002539		75.00		300.00		0.16327		0.64921	-0.48594
24		0.0002701		80.00		300.00		0.19811		0.73859	-0.54047
26		0.0002934		85.00		300.00		0.23759		0.83372	-0.59613
28		0.0003106		90.00		300.00		0.28199		0.93462	-0.65263
30		0.0004278		95.00		300.00		0.33160		1.04128	-0.70968
32		0.0004451		100.00		300.00		0.38671		1.15370	-0.76659
34											
36											
38											
40											
42											
44											
46											
48											
50											
52											
54											
56											
58											
60		0.0000546		10.00		400.00		0.00044		0.01338	-0.01293
62		0.0000517		15.00		400.00		0.00150		0.03004	-0.02454
64											

 DEEP DIAMETER PHASE RATIO KOTAK SPEED MODEL ONE MODEL TWO ONE-TWO

	DROP DIAMETER	PHASE RATIO	ROTAR SPEED	MODEL ONE	MODEL TWO	DIFF-TWO
2	0.0000518	15.00	500.00	0.00165	0.03355	-0.03188
4	0.0000660	20.00	500.00	0.00391	0.05958	-0.05567
6	0.0000862	25.00	500.00	0.00764	0.09307	-0.08356
8	0.0001195	30.00	500.00	0.01320	0.13399	-0.12080
10	0.0001697	35.00	500.00	0.02095	0.18255	-0.16166
12	0.0002379	40.00	500.00	0.03126	0.23815	-0.20949
14	0.0003352	45.00	500.00	0.04451	0.30139	-0.25688
16	0.0004724	50.00	500.00	0.06105	0.37206	-0.31101
18	0.0006496	55.00	500.00	0.08124	0.45017	-0.36892
20	0.0008669	60.00	500.00	0.10547	0.53572	-0.43025
22	0.0011241	65.00	500.00	0.13408	0.62870	-0.49462
24	0.0014213	70.00	500.00	0.16746	0.72912	-0.56176
26	0.0017555	75.00	500.00	0.20595	0.83698	-0.63192
28	0.0021258	80.00	500.00	0.24994	0.95227	-0.70233
30	0.0025310	85.00	500.00	0.29978	1.07501	-0.77522
32	0.0029702	90.00	500.00	0.35585	1.20518	-0.84943
34	0.0034447	95.00	500.00	0.41850	1.34278	-0.92429
36	0.0039467	100.00	500.00	0.48810	1.48763	-0.99973

54
56
58
60
62
64

54
56
58
60
62
64

	DRUP DIAMETER	PHASE RATIO	POTAR SPEED	MODEL 018	MODEL TWO	ONE-TWO
2	0.0000345	10.00	600.00	0.00053	0.01632	-0.01579
4	0.0000517	15.00	600.00	0.00179	0.03670	-0.03491
6	0.0000690	20.00	600.00	0.00425	0.06523	-0.06098
8	0.0000862	25.00	600.00	0.00830	0.10190	-0.09360
10	0.0001034	30.00	600.00	0.01434	0.14672	-0.13698
12	0.0001207	35.00	600.00	0.02277	0.19969	-0.17692
14	0.0001379	40.00	600.00	0.03398	0.26080	-0.22612
16	0.0001551	45.00	600.00	0.04838	0.33006	-0.28169
18	0.0001724	50.00	600.00	0.06635	0.40747	-0.34112
20	0.0001896	55.00	600.00	0.08831	0.49303	-0.40471
22	0.0002068	60.00	600.00	0.11465	0.58673	-0.47208
24	0.0002240	65.00	600.00	0.14576	0.68857	-0.54662
26	0.0002413	70.00	600.00	0.18204	0.79857	-0.61653
28	0.0002585	75.00	600.00	0.22390	0.91671	-0.69251
30	0.0002757	80.00	600.00	0.27172	1.04300	-0.77128
32	0.0002930	85.00	600.00	0.32591	1.17743	-0.85152
34	0.0003102	90.00	600.00	0.38687	1.32002	-0.93315
36	0.0003274	95.00	600.00	0.45493	1.47074	-1.01976
38	0.0003447	100.00	600.00	0.53066	1.62962	-1.09656

2	0.0000565	10.00	700.00	0.000957	0.01762	-0.01705
4	0.0000517	15.00	700.00	0.00192	0.03965	-0.03970
6	0.0000690	20.00	700.00	0.00456	0.07042	-0.06667
8	0.0000862	25.00	700.00	0.00891	0.11004	-0.10113
10	0.0001054	30.00	700.00	0.01539	0.15845	-0.14506
12	0.0001206	35.00	700.00	0.02443	0.21565	-0.19122
14	0.0001379	40.00	700.00	0.03646	0.28166	-0.26519
16	0.0001551	45.00	700.00	0.05192	0.35646	-0.36654
18	0.0001723	50.00	700.00	0.07121	0.44006	-0.48665
20	0.0001896	55.00	700.00	0.09478	0.53247	-0.61769
22	0.0002068	60.00	700.00	0.12305	0.63367	-0.81062
24	0.0002240	65.00	700.00	0.15644	0.74367	-0.98723
26	0.0002413	70.00	700.00	0.19538	0.86247	-0.166709
28	0.0002585	75.00	700.00	0.24031	0.99007	-0.274977
30	0.0002757	80.00	700.00	0.29164	1.12647	-0.835613
32	0.0002929	85.00	700.00	0.34981	1.27167	-0.92167
34	0.0003102	90.00	700.00	0.41523	1.42567	-1.01644
36	0.0003274	95.00	700.00	0.48835	1.58847	-1.11012
38	0.0003446	100.00	700.00	0.56958	1.76007	-1.19069

	DROP DIAMETER	PHASE RATIO	ROTAR SPEED	MODEL ONE	MODEL TWO	ONE-TWO
6	0.0000345	10.00	800.00	0.00061	0.01862	-0.01822
8	0.0000517	15.00	600.00	0.00205	0.04235	-0.04031
10	0.0000619	20.00	600.00	0.00485	0.07528	-0.07643
12	0.0000662	25.00	600.00	0.00947	0.11762	-0.10815
14	0.0001034	30.00	800.00	0.01636	0.16937	-0.15301
16	0.0001216	35.00	800.00	0.02597	0.23052	-0.20654
18	0.0001379	40.00	800.00	0.03877	0.30108	-0.26231
20	0.0001551	45.00	800.00	0.05520	0.38104	-0.33585
22	0.0001723	50.00	800.00	0.07571	0.47041	-0.39670
24	0.0001896	55.00	800.00	0.10077	0.56919	-0.46862
26	0.0002068	60.00	800.00	0.13083	0.67738	-0.54655
28	0.0002240	65.00	800.00	0.16633	0.79497	-0.62864
30	0.0002412	70.00	800.00	0.20774	0.92197	-0.71624
32	0.0002585	75.00	800.00	0.25551	1.05835	-0.80288
34	0.0002757	80.00	500.00	0.31009	1.20420	-0.89411
36	0.0002929	85.00	100.00	0.37193	1.35942	-0.98746
38	0.0003102	90.00	800.00	0.44150	1.52405	-1.08254
40	0.0003274	95.00	600.00	0.51924	1.69808	-1.17864
42	0.0003446	100.00	800.00	0.60562	1.88152	-1.27591

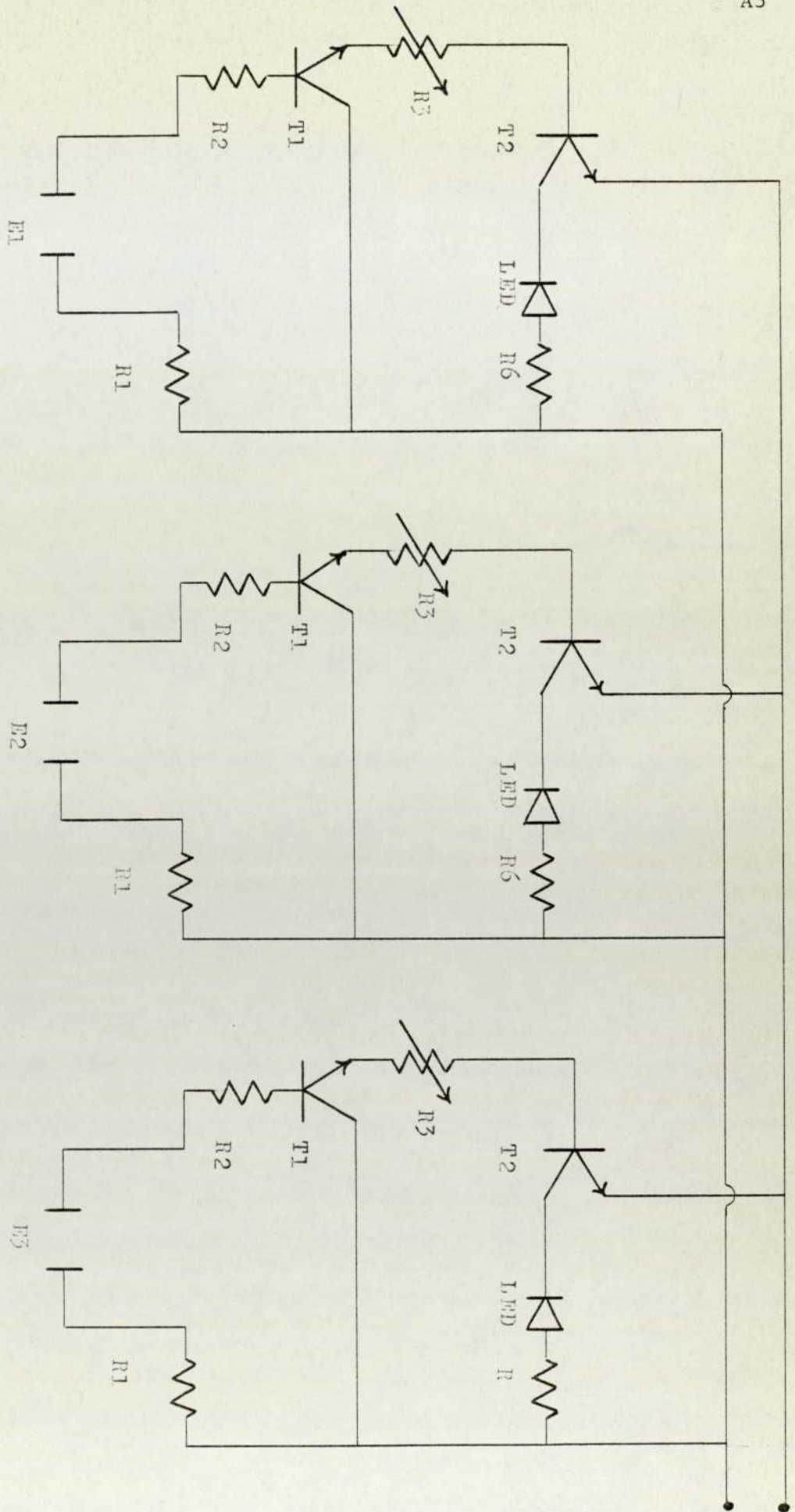
	DROP DIAMETER	PHASE RATIO	ROTAR SPEED	MODEL ONE	MODEL TWO	ONE-TWO
2						
4						
6						
8	0.0000345	10.00	900.00	0.000064	0.01997	-0.01995
10						
12	0.0000517	15.00	900.00	0.00216	0.04491	-0.04276
14						
16	0.0000679	20.00	900.00	0.00512	0.07984	-0.07472
18	0.0000662	25.00	900.00	0.00999	0.12474	-0.11475
20						
22	0.0001024	30.00	900.00	0.01727	0.17963	-0.16256
24	0.0001206	35.00	900.00	0.02742	0.24449	-0.21707
26						
28	0.0001379	40.00	900.00	0.04092	0.31932	-0.27840
30	0.0001551	45.00	900.00	0.05826	0.40414	-0.34587
32						
34	0.0001723	50.00	900.00	0.07992	0.49993	-0.41901
36	0.0001895	55.00	900.00	0.10637	0.60370	-0.49732
38						
40	0.0002068	60.00	900.00	0.13810	0.71844	-0.58034
42	0.0002240	65.00	900.00	0.17558	0.84317	-0.66759
44						
46	0.0002412	70.00	900.00	0.21929	0.97787	-0.75856
48	0.0002575	75.00	900.00	0.26972	1.12255	-0.85283
50						
52	0.0002757	90.00	900.00	0.32733	1.27721	-0.94937
54	0.0002929	15.00	900.00	0.39262	1.44154	-1.04922
56						
58	0.0003101	90.00	900.00	0.46606	1.61645	-1.15039
60	0.0003274	95.00	900.00	0.54813	1.80104	-1.25292
62						
64	0.0003446	160.00	900.00	0.63530	1.99561	-1.35631

.....

APPENDIA THREE

CONTINUOUS PHASE DETECTOR UNIT

The Continuous Phase Detector Unit, as shown in the diagram, is based on a circuit which, when completed across E_1 , - E_3 , L.E.D. from the completed circuit is lit, indicating that the continuous phase is aqueous. When the light is off, organic phase is dispersed.



APPENDIX FOUR

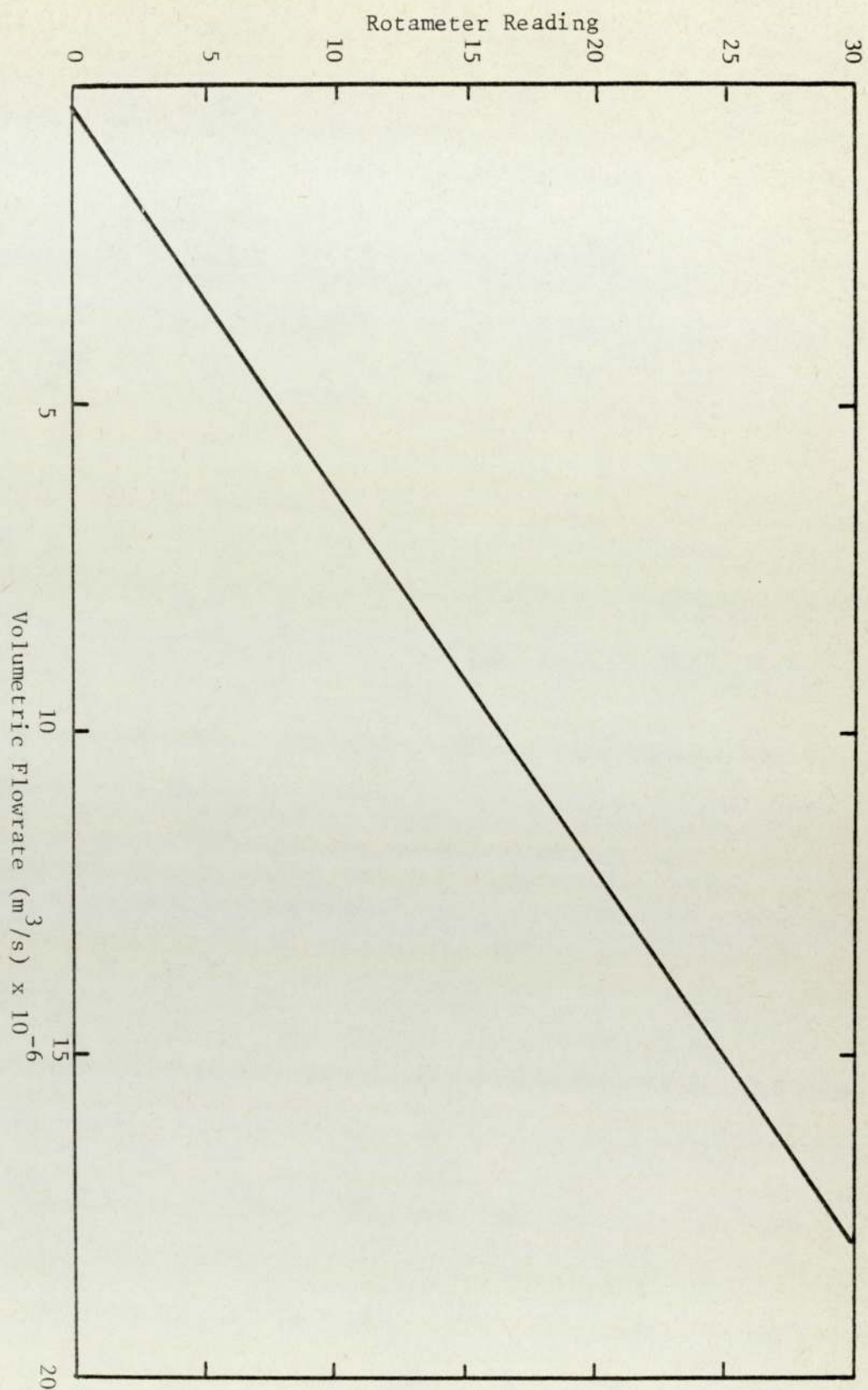
PHYSICAL PROPERTIES OF LIQUID-LIQUID SYSTEMS

PHYSICAL PROPERTIES

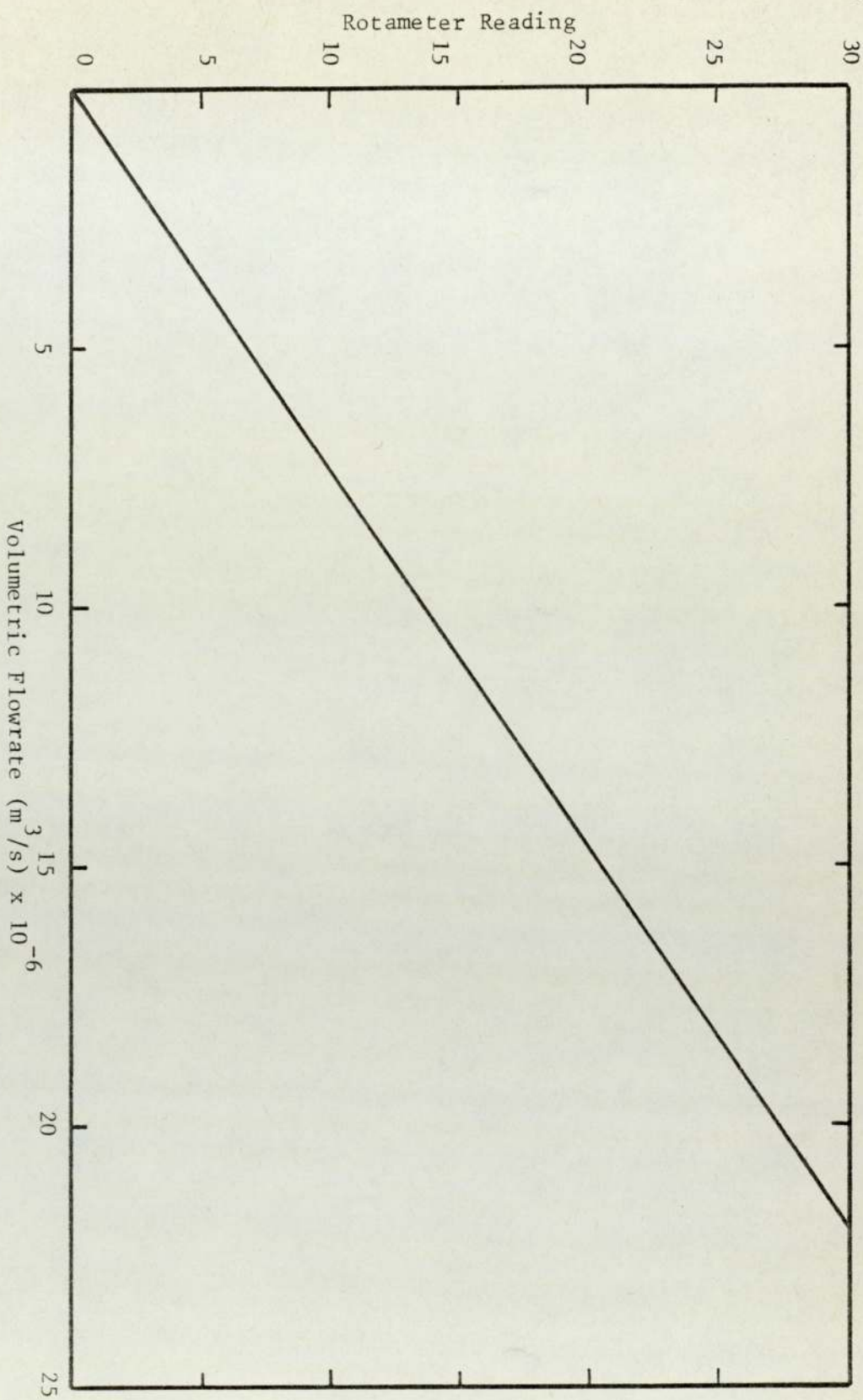
SYSTEM	DENSITY	INTERFACIAL TENSION	SURFACE TENSION	VISCOSITY kg./ms
	kg/m ³	N/m	Newtons/m	
Toluene	870	0.024	0.0300	0.0078
Water	995	0.024	0.0537	0.0101
CCl ₄	1301	0.031	0.0282	0.0062
Water	995	0.031	0.0525	0.0099
70% Toluene 30% CCl ₄	999	0.0001	0.0304	0.0059
Water	1013	0.0001	0.0303	0.0091
63% Toluene 37% CCl ₄	1029	0.0056	0.0310	0.0082
Water	998	0.0056	0.0366	0.0111
30% Toluene 70% CCl ₄	1172	0.031	0.0282	0.0062
Water	995	0.031	0.0525	0.0099

APPENDIX FIVE

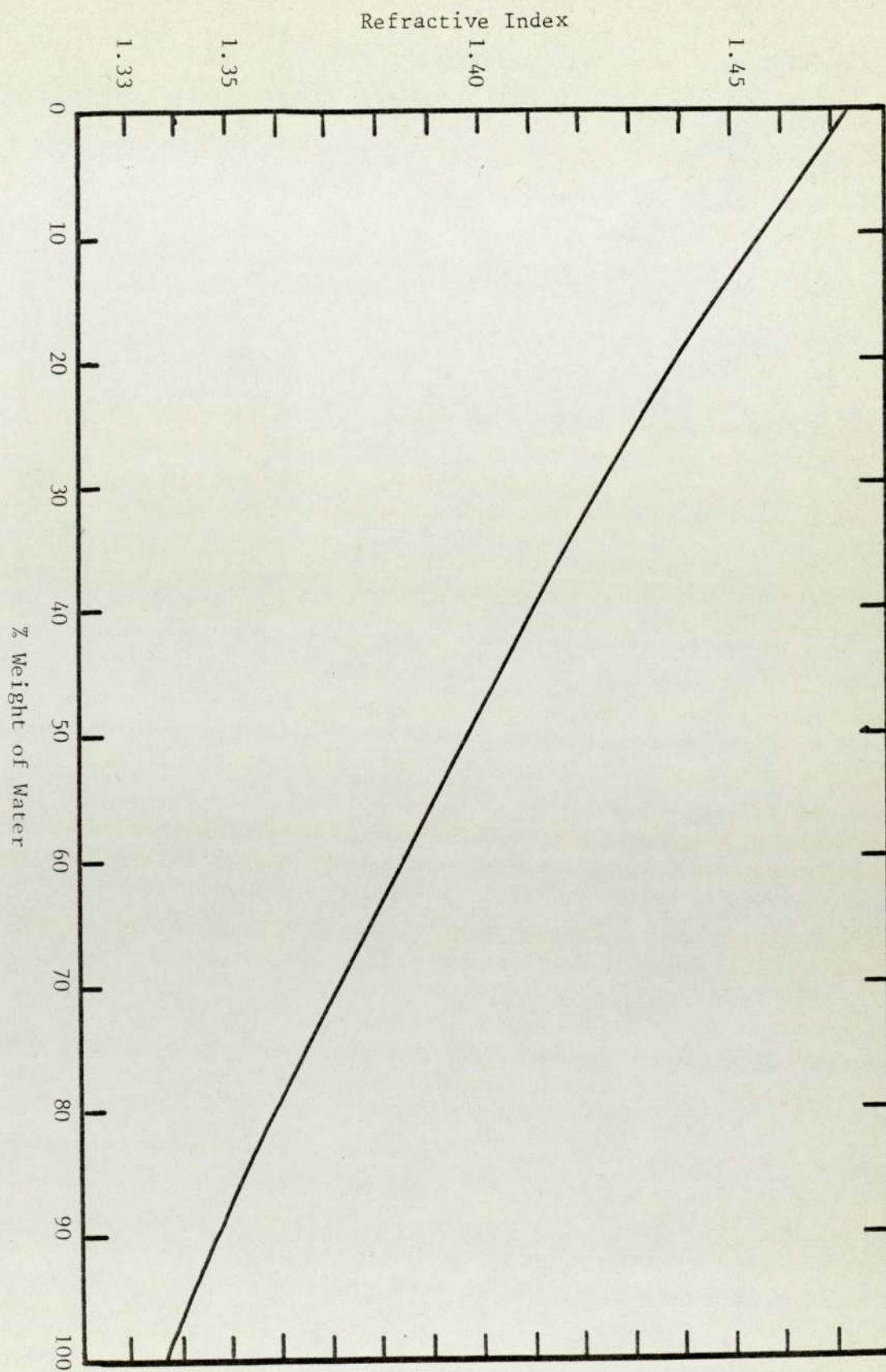
CALIBRATION OF ROTAMETERS



CALIBRATION FOR WATER

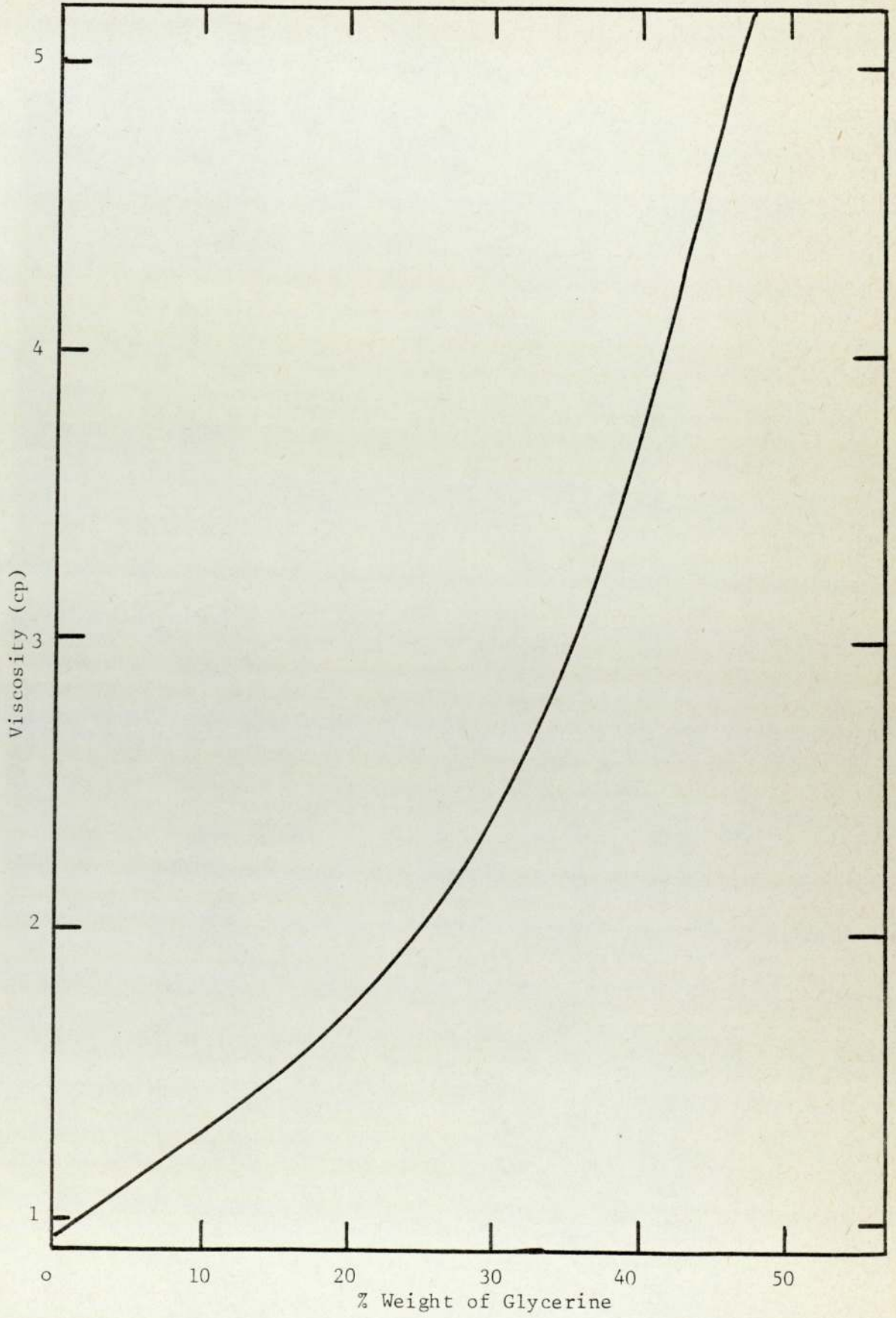


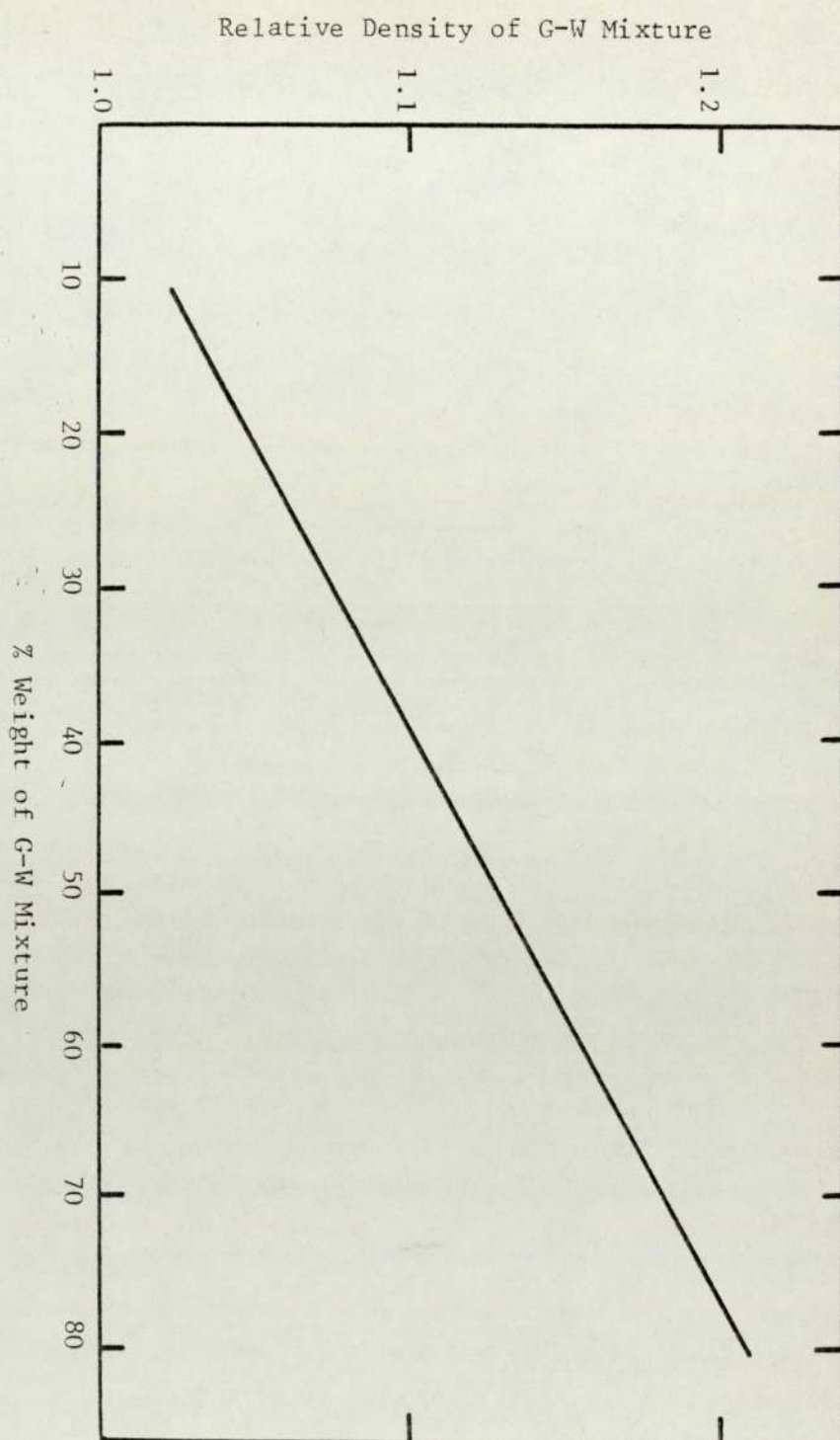
CALIBRATION FOR TOLUENE



APPENDIX SIX

PHYSICAL PROPERTIES OF GLYCERINE-WATER SYSTEM





APPENDIX SEVEN

DROP SIZE ANALYSIS PROGRAMME

```

TRACE 1
TRACE 2
MASTER ARASH
REAL MF, ND1, ND2, ND3, MVD
MAGNIFYING FACTOR, MF
INTEGER B, CM, F, A, Z
C Z IS THE NUMBER OF SETS OF DATA SUPPLIED
Z=14
DO 10 A=1,Z
5 READ(1,200)I,B,K,MF
200 FORMAT(3I0,F0.0)
WRITE(2,201)I,B
201 FORMAT(1I1,5X,'SERIALNO= ',I5,5X,'PHOT.NO= ',I5)
WRITE(2,111)
111 FORMAT(1H0,36X,'SAUTER MEAN DIAMETER AND ST.DEVIATION CALCULATION'
1)
WRITE(2,112)
112 FORMAT(24X,'DM',5X,'D',9X,'N',9X,'D2',5X,'D3',7X,'ND1',7X,'ND2',
17X,'ND3')
SUMV=0
SUMW=0
SUMND1=0
SUMND2=0
SUMND3=0
CROP MEAN DIAMETER, CM
NUMBER OF DROPS, N
DO 200 J=1,K
READ(1,114)DM,F
114 FORMAT(9(I0,I0))
D=DN/MF
D2=D**2
D3=D**3
N1=F*D
ND2=F*D2
ND3=F*D3
SUMD=SUMD+D

```

```

SUMN=SUMN+F
SUMNT1=SUMND1+N*1
SUMND2=SUMND2+L*02
SUMND3=SUMND3+N*03
20 WRITE(2,115)DF,D,F,D2,D3,ND1,ND2,ND3
115 FORMAT(22X,I5,3X,F9.5,4X,I5,4X,F9.5,1X,F9.4,2X,F9.4,2X,F9.4,
11X,F9.4)
GO TO 21
21 WRITE(2,116)
116 FORMAT(3X,1,4X,1,24X,1,1X,1,2X
1,1,1)
WRITE(2,117)SUMD,SUMN,SUMND1,SUMND2,SUMND3
117 FORMAT(70X,F9.5,3X,F4.0,22X,F9.4,2X,F9.4,1X,F9.4)
C
C ARITHMETIC MEAN, DIAMETER,  $\mu$ 
C SAUER MEAN DIAMETER,  $\mu_{SD}$ 
C ST. DEVIATION,  $\sigma$ 
AMD=SUMND1/SUMN
SMD=SUMND3/SUMND2
SD=SQRT((SUMND2-(SUMN*AMD**2))/(SUMN-1))
MVD=(SUMND3/SUMN)*C_3333
WRITE(2,118)AMD
118 FORMAT(20X,10X,ARITHMETIC MEAN, DIA= ,F10.5)
WRITE(2,119)SMD
119 FORMAT(20X,15X,SAUER MEAN DIA= ,F10.5)
WRITE(2,120)SD
120 FORMAT(20X,15X,ST. DEV = ,F10.6)
WRITE(2,121)MVD
121 FORMAT(20X,15X,MEAN VOLUME DIA= ,F10.5)
IF(I-100)25,26,26
I=I+1
25 GO TO 5
10 CONTINUE
26 STOP
END

```


APPENDIX EIGHT

BATCH EQUIPMENT RESULTS

BATCH EQUIPMENT

Phase Inversion Hold-up vs Rotor Speed

System: Toluene/Water (Toluene Dispersed)

Rotor Speed (r.p.m.)	Hold-up (%)
350	67.03
420	67.50
450	67.14
500	65.50
550	65.02
600	64.88
650	64.21
700	62.56
750	61.90

Phase Inversion Hold-up vs Rotor Speed

System: Toluene/Water (Water Dispersed)

Rotor Speed (r.p.m.)	Hold-up (%)
380	53.25
450	55.14
500	57.55
530	58.38
560	58.99
600	59.50
650	60.45
700	61.53
750	62.31

Phase Inversion Hold-up Vs Rotor Speed

System: 70% Toluene + 30% CCl₄/Water

(Organic Dispersed)

Rotor Speed (r.p.m.)	Hold-up (%)
290	48.23
340	52.25
400	57.52
490	65.09
550	70.52
650	79.38
700	82.19

Phase Inversion Hold-up Vs Rotor Speed

System: 70% Toluene + 30% CCl₄/Water

(Water Dispersed)

Rotor Speed (r.p.m.)	Hold-up (%)
220	90.15
290	88.73
350	87.83
410	86.69
480	86.41
560	85.97
610	85.50
680	84.02
750	83.82

Phase Inversion Hold-up Vs Rotor Speed

System: 63% Toluene + 37% CCl₄/Water

(Organic Dispersed)

Rotor Speed (r.p.m.)	Hold-up (%)
200	62.05
250	66.13
260	67.82
300	70.37
310	72.28
350	75.09
400	79.53
450	84.92

Phase Inversion Hold-up Vs Rotor Speed

System: 63% Toluene + 37% CCl₄/Water

(Water Dispersed)

Rotor Speed (r.p.m.)	Hold-up (%)
200	47.82
220	56.23
260	71.67
290	84.53

Phase Inversion Hold-up vs Rotor Speed

System: 30% Toluene + 70% CCl₄/Water

(Organic Dispersed)

Rotor Speed (r.p.m.)	Hold-up (%)
300	56.13
410	64.51
510	70.08
560	73.25
600	76.39
690	82.48

Phase Inversion Hold-up Vs Rotor Speed

System: 30% Toluene + 70% CCl₄/Water

(Water Dispersed)

Rotor Speed (r.p.m.)	Hold-up (%)
300	88.02
370	87.53
460	86.93
500	85.52
580	84.09
650	82.57
750	82.19

Toluene Drop Size vs Hold-up

Rotor Speed = 300 r.p.m.

Drop Size d_{32} (m)	Hold-up (%)
1.72×10^{-3}	25
1.95×10^{-3}	30
2.20×10^{-3}	35
2.43×10^{-3}	40
2.68×10^{-3}	45
2.89×10^{-3}	50
2.98×10^{-3}	52
3.18×10^{-3}	56
5.35×10^{-3}	60

Toluene Drop Size vs Hold-up

Rotor Speed = 350 r.p.m.

Drop Size d_{32} (m)	Hold-up (%)
1.65×10^{-3}	25
1.91×10^{-3}	30
2.15×10^{-3}	35
2.42×10^{-3}	40
2.65×10^{-3}	45
2.98×10^{-3}	50
3.05×10^{-3}	54
4.61×10^{-3}	58
8.03×10^{-3}	62

Toluene Drop Size vs Hold-up

Rotor Speed = 400 r.p.m.

Drop Size d_{32} (m)	Hold-up (%)
1.65×10^{-3}	25.0
1.91×10^{-3}	30.0
2.15×10^{-3}	35.0
2.40×10^{-3}	40.0
2.65×10^{-3}	45.0
2.90×10^{-3}	49.0
2.95×10^{-3}	50.0
3.20×10^{-3}	54.0
3.34×10^{-3}	55.5
3.75×10^{-3}	56.5
3.95×10^{-3}	57.2
4.62×10^{-3}	59.0
5.33×10^{-3}	59.5
6.10×10^{-3}	60.0

Toluene Drop Size vs Hold-up

Rotor Speed = 450 r.p.m.

Drop Size d_{32} (m)	Hold-up (%)
1.55×10^{-3}	25
1.95×10^{-3}	30
2.20×10^{-3}	35
2.40×10^{-3}	40
2.51×10^{-3}	45
2.93×10^{-3}	50
3.00×10^{-3}	52
3.15×10^{-3}	54
3.12×10^{-3}	56
4.35×10^{-3}	60

Toluene Drops vs Hold-up

Rotor Speed = 500 r.p.m.

Drop Size d_{32} (m)	Hold-up (%)
1.52×10^{-3}	25
1.95×10^{-3}	30
2.10×10^{-3}	35
2.30×10^{-3}	40
2.52×10^{-3}	45
2.95×10^{-3}	50
3.03×10^{-3}	52
3.11×10^{-3}	56
5.02×10^{-3}	60

Drop Size Growth at Phase Inversion

Rotor Speed = 300 r.p.m.

d_{32} (m)	time (seconds)
7.45×10^{-3}	0.0
7.82×10^{-3}	0.5
8.15×10^{-3}	1.0
8.63×10^{-3}	1.5
9.85×10^{-3}	2.0
2.06×10^{-2}	2.5
3.57×10^{-2}	3.0
6.05×10^{-2}	3.5

Drop Size Growth at Phase Inversion

Rotor Speed = 350 r.p.m.

Drop Size d_{32} (m)	Time (seconds)
8.02×10^{-3}	0.0
9.53×10^{-3}	0.5
1.15×10^{-2}	1.0
1.31×10^{-2}	1.5
1.85×10^{-2}	2.0
1.72×10^{-2}	2.5
2.12×10^{-2}	3.0
3.25×10^{-2}	3.5
4.89×10^{-2}	4.0

Drop Size Growth at Phase Inversion

Rotor Speed = 400 r.p.m.

d_{32} (m)	time (seconds)
7.55×10^{-3}	0.0
7.92×10^{-3}	0.5
8.42×10^{-3}	1.0
8.93×10^{-3}	1.5
9.62×10^{-3}	2.0
1.04×10^{-2}	2.5
1.42×10^{-2}	3.0
1.93×10^{-2}	3.5
2.98×10^{-2}	4.0
4.35×10^{-2}	4.5
6.30×10^{-2}	5.0

Drop Size Growth at Phase Inversion

Rotor Speed = 450 r.p.m.

d_{32} (m)	time (seconds)
7.63×10^{-3}	0
7.95×10^{-3}	0.5
8.32×10^{-3}	1.0
8.95×10^{-3}	1.5
9.42×10^{-3}	2.0
1.15×10^{-2}	2.5
1.95×10^{-2}	3.0
3.45×10^{-2}	3.5
6.82×10^{-2}	4.0

APPENDIX NINE

CONTINUOUS FLOW EQUIPMENT RESULTS

SYSTEM: TOLUENE - WATER (TOLUENE DISPERSED)

Rotor Speed (r.p.m.)	Inversion Phase Ratio (%)	Continuous Phase Hold-up (m^3)	Dispersed Phase Hold-up (m^3)
255	88.57	0.58×10^{-3}	4.53×10^{-3}
325	88.11	0.61×10^{-3}	4.48×10^{-3}
400	87.45	0.64×10^{-3}	4.42×10^{-3}
475	85.97	0.70×10^{-3}	4.29×10^{-3}
550	85.12	0.74×10^{-3}	4.24×10^{-3}
620	83.90	0.80×10^{-3}	4.17×10^{-3}

SYSTEM: TOLUENE - WATER (WATER DISPERSED)

Rotor Speed (R.P.M.)	Inversion Phase Ratio (%) (Dispersed Phase)	Continuous Phase Hold-up (m^3)	Dispersed Phase Hold-up (m^3)
200	68.65	1.61×10^{-3}	3.52×10^{-3}
250	69.14	1.58×10^{-3}	3.55×10^{-3}
300	68.75	1.60×10^{-3}	3.52×10^{-3}
350	70.77	1.48×10^{-3}	3.59×10^{-3}
360	69.46	1.55×10^{-3}	3.53×10^{-3}
420	70.52	1.48×10^{-3}	3.54×10^{-3}
495	71.97	1.40×10^{-3}	3.59×10^{-3}
550	72.01	1.39×10^{-3}	3.58×10^{-3}
615	72.49	1.37×10^{-3}	3.61×10^{-3}

SYSTEM: TOLUENE - WATER (TOLUENE DISPERSED)

Total Flow Rate = $6 \times 10^{-5} \text{ m}^3/\text{s}$

Rotor Speed (R.P.M.)	Inversion Phase Ratio (%) (Dispersed Phase)	Continuous Phase Hold-up (m^3)	Dispersed Phase Hold-up (m^3)
200	89.4	0.53×10^{-3}	4.47×10^{-3}
260	89.2	0.54×10^{-3}	4.46×10^{-3}
340	87.8	0.61×10^{-3}	4.39×10^{-3}
400	86.4	0.68×10^{-3}	4.32×10^{-3}
460	86.4	0.68×10^{-3}	4.32×10^{-3}
540	84.8	0.76×10^{-3}	4.24×10^{-3}
600	84.6	0.77×10^{-3}	4.23×10^{-3}

SYSTEM: WATER - TOLUENE (WATER DISPERSED)

Total Flow Rate = $6 \times 10^{-5} \text{ m}^3/\text{s}$

Rotor Speed (R.P.M.)	Phase Ratio (%)	Continuous Phase Hold-up (m^3)	Dispersed Phase Hold-up (m^3)
250	69.0	1.55×10^{-3}	3.45×10^{-3}
320	69.6	1.52×10^{-3}	3.48×10^{-3}
390	70.4	1.48×10^{-3}	3.52×10^{-3}
460	72.6	1.37×10^{-3}	3.63×10^{-3}
530	71.8	1.41×10^{-3}	3.59×10^{-3}
600	72.4	1.38×10^{-3}	3.62×10^{-3}

SYSTEM: TOLUENE - WATER (TOLUENE DISPERSED)

Total Flow Rate = $8 \times 10^{-5} \text{ m}^3/\text{s}$

Rotor Speed (r.p.m.)	Inversion Phase Ratio (%)	Continuous Phase Hold-up (m^3)	Dispersed Phase Hold-up (m^3)
200	90.6	0.47×10^{-3}	4.53×10^{-3}
260	89.4	0.53×10^{-3}	4.47×10^{-3}
340	87.8	0.61×10^{-3}	4.39×10^{-3}
400	86.0	0.70×10^{-3}	4.30×10^{-3}
460	85.8	0.71×10^{-3}	4.29×10^{-3}
540	85.6	0.72×10^{-3}	4.28×10^{-3}
600	83.8	0.81×10^{-3}	4.19×10^{-3}

SYSTEM: WATER - TOLUENE (WATER DISPERSED)

$$\text{Total Flow Rate} = 8 \times 10^{-5} \text{ m}^3/\text{s}$$

Rotor Speed (r.p.m.)	Phase Ratio (%)	Continuous Phase Hold-up (m^3)	Dispersed Phase Hold-up (m^3)
250	70.0	1.50×10^{-3}	3.50×10^{-3}
320	69.8	1.51×10^{-3}	3.49×10^{-3}
390	70.2	1.49×10^{-3}	3.51×10^{-3}
460	71.0	1.45×10^{-3}	3.55×10^{-3}
530	72.2	1.39×10^{-3}	3.61×10^{-3}
600	71.8	1.41×10^{-3}	3.59×10^{-3}

SYSTEM: TOLUENE - WATER (TOLUENE DISPERSED)

Total Flow Rate = $10 \times 10^{-5} \text{ m}^3/\text{s}$

Rotor Speed (r.p.m.)	Inversion Phase Ratio (%)	Continuous Phase Hold-up (m^3)	Dispersed Phase Hold-up (m^3)
250	89.8	0.51×10^{-3}	4.49×10^{-3}
320	88.2	0.59×10^{-3}	4.41×10^{-3}
390	87.8	0.61×10^{-3}	4.39×10^{-3}
450	86.4	0.68×10^{-3}	4.32×10^{-3}
500	86.0	0.70×10^{-3}	4.30×10^{-3}
550	84.8	0.76×10^{-3}	4.24×10^{-3}
600	84.6	0.77×10^{-3}	4.23×10^{-3}

SYSTEM: WATER - TOLUENE (WATER DISPERSED)

Total Flow Rate = $1 \times 10^{-4} \text{ m}^3/\text{s}$

Rotor Speed (r.p.m.)	Phase Ratio (%)	Continuous Phase Hold-up (m^3)	Dispersed Phase Hold-up (m^3)
280	69.2	1.54×10^{-3}	3.46×10^{-3}
350	69.6	1.52×10^{-3}	3.48×10^{-3}
420	70.8	1.46×10^{-3}	3.54×10^{-3}
490	71.8	1.41×10^{-3}	3.59×10^{-3}
550	72.0	1.40×10^{-3}	3.60×10^{-3}
600	72.6	1.37×10^{-3}	3.63×10^{-3}

SYSTEM TOLUENE - WATER (TOLUENE DISPERSED)

$$\text{Total Flow Rate} = 12 \times 10^{-5} \text{ m}^3/\text{s}$$

Rotor Speed (r.p.m.)	Inversion Phase Ratio (%)	Continuous Phase Hold-up (m^3)	Dispersed Phase Hold-up (m^3)
250	88.2	0.59×10^{-3}	4.41×10^{-3}
320	88.4	0.58×10^{-3}	4.42×10^{-3}
390	87.0	0.65×10^{-3}	4.35×10^{-3}
450	86.8	0.66×10^{-3}	4.34×10^{-3}
500	84.8	0.76×10^{-3}	4.24×10^{-3}
550	84.2	0.79×10^{-3}	4.21×10^{-3}
600	84.0	0.8×10^{-3}	4.20×10^{-3}

SYSTEM: WATER-TOLUENE (WATER DISPERSED)

Total Flow Rate = $1.2 \times 10^{-4} \text{ m}^3/\text{s}$

Rotor Speed (r.p.m.)	Phase Ratio (%)	Continuous Phase Hold-up (m^3)	Dispersed Phase Hold-up (m^3)
280	69.6	1.52×10^{-3}	3.48×10^{-3}
350	70.0	1.50×10^{-3}	3.50×10^{-3}
420	70.8	1.46×10^{-3}	3.54×10^{-3}
490	72.0	1.40×10^{-3}	3.60×10^{-3}
550	72.6	1.37×10^{-3}	3.63×10^{-3}
600	73.2	1.34×10^{-3}	3.66×10^{-3}

NOMENCLATURE

A (h)	Adhesion energy
a	Drop surface area, constant
b	Constant
c_1, \dots	Constant
C	Clearance of impeller off vessel bottom
D	Impeller diameter
D_k	Constant
d	Drop diameter
d_{32}	Sauter mean diameter
E	Kinetic energy
Fr	Froude number
H	Compartment height
G	Mass flowrate
g	Gravitational acceleration
K	Constant
k	Constant
l	Impeller blade length
N	Impeller speed
n	Number of blades
N_c	Coalescence frequency
N_t	Collision frequency
N_p	Power number
N_{vi}	Viscosity group
N_Q	Discharge number

P	Power input
p	Blade pitch
Re	Reynolds number
r	Distance between two drops
Q	Discharge rate
T	Tank diameter
t	Time
V	Volumetric flowrate
v	Fluid velocity
We	Weber number
w	Blade width
X	Inversion concentration
Z	Coalescence constant
z	Liquid depth

Greek Symbols

σ	Interfacial tension
ρ	Density
μ	Viscosity
ξ	Kinematic viscosity
λ	Eddy length
\emptyset	Dispersed phase ratio
Θ	Mixing time
λ_n	Scale of turbulence
τ	Deformation force
ψ	Kolmogoroff length
ε	energy dissipated by impeller

ϵ_v Energy dissipated per unit volume
 ν Kinematic viscosity

Subscript

c Continuous
d Dispersed
m Mean
av Average
cr Critical
i Inversion
max Maximum
min Minimum

LITERATURE REFERENCES

- 1 Mumford, C.J., Brit. Chem. Engng., 13, (7)981, (1968).
- 2 Bailes, P.J. and Windward, A., Trans. Inst. Chem. Engrs., 50, 240, (1972).
- 3 Logsdail, D.H. and Lowes, L., 'Industrial Contacting Equipment' in Hanson, C. (ed) "Recent Advances in Liquid-Liquid Extraction" pp. 139 - 168 (1970).
- 4 Reman, G.H., Proc. 3rd World Petr. Congr., The Hague (1951).
- 5 Misek, T., 'Rotating Disc Contactor' (1964) (Prague, Statni Nakadelokei Technicke Literatury).
- 6 Hanson, D., (ed) "Recent Advances in Liquid-Liquid Extraction" Pergamon (1971).
- 7 Arnold, D.R., Ph.D. Thesis, Uni of Aston in Birmingham (1974).
- 8 Al-Hemiri, A.A.A., Ph.D. Thesis, Uni of Aston in Birmingham (1973).
- 9 Khandelwal, A.N., Ph.D. Thesis, Uni of Aston in Birmingham (1978).
- 10 Sarkar, S., Ph.D. Thesis, Uni of Aston in Birmingham (1976).
- 11 Molyneux, F., Chem. Proc. Eng. 502 (1962).
- 12 Hossain, K.T., Ph.D. Thesis, Uni of Aston in Birmingham (1978).
- 13 Treybal, R.E., Liquid Extraction, 2nd Edition (1963) McGraw-Hill.
- 14 Hanson, C., Brit. Chem. Eng., 10, 34, (1965).
- 15 Arashmid, M. and Jeffreys, G.V., A.I.Ch.E. Jnl., 51, 26, (1980).

- 16 A.I.Ch.E., "Standard Testing Procedure, Impeller - Type Mixing Equipment." A.I.Ch.E., New York, 1960.
- 17 Uhl, V.W., Mixing: Theory and practice, Academic Press 1966.
- 18 Thomson, J., Proc. Roy. Soc., 7,509, (1855).
- 19 Unwin, W.C., Proc. Roy. Soc., A31,54, (1880).
- 20 White, A.M., and Brenner, E., Trans. A.I.Ch.E. 30, 585, (1934).
- 21 White, A.M., Brenner, E., Phillips, G.A., and Morrison, M.S., Trans. A.I.Ch.E., 30, 570 (1934).
- 22 White, A.M. and Somerford, S.D., Chem. & Met. Eng., 43, 370, (1936).
- 23 Hixson, A.W. and Baum, S.J., Ind. Eng. Chem., 34,194, (1942).
- 24 Hixson, A.W. and Luedeke, V.D., Ind. Eng. Chem., 29, 927 (1937).
- 25 Hixson, A.W. and Wilkins, G.A., Ind. Eng. Chem., 25, 1196 (1933)
- 26 Hixson, A.W. and Tenney, A.H., Trans. A.I.Ch.E., 31, 113 (1935).
- 27 Martin, J.J., Trans. A.I.Ch.E., 42, 777, (1946).
- 28 Brown, G.G., "Unit Operations". p. 507. Wiley, New York, 1950.
- 29 Hooker, T., Chem. Eng. Progr., 44, 833, (1948).
- 30 Mann, C.A., Trans. A.I.Ch.E., 40, 709 (1944).
- 31 Vermeulen, T., Williams, G.M. and Langlois, G.E., Chem. Eng. Progr., 51, 85 (1955).
- 32 Vanderveen, J.H., M.S. Thesis, Uni. of California, 1960.
- 33 Stepanoff, A.J., "Centrifugal and Axial Flow Pumps", 2nd ed., Wiley, New York, 1957.
- 34 Wislicenus, G.F., "Fluid Mechanics of Turbomachinery", McGraw-Hill, New York, 1947.

- 35 Miller, S.A., and Mann, C.A., Trans. A.I.Ch.E., 40, 709 (1944).
- 36 Nagata, S., Yoshioka, N. and Yokoyama, T., Mem. Fac. Eng. Kyoto Uni., 17, 175 (1955).
- 37 Rushton, J.H. and Oldshue, J.Y., Chem. Eng. Progr., 44, 161, 267, (1953).
- 38 Marr, G.R., PH.D. Thesis, Princeton University, (1959).
- 39 Marr, G.R., A.I.Ch.E. Jnl., 9, 383, (1963).
- 40 Rushton, J.H., Mack, D.E. and Everett, H.J., Trans. A.I.Ch.E., 42, 441, (1948).
- 41 Van de Vusse, J.G., Chem Eng. Sci., 4, 178, 209, (1955).
- 42 Sachs, J.P. and Rushton, J.H., Chem. Eng. Progr., 50, 597, (1954).
- 43 Norwood, K.W. and Metzner, A.B., A.I.Ch.E. Jnl., 6, 432, (1960).
- 44 Holmes, D.B., Voncken, R.M. and Dekker, J.A., Chem. Eng. Sci., 19, 201, (1964).
- 45 Nagata, S., Yamamoto, K., Hashimoto, K. and Naruse, Y., Mem. Fac. Eng. Kyoto Univ., 21, 260, (1959).
- 46 Mumford, C.J. and Jeffreys, G.V., Paper presented to 3rd. C.H.I.S.A. Congress, Marianske Lazne, September 1969.
- 47 Thornton, J.D. and Bouyatiotis, B.A., I. Chem. E. Symposium Series, 26, 43, (1967).
- 48 Null, R. and Johnson, H.E., A.I.Ch.E. Jnl., 4, 273, (1958).
- 49 Harkins, W.D. and Brown, F.E., Am. Chem. Soc. Jnl., 41, 499, (1919).
- 50 Scheele, G.F. and Meister, B.J., A.I.Ch.E. Jnl., 14, 9, (1968).
- 51 Hayworth, C.B. and Treybal, R.E., Ind. Eng. Chem., 42, 1174, (1950).
- 52 Ryan, J.T., Ph.D. Thesis, Uni. of Missouri, (1966).
- 53 Rao, E.V.L.N., Kumar, R. and Kuloor, N.R., Chem Eng. Sci., 21, 867, (1966).
- 54 Heertzes, P.M., de Nie, L.H. and de Vries, Chem. Eng. Sci., 26, 441, and 755, (1971).

- 55 Nodberg, S., Dechema Monagr., 41, 257, (1962).
- 56 Dixon, B.E. and Russell, A.A.W., J. Soc. Chem. Ind., London, 69, 284, (1950).
- 57 Angels, J.B., Lightfoot, E.M. and Howard, D.W., A.I.Ch.E. Jnl., 12, 751, (1966).
- 58 Al Hassani, T., Ph.D. Thesis, University of Aston in Birmingham, (1979).
- 59 Kolmogoroff, A.N., Doklady Acad. Nank., U.S.S.R., 30, 301, (1941); 31, 538, (1941).
- 60 Heinze, J.O., A.I.Ch.E. Jnl, 1, 289, (1955).
- 61 Rushton, J.H., Rodger, W.A. and Trice, V.G., Chem. Eng. Prog., 52, 515, (1956).
- 62 Shinnar, R. and Church, J.M., Ind. Engng. Chem., 52, 253, (1960).
- 63 Levich, V.G. "Physico Chemical Hydrodynamics", Prentice-Hall, N.Y. (U.S.A.), (1962).
- 64 Endoh, K. and Oyama, Y., Jnl. Sci. Research Inst. (Tokyo) 52, 253, (1966).
- 65 Baranayev, M.K., Ye. Taverovskiy, N., and Tregubova, E.L., Doklady Akad. Nank U.S.S.R., 66, 821, (1949).
- 66 Chen, H.T. and Middleman, S., A.I.Ch.E. Jnl., , 989, (1967).
- 67 Brown, D.E. and Pitt, K., Proc. Chemica, 70, Butterworth, Australia, (1970).
- 68 Pebalk, V.L. and Mishev, V.M., Teor, Osnary. Khim. Tekhnol., 3, 418, (1969).
- 69 Giles, J.G., Hanson, C. and Marsland, J.H., Proc. I.S.E.C., (1974), The Hague.
- 70 Howarth, W.J., Chem. Eng. Sci., 19, 33, (1966).
- 71 Madden, A.J. and Damarell, G.L., A.I.Ch.E. Jnl. 8, 233, (1962).
- 72 Misek, T., Coll. Czech. Chem. Comm., 29, 2086, (1964).
- 73 Kafanov, V.V. and Babanov, D.M., Zh. Prikl. Khim., 32, 789, (1959).
- 74 Calderbank, P.H., Trans. Instn. Chem. Engrs., 36, 443, (1958).
- 75 Olney, R.B., A.I.Ch.E. Jnl., 10, 827, (1964).

- 76 Sprow, F.B., A.I.Ch.E. Jnl. 13, 995, (1967).
- 77 Harkins, W.D., "The Physical Chemistry of Surface Films", Reinhold Publishing Corp., (1952).
- 78 Smoluchowski, M., Coll. Brounovskoye Dvizheniye, ONTI, (1936).
- 79 Oswaldt, W., Kolloid Z, 6, 103, (1910).
- 80 Ahmad, K.E., M.Sc. Thesis, Uni. of Aston in Birmingham, (1978).
- 81 Luhning, R.W. and Sawistowski, H., I.S.E., C., Session 5A, 136, 51, (1971).
- 82 McClarey, M.J. and Mansoori, G.R., A.I.Ch.E. Symp. Series, 74, 173, (1978).
- 83 Selker, A.H. and Sleicher, C.A., Jnr., Can. J. Chem. Eng., 17, 298, (1965).
- 84 Quinn, J.A. and Sigloh, D.B., Can. J. Chem. Eng., 41, 15, (1963).
- 85 Yeh, G.C., Haynie, F.H., Jnr. and Moses, R.A., A.I.Ch.E., Jnl, 10, 260, (1964).
- 86 Clarke, S.J. and Sawistowski H., Trans. I. Chem. E., 56, 50, (1978).
- 87 Ali, F.A., M.Sc. Thesis, Uni. of Manchester, (1969).
- 88 Al Saadi, A., Ph.D. Thesis, Uni. of Aston in Birmingham, (1978).
- 89 Coulaloglou, C.A. and Tavlarides, L.L., A.I.Ch.E. Jnl., 22, 285, (1976).
- 90 Miller, R.S., Ralph, J.L., Curl, R.L. and Towell, G.D., A.I.Ch.E. Jnl., 9, 196, (1963).
- 91 Logsdail, D.H., Thornton, J.D. and Pratt, H.R.C., Trans. Instn, Chem. Eng., 35, 301, (1957).
- 92 Arnold, D.R. Unpublished Work, Uni. of Aston in Birmingham, (1973).
- 93 Jeffreys, G.V., Unpublished Work, Uni. of Aston in Birmingham (1975).
- 94 Clay, P.H., Proc. Royal Acad. Sci., Amsterdam, 43, 852, 979, (1940).

- 95 Mumford, C.J. and Jeffreys, G.V., Paper presented to the the 3rd C.H.I.S.A. Congress, Marianske Lazne, Sept. 1969.
- 96 Davies, J.T. Turbulence Phenomena, Academic Press, (1972).
- 97 Stephenson, R., I. Chem. Eng. Symp. Series, 38, 1, (1974).
- 98 Nakada, K. and Tanaka, M. Trans. Instn. Chem. Engrs., 55, 143, (1977).
- 99 Ponter, A.B., Polymer Eng. and Sci., 17, 7, (1977).
- 100 Hittit, A., Ph.D. Thesis, Univ. of Aston in Birmingham, (1972).
- 101 Angelo, J.B., Lightfoot, E.N. and Howard, D.W., A.I.Ch.E., Jnl., 12, 751, (1966).
- 102 Misek, T., Collection Czeck. Chem. Comm., 29, 2086, (1964).
- 103 Rodger, W.A., Trice, V.G., Jr. and Rushton, J.H., Chem. Eng. Prog., 52, 515, (1956).
- 104 Sawistowski, H., Private Communication, (1980).
- 105 Harkins, W.D., "The Physical Chemistry of Surface Films", Reinhold Publishing Corp., (1952).

- Miller, L. and P. C. Carmen, "Self-Diffusion in Mixtures—II," *Trans. Fara. Soc.*, **55**, 1831-1837 (1959).
- Miyake, Y., Y. Tzumi, and R. Kono, "Static and Dynamic Viscosities in the Binary Mixture Nitrobenzene-n-Hexane Near a Critical Point," *Phys. Rev. A*, **15**, 2065-8 (1977).
- Prigogine, I. and R. Defay, *Treatise on Thermodynamics*, London, Longmans (1954).
- Reed, T. M. and K. E. Gubbins, *Applied Statistical Mechanics*, McGraw-Hill, New York (1973).
- Robinson, R. A. and R. H. Stokes, *Electrolyte Solutions*, Butterworths, London (1965).
- Stanley, H. E., *Introduction to Phase Transitions and Critical Phenomena*, Oxford, New York (1971).
- Swift, J., "Transport Coefficients Near the Consolute Temperature of a Binary Liquid Mixture," *Phys. Rev.*, **173** (1), 257-260 (1968).
- Thiel, D., B. Chu, A. Stein, and G. Allen, "Light Scattering from a Binary Liquid Mixture Above its Critical Consolute Point," *J. Chem. Phys.*, **62**, 3689-3711 (1975).
- Turner, J. C. R., "Formulation of the Diffusion Coefficient in Isothermal Binary Systems," *Chem. Engr. Sci.*, **30**, 151 (1975a).
- Turner, J. C. R., "Diffusion Coefficients Near Consolute Points," *Chem. Engr. Sci.*, **30**, 1304-5 (1975b).
- Vignes, A., "Diffusion in Binary Solutions," *IEC Fund.*, **5**, 189-199 (1966).

Manuscript received February 20, 1978; revision received December 7, and accepted January 3, 1979.

Analysis of the Phase Inversion Characteristics of Liquid-Liquid Dispersions

Correlations of the collision frequency and the coalescence frequency of an agitated dispersion are combined with models relating drop sizes and hold-up to agitator speed, to predict the ambivalence range and phase inversion composition of liquid-liquid dispersions. Our model was tested by comparing predicted and experimental phase inversion compositions of the systems toluene-water and carbon tetrachloride-water. In addition, the predicted results have been compared with published results for the system kerosene-water, and in all cases, agreement between predicted and experimental results are excellent.

M. ARASHMID

and

G. V. JEFFREYS

Chemical Engineering Department
University of Aston in Birmingham
Gosta Green, Birmingham, United Kingdom

SCOPE

Liquid-liquid dispersions are generated in solvent extraction operations, direct contact heat exchangers and in two-phase chemical reactors. The identification of the dispersed phase under all conditions and the limits of stability of these heterogeneous mixtures are most important in these process operations. Hitherto, the limits of the ambivalence range and the phase inversion concentrations have been treated qualitatively, and there has been no

attempt to predict either limit or assess the effect of agitator speed and the physical properties of the system on the inversion characteristics. In this article, phase inversion is analyzed in terms of the collision frequency and coalescence frequency of agitated dispersions. It was possible to combine models of these two phenomena with the effects of disperse phase hold-up on drop size, to accurately predict the ambivalence range and the phase inversion compositions.

CONCLUSIONS AND SIGNIFICANCE

The collision frequency and the coalescence frequency of agitated dispersions have been studied extensively, and both have been found to depend on the turbulence level of the agitation, the disperse phase hold-up, and the physical properties of the system. These phenomena can be combined to accurately predict the ambivalence range and the phase inversion concentration. Thus the ambivalence range can vary from 20% dispersed to 90%, depending on how the dispersion was produced. Recently, Arnold (1975) showed that a solvent extractor operates most efficiently under sequential phase inversion conditions. There-

fore, it is necessary to be able to predict the ambivalence range and the phase inversion concentrations, and the model presented here has been tested on two systems of widely different physical properties, together with a third studied qualitatively by another researcher (Ali 1969). We found that the ambivalence range and the phase inversion concentration can be predicted accurately as a function of agitator speed, dispersed phase hold-up and the physical properties of the system. This has significance in the design and operation of extraction equipment, direct contact heat exchangers, and two-phase liquid-liquid reactors.

Characterization of a liquid-liquid dispersion is an important requirement in many industrial chemical engineer-

ing operations such as solvent extraction, direct contact heat exchangers, and batch and continuous heterogeneous reactors. These dispersions are produced by injecting one phase through a distributor into the second phase, or mechanically agitating the two phases in the equipment in

0001-1541-80-3250-0051-\$00.75. © The American Institute of Chemical Engineers, 1980.

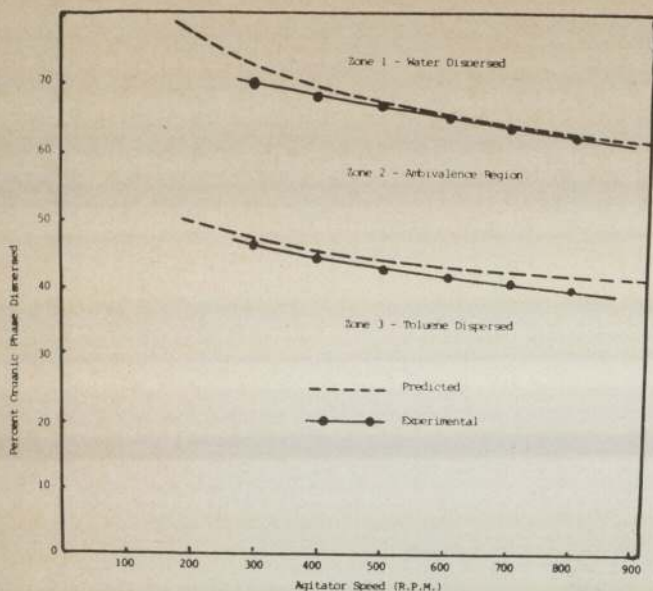


Figure 1. Ambivalence range for system toluene-water.

which the dispersion is to reside. If the energy transmitted to the liquid-liquid system is large, very small drops of the dispersed phase are produced and a metastable emulsion could result, but in the majority of chemical engineering operations this is unlikely and undesirable. In most process operations of the types cited above, a large interfacial area between the phases is essential. This may be achieved by applying mechanical energy to produce small droplets, or by adjusting the phase ratio to increase the number of droplets, albeit larger droplets. In practice, the adjustment of the phase ratio is generally more preferable, because of the subsequent inherent difficulties associated with the phase separation of dispersions consisting of small drops (for example, secondary dispersions). There are, however, limits to which one liquid phase can be dispersed in another. If the droplets remained spherical, the maximum volume fraction of the dispersed phase would correspond to Ostwald's ratio, but because of distortion of the drops in the dispersion, phase inversion ratios in excess of 90% have been reported. Phase inversion is generally presented graphically by plotting the volume fraction of the dispersed phase in the heterogeneous mixture at inversion against the speed of the agitator. A typical plot is shown in Figure 1 for the system water-toluene.

In this figure, two curves separate three zones. These are:

Zone 1—in which the composition of the mixture and agitation rate are such that only water can exist as the dispersed phase.

Zone 3—in which the mixture composition and agitation rate are such that only toluene can exist as the dispersed phase.

Zone 2—where either phase can be dispersed. In Zone 2 the phase dispersed depends on the method by which the dispersion was formed. The difference in the composition of the dispersed phase in this zone, at any agitation rate, is generally termed the "ambivalence range." All agitated heterogeneous liquid-liquid systems exhibit this hysteresis region and, although there are several studies of this phenomenon (Sawistowski 1971, McClarey & Mansoori 1978) no attempt has been made to quantify the parameters controlling phase inversion. We considered this essential, because it has been observed that phase inversion phenomena has a pronounced effect on the performance of mechanically agitated extraction columns

(Arnold 1975, Al-Saadi 1978). Therefore we initiated an investigation to identify properties of the system that control the phase inversion characteristics of a heterogeneous liquid mixture in an agitated environment. The results obtained follow.

MATHEMATICAL MODEL

Consider a heterogeneous liquid-liquid mixture to be agitated in a tank of suitable dimensions so that 1) isotropic turbulence persists throughout its contents and that 2) the energy input is sufficient to produce and maintain a dispersion in the tank. When steady state is attained, there will be equilibrium between the kinetic energy transmitted from the agitator causing drop break-up, and the energy of adhesion inducing the drops to coalesce (Shinnar 1960).

Both the break-up and coalescence processes proceed simultaneously throughout the contents of the tank, if the turbulence is isotropic. This will manifest itself through frequent collisions of adjacent drops, and some coalescence will result. Under these conditions, the smaller drops will be coalescing and the larger drops will be breaking up. The scale of turbulence will be such that the collision frequency of the drops in the turbulent regime may be estimated from the expression deduced by Levich (1962). Thus, following Misek (1964) for drops of initial size p , the frequency of collision N_T is

$$N_T = \frac{\rho_d n^2 \epsilon_0^{3/4} p^4}{\rho_c \nu_c^{5/4}} \quad (1)$$

where n is the number of drops per unit volume. Other terms are identified in the nomenclature.

$$n = \frac{6 \cdot \phi}{\pi \cdot p^3} \quad (2)$$

The energy per unit volume of mixture transmitted to the liquids is proportional to the density of the continuous phase and the agitator speed, or

$$\epsilon_0 = k_1 \rho_c N^3 \quad (3)$$

where k_1 is the proportionality constant. Substituting Equations (2) and (3) into Equation (1), and introducing the viscosity ratio to allow for the shearing effect of turbulence on the drops in the turbulent field, gives

$$N_T = \frac{K \cdot \phi^2 \cdot \mu_d \cdot \rho_d \cdot \rho_c N^{9/4}}{p^2 \cdot \mu_c^{9/4}} \quad (4)$$

where $K = 3.65 k_1^{3/4}$, and k_1 is a constant characteristic of the type of agitator.

The coalescence frequency of drops in a dispersion in an agitated tank has been studied by Howarth (1967), who stated that the coalescence frequency could be estimated by

$$N_c = \frac{6.0 \phi [dp/d\theta]}{(2.0 - 2.0^{0.667}) p^4} \quad (5)$$

Howarth found that the rate of change of drop size with time following a disturbance was proportional to $N^{1.9-2.25}$ for agitator speeds in the range 200-400 rpm. Whereas, Maddern and Damerell (1962) found that the coalescence frequency dependence on agitator speed was proportional to $N^{1.5-3.3}$. This range of the exponent of the agitator speed agrees with the tabulated results of Miller (1963). Extrapolating Miller's results for a turbine agitator and dispersed phase hold-up's greater than 60% gives an exponent of 1.8. That is,

$$\frac{dp}{d\theta} \propto N^{1.8} \quad (6)$$

is the most suitable relationship to substitute into Equation (5) for the variation of drop size with time following a disturbance.

The steady state drop size is a function of both the agitator speed and the dispersed phase hold-up, and the effects of hold-up on drop size have been the subject of a large number of research studies. These are summarized by Tavlarides and Coualaloglou (1976) who stated that the different correlations proposed are equally valid, within the limits of their derivation. The correlations of Thornton and Bouyotiotes (1967) will be applied to estimate the mean drop size at different dispersed phase hold-ups. Thornton and Bouyotiotes showed that the sauter mean drop size at hold-up ϕ is related to the sauter mean drop size at zero hold-up by

$$p = p_0 + m\phi \quad (7)$$

where m is related to the physical properties by

$$m = k_2 \left(\frac{\sigma}{\mu_c^2 g} \right) \left(\frac{\Delta\rho\sigma^3}{\mu_c^4 g} \right)^{-0.62} \left(\frac{\Delta\rho}{\rho_c} \right)^{0.05} \quad (8)$$

and where k_2 is a geometric constant.

These authors further showed that the drop size at zero hold-up p_0 could be correlated by the expression

$$\left(\frac{p_0 \rho_c^2 g}{\mu_c^3} \right) = 29.0 \left(\frac{P_0^3 g_c}{\rho_c^2 \mu_c g^4} \right)^{-0.32} \left(\frac{\rho_c \sigma^3}{\mu_c^4 g} \right)^{0.14} \quad (9)$$

Replacing P_0 by $(k_1 \rho_c N^3)$ and converting to SI units, and then rearranging Equation (9) gives

$$P_0 = k_3 \cdot m_1 N^{-2.88} \quad (10)$$

where the parameter m_1 is correlated to be

$$m_1 = \left(\frac{\mu_c^3}{\rho_c^2 g} \right) \left(\frac{\rho_c \sigma^3}{\mu_c^4 g} \right)^{0.14} \left(\frac{\rho_c}{\mu_c g^4} \right)^{-0.32} \quad (11)$$

Combining Equations (7) and (10) leads to

$$p = k_3 \cdot m_1 N^{-2.88} + m\phi \quad (12)$$

Expressions similar to Equation (12) can be developed from many of the other correlations quoted by Tavlarides (1976).

When the dispersion is agitated, the drops will collide and some will coalesce. As the dispersed phase hold-up increases, at constant agitator speed, the proportion of the pairs of drops coalescing at each collision will increase until, at phase inversion, coalescence will occur at every collision. That is when coalescence frequency is equal to collision frequency, and phase inversion occurs, or when N_T in Equation (4) is equal to N_c in Equation (5). Let the ratio (N_c/N_T) be T or

$$T = \frac{K}{\phi p^2 N^{0.46}} \quad (13)$$

By Equation (13), phase inversion occurs when $T = 1.0$, and the inversion composition for any system should be capable of predicting from Equations (12) and (13) for the condition $T = 1.0$.

EXPERIMENTAL

Batch phase inversion studies were performed in a 0.102 m diameter round bottom glass vessel 0.102 m high,

containing four equally spaced stainless steel baffles, 0.01 m wide. The tank's contents were agitated by a four blade stainless steel open turbine, 0.05 m diameter. It is powered by a 10 kW electric motor with a variable speed attachment, and is capable of a maximum agitator speed of 800 rpm. The agitator speed was kept constant during each phase inversion test, and was monitored by an electronic tachometer.

Phase inversion was detected by inserting two electrodes into the side walls of the glass mixing vessel; the inversion point could be detected very accurately by violent deflection of the ammeter placed in the electrode circuit.

SYSTEMS STUDIED

Two immiscible liquid systems were studied: toluene-water, and carbon tetrachloride-water. The toluene and carbon tetrachloride were both of G.P.R. grade and mixed with deionized distilled water until they were saturated. This was accomplished by agitating each organic liquid with the water in an aspirator bottle for three days at 25°C. When the phases had been saturated, the relevant physical properties of each were determined by the usual methods.

EXPERIMENTAL TECHNIQUE

The mixing vessel and all the measuring cylinders used for the experimental work were thoroughly cleaned by soaking in a 1.0% Decon solution overnight, then by rinsing with hot running water, and finally with deionized distilled water. The mixing vessel was cleaned after each six experiments, and the purity of each system studied was tested by immersing 400 mL of each phase in the mixing vessel, agitating at 450 rpm for ten minutes and then switching off the agitator. Time taken for the dispersion to collapse to a clear interface was determined. This time was compared with that for fresh liquids, and if there was a 5.0% deviation from the original value, the particular mixture was rejected and replaced.

Phase inversion experiments were performed by placing the continuous phase in the mixing vessel until the impeller was immersed; the continuous phase volume was noted. Usually this was of the order of 500 mL. The impeller was then started and its speed adjusted to that desired for the particular experiment. After this, small quantities of the dispersed phase were added at frequent intervals to produce a dispersion occupying 800 mL total volume. The phase ratio was then periodically adjusted by adding or removing 3.0 mL portions of either phase, until phase inversion was observed. After phase inversion, the agitator was stopped and the volume of each phase ascertained.

Experiments were conducted at agitator speeds between 300 and 800 rpm. The results are presented in Figures 1 and 2, for the systems toluene-water and carbon tetrachloride-water, respectively.

During a number of experiments, the variation in drop size with hold-up was estimated, and the Thornton-Bouyotiotes correlation up to phase inversion was tested by taking photographs of the dispersion with a 35 mm camera. The photographs were evaluated on a Zeiss particle counter. These results are presented in Figure 3.

RESULTS

In all experiments, we observed that the variation in drop size with hold-up conformed to the Thornton-Bouyotiotes correlation close-up to the phase inversion concentration. But, in the vicinity of phase inversion, the

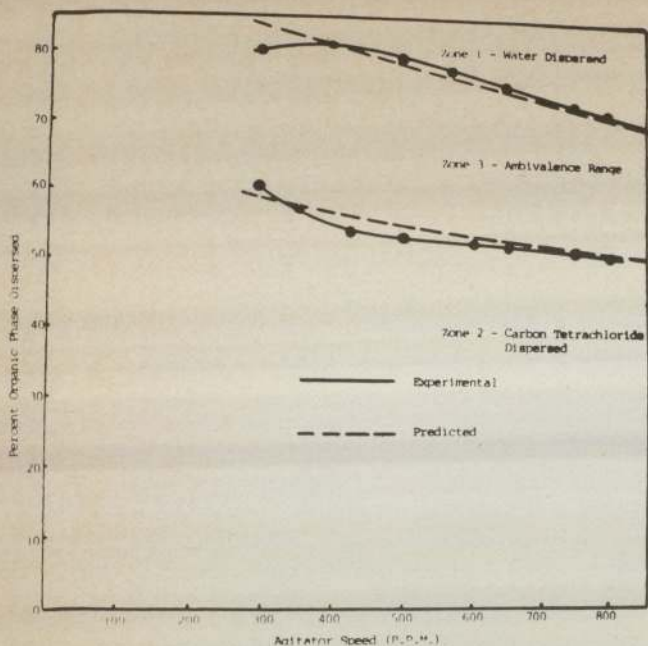


Figure 2. Ambivalence limits for the system carbon tetrachloride-water.

drop size increased rapidly with very small additions of the dispersed phase. Immediately prior to phase inversion, globules of the dispersed phase were discharged from the periphery of the impeller region. This could be expected, since in this region of the mixing vessel, rapidly moving drops discharged from the impeller come into contact with the slower moving dispersion near the walls of the mixer. Phase inversion followed rapidly after these conditions were passed. Still, while the actual phase inversion process was much more abrupt at slow agitator speeds than at high speeds, in all experiments the change occurred quite fast and was accompanied by violent fluctuations through the vessel.

The model describing phase inversion was tested on the two systems studied. In addition, the data of Ali (1969) for the system kerosene-water were also analyzed. Results for this system are presented in Figure 4. The constants in Equations (12) and (13) were evaluated for one experimental result for each system, and these are presented in Table I. The values of the constants so obtained were then inserted into all the other results. Equations (8), (11), (12) and (13) were solved by an appropriate computer program (Arashmid 1979), and all the results

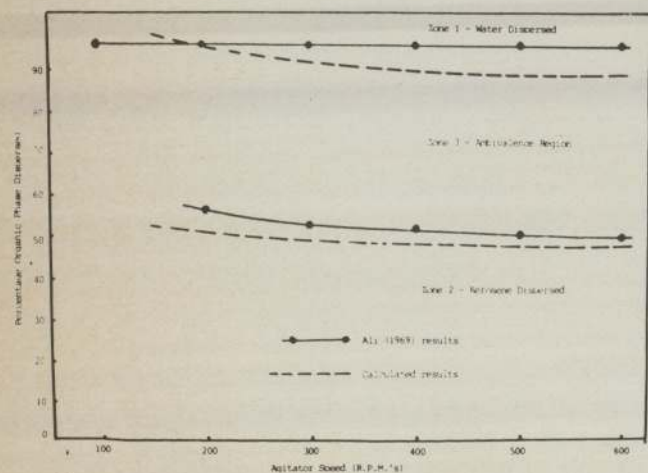


Figure 4. Ambivalence range for the system kerosene-water.

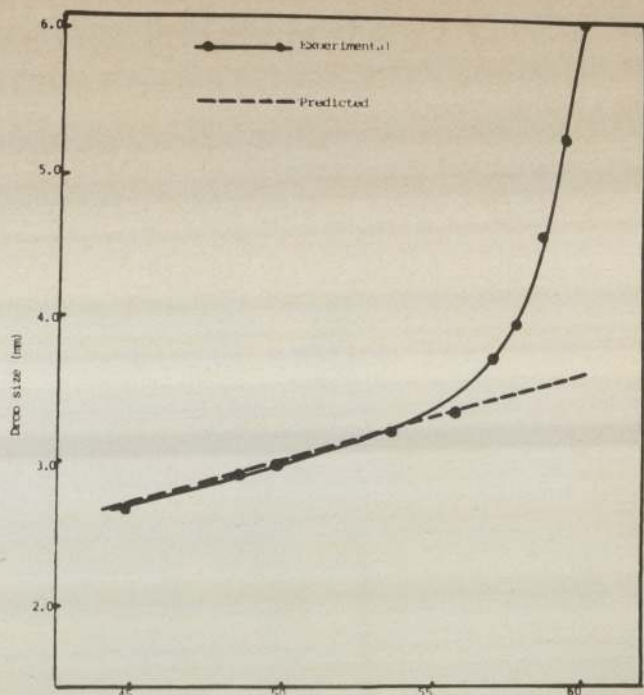


Figure 3. Drop size vs. dispersed phase hold-up for an agitator speed of 400 rpm.

TABLE I. OVERALL CONSTANT FOR PREDICTION OF PHASE INVERSION

Dispersed phase	Continuous phase	K
Water	Toluene	2.62×10^5
Water	Carbon tetrachloride	6.85×10^4
Water	Kerosene	1.83×10^{-3}
Toluene	Water	2.91×10^4
Carbon tetrachloride	Water	9.75×10^4
Kerosene	Water	6.09×10^7

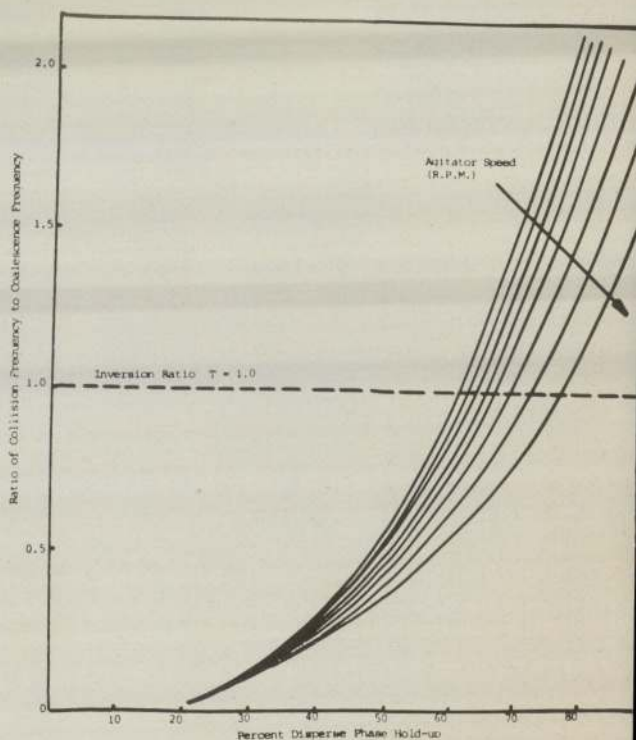


Figure 5. Variation of collision frequency/coalescence frequency with dispersed phase hold-up and agitator speed.

calculated for the three systems are shown in Figures 1, 2 and 4, where they can be compared with the experimental results.

Variation in the value of T with the volume fraction dispersed for the system toluene-water, with toluene dispersed, is plotted in Figure 5, using agitator speed as parameter. The line for " $T = 1.0$ " is also shown, and the abscissa for the intersection of this line with each curve gives the inversion point. Corresponding plots for the other systems studied here have been prepared by Arashmid (1979). The points obtained from this type of curve were then transferred to the normal phase inversion curve as shown in Figures 1, 2 and 4. In all cases, the agreement between the predicted phase inversion curve and the experimental curve is exceptionally good. The difference between the experimental and predicted inversion concentration was generally less than 2.0% volume fraction. The greatest difference was observed with the system carbon tetrachloride-water with water dispersed. In that case, differences of the order of 4% were observed. Generally better agreement was obtained when the organic liquid was dispersed, and improved agreement can be seen for each system as the agitator speed increases.

NOTATION

- g = gravity acceleration constant
 k_1 = proportionality constant characteristic of the agitator
 k_3 = combined constant in drop size equation
 m = gradient of drop size vs. hold-up relationship
 m_1 = parameter correlated by Equation (11)
 n = number of drops per unit volume
 N = agitator speed in rpm
 N_c = coalescence frequency
 N_T = collision frequency
 p = drop size
 p_0 = drop size at zero hold-up
 P_0 = power transmitted by agitator
 T = ratio of N_c/N_T

Greek Symbols

- ζ = energy of turbulence
 ν_c = kinematic viscosity of continuous phase
 ρ_c = density of continuous phase
 ρ_d = density of dispersed phase

- θ = time
 μ_c = viscosity of continuous phase
 μ_d = viscosity of dispersed phase
 ϕ = fractional hold-up of dispersed phase

LITERATURE CITED

- Al-Hemiri, A. M., "The Effects of Surface Renewal on Mass Transfer in Agitated Contactors," Ph.D. thesis, University of Aston, Birmingham (1973).
 Ali, F. A., "Ambivalence Studies in Mixer Settlers," M.Sc. (Tech.) thesis, University of Manchester (1969).
 Al-Saadi, A., "Studies of Liquid Extraction with Simultaneous Chemical Reaction," Ph.D. thesis, University of Aston, Birmingham (1978).
 Arashmid, M., "Phase Inversion Studies in Liquid-Liquid Dispersions," Ph.D. thesis, University of Aston, Birmingham (1979).
 Arnold, D. R., "Liquid Extraction in Agitated Contactors Involving Droplet Coalescence and Redispersion," Ph.D. thesis, University of Aston, Birmingham (1975).
 Coulaloglou, C. A. & L. L. Tavlarides, "Drop Size Distribution & Coalescence Frequencies of Liquid-Liquid Dispersions in Flow Vessels," *AIChE J.*, **22**, 289 (1976).
 Howarth, W. J., "Measurement of Coalescence Frequencies in Agitated Tanks," *AIChE J.*, **13**, 1007 (1967).
 Luning, R. W. & H. Sawistowski, "Phase Inversion in Stirred Liquid-Liquid Systems," *I.S.E.C.*, Session 5A, **136**, 51 (1971).
 Levich, V. G., *Physicochemical Hydrodynamics*, Prentice-Hall Int, Englewood Cliffs, N.J. (1962).
 Maddern, A. J. & G. L. Damerell, "Coalescence Frequencies in Agitated Liquid-Liquid Systems," *AIChE J.*, **8**, 233 (1962).
 McClarey, M. J. & G. R. Mansoori, "Effects of Density Differences, Temperature and Interfacial Tension on Dispersion Shift of Immiscible Liquids," *AIChE Symposium Series*, **74**, 173 (1978).
 Miller, R. S., J. L. Ralph, R. L. Curl, & G. D. Towell, "Dispersed Phase Mixing: Measurements in Organic Dispersed Systems," *AIChE J.*, **9**, 196 (1963).
 Misek, T., "Coalescence of Drops in an Agitated Liquid-Liquid Extractor," *Collection Czech. Chem. Comm.*, **29**, 2086 (1964).
 Quinn, J. A. & B. D. Jigloh, "Phase Inversion in the Mixing of Immiscible Liquids," *Can. J. Chem. Eng.*, **42**, 15 (1963).
 Shinnar, R. & J. M. Church, "Predicting Particle Size in Agitated Dispersions," *Ind. Eng. Chem.*, **52**, 253 (1960).
 Thornton, J. D. & B. A. Bonyototes, *I. Chem. E. Symp. Series*, **26**, 43 (1967).

Manuscript received March 21, 1979; revision received August 2, and accepted August 30, 1979.

Effectiveness and Deactivation of a Diluted Catalyst Pellet

PHILIP VARGHESE

and

EDUARDO E. WOLF

Department of Chemical Engineering
 University of Notre Dame
 Notre Dame, Indiana 46556

In this article, we analyze the performance of a diluted catalyst pellet consisting of inert and active particles, under diffusion influenced conditions and pore-mouth poisoning. First, we establish the requirements for validity of the analytical solutions of the diluted pellet equations. Secondly, we show that, under pore-mouth poisoning conditions, a diluted pellet can display considerably longer lifetimes than a uniformly impregnated catalyst. Conversely, for the same lifetime, use of a diluted pellet can result in savings of the catalytic agent. These advantages are not offset by difficulties in catalyst manufacture, as is the case for previous designs.

SCOPE

Many catalytic processes of industrial importance operate in the temperature region where the reaction is essen-

tially diffusion controlled, and only a small fraction of total catalyst volume is effective in the reaction. In situations where shell-progressive or pore-mouth type poisoning describes the deactivation process, the catalyst may suffer a precipitous decline in activity by virtue of the fact that

Address correspondence to E. Wolf.

it is these very outer layers of active material that are poisoned first. However, proper design of the diffusion characteristics of a catalyst shows promise for more efficient utilization of active material and of mitigating the effects of poisoning processes.

These goals have been actively pursued in relation to the important area of catalysts for automotive exhaust pollution control. Previous proposed designs that, in theory showed promise for improvement, consisted of catalysts with non-uniform distribution of active materials, and composite catalysts made of layers of different diffusive properties. Ruckenstein (1970) analyzed the effectiveness of a diluted catalyst pellet consisting of microspheres imbedded in an inert porous media. With this configuration, pellet effectiveness can be modified by selecting the

proper diffusivity of the inert media. The objective here is to analyze the performance of such diluted catalysts under conditions of pore-mouth poisoning, a question which has not been investigated before. First, we analyze the effectiveness of the diluted pellet using more realistic assumptions regarding its effective diffusivity, to represent pellet behavior over the entire possible range of dilution more correctly than in previous models. Results indicate that for a given value of the diffusivities of the porous inert media and active particles, there is an optimal dilution which gives maximum effectiveness. Secondly, these results are combined with pore-mouth poisoning equations to predict the reaction rate versus time-on-stream behavior of the diluted catalysts, relative to that of undiluted catalysts of the same dimensions.

CONCLUSIONS AND SIGNIFICANCE

The analysis of the diffusion-reaction equations used to describe a diluted catalyst pellet showed that a valid analytical solution is possible with the use of a consistent expression for the effective diffusivity. This is true only when the active porous particles within the diluted pellet are themselves not diffusion limited. Our results validate the assumptions made in the model depicting the diluted pellet. The analysis of pore-mouth poisoning in the diluted catalyst showed that increasing the diffusivity of the inert

media and its "poison-getter" capacity can increase catalyst lifetime and savings in active material required.

A diluted catalyst pellet should not present significant manufacturing difficulties: diffusivity and poison-getter capacity can be enhanced by selecting an appropriate pore structure for the inert media and/or a modifying of its chemical nature. Results suggest that there are significant advantages to using diluted catalysts where diffusion limitations and pore-mouth poisoning conditions exist.

Remedies to diffusional intrusions in catalyst pellets and mitigation of their poisoning have been the preoccupation of many investigators, particularly in connection with catalysts for the control of automobile emissions. Two

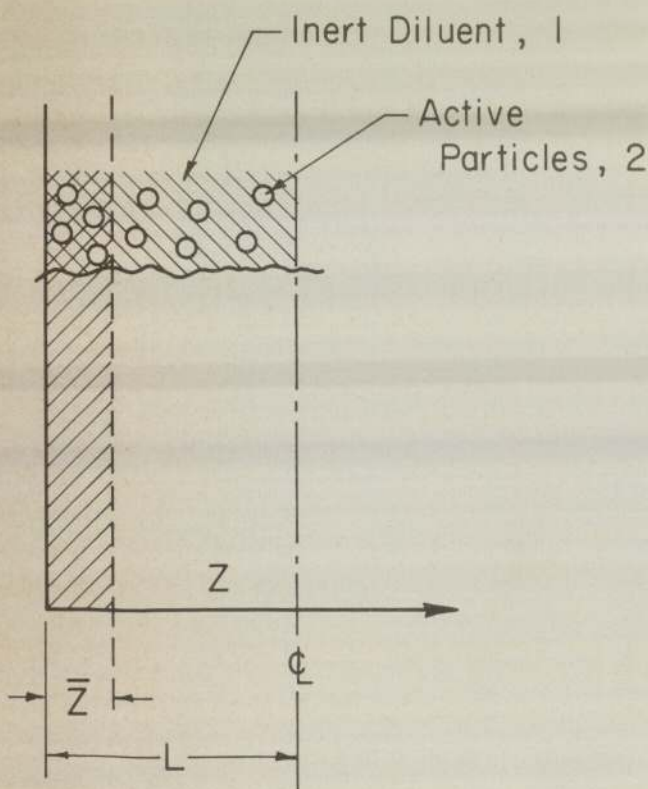


Figure 1. Schematic diagram of the diluted pellet showing the coordinate system and the poison front.

approaches, namely that of nonuniform distribution of active material on supports, and that of composite catalysts having layers of different diffusive properties, have been proposed. Becker and Wei (1977) examined the effects of 'egg yolk,' 'egg white' and 'egg shell' modes of active material deposition within a uniform support on their activity in reactions of bimolecular Langmuir kinetics, and on their resistance to poisoning in first order reactions. Wolf (1977) proposed the use of a composite catalyst having a protective outer layer of higher reactant diffusivity and analyzed its performance under pore-mouth poisoning conditions, such as those described by Wheeler (1951). Polomski and Wolf (1978) extended the analysis to include the bimolecular Langmuir type kinetics. The above analyses indicate that the deposition of active material in the interior of the catalyst pellet can lead to higher activity in the high reactant concentration region for bimolecular Langmuir kinetics and improve substantially the deactivation characteristics for both first order and bimolecular Langmuir kinetics under pore-mouth poisoning conditions. These advantages were more pronounced for the composite catalysts where the opportunity of minimizing the diffusion resistance of the protective layer of inert material existed. It may be noted that poison precursors in automotive exhausts (P, Pb and S compounds) typically result in pore-mouth type poisoning by strong adsorption on supports, as well as on active components (Hegedus and Cavendish, 1977; McArthur, 1975).

Ruckenstein (1970) proposed the use of a diluted catalyst pellet, composed of microspheres of active catalyst imbedded in an inert porous medium of advantageous diffusion characteristics, to permit more efficient utilization of the active material. Such a catalyst allows the use of a high area support, such as is necessary to obtain